BST

BioScience Trends

IRCA
BSSA

IACMHR

www.biosciencetrends.com

BioScience Trends is one of a series of peer-reviewed journals of the International Research and Cooperation Association for Bio & Socio-Sciences Advancement (IRCA-BSSA) Group. It is published bimonthly by the International Advancement Center for Medicine & Health Research Co., Ltd. (IACMHR Co., Ltd.) and supported by the IRCA-BSSA.

BioScience Trends devotes to publishing the latest and most exciting advances in scientific research. Articles cover fields of life science such as biochemistry, molecular biology, clinical research, public health, medical care system, and social science in order to encourage cooperation and exchange among scientists and clinical researchers.

BioScience Trends publishes Original Articles, Brief Reports, Reviews, Policy Forum articles, Communications, Editorials, News, and Letters on all aspects of the field of life science. All contributions should seek to promote international collaboration.

BioScience Trends

Editorial and Head Office

Pearl City Koishikawa 603, 2-4-5 Kasuga, Bunkyo-ku,
Tokyo 112-0003, Japan

E-mail: office@biosciencetrends.com
URL: www.biosciencetrends.com

Editorial Board Members

CONTENTS

Volume 18, Number 2, 2024

CONTENTS   (*Continued*)

Comment

Letter to the Editor

Policy Forum

A multidisciplinary collaborative diagnosis and rehabilitation program for dysphagia in general hospitals

Dysphagia Research Team (Alphabetical order)[1,*]: Juan Chen[1], Lili Dai[1], Min Guo[1], Hui Huang[1], Rongfen He[1], Hui Jin[1], Xin Jin[1], Xiaoxiao Li[1], Yumin Li[1], Yonggang Liu[1], Chao Wang[1], Yukai Wang[1], Li Wu[1], Zhongcheng Xing[1]; Japan NCGM Cooperation Team[2]: Junko Fujitani[2], Yasuo Sugiura[2], Chihaya Hinohara[2], Wei Tang[2]

[1] Huaibei People's Hospital Affiliated to Bengbu Medical University, Anhui Province, China;
[2] National Center for Global Health and Medicine, Tokyo, Japan.

SUMMARY Dysphagia is a common complication of various clinical conditions, with an increased incidence as age advances. Complications such as aspiration, malnutrition, and aspiration pneumonia caused by dysphagia significantly affect the overall treatment outcomes of patients. Scholars both domestically and internationally are increasingly focusing on early rehabilitation for dysphagia. This article summarizes common conditions causing dysphagia, clinical manifestations, complications, screening assessment, diagnosis, rehabilitation, and nutritional support related to dysphagia. It emphasizes the arrival at a multidisciplinary collaborative diagnosis and formulation of a rehabilitation management plan for dysphagia in general hospitals in order to provide strategic suggestions for establishing a multidisciplinary collaborative model for swallowing disorder management in general hospitals.

Keywords general hospitals, dysphagia, multidisciplinary collaboration, management

Swallowing is a crucial aspect of human physiology, serving not only as a means of ingesting nutrients and fluids but also as a result of the coordinated functioning of several organs, including the mouth, pharynx, and esophagus. However, dysphagia, a common and serious disorder, poses a significant challenge to the quality of life and overall health of patients. Dysphagia can be caused by a variety of factors, including neuromuscular disorders, anatomical abnormalities, neurological injuries, or post-surgical complications (*1-4*). Dysphagia can lead to serious complications, including aspiration pneumonia, malnutrition, and psychological and social interaction disorders. In severe cases, it can even be life-threatening (*5*).

Traditionally, physicians have relied on clinical experience and routine examinations to diagnose and treat dysphagia, but this approach has limitations. The diagnosis and treatment of dysphagia require multidisciplinary collaboration, involving specialists in otorhinolaryngology, neurology, rehabilitation medicine, nutrition, and speech-language pathology. This approach allows for a comprehensive understanding of the patient's condition and the formulation of personalized treatment plans to maximize the improvement of the patient's swallowing and quality of life (*6-9*). Rehabilitation for dysphagia is crucial, particularly in countries like China where the aging population is increasing. Objective evaluations should be prioritized over subjective ones. This can help prevent complications such as aspiration and swallowing pneumonia, reduce medical expenses, and alleviate the burden on the social healthcare system. Moreover, focusing on rehabilitation for dysphagia can advance the development of related medical technology and equipment, enhance the effectiveness and quality of rehabilitation, and advance medical care.

One aim of the current work was to investigate the use of a multidisciplinary collaborative diagnosis and treatment model for the rehabilitation of patients with dysphagia in general hospitals. Another aim was to propose a detailed and effective diagnosis, treatment, and rehabilitation program by combining practical experience and clinical research (Figure 1). This program will serve as a valuable reference for assessing the quality of life and therapeutic outcomes of patients with dysphagia. In addition, it will offer practical guidance and inspiration for medical professionals and researchers in related fields.
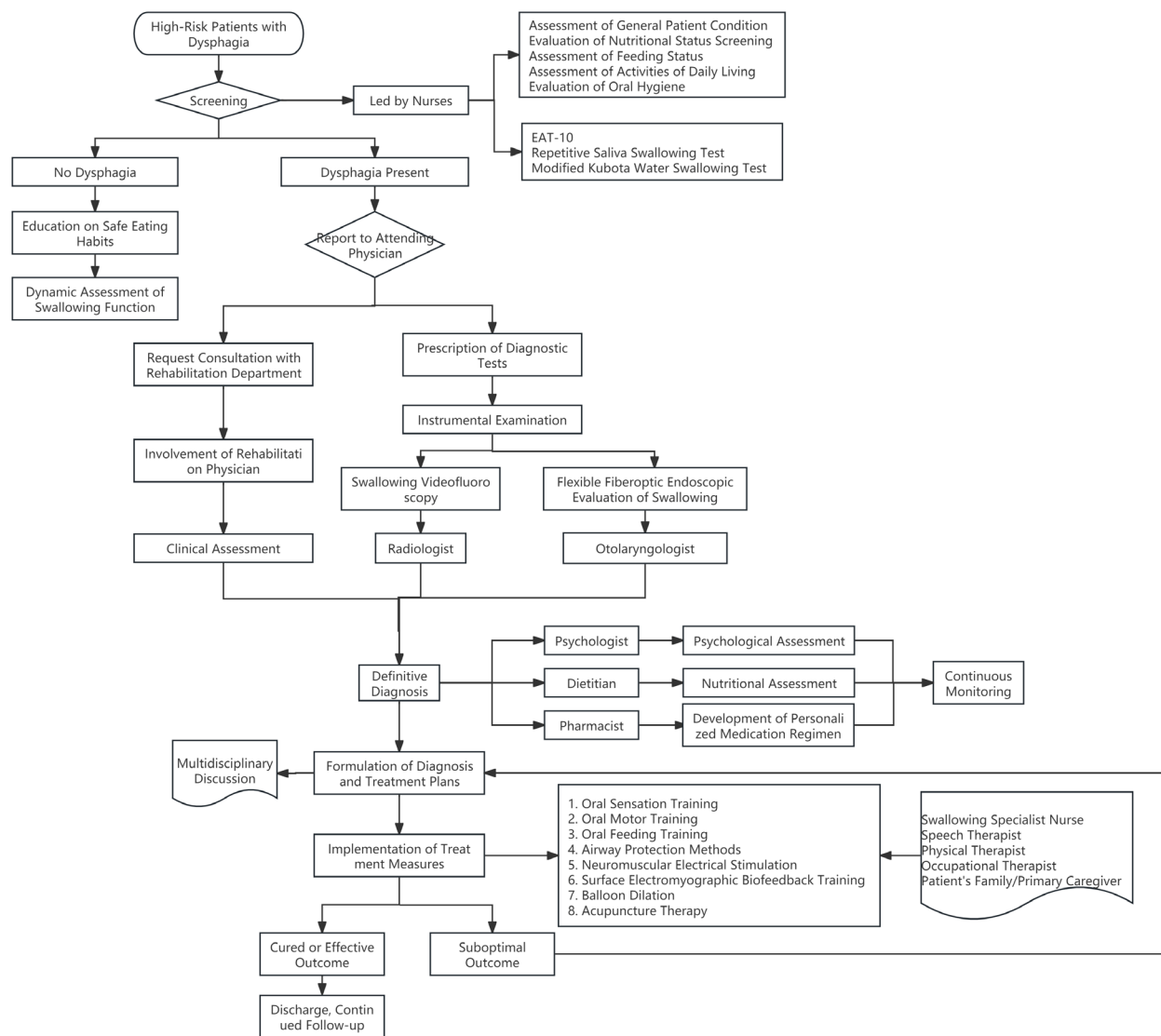
Figure 1. Multidisciplinary Collaboration Workflow for the Diagnosis, Treatment, and Rehabilitation of Dysphagia.

1. An Overview of Dysphagia

1.1. Definition

Dysphagia is a clinical manifestation resulting from structural and/or functional impairment of organs such as the mandible, lips, tongue, soft palate, pharynx, and esophagus, preventing the safe and effective passage of food from the mouth to the stomach. The broad concept of dysphagia should encompass behavioral and action abnormalities caused by cognitive, psychological, and mental issues leading to swallowing and feeding problems, known as feeding-dysphagia. Dysphagia typically meets the following criteria: (*i*) Difficulty in the passage of food or liquid from the mouth to the stomach; (*ii*) Impaired muscle control or coordination in the oral cavity and pharynx, resulting in malnutrition; and (*iii*) Accidental entry of food into the trachea, leading to recurrent pulmonary infections and aspiration pneumonia. Dysphagia can be categorized based on different stages of development: a swallowing disorder in the oral preparatory phase, a swallowing disorder in the oral phase, a swallowing disorder in the pharyngeal phase, and a swallowing disorder in the esophageal phase.

1.2. Conditions Causing Dysphagia

Normal swallowing is a complex and coordinated process involving structures and their related nerves and muscles in the upper respiratory tract, oral cavity, pharynx, and esophagus. Any disease along the pathway from the mouth to the stomach can cause dysphagia. This includes central nervous system diseases, peripheral neuropathies, neuromuscular junction disorders, muscle diseases, structural lesions of the oropharynx, diseases of the digestive and respiratory

systems, as well as undergoing radiation therapy and surgery in the oropharyngeal region.

Common conditions causing dysphagia include:

Neurological diseases: Stroke, Parkinson's disease, multiple sclerosis, amyotrophic lateral sclerosis (ALS), and facial nerve paralysis.

Structural abnormalities: Dysphagia can also result from structural abnormalities in the oral cavity, pharynx, and esophagus. Examples include esophagitis, esophageal strictures, esophageal hiatus hernia, tumors, trauma, and surgery on the oral cavity and pharynx.

Muscle diseases: Such as myasthenia gravis, muscular dystrophy, and disorders of muscle tone.

Other conditions: These conditions include thyroid enlargement, hyperthyroidism, esophageal ulcers, and esophagitis.

1.3. Clinical Manifestations of Dysphagia

Common clinical manifestations include: drooling or food spillage from the mouth, food residue in the oral cavity, a foul taste in the mouth, nasal regurgitation, food sticking in the mouth or throat, coughing or choking while eating or drinking, wheezing, difficulty breathing, the sensation of choking, swallowing pain, changes in eating habits, inability to eat certain foods, needing extra fluids to moisten food or aid in swallowing, multiple swallows required to clear food, a hoarse voice, frequent mouth clearing, difficulty or pain while chewing, a hoarse voice after swallowing, recurrent pneumonia, an unexplained fever, malnutrition, weight loss, other digestive system symptoms such as decreased appetite or refusal to eat, belching, acid reflux, nausea, vomiting, and abdominal bloating.

1.4. Common Complications of Dysphagia

Dysphagia can lead to serious complications that significantly impact the health and quality of life of patients.

1.4.1. Aspiration
Aspiration refers to the inhalation of substances from the oral or pharyngeal region into the lower respiratory tract. Aspiration is the most common and immediately actionable complication of dysphagia. After aspiration, patients may experience immediate irritative coughing, shortness of breath, or even wheezing, known as overt aspiration. In covert aspiration (>1 min), patients do not exhibit external signs such as coughing for more than one minute after aspiration, so it often goes undetected.

1.4.2. Pneumonia
Inhalation of oral or pharyngeal secretions containing pathogens or food particles can introduce bacteria into the lungs, leading to bacterial colonization

and subsequent pulmonary infections. In addition, gastroesophageal reflux can introduce gastric contents into the trachea and lungs, causing chemical injury to the lungs and eventual mixed infections.

1.4.3. Malnutrition
Malnutrition refers to deficiencies or excesses of energy, protein, and other nutrients that adversely affect bodily functions and clinical outcomes, including undernutrition and obesity.

1.4.4. Psychological and Social Interaction Disorders
Patients may experience depression, social isolation, or other psychological symptoms due to an inability to eat orally or the use of nasal feeding tubes, leading to impaired language and communication skills in children.

2. Swallowing Disorder Screening and Assessment

Using methods such as the EAT-10 Swallowing Screening Scale, repetitive saliva swallowing test, and the modified Wakita water swallowing test for screening and assessment, the initial assessment identifies swallowing issues in patients. Based on the assessment results, dietary and treatment plans are formulated to prevent aspiration and aspiration pneumonia.

2.1. Pre-screening Assessment

The patient's consciousness, speech, cognition, head control ability, and cooperation level are assessed. The patient's nutritional status, intake route, oral condition, and psychological state are simultaneously evaluated. Screening is postponed for patients with impaired consciousness or elderly and frail patients who cannot cooperate with the process, and appropriate nutritional routes are selected as needed. Screening tools include:

2.1.1. EAT-10 Swallowing Screening Scale
Developed by Belafsky *et al.*, the EAT-10 can improve the sensitivity and specificity of screening when used in conjunction with the water swallowing test. A total score of 3 or higher is considered abnormal swallowing, requiring further examination and evaluation.

2.1.2. Repetitive Saliva Swallowing Test (RSST)
As a screening test for functional dysphagia (*10*), the RSST assesses induction of the patient's swallowing reflex by observing the initiation time, number of swallows, and extent of laryngeal elevation within 30 seconds. This method of assessment is simple, quick, and safe.

2.1.3. Modified Kubota Water Swallowing Test
Proposed by Toshio Kubota *et al.* (*11*), this water swallowing test screens for the presence and severity of
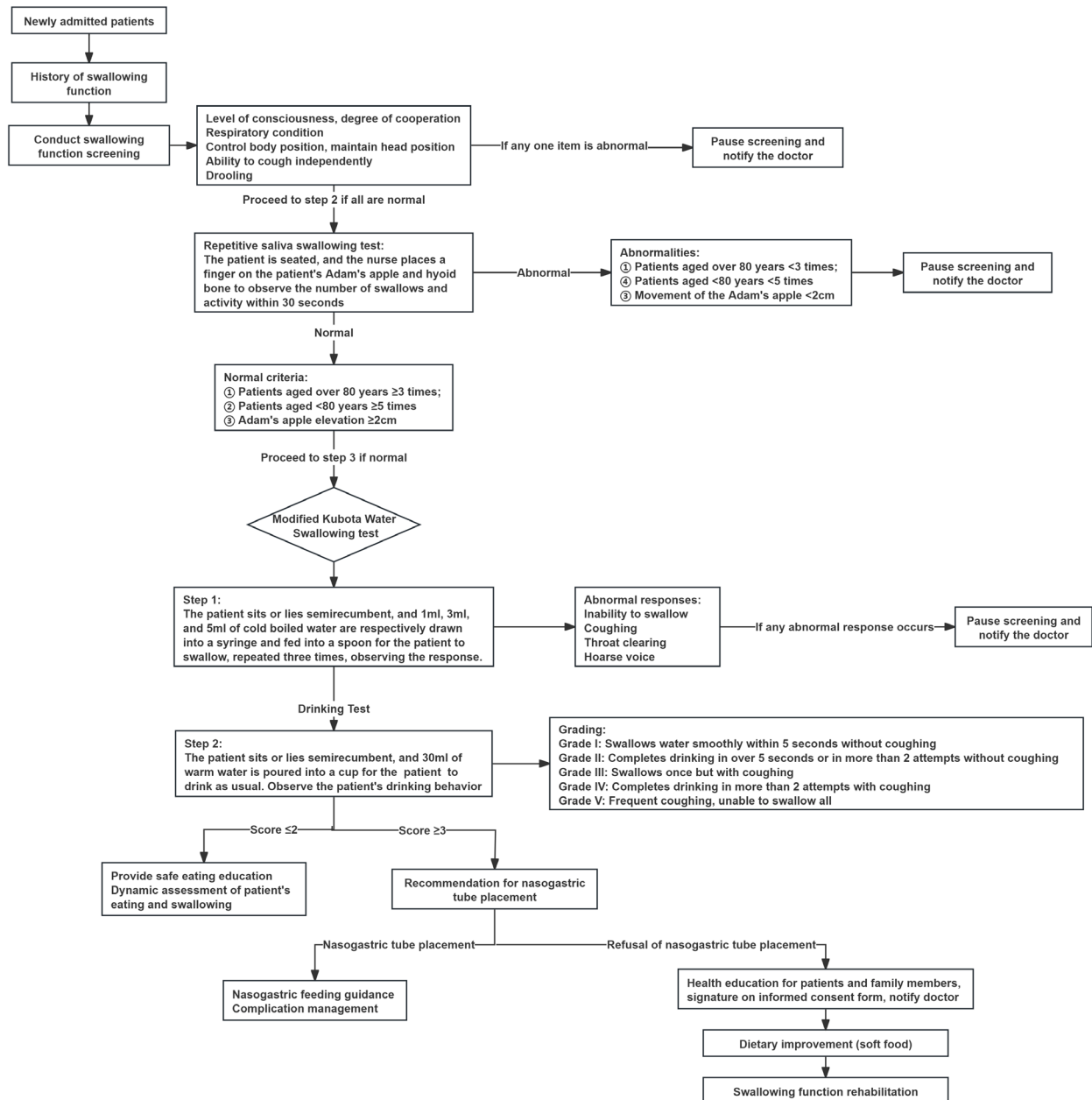
Figure 2. Swallowing Screening and Assessment Process.

dysphagia by having a patient drink 30 ml of water. The modified Kubota *et al.* water swallowing test involves administering 1 ml, 3 ml, and 5 ml of water before the actual test to reduce the risk of aspiration caused by screening. If the patient passes this pre-screening, the water swallowing test is continued to assess the presence and severity of dysphagia. This test can serve as a screening criterion for whether a patient can undergo swallowing imaging.

2.1.4. Swallowing Screening and Assessment Process
The swallowing screening and assessment workflow is shown in Figure 2.

2.2. Clinical Swallow Evaluation (CSE)

The CSE is an essential component of an intervention to diagnose or identify suspected dysphagia. It includes three main parts: a comprehensive medical history, a physical examination of oral and motor function, and assessment of food intake.

2.2.1. Medical History
This involves a comprehensive assessment of the patient's chief complaints, medical history, mental status, cognitive ability, treatment compliance, communication ability, nutritional status, oral hygiene,

respiratory function, and general motor function. It aims to further clarify the diagnosis of dysphagia and identify existing risks.

2.2.2. Bedside Feeding Evaluation
The volume-viscosity swallow test (V-VST) is used to evaluate bedside feeding. It observes the patient's swallowing to help choose the most appropriate volume and viscosity for fluid intake, ensuring the safety and effectiveness of feeding.

2.2.3. Direct Feeding Assessment
In addition to the V-VST, direct feeding is assessed in patients capable of oral intake, observing the process of the patient bringing food into his or her mouth. Key observations include the amount of food taken in one bite, swallowing time, coordination between breathing and swallowing, suitable shapes of food for safe swallowing, and assessment of oral medication.

2.2.4. Functional Oral Intake Scale (FOIS)
The FOIS is a tool used to assess a patient's ability to take food in orally. It evaluates whether the patient can consume foods of different consistencies and maintain the correct posture and breathing during eating. This scale is suitable for adult patients with varying degrees of dysphagia and is used to assess the progress of treatment and rehabilitation outcomes in patients with a swallowing disorder.

2.3. Instrumental Assessment of Dysphagia

2.3.1. Videofluoroscopic Swallowing Study (VFSS)
The VFSS is a specialized imaging study conducted under X-ray fluoroscopy to assess swallowing movements of the mouth, pharynx, larynx, and esophagus. It dynamically and comprehensively evaluates swallowing in the upper aerodigestive tract, identifying the presence of aspiration and its causes. The VFSS is considered the "gold standard" for assessing dysphagia.

2.3.2. Fiberoptic Endoscopic Evaluation of Swallowing
The Fiberoptic Endoscopic Evaluation of Swallowing (FEES) involves the use of a flexible endoscope inserted through the nose to depict the structures of the nasopharynx, oropharynx, and larynx on a monitor. It allows direct observation of various physiological activities, including quiet breathing, forced breathing, coughing, speaking, and swallowing. The FEES assesses the condition of these structures during swallowing, identifies the location and amount of residue after swallowing, and detects signs of leakage, penetration, or aspiration. It can be repeated multiple times over a given period to evaluate the effectiveness of different swallowing strategies.

3. Treatment and Rehabilitation Plan for Dysphagia

3.1. Oral Phase Rehabilitation

3.1.1. Drooling
Forms of Rehabilitation (12-14):
3.1.1.1. Sensory perception training for the lips: Alternating cold and hot water stimulation.
3.1.1.2. Massage therapy for the orbicularis oris muscle to improve muscle strength and tone.
3.1.1.3. Lip rounding exercises: Pronouncing syllables such as "i-l-i," "u-U-u," and "i-I-U-1" (combined with rhythm training).
3.1.1.4. Jaw opening and chewing exercises (can be combined with a chewable device).
3.1.1.5. Neuromuscular low-frequency electrical stimulation.
3.1.1.6. Traditional Chinese acupuncture to treat drooling: The main acupuncture points include the Lianquan acupoint, Chengjiang acupoint, Dicang acupoint, and Jiache acupoint (*15-17*).

3.1.2. Prolonged Oral Phase
Forms of Rehabilitation:
3.1.2.1. Sensory stimulation training: Ice stimulation, sour stimulation, *etc.*
3.1.2.2. Tongue massage therapy and tongue movement exercises.
3.1.2.3. Simulated chewing and bolus propulsion training for the tongue.
3.1.2.4. Compensatory treatment: Placing the bolus at the base of the tongue, eating with the head tilted back, and consuming smooth and thin liquid boluses.

3.1.3. Inadequate Tongue Elevation
Forms of Rehabilitation:
3.1.3.1. Compensatory strategies
Choosing foods with a thin, liquid texture, using a head-backward tilt, or placing the bolus at the base of the tongue.
3.1.3.2. Indirect strategies
Passive and active tongue movement exercises (*14*), resistance exercises for tongue elevation, and bolus propulsion exercises.

3.2. Pharyngeal Phase Issues

3.2.1. Delayed Pharyngeal Initiation
Forms of Rehabilitation (12-13):
3.2.1.1. Compensatory strategies: Increasing the viscosity of liquids (nectar-like fluids) or adopting a forward head tilt.
3.2.1.2. Indirect strategies: Thermal tactile stimulation.

3.2.2. Insufficient Laryngeal Elevation (*12-13*)
Forms of Rehabilitation:

3.2.2.1. Compensatory strategies
Increasing the viscosity of liquids (thin to moderately thick) or adopting a forward head tilt.
3.2.2.2. Indirect strategies
Singing therapy: Singing from low to high pitches, maintaining a high pitch for several seconds; the Mendelsohn maneuver (*18*). Laryngeal neuromuscular electrical stimulation at a low frequency (*19*).

3.2.3. Weak Pharyngeal Contraction
Forms of Rehabilitation:
3.2.3.1. Compensatory strategies (*12-13*)
Alternating between solid and liquid foods, preferring liquids; for unilateral pharyngeal muscle weakness, tilting the head towards the unaffected side; for bilateral pharyngeal muscle weakness, adopting a lateral recumbent position.
3.2.3.2. Indirect and direct strategies
The Mendelsohn maneuver; effortful swallowing.

3.2.4. Residue in Pharyngeal Recesses (Valleculae Residue, Piriform Sinus Residue)
3.2.4.1. Treatments for Valleculae Residue
   (*i*) Compensatory strategies: Reducing bolus viscosity (thin liquids), adopting a forward head tilt.
   (*ii*) Indirect strategies: The Masako maneuver (*12-14*); base of the tongue movement training.
   (*iii*) Direct strategy: Effortful swallowing.
3.2.4.2 Treatments for Piriform Sinus Residue
   (*i*) Compensatory strategies: Reducing bolus viscosity (water-like liquids), performing head turns during swallowing.
   (*ii*) Indirect strategies: The Mendelsohn maneuver; the Shaker exercise; occasionally, cricopharyngeal dilation may be necessary.

3.3. Aspiration

3.3.1. Treatment of Pre-swallowing Aspiration
3.3.1.1. Compensatory strategies: Increasing bolus viscosity (nectar-thick liquids, reducing powdered foods such as biscuits); adopting a forward head tilt; adjusting the volume and speed of intake (small sips).
3.3.1.2. Indirect strategies
Enhancing orofacial sensory perception.

3.3.2. Treatment of Mid-swallowing Aspiration
3.3.2.1. Compensatory strategies
Chin down, head turned towards the affected side; increasing bolus viscosity.
3.3.2.2. Indirect strategies
Training to promote glottal closure (*12-14*).
3.3.2.3. Direct strategies
Supraglottic swallow (*12-14*).

3.3.3. Treatment of Post-swallowing Aspiration

3.3.3.1. Compensatory strategies
Reducing bolus viscosity (water-like liquids); head turn during swallowing.
3.3.3.2. Indirect strategies
The Mendelsohn maneuver; effortful swallowing (*12-14*); if necessary, cricopharyngeal dilation (*12-13*). Individualized application of non-invasive central nervous system stimulation techniques such as transcranial magnetic stimulation and transcranial direct current stimulation based on the patient's condition.

4. Nutritional Management of Dysphagia

Dysphagia is closely related to malnutrition. Once diagnosed, patients with dysphagia undergo nutritional risk screening. Screening tools include Nutritional Risk Screening (NRS-2002), the Malnutrition Universal Screening Tool (MUST), and the Mini-Nutritional Assessment (MNA). A score of ≥ 3 on the NRS-2002 indicates nutritional risk; if the score is < 3, reassessment is performed after one week. Nutritional assessment and therapy are provided for patients at nutritional risk.

   For patients with mild swallowing difficulties who have undergone safety and efficacy testing or instrumental assessments without obvious aspiration or significant residue, oral intake is the preferred route of nutritional intake. Foods that are easily chewed, swallowed, or modified in texture may be chosen (*20*). Food texture should adhere to the following principles: 1. Hard foods should be softened; 2. Thin liquids should be thickened; 3. Avoidance of heterogeneous mixtures; and 4. Food should be homogeneous and smooth. When oral intake cannot meet nutritional needs, provided the patient's intestinal function is normal, enteral nutrition preparations or specialized medical foods adjusted for food texture are recommended for oral administration.

   For patients with severe swallowing difficulties, continuous or intermittent enteral nutrition preparations or specialized medical foods adjusted for food texture *via* tube feeding should be selected. When enteral nutrition cannot meet 60% of nutritional requirements, supplementation with parenteral nutrition should be considered.

   Regular nutritional monitoring is necessary during the implementation of nutritional therapy to assess current eating status, gastrointestinal symptoms, nutrient intake, and nutritional status in order to promptly modify the nutritional treatment plan.

5. Swallowing Disorder Rehabilitation Management

5.1. Risk Management

5.1.1. Informed consent
An adequate explanation should be provided to and

consent should be obtained from patients and their families before assessment and treatment, following standardized medical recording procedures and relevant requirements. For high-risk procedures or treatments, informed consent forms must be signed according to regulations.

5.1.2. Emergency management
Emergency plans for aspiration and choking.

5.2. Multidisciplinary Consultation and Case Discussions

The rehabilitation team holds regular case conferences where the focus is on reporting the patient's eating status. Other team members provide opinions, raise questions, and propose solutions. The attending physician compiles and determines the treatment plan, which is then implemented according to each team member's responsibilities.

5.3. Communication

Timely communication and exchanges of information among members of the multidisciplinary team can be facilitated through regular case conferences, phone calls, or messaging apps like WeChat. A dedicated communication platform for diagnosis, treatment, and rehabilitation of a swallowing disorder can ensure the prompt exchange of opinions on treatment.

5.4. Discharge Follow-up and Continuation of Rehabilitation Guidance

Upon discharge, patients and their families should be provided with guidance on home treatment, rehabilitation, and care, including knowledge and skills in preventing aspiration, self-management, caregiver abilities, food selection and portion control, eating posture, and knowledge of medication. Regular follow-up visits after discharge should be scheduled, with home visits conducted when necessary.

6. Conclusion

In summary, dysphagia is receiving increasing attention. This article has provided an overview of comprehensive management of dysphagia at a tertiary hospital, including screening and assessment, rehabilitation programs, nutritional management, multidisciplinary collaboration, risk prevention and control, and discharge follow-up. The aim is to promote the restoration of swallowing, reduce complications, and improve quality of life. Multidisciplinary collaboration is particularly important in the diagnosis and treatment of dysphagia, and it plays a significant role in enhancing the level of diagnosis and treatment and improving the quality of life for patients.

Conflict of Interest: The authors have no conflicts of interest to disclose.

References

1. Schindler A, Pizzorni N, Cereda E, *et al*. Consensus on the treatment of dysphagia in Parkinson's disease. J Neurol Sci. 2021; 430:120008.
2. Calandra-Buonaura G, Alfonsi E, Vignatelli L, *et al*. Dysphagia in multiple system atrophy consensus statement on diagnosis, prognosis and treatment. Parkinsonism Relat Disord. 2021; 86:124-132.
3. Kristensen MB, Isenring E, Brown B. Nutrition and swallowing therapy strategies for patients with head and neck cancer. Nutrition. 2020; 69:110548.
4. Boccardi V, Ruggiero C, Patriti A, Marano L. Diagnostic assessment and management of dysphagia in patients with Alzheimer's disease. J Alzheimers Dis. 2016; 50:947-955.
5. Marik PE, Kaplan D. Aspiration pneumonia and dysphagia in the elderly. Chest. 2003; 124:328-336.
6. Starmer HM, Dewan K, Kamal A, *et al*. Building an integrated multidisciplinary swallowing disorder clinic: Considerations, challenges, and opportunities. Ann N Y Acad Sci. 2020; 1481:11-19.
7. Umay E, Eyigor S, Giray E, *et al*. Pediatric dysphagia overview: Best practice recommendation study by multidisciplinary experts. World J Pediatr. 2022; 18:715-724.
8. Jukic Peladic N, Orlandoni P, Di Rosa M, Giulioni G, Bartoloni L, Venturini C. Multidisciplinary assessment and individualized nutritional management of dysphagia in older outpatients. Nutrients. 2023; 15:1103.
9. Di Pede C, Mantovani ME, Del Felice A, Masiero S. Dysphagia in the elderly: Focus on rehabilitation strategies. Aging Clin Exp Res. 2016; 28:607-617
10. Oguchi K, Saito E, Mizuno M, Baba M, Okui M, Suzuki M. The Repetitive Saliva Swallowing Test (RSST) as a Screening Test of Functional Dysphagia. Jpns J Rehab Med. 2000; 37:375-382. (in Japanese)
11. Kubota T, Mishima H, Hanada M, Namba I, Kojima Y. Dysphagia paralytica in cerebrovascular disease: screening test and its clinical application. Sogo Rihabiriteshon. 1982; 10:271-276. (in Japanese)
12. Dou ZL, Lan Y, Wan GF, *et al*. Assessment and Treatment of Dysphagia. People's Medical Publishing House, 2009, Beijing, China. (in Chinese)
13. Dou ZL, Wan GF. Dysphagia Rehabilitation Technology. Electronic Industry Press, 2019, Beijing, China. (in Chinese)
14. Rosenfeld-Johnson S. Oral-Motor Exercises for Speech Clarity: A comprehensive, step-by-step guide, that fills the gap between what we were taught and what we need to know. TalkTools/Innovative Therapists International, 2001.
15. Xia WG, Zheng CJ, Zhu SQ, *et al*. Does the addition of specific acupuncture to standard swallowing training

improve outcomes in patients with dysphagia after stroke? A randomized controlled trial. Clin Rehabil. 2016; 30:237-246.

16. Mao LY, Li LL, Mao ZN, *et al.* Therapeutic effect of acupuncture combining standard swallowing training for post-stroke dysphagia: A prospective cohort study. Chin J Integrative Med. 2016; 22:525-531

17. Chen LF, Fang JQ, Ma RJ, *et al*. Additional effects of acupuncture on early comprehensive rehabilitation in patients with mild to moderate acute ischemic stroke: a multicenter randomized controlled trial. BMC Complement Altern Med. 2016; 16:226.

18. Tatsuyuki F, Takahiro. Effect of the effortful swallow and the Mendelsohn maneuver on tongue pressure production against the hard palate. Dysphagia. 2013; 28:539-547

19. Li L, Li Y, Wu X, *et al.* The value of adding transcutaneous neuromuscular electrical stimulation (VitalStim) to traditional therapy for poststroke dysphagia: A randomized controlled trial. Topics in Geriatric Rehabilitation. 2018; 34:200-206

20. Chinese Expert Consensus Group on Dietary and Nutritional Management of Dysphagia. Chinese expert consensus on dietary and nutritional management of dysphagia (2019 edition). Chin J Phys Med and Rehab. 2019; 41:881-888. (in Chinese)

Address correspondence to:
Lili Dai, Huaibei People's Hospital Affiliated to Bengbu Medical University, Anhui Province, China.
E-mail: lilidai710606@foxmail.com

Comprehensive assessment and treatment strategies for dysphagia in the elderly population: Current status and prospects

Xiqi Hu[1], Ya-nan Ma[2], Kenji Karako[3], Wei Tang[3,4], Peipei Song[4,*], Ying Xia[1,*]

[1] Department of Neurosurgery, Central South University, Xiangya School of Medicine Affiliated Haikou Hospital, Haikou, China;
[2] Department of Gastroenterology, Hainan General Hospital, Hainan Affiliated Hospital of Hainan Medical University, Haikou, China;
[3] Department of Surgery, Graduate School of Medicine, The University of Tokyo, Tokyo, Japan;
[4] National Center for Global Health and Medicine, Tokyo, Japan.

SUMMARY   As the population ages, the prevalence of dysphagia among older adults is a growing concern. Age-related declines in physiological function, coupled with neurological disorders and structural changes in the pharynx associated with aging, can result in weakened tongue propulsion, a prolonged reaction time of the submental muscles, delayed closure of the laryngeal vestibule, and delayed opening of the upper esophageal sphincter (UES), increasing the risk of dysphagia. Dysphagia impacts the physical health of the elderly, leading to serious complications such as dehydration, aspiration pneumonia, malnutrition, and even life-threatening conditions, and it also detrimentally affects their psychological and social well-being. There is a significant correlation between frailty, sarcopenia, and dysphagia in the elderly population. Therefore, older adults should be screened for dysphagia to identify both frailty and sarcopenia. A reasonable diagnostic approach for dysphagia involves screening, clinical assessment, and instrumental diagnosis. In terms of treatment, multidisciplinary collaboration, rehabilitation training, and the utilization of new technologies are essential. Future research will continue to concentrate on these areas to enhance the diagnosis and treatment of dysphagia, with the ultimate aim of enhancing the quality of life of the elderly population.

Keywords   dysphagia, aging, frailty, sarcopenia, rehabilitation, diagnosis

1. Introduction

Globally, aging has emerged as a prominent phenomenon in modern society, driven by advances in medical care and higher living standards (*1*). As of 2022, the population age 65 and older has surpassed 500 million worldwide, with projections indicating a rise to 1.2 billion by 2050. This trend underscores the pervasive challenge of aging faced by nations across the globe (*2*). As aging becoming more pronounced, the prevalence of chronic conditions among the elderly, including dysphagia, has increased (*3*). Despite its prevalence, dysphagia often remains overlooked, despite being a widespread health concern (*4*). Estimates suggest that 30% to 40% of the elderly population experience dysphagia (*5-7*).

Dysphagia manifests as abnormal difficulty or discomfort in the swallowing process, stemming from problems with the muscles and nervous system of the pharynx (*8*). It impacts dietary intake and nutritional status and also poses risks for various complications, including potentially life-threatening lung infections (*9*). In a cross-sectional study among elderly nursing home residents, those with dysphagia had a 6-month mortality rate of 24.7%, compared to 11.9% among those without dysphagia (*p* < 0.001) (*10*). In addition, dysphagia was found to be an independent risk factor for mortality in this population (*10*). As a result of the aging process, dysphagia is thus a significant health concern among the elderly, significantly affecting their quality of life and overall health status.

Therefore, obtaining a comprehensive understanding of dysphagia's current status, etiology, diagnostic approaches, and therapeutic interventions in aging populations is crucial to improving the well-being and health outcomes of older adults. The current work aims to provide an in-depth analysis and discussion of dysphagia in order to offer theoretical insights and practical recommendations to support future research endeavors and clinical interventions.

2. Current status of dysphagia in the context of aging

2.1. Pathophysiological characteristics of dysphagia in the aging population

Swallowing is a complex process involving coordinated interactions among various systems and tissues, including the central nervous system, sensory nerves, motor nerves, and peripheral receptors (*11*). In addition, the intact anatomical structure of the pharynx is crucial to proper swallowing. The normal swallowing process consists of four phases: oral preparatory, oral propulsive, pharyngeal, and esophageal (*7*). In the oral preparatory phase, an individual forms a homogeneous food bolus in the anterior part of the mouth. In the oral propulsive phase, the tongue applies pressure on the palate to propel the food through the upper esophageal sphincter (UES) with minimal resistance (*12*). Pharyngeal contractions primarily contribute to pharyngeal clearance (*12*). The pharyngeal phase entails a series of automatic, involuntary neuromuscular events initiated by the passage of gastric juices through the pharyngeal column, driven by the tongue. The soft palate ascends to close the nasopharynx, preventing regurgitation of food into the nasal cavity. The suprahyoid muscles elevate the hyoid bone and raise the larynx, and the epiglottis closes the entrance to the larynx. During the esophageal phase, the tongue's root contacts the pharyngeal wall while the hyoid bone moves forward, coinciding with the relaxation of the cricopharyngeal muscles and the opening of the UES. Involuntary esophageal peristalsis propels the homogeneous food bolus through the upper gastrointestinal tract and into the stomach.

In the elderly, alterations in the swallowing reflex can arise due to declining physiological function, nervous system diseases, and structural changes in the pharynx (*13*). These alterations encompass reduced tongue propulsive force, a prolonged response time of the submental muscles, delayed closure of the laryngeal vestibule, and delayed opening of the UES (*14*). Notably, delayed closure of the laryngeal vestibule and delayed opening of the UES are pivotal contributors to impaired swallowing particularly in the elderly. Decreased thrust force may lead to post-swallowing oropharyngeal food retention, potentially resulting in malnutrition, neuromuscular conditions, and sarcopenia according to several studies (*15-17*). Various factors, such as diminished oropharyngeal sensitivity, reduced neuron counts, and damage to the swallowing-related areas in the cerebral cortex or brainstem, may contribute to delayed swallowing, particularly prevalent in the elderly, prompting delayed swallowing maneuvers (*16,18,19*). Moreover, reduced sphincter opening in the elderly may signify decreased upper dental support and/or weakened food propulsion (*20*). Physiological apnea occurs during swallowing in healthy individuals (*21*), but older adults or those with concurrent nervous system diseases or chronic obstructive pulmonary disease may have increased swallowing frequency during the inspiratory phase, increasing the risk of aspiration linked to swallowing (*22*).

2.2. Prevalence of dysphagia in an aging population

As individuals age, systems in the elderly gradually fall out of balance and functionally decline, resulting in a decrease in neural and muscular functional reserve, which impacts swallowing function (*23*). In addition, as muscle strength, including that of the muscles of the larynx and oropharynx, diminishes over time, coordination and strength during swallowing are compromised, thereby increasing the risk of dysphagia (*24*). Decreased muscle mass have been identified as an independent risk factor for dysphagia (*25*). The risk of oropharyngeal dysphagia increases in individuals of advanced age with the increased incidence of frailty, muscle loss, and comorbidities (*26*). A study has indicated that frailty correlates with dysphagia and reduced quality of life, irrespective of age, the presence of dementia, or nutritional status (*27*). The prevalence of oropharyngeal dysphagia among independently living seniors (mean age: 78.2 years) was 27.2% (*28*). In healthy seniors, alterations in swallowing function do not signify pathology (*29*) (as shown in Table 1).

There is a significant correlation between decreased tongue strength and aspiration (*41*). Sarcopenia was observed in 45% of the elderly with concurrent dysphagia residing in nursing homes (*35*). Within geriatric outpatient clinics, 6.7% of patients over the age of 60 had dysphagia (*38*). Among elderly patients with concomitant frailty hospitalized in emergency departments, 47.4% had dysphagia (*42,43*).

As the elderly population continues to grow, there is a corresponding increase in the proportion of elderly individuals with combined neurological disorders (*1,8*), which increases the risk of developing dysphagia. Over the years, the prevalence of stroke surged by 102% from 1990 to 2019, with approximately 42% or more of stroke survivors experiencing dysphagia (*44,45*). In 2018, the global prevalence of Alzheimer's disease (AD) stood at 50 million, a figure projected to triple by 2050 (*46*). Roughly 80% of individuals with AD have dysphagia (*47*). A study conducted in the US revealed that Parkinson's disease was diagnosed in over 50% of individuals age 85 and over (*48*), with 60% of Parkinson's patients experiencing pharyngeal dysphagia (*7,47*). In addition, other neurological disorders such as traumatic brain injury and neurological tumors can also affect the neural control of the pharynx, consequently impacting swallowing (*49-51*). Moreover, oral health issues such as tooth loss and dry mouth, cervical and laryngeal tumors, and postoperative esophageal stenosis can exacerbate dysphagia (*52,53*). Alterations in oral function and oral sensorimotor function among older adults and those receiving long-term care in senior populations are linked to a higher prevalence of oropharyngeal dysphagia (*54*). Consequently, swallowing function in older adults typically declines

Table 1. Prevalence of dysphagia in different elderly populations

Author (Year) References	Study population	Age	Screening methods	Prevalence of dysphagia
Jones *et al.* (2023) (*30*)	Individuals residing in the community	> 65 years	Questionnaire (Self-reported dysphagia)	10.6%
Mello *et al.* (2022) (*31*)	Individuals residing in the community	> 60 years	Questionnaire	8.1%
Takeuchi *et al.* (2014) (*32*)	Individuals residing in the community	Average age: 80.7 years for men and 82.9 years for women	Questionnaire (DRACE)	13.3%
Serra-Prat *et al.* (2012) (*33*)	Individuals age 70 and over who are living alone	Average age: 78 years	Questionnaire (V-VST)	18.8%
Igarashi *et al.* (2019) (*34*)	Older individuals living alone	Average age: 75.0 years	Questionnaire (EAT-10)	25.1%
	Dependent elderly	Average age: 82.3 years	Questionnaire (EAT-10)	53.8%
Campo-Rivera *et al.* (2022) (*35*)	Nursing home residents	Average age: 84 years	V-VST	65%
Yuan *et al.* (2022) (*36*)	Nursing home residents	Average age: 84.28 years	WST	75.3%
Lin *et al.* (2002)(*37*)	Long-term care facility residents	Average age: 77.07 years	Questionnaire	51%
Bahat *et al.* (2019) (*38*)	Hospital geriatric outpatient clinic	Average age: 74.1 years	Questionnaire (EAT-10)	6.7%
Mateos-Nozal *et al.* (2020) (*39*)	Emergency geriatric ward	Average age: 93.5 years	V-VST	82.4%
Maeda *et al.* (2016) (*40*)	Hospitalized elderly	Average age: 82.5 years	FOIS	30.0%

Abbreviations: DRACE, Dysphagia Risk Assessment for the Community-dwelling Elderly; EAT-10, 10-item Eating Assessment Tool; FOIS, Functional Oral Intake Scale; V-VST, Volume-Viscosity Swallow Test; WST, Water Swallow Test.

with age, compounded by the presence of multiple chronic conditions common in the elderly population, such as stroke and geriatric diseases, thereby further increasing the prevalence of dysphagia.

2.3. Complications associated with dysphagia in elderly individuals

Dysphagia in the elderly impacts their physical health and also detrimentally affects their psychological and social well-being. This condition can lead to serious complications, such as dehydration, aspiration, aspiration pneumonia, and malnutrition, significantly increasing the complexity of their health status and posing life-threatening risks. More than 50% of elderly individuals in nursing homes experience dysphagia, with approximately 19.7% requiring nasal feeding tubes due to severe aspiration (*42*). Moreover, over 22% of elderly individuals with concurrent dysphagia suffer from malnutrition (*55*). Among stroke patients, dysphagia has been associated with a 1.7-fold higher in-hospital mortality rate compared to controls (95% CI 1.67-1.74). In addition, dysphagia is correlated with prolonged hospitalization, increased healthcare costs, and a higher likelihood of readmission to acute care facilities following discharge (*4*). Moreover, dysphagia has been identified as an independent risk factor for mortality among elderly nursing home residents (*10*). In patients with dementia, dysphagia is linked to increased rates of malnutrition, respiratory infections, and mortality (*47*). Hence, dysphagia impacts the physical health of individuals and also increases the risk of aspiration, exacerbates the severity of disease, and jeopardizes their safety and survival.

Moreover, dysphagia can exacerbate social and psychological burdens on patients, leading to

psychological issues like anxiety and depression and diminishing their overall quality of life. A study found that 41% of dysphagia patients experience anxiety or panic during meals, and more than one-third avoid communal dining due to dysphagia-related concerns (*5*). Intermittent dysphagia is often linked to anxiety, whereas progressive dysphagia is primarily associated with depression (*56*). Studies have indicated that depression affects 7.2–49% of the elderly population (*57*) while anxiety disorders affect 3–14% (*58*). These psychological factors can further disrupt normal swallowing function and exacerbate dysphagia symptoms, perpetuating a vicious cycle. Complications stemming from dysphagia can lead to muscle frailty, decreased functionality, hospital admission, increased comorbidities, readmission, increased use of medication, and prolonged hospitalization (*59*). Consequently, dysphagia poses a significant socioeconomic burden, intensifying both the social and psychological strain on patients and placing substantial pressure on national healthcare budgets (*60*).

3. Screening and evaluation of dysphagia

3.1. Screening for frailty and sarcopenia in the elderly population

Frailty and sarcopenia are prevalent among elderly individuals and are closely linked to the onset of dysphagia. Therefore, comprehensive screening, including assessments for frailty and sarcopenia, is advisable in this demographic. Currently, widely utilized screening tools for frailty include the Clinical Frailty Scale (CFS) and the Comprehensive Geriatric Assessment (CGA) (*61*). A study has indicated that use of the CGA yielded favorable outcomes among hospitalized elderly patients, such as decreased mortality

and rehospitalization rates, along with enhanced physical functioning (*61*). The European Working Group on Sarcopenia in Older People (EWGSOP2) has proposed a clinical pathway for sarcopenia evaluation comprising four steps: find, assess, confirm, and severity. Initially, individuals are identified using the Strength, Assistance with walking, Rising from a chair, Climbing stairs, and Falls (SARC-F) questionnaire (*62*). Subsequently, they are assessed using the chair stand test. Afterwards, dual-energy X-ray absorptiometry (DXA) or bioelectrical impedance analysis (BIA) is used to verify muscle mass. Finally, somatic functional status is further evaluated (*63*).

3.2. Dysphagia screening

Screening for dysphagia is crucial in the elderly population due to its varied causes and often subtle clinical manifestations (*64*). Older adults at risk for dysphagia, including those who are frail, who have sarcopenia, who suffered a stroke, or who have neurodegenerative diseases or head and neck tumors, should undergo screening. This screening should be conducted by specialized clinicians or nurses using specific questionnaires and swallowing assessment tests.

Two widely used questionnaires are the Sydney Swallow Questionnaire (SSQ) and the 10-Item Eating Assessment Tool (EAT-10) (*65*). The SSQ is particularly effective at assessing the severity of dysphagia in patients with neuromuscular disorders (*66*). Both the SSQ and the EAT-10 are valuable for dysphagia assessment. The SSQ focuses on evaluating dysphagia severity in patients with neuromuscular conditions, while the EAT-10 demonstrates good sensitivity and specificity across various etiologies (*38,67*).

Common swallowing assessment tests include the Toronto Bedside Swallowing Screening Test (TOR-BSST), Volume-Viscosity Swallow Test (V-VST), Gugging Swallowing Screen (GUSS), and Standard Swallowing Assessment. The TOR-BSST and V-VST are validated tools for assessing dysphagia related to neurological disorders. The TOR-BSST is a risk screening tool for dysphagia that requires training to administer, boasting a sensitivity of 80–96% and a specificity of 64–68% (*68,69*). The V-VST is a dysphagia risk screening tool that involves up to nine swallows, utilizing three different viscosities and three different volumes. It screens for dysphagia risk and also offers guidance on oral intake. Its sensitivity ranges from 69% to 100%, and its specificity ranges from 29% to 87% (*70,71*). Patients testing positive on the swallowing assessment should undergo additional clinical evaluation and instrumental assessment to confirm the diagnosis and formulate an appropriate treatment plan.

3.3. Clinical assessment of swallowing function

The clinical assessment of swallowing function is pivotal for pinpointing the location and severity of dysphagia as well as determining the necessity for further diagnostic procedures and treatment (*52*). This assessment typically entails gathering a comprehensive medical history, conducting a physical examination, performing an oral motor examination, and administering swallowing assessment tests. When taking the patient's history, the assessor needs to inquire about any neurologic, psychiatric, head and neck, or upper gastrointestinal disorders, as well as the patient's nutritional status. An oral motor examination, overseen by an otolaryngologist and a speech-language pathologist, evaluates the structure and function of the jaw, tongue, pharynx, and larynx, along with the associated cranial nerves (V, VII, IX, and XII) (*70*). Given the correlation between dysphonia and swallowing function, assessing articulation is also essential (*72*). Moreover, absence of the cough reflex has been linked to silent malabsorption, and a simplified cough test may have some predictive value in dysphagia screening (*73*). Patients suspected of having dysphagia should undergo swallowing assessment tests such as the V-VST and the GUSS. Further instrumental assessment is recommended for patients testing positive on the swallowing assessment tests.

3.4. Instrumental assessment

Instrumental assessment serves as a crucial method for accurately evaluating the functional status of swallowing. This evaluation aids physicians in devising individualized treatment plans and monitoring treatment effectiveness to enhance the patient's quality of life. Ultrasonography offers a means to measure swallowing muscle mass and quality in elderly patients with sarcopenic dysphagia. It can identify specific factors indicative of sarcopenic dysphagia, such as lingual muscle area (sensitivity of 0.389, specificity of 0.947, and critical value of 1,536.0) and lingual root muscle area brightness (sensitivity of 0.806, specificity of 0.632, and critical value of 20.1) (*74*). Videofluoroscopy (VFS) and fiberoptic endoscopic evaluation of swallowing (FEES) are recognized as the gold standard for dysphagia assessment. VFS allows for monitoring of the anatomy and function of the oral cavity, pharynx, and larynx. It assesses the functionality of airway protective mechanisms by providing insights into the function of various anatomical structures (tongue-pharyngeal junction, pharyngeal junction, and epiglottis opening and closing times) (*75,76*). Despite its advantages, VFS is limited by its use of radiation and its predictive capability regarding aspiration pneumonia (*77,78*). In contrast, FEES, conducted at the bedside, enables precise visualization of mucosal surfaces and movements within the base of the tongue, pharynx, and larynx and it is well-tolerated by patients (*79*). Its utility extends to assessing dysphagia in the elderly and evaluating dysphagia associated with various conditions, including head and neck neoplasms, post-

stroke complications, and neurological disorders (*80-83*). Nevertheless, FEES is constrained by its inability to quantify physiological swallowing processes, relying instead on subjective interpretation of residual findings.

Swallowing electromyography (EMG) and high-resolution manometry (HRM) of the esophagus offer detailed insights into physiological function (*84,85*). These modalities assess muscular coordination and strength relevant to swallowing, alongside normalizing esophageal movements and pressure changes. Notably, they present advantages in diagnosing post-stroke dysphagia (PSD), providing more objective and sensitive assessments compared to clinical methods (*86*). For acute stroke scenarios, the use of standardized, validated, and reliable instruments in PSD assessment should consider various factors like the type of stroke, history, severity, diabetes, and sex to mitigate pneumonia risks and reduce mortality (*45*). Moreover, assessment of swallowing function through ultrasonography, functional magnetic resonance imaging (fMRI), and real-time MRI furnishes critical insights, capitalizing on advantages such as soft-tissue visualization, reliable timing analysis, and eliminating x-ray exposure (*87-89*). A comprehensive assessment incorporating these diverse tools and methods aids in diagnosing and devising treatment plans for patients with dysphagia (as shown in Figure 1).

4. Interventions for dysphagia

Interventions aimed at addressing dysphagia encompass a range of strategies, including postural adjustments, dietary modifications, and swallowing rehabilitation (*90-92*). These interventions aim to improve swallowing function, enhance coordination and efficiency, and mitigate the incidence of dysphagia and associated complications. Postural adjustments play a pivotal role in enhancing swallowing function and mitigating the risk of aspiration. This can be achieved by optimizing the patient's posture during meals, such as maintaining an upright position and performing the chin-down maneuver (*93,94*). In addition, dietary management involves altering food consistency, regulating bolus flow, and alternating between solid and liquid intake (*95*). Such therapeutic interventions seek to bolster patient tolerance and reduce the likelihood of aspiration pneumonia and pulmonary infections (*95,96*).

Swallowing rehabilitation entails targeted exercises aimed at strengthening specific muscles or muscle groups in the oral cavity and pharynx. Techniques such as progressive tongue resistance exercises and the Shaker exercise are used to enhance physiological swallowing function and mitigate complications associated with dysphagia (*15,97*).
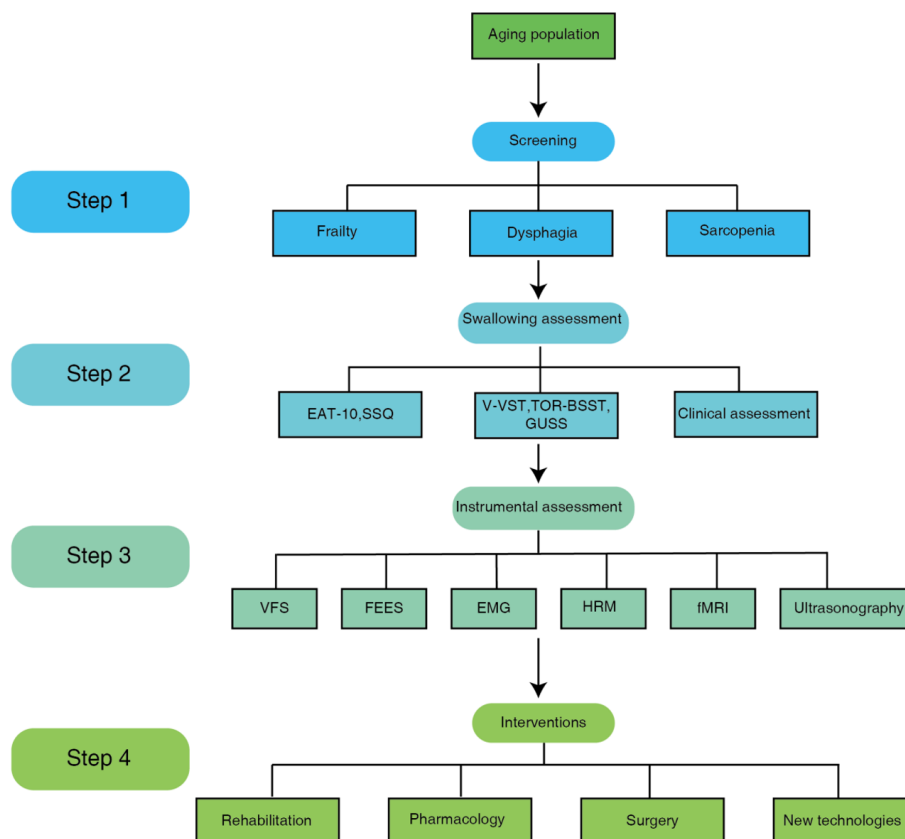
Figure 1. Diagnosis and treatment options for dysphagia in the aging population. Abbreviations: EAT-10, 10-Item Eating Assessment Tool; EMG, electromyography; FEES, fiberoptic endoscopic evaluation of swallowing; fMRI, functional magnetic resonance imaging; GUSS, Gugging Swallowing Screen; HRM, high-resolution manometry; SSQ, Sydney Swallow Questionnaire; TOR-BSST, Toronto Bedside Swallowing Screening Test; VFS, videofluoroscopy; V-VST, Volume-Viscosity Swallow Test.

Pharmacologic and surgical interventions are pivotal in addressing dysphagia, serving as adjuncts or primary treatments tailored to specific etiologies. In terms of pharmacotherapy, patients with dysphagia are advised to consider reducing the use of medications known to adversely affect swallowing function, such as antipsychotics (*98*). In addition, certain excitatory drugs like capsaicin, which activates transient receptor potential vanilloid type 1 (TRPV1), can enhance the swallowing response, thereby shortening swallowing response times and improving safety and efficacy (*99*).

Common options for surgical interventions include cricopharyngeal myotomy, UES dilatation, and cricopharyngeal botulinum toxin injections, aimed at enhancing push flow and eliminating UES outlet obstruction (*100-102*). Procedures such as laryngectomy, tracheoesophageal diversion, and laryngeal suspension are used to safeguard the airway and mitigate the risk of aspiration (*103-106*). In addition, endoscopic Zenker repair can improve push flow and alleviate UES outlet obstruction and push retention in diverticular pockets (*107-109*).

Moreover, physiotherapy and nutritional support, such as transgastric or transnasal gastrostomy tube (NGT) feeding, play crucial roles in dysphagia management (*110*). Among individuals with oropharyngeal dysphagia, those undergoing percutaneous endoscopic gastrostomy (PEG) requiring hospitalization have a significantly lower prevalence of pneumonia compared to those receiving NGT feeding (*111*). When formulating a treatment plan, the patient's specific circumstances and etiology, along with the effects and risks of treatment, should be carefully considered and personalized under the guidance of a physician.

The management of swallowing function necessitates the coordination of multiple systems, including the oral, pharyngeal, neurological, and muscular systems, highlighting the importance of collaborative management strategies by a multidisciplinary team. A survey of clinic attendees revealed that 43% of dysphagia patients had a history of esophageal disease, 22% had undergone head and neck radiation therapy, 14% had an underlying neurological diagnosis, 10% had undergone cervical spine surgery, and only 1% had no known medical history (*112*). Consequently, effectively treating and managing dysphagia in the elderly population with comorbidities necessitates drawing on multidisciplinary expertise.

A multidisciplinary care team typically consists of otolaryngologists, neurologists, rehabilitation medicine specialists, dietitians, and speech therapists (*113,114*). At the McGill University Health Center, for example, a comprehensive treatment plan is offered to patients, incorporating flexible endoscopic swallowing assessment, dietary modifications, swallowing therapy, medication, and surgery, thus enhancing treatment adaptability and effectiveness (*115*). Similarly, Stanford University has established a multidisciplinary dysphagia center, bringing together physicians and therapists specializing in otolaryngology, speech-language pathology, nutrition, and gastroenterology. This center delivers comprehensive treatment plans addressing symptoms and issues associated with various dysphagia types (*112*).

The multidisciplinary teamwork model is instrumental in managing dysphagia among the elderly population. It plays a crucial role in minimizing duplicate examinations, shortening the duration of treatment, and increasing satisfaction with care. Overall, this approach ensures comprehensive treatment and care for patients with dysphagia.

5. Use of new technologies

The use of new technologies holds significant promise in the treatment of dysphagia. Neuromodulation techniques, such as repetitive transcranial magnetic stimulation (rTMS), transcranial direct current stimulation (tDCS), and pharyngeal electrical stimulation (PES), have garnered considerable attention for their ability to address neurogenic dysphagia (*116-119*). These techniques primarily aim to enhance the function of the swallowing neuron network by modulating central nervous system activity, thereby improving patients' swallowing ability. In stroke patients with dysphagia, for example, rTMS treatment has been found to induce changes in the functional motor system of swallowing, including increased excitability of the pharyngeal cortex and enhanced pharyngeal sensory conduction (*118-120*). A clinical study has demonstrated the effectiveness of various rTMS protocols, including ipsilateral, contralateral, and cerebellar stimulation, in improving swallowing function and reducing dysphagia severity (*121*). Similarly, anodal tDCS applied to the contralateral sensorimotor cortex has been found to alleviate the functional severity of dysphagia in patients without adverse effects (*122*). These neuromodulation techniques offer novel treatment options for elderly patients with dysphagia of neurological origin.

As a complement to swallowing therapy, biofeedback offers patients visual or auditory signals to adjust the conscious or subconscious mechanisms involved in swallowing, thereby improving their swallowing ability (*123,124*). One such biofeedback technique, surface electromyography (sEMG), is widely used. sEMG biofeedback uses two small electrodes on the submental muscles to measure the timing and force of muscle contractions, displayed graphically on a screen (*125,126*). When combined with swallowing maneuvers, sEMG biofeedback enhances hyoid displacement in post-stroke dysphagia patients (*126*). Another innovative dysphagia treatment is Biofeedback in Strength and Skill Training (BiSSkiT) (*127*). Initial studies in neurodegenerative diseases suggest that skill training may improve

swallowing coordination and timing, potentially aiding dysphagia rehabilitation (*128,129*).

The use of stem cells to repair damaged tissue or promote tissue regeneration holds promise for dysphagia treatment. Stem cells possess the remarkable ability to self-renew and differentiate into various cell types, offering the potential to repair damaged pharyngeal tissues or reconstruct impaired neuronal networks, thereby restoring swallowing function in patients (*130*). In a clinical pilot study involving 12 patients with oculopharyngeal muscular dystrophy (OPMD) and indications for cricopharyngeus muscle myotomy, stem cell injections were administered at different pharyngeal constrictor sites post-myotomy (*131*). Six out of 12 patients had improved upper pharyngeal function at 24 months according to video endoscopy, but only 2 out of 12 patients displayed improvement according to the more sensitive videofluoroscopy (*131*). In another study, 30 patients who underwent radiotherapy for HPV-positive squamous cell carcinoma of the oropharynx were randomized to receive ultrasound-guided injections of autologous adipose tissue-derived stem cells (ADSCs) or a placebo in the submandibular gland (*131*). Patients treated with ADSCs had a significant increase in non-stimulated salivary flow rate at both 1 and 4 months, along with reduced symptoms and improved eating and thirst compared to those receiving a placebo (*131*). A tissue examination also revealed positive changes in gland tissue morphology in patients treated with ADSCs, indicating potential benefits of stem cell therapy in dysphagia management (*131*). While stem cell therapy remains in the research phase, these preliminary findings offer hope for advancing dysphagia treatment.

6. Conclusion

The current status of dysphagia in the context of aging highlights its prevalence and complexity. As the global population ages, dysphagia has emerged as a significant issue among older adults. Physiological changes related to aging, such as diminished muscle strength and coordination in the oropharyngeal region, contribute to the increased risk of swallowing problems in this demographic. In addition, age-related conditions like neurological disorders and structural changes in the pharynx further increase the likelihood of dysphagia, posing risks of complications such as aspiration pneumonia, malnutrition, and dehydration. Moreover, beyond the physical challenges, dysphagia profoundly affects the overall well-being of the elderly, leading to diminished quality of life, social isolation, and psychological distress, which in turn presents considerable challenges for caregivers and healthcare providers.

Addressing these challenges necessitates a comprehensive approach involving early detection and intervention strategies tailored to individual needs.

Screening protocols, along with diagnostic tools like videofluoroscopy and fiberoptic endoscopic evaluation, play crucial roles in effective dysphagia management. Moreover, interdisciplinary collaboration among healthcare professionals including speech-language pathologists, dietitians, and physicians is essential for providing integrated care. Moving forward, continued research is vital to refining diagnostic techniques, optimizing treatment modalities, and promoting holistic approaches to improve the well-being and quality of life of older adults with dysphagia.

Conflict of Interest: The authors have no conflicts of interest to disclose.

References

1. Partridge L, Deelen J, Slagboom PE. Facing up to the global challenges of ageing. Nature. 2018; 561:45-56.
2. Affairs UDoEaS. Population division -world population prospects 2022. online, 2024. *https://population.un.org/wpp* (accessed April 10, 2024)
3. Tchkonia T, Kirkland JL. Aging, cell senescence, and chronic disease: Emerging therapeutic strategies. JAMA. 2018; 320:1319-1320.
4. Patel DA, Krishnaswami S, Steger E, Conover E, Vaezi MF, Ciucci MR, Francis DO. Economic and survival burden of dysphagia among inpatients in the United States. Dis Esophagus. 2018; 31:1-7.
5. Ekberg O, Hamdy S, Woisard V, Wuttge-Hannig A, Ortega P. Social and psychological burden of dysphagia: Its impact on diagnosis and treatment. Dysphagia. 2002; 17:139-146.
6. Cho SY, Choung RS, Saito YA, Schleck CD, Zinsmeister AR, Locke GR, 3rd, Talley NJ. Prevalence and risk factors for dysphagia: A USA community study. Neurogastroenterol Motil. 2015; 27:212-219.
7. Clave P, Shaker R. Dysphagia: Current reality and scope of the problem. Nat Rev Gastroenterol Hepatol. 2015; 12:259-270.
8. Thiyagalingam S, Kulinski AE, Thorsteinsdottir B, Shindelar KL, Takahashi PY. Dysphagia in older adults. Mayo Clin Proc. 2021; 96:488-497.
9. Tagliaferri S, Lauretani F, Pela G, Meschi T, Maggio M. The risk of dysphagia is associated with malnutrition and poor functional outcomes in a large population of outpatient older individuals. Clin Nutr. 2019; 38:2684-2689.
10. Wirth R, Pourhassan M, Streicher M, Hiesmayr M, Schindler K, Sieber CC, Volkert D. The impact of dysphagia on mortality of nursing home residents: Results from the nutrition day project. J Am Med Dir Assoc. 2018; 19:775-778.
11. Jean A. Brain stem control of swallowing: neuronal network and cellular mechanisms. Physiol Rev. 2001; 81:929-969.

12. Kahrilas PJ, Logemann JA, Lin S, Ergun GA. Pharyngeal clearance during swallowing: A combined manometric and videofluoroscopic study. Gastroenterology. 1992; 103:128-136.

13. Clave P, Verdaguer A, Arreola V. Oral-pharyngeal dysphagia in the elderly. Med Clin (Barc). 2005; 124:742-748.

14. Nagaya M, Sumi Y. Reaction time in the submental muscles of normal older people. J Am Geriatr Soc. 2002; 50:975-976.

15. Robbins J, Gangnon RE, Theis SM, Kays SA, Hewitt AL, Hind JA. The effects of lingual exercise on swallowing in older adults. J Am Geriatr Soc. 2005; 53:1483-1489.

16. Rofes L, Arreola V, Romea M, Palomera E, Almirall J, Cabre M, Serra-Prat M, Clave P. Pathophysiology of oropharyngeal dysphagia in the frail elderly. Neurogastroenterol Motil. 2010; 22:851-858, e230.

17. Clave P, de Kraa M, Arreola V, Girvent M, Farre R, Palomera E, Serra-Prat M. The effect of bolus viscosity on swallowing function in neurogenic dysphagia. Aliment Pharmacol Ther. 2006; 24:1385-1394.

18. Teismann IK, Steinstrater O, Warnecke T, Suntrup S, Ringelstein EB, Pantev C, Dziewas R. Tactile thermal oral stimulation increases the cortical representation of swallowing. BMC Neurosci. 2009; 10:71.

19. Turley R, Cohen S. Impact of voice and swallowing problems in the elderly. Otolaryngol Head Neck Surg. 2009; 140:33-36.

20. Cook IJ. Clinical disorders of the upper esophageal sphincter. GI Motility online. 2006. DOI:10.1038/gimo37

21. Martin-Harris B, Brodsky MB, Michel Y, Ford CL, Walters B, Heffner J. Breathing and swallowing dynamics across the adult lifespan. Arch Otolaryngol Head Neck Surg. 2005; 131:762-770.

22. Martin-Harris B. Clinical implications of respiratory-swallowing interactions. Curr Opin Otolaryngol Head Neck Surg. 2008; 16:194-199.

23. Thuault S. Reflections on aging research from within the National Institute on Aging. Nat Aging. 2021; 1:14-18.

24. Hu X, Ma Y, Jiang X, Tang W, Xia Y, Song P. Neurosurgical perioperative management of frail elderly patients. Biosci Trends. 2023; 17:271-282.

25. Maeda K, Takaki M, Akagi J. Decreased skeletal muscle mass and risk factors of sarcopenic dysphagia: A prospective observational cohort study. J Gerontol A Biol Sci Med Sci. 2017; 72:1290-1294.

26. Roy N, Stemple J, Merrill RM, Thomas L. Dysphagia in the elderly: Preliminary evidence of prevalence, risk factors, and socioemotional effects. Ann Otol Rhinol Laryngol. 2007; 116:858-865.

27. Guner M, Bas AO, Ceylan S, Kahyaoglu Z, Coteli S, Unsal P, Cavusoglu C, Ozsurekci C, Dogu BB, Cankurtaran M, Halil MG. Dysphagia is closely related to frailty in mild-to-moderate Alzheimer's disease. BMC Geriatr. 2023; 23:304.

28. Serra-Prat M, Hinojosa G, Lopez D, Juan M, Fabre E, Voss DS, Calvo M, Marta V, Ribo L, Palomera E, Arreola V, Clave P. Prevalence of oropharyngeal dysphagia and impaired safety and efficacy of swallow in independently living older persons. J Am Geriatr Soc. 2011; 59:186-187.

29. Humbert IA, Robbins J. Dysphagia in the elderly. Phys Med Rehabil Clin N Am. 2008; 19:853-866, ix-x.

30. Jones HN, Leiman DA, Porter Starr KN, North R, Pieper CF, Robison RD, Cohen SM. Dysphagia in older adults is associated with food insecurity and being homebound. J Appl Gerontol. 2023; 42:1993-2002.

31. Mello RP, Xavier MO, Tomasi E, Gonzalez MC, Demarco FF, Bielemann RM. Dysphagia perception among community-dwelling older adults from a municipality in southern Brazil. Dysphagia. 2022; 37:879-888.

32. Takeuchi K, Aida J, Ito K, Furuta M, Yamashita Y, Osaka K. Nutritional status and dysphagia risk among community-dwelling frail older adults. J Nutr Health Aging. 2014; 18:352-357.

33. Serra-Prat M, Palomera M, Gomez C, Sar-Shalom D, Saiz A, Montoya JG, Navajas M, Palomera E, Clave P. Oropharyngeal dysphagia as a risk factor for malnutrition and lower respiratory tract infection in independently living older persons: A population-based prospective study. Age Ageing. 2012; 41:376-381.

34. Igarashi K, Kikutani T, Tamura F. Survey of suspected dysphagia prevalence in home-dwelling older people using the 10-Item Eating Assessment Tool (EAT-10). PLoS One. 2019; 14:e0211040.

35. Campo-Rivera N, Ocampo-Chaparro JM, Carvajal-Ortiz R, Reyes-Ortiz CA. Sarcopenic dysphagia is associated with mortality in institutionalized older adults. J Am Med Dir Assoc. 2022; 23:1720 e1711-1720 e1717.

36. Yuan J, Lin Y, Song J, Xia R, Jiang Y, Yang X, Li Y, Dong B. Associations of sarcopenic parameters with dysphagia in older nursing home residents: A cross-sectional study. J Nutr Health Aging. 2022; 26:339-345.

37. Lin LC, Wu SC, Chen HS, Wang TG, Chen MY. Prevalence of impaired swallowing in institutionalized older people in Taiwan. J Am Geriatr Soc. 2002; 50:1118-1123.

38. Bahat G, Yilmaz O, Durmazoglu S, Kilic C, Tascioglu C, Karan MA. Association between dysphagia and frailty in community dwelling older adults. J Nutr Health Aging. 2019; 23:571-577.

39. Mateos-Nozal J, Montero-Errasquin B, Sanchez Garcia E, Romero Rodriguez E, Cruz-Jentoft AJ. High prevalence of oropharyngeal dysphagia in acutely hospitalized patients aged 80 years and older. J Am Med Dir Assoc. 2020; 21:2008-2011.

40. Maeda K, Akagi J. Sarcopenia is an independent risk factor of dysphagia in hospitalized older people. Geriatr Gerontol Int. 2016; 16:515-521.

41. Butler SG, Stuart A, Leng X, Wilhelm E, Rees C, Williamson J, Kritchevsky SB. The relationship of aspiration status with tongue and handgrip strength in healthy older adults. J Gerontol A Biol Sci Med Sci. 2011; 66:452-458.

42. Leder SB, Suiter DM. An epidemiologic study on aging and dysphagia in the acute care hospitalized population: 2000-2007. Gerontology. 2009; 55:714-718.

43. Carrion S, Cabre M, Monteis R, Roca M, Palomera E, Serra-Prat M, Rofes L, Clave P. Oropharyngeal dysphagia is a prevalent risk factor for malnutrition in a cohort of older patients admitted with an acute disease to a general hospital. Clin Nutr. 2015; 34:436-442.

44. Labeit B, Michou E, Hamdy S, Trapl-Grundschober M, Suntrup-Krueger S, Muhle P, Bath PM, Dziewas R. The assessment of dysphagia after stroke: State of the art and future directions. Lancet Neurol. 2023; 22:858-870.

45. Banda KJ, Chu H, Kang XL, Liu D, Pien LC, Jen HJ, Hsiao SS, Chou KR. Prevalence of dysphagia and risk of pneumonia and mortality in acute stroke patients: A meta-analysis. BMC Geriatr. 2022; 22:420.

46. International AsD. World Alzheimer Report 2018. The

state of the art of dementia research: new frontiers. online, September 2018. *https://www.alzint.org/u/ WorldAlzheimerReport2018.pdf* (accessed April 10, 2024)

47. Espinosa-Val MC, Martin-Martinez A, Graupera M, Arias O, Elvira A, Cabre M, Palomera E, Bolivar-Prados M, Clave P, Ortega O. Prevalence, risk factors, and complications of oropharyngeal dysphagia in older patients with dementia. Nutrients. 2020; 12:863.

48. Bennett DA, Beckett LA, Murray AM, Shannon KM, Goetz CG, Pilgrim DM, Evans DA. Prevalence of parkinsonian signs and associated mortality in a community population of older people. N Engl J Med. 1996; 334:71-76.

49. Kenny C, Regan J, Balding L, Higgins S, O'Leary N, Kelleher F, McDermott R, Armstrong J, Mihai A, Tiernan E, Westrup J, Thirion P, Walsh D. Dysphagia in solid tumors outside the head, neck or upper GI tract: Clinical characteristics. J Pain Symptom Manage. 2022; 64:546-554.

50. Nieto K, Ang D, Liu H. Dysphagia among geriatric trauma patients: A population-based study. PLoS One. 2022; 17:e0262623.

51. Cosentino G, Avenali M, Schindler A, *et al.* A multinational consensus on dysphagia in Parkinson's disease: Screening, diagnosis and prognostic value. J Neurol. 2022; 269:1335-1352.

52. Baijens LW, Clave P, Cras P, Ekberg O, Forster A, Kolb GF, Leners JC, Masiero S, Mateos-Nozal J, Ortega O, Smithard DG, Speyer R, Walshe M. European Society for Swallowing Disorders - European Union Geriatric Medicine Society white paper: Oropharyngeal dysphagia as a geriatric syndrome. Clin Interv Aging. 2016; 11:1403-1428.

53. Clave P, Terre R, de Kraa M, Serra M. Approaching oropharyngeal dysphagia. Rev Esp Enferm Dig. 2004; 96:119-131.

54. Rech RS, Baumgarten A, Colvara BC, Brochier CW, de Goulart B, Hugo FN, Hilgert JB. Association between oropharyngeal dysphagia, oral functionality, and oral sensorimotor alteration. Oral Dis. 2018; 24:664-672.

55. Jukic Peladic N, Orlandoni P, Di Rosa M, Giulioni G, Bartoloni L, Venturini C. Multidisciplinary assessment and individualized nutritional management of dysphagia in older outpatients. Nutrients. 2023; 15:1103.

56. Eslick GD, Talley NJ. Dysphagia: Epidemiology, risk factors and impact on quality of life--A population-based study. Aliment Pharmacol Ther. 2008; 27:971-979.

57. Djernes JK. Prevalence and predictors of depression in populations of elderly: A review. Acta Psychiatr Scand. 2006; 113:372-387.

58. Barton S, Karner C, Salih F, Baldwin DS, Edwards SJ. Clinical effectiveness of interventions for treatment-resistant anxiety in older people: A systematic review. Health Technol Assess. 2014; 18:1-59, v-vi.

59. Altman KW, Yu GP, Schaefer SD. Consequence of dysphagia in the hospitalized patient: Impact on prognosis and hospital resources. Arch Otolaryngol Head Neck Surg. 2010; 136:784-789.

60. Bonilha HS, Simpson AN, Ellis C, Mauldin P, Martin-Harris B, Simpson K. The one-year attributable cost of post-stroke dysphagia. Dysphagia. 2014; 29:545-552.

61. Stuck AE, Siu AL, Wieland GD, Adams J, Rubenstein LZ. Comprehensive geriatric assessment: A meta-analysis of controlled trials. Lancet. 1993; 342:1032-1036.

62. Cruz-Jentoft AJ, Bahat G, Bauer J, *et al.* Sarcopenia:

63. Cao L, Morley JE. Sarcopenia is recognized as an independent condition by an International Classification of Disease, Tenth Revision, Clinical Modification (ICD-10-CM) Code. J Am Med Dir Assoc. 2016; 17:675-677.

64. Sheikhany AR, Shohdi SS, Aziz AA, Abdelkader OA, Abdel Hady AF. Screening of dysphagia in geriatrics. BMC Geriatr. 2022; 22:981.

65. Dwivedi RC, St Rose S, Roe JW, Khan AS, Pepper C, Nutting CM, Clarke PM, Kerawala CJ, Rhys-Evans PH, Harrington KJ, Kazi R. Validation of the Sydney Swallow Questionnaire (SSQ) in a cohort of head and neck cancer patients. Oral Oncol. 2010; 46:e10-e14.

66. Boaden E, Burnell J, Hives L, Dey P, Clegg A, Lyons MW, Lightbody CE, Hurley MA, Roddam H, McInnes E, Alexandrov A, Watkins CL. Screening for aspiration risk associated with dysphagia in acute stroke. Cochrane Database Syst Rev. 2021; 10:CD012679.

67. Zhang H, Ye C, Zhang S, Yang D, Gong X, Li S, Xue W, Su J, Zhao L, Qiu Y, He X, Zhang Y, Tang M. Association between health literacy and dysphagia in the community-dwelling older population: A cross-sectional study. Aging Clin Exp Res. 2023; 35:2165-2172.

68. Martino R, Silver F, Teasell R, Bayley M, Nicholson G, Streiner DL, Diamant NE. The Toronto Bedside Swallowing Screening Test (TOR-BSST): Development and validation of a dysphagia screening tool for patients with stroke. Stroke. 2009; 40:555-561.

69. Kertscher B, Speyer R, Palmieri M, Plant C. Bedside screening to detect oropharyngeal dysphagia in patients with neurological disorders: An updated systematic review. Dysphagia. 2014; 29:204-212.

70. Clave P, Arreola V, Romea M, Medina L, Palomera E, Serra-Prat M. Accuracy of the volume-viscosity swallow test for clinical screening of oropharyngeal dysphagia and aspiration. Clin Nutr. 2008; 27:806-815.

71. Rofes L, Arreola V, Clave P. The volume-viscosity swallow test for clinical screening of dysphagia and aspiration. Nestle Nutr Inst Workshop Ser. 2012; 72:33-42.

72. Hughes TA, Wiles CM. Neurogenic dysphagia: The role of the neurologist. J Neurol Neurosurg Psychiatry. 1998; 64:569-572.

73. Lee JY, Kim DK, Seo KM, Kang SH. Usefulness of the simplified cough test in evaluating cough reflex sensitivity as a screening test for silent aspiration. Ann Rehabil Med. 2014; 38:476-484.

74. Ogawa N, Mori T, Fujishima I, Wakabayashi H, Itoda M, Kunieda K, Shigematsu T, Nishioka S, Tohara H, Yamada M, Ogawa S. Ultrasonography to measure swallowing muscle mass and quality in older patients with sarcopenic dysphagia. J Am Med Dir Assoc. 2018; 19:516-522.

75. Baijens L, Barikroo A, Pilz W. Intrarater and interrater reliability for measurements in videofluoroscopy of swallowing. Eur J Radiol. 2013; 82:1683-1695.

76. Langmore SE, Terpenning MS, Schork A, Chen Y, Murray JT, Lopatin D, Loesche WJ. Predictors of aspiration pneumonia: How important is dysphagia? Dysphagia. 1998; 13:69-81.

77. Nativ-Zeltzer N, Kahrilas PJ, Logemann JA. Manofluorography in the evaluation of oropharyngeal dysphagia. Dysphagia. 2012; 27:151-161.

78. Cook IJ. Oropharyngeal dysphagia. Gastroenterol Clin North Am. 2009; 38:411-431.

79. Hiss SG, Postma GN. Fiberoptic endoscopic evaluation of swallowing. Laryngoscope. 2003; 113:1386-1393.

80. McGowan SL, Gleeson M, Smith M, Hirsch N, Shuldham CM. A pilot study of fibreoptic endoscopic evaluation of swallowing in patients with cuffed tracheostomies in neurological intensive care. Neurocrit Care. 2007; 6:90-93.

81. Leder SB, Joe JK, Hill SE, Traube M. Effect of tracheotomy tube occlusion on upper esophageal sphincter and pharyngeal pressures in aspirating and nonaspirating patients. Dysphagia. 2001; 16:79-82.

82. Thottam PJ, Silva RC, McLevy JD, Simons JP, Mehta DK. Use of fiberoptic endoscopic evaluation of swallowing (FEES) in the management of psychogenic dysphagia in children. Int J Pediatr Otorhinolaryngol. 2015; 79:108-110.

83. Badenduck LA, Matthews TW, McDonough A, Dort JC, Wiens K, Kettner R, Crawford S, Kaplan BJ. Fiber-optic endoscopic evaluation of swallowing to assess swallowing outcomes as a function of head position in a normal population. J Otolaryngol Head Neck Surg. 2014; 43:9.

84. Lang IM, Medda BK, Kern M, Shaker R. A biomechanical response of the esophagus participates in swallowing. Am J Physiol Gastrointest Liver Physiol. 2023; 324:G131-G141.

85. Malvuccio C, Kamavuako EN. The effect of EMG features on the classification of swallowing events and the estimation of fluid intake volume. Sensors (Basel). 2022; 22:3380.

86. Cohen DL, Roffe C, Beavan J, *et al.* Post-stroke dysphagia: A review and design considerations for future trials. Int J Stroke. 2016; 11:399-411.

87. Chen KC, Jeng Y, Wu WT, Wang TG, Han DS, Ozcakar L, Chang KV. Sarcopenic dysphagia: A narrative review from diagnosis to intervention. Nutrients. 2021; 13:4043.

88. Zeng M, Wang Z, Chen X, Shi M, Zhu M, Ma J, Yao Y, Cui Y, Wu H, Shen J, Xie L, Fu J, Gu X. The effect of swallowing action observation therapy on resting fMRI in stroke patients with dysphagia. Neural Plast. 2023; 2023:2382980.

89. Olthoff A, Carstens PO, Zhang S, von Fintel E, Friede T, Lotz J, Frahm J, Schmidt J. Evaluation of dysphagia by novel real-time MRI. Neurology. 2016; 87:2132-2138.

90. McCulloch TM, Hoffman MR, Ciucci MR. High-resolution manometry of pharyngeal swallow pressure events associated with head turn and chin tuck. Ann Otol Rhinol Laryngol. 2010; 119:369-376.

91. Schindler A, Vincon E, Grosso E, Miletto AM, Di Rosa R, Schindler O. Rehabilitative management of oropharyngeal dysphagia in acute care settings: Data from a large Italian teaching hospital. Dysphagia. 2008; 23:230-236.

92. Rofes L, Arreola V, Mukherjee R, Swanson J, Clave P. The effects of a xanthan gum-based thickener on the swallowing function of patients with dysphagia. Aliment Pharmacol Ther. 2014; 39:1169-1179.

93. Sura L, Madhavan A, Carnaby G, Crary MA. Dysphagia in the elderly: Management and nutritional considerations. Clin Interv Aging. 2012; 7:287-298.

94. Terre R, Mearin F. Effectiveness of chin-down posture to prevent tracheal aspiration in dysphagia secondary to acquired brain injury. A videofluoroscopy study. Neurogastroenterol Motil. 2012; 24:414-419, e206.

95. Steele CM, Alsanei WA, Ayanikalath S, *et al.* The influence of food texture and liquid consistency modification on swallowing physiology and function: A systematic review. Dysphagia. 2015; 30:2-26.

96. Low J, Wyles C, Wilkinson T, Sainsbury R. The effect of compliance on clinical outcomes for patients with dysphagia on videofluoroscopy. Dysphagia. 2001; 16:123-127.

97. Shaker R, Easterling C, Kern M, Nitschke T, Massey B, Daniels S, Grande B, Kazandjian M, Dikeman K. Rehabilitation of swallowing by exercise in tube-fed patients with pharyngeal dysphagia secondary to abnormal UES opening. Gastroenterology. 2002; 122:1314-1321.

98. Dziewas R, Warnecke T, Schnabel M, Ritter M, Nabavi DG, Schilling M, Ringelstein EB, Reker T. Neuroleptic-induced dysphagia: Case report and literature review. Dysphagia. 2007; 22:63-67.

99. Rofes L, Arreola V, Martin A, Clave P. Natural capsaicinoids improve swallow response in older patients with oropharyngeal dysphagia. Gut. 2013; 62:1280-1287.

100. Kelly EA, Koszewski IJ, Jaradeh SS, Merati AL, Blumin JH, Bock JM. Botulinum toxin injection for the treatment of upper esophageal sphincter dysfunction. Ann Otol Rhinol Laryngol. 2013; 122:100-108.

101. Moerman MB. Cricopharyngeal Botox injection: Indications and technique. Curr Opin Otolaryngol Head Neck Surg. 2006; 14:431-436.

102. Kocdor P, Siegel ER, Tulunay-Ugur OE. Cricopharyngeal dysfunction: A systematic review comparing outcomes of dilatation, botulinum toxin injection, and myotomy. Laryngoscope. 2016; 126:135-141.

103. Kos MP, David EF, Aalders IJ, Smit CF, Mahieu HF. Long-term results of laryngeal suspension and upper esophageal sphincter myotomy as treatment for life-threatening aspiration. Ann Otol Rhinol Laryngol. 2008; 117:574-580.

104. Brasnu DF. Supracricoid partial laryngectomy with cricohyoidopexy in the management of laryngeal carcinoma. World J Surg. 2003; 27:817-823.

105. Tomita T, Tanaka K, Shinden S, Ogawa K. Tracheoesophageal diversion versus total laryngectomy for intractable aspiration. J Laryngol Otol. 2004; 118:15-18.

106. Kawamoto A, Katori Y, Honkura Y, Kakuta R, Higashi K, Ogura M, Miyazaki M, Arakawa K, Kashima K, Asada Y, Matsuura K. Central-part laryngectomy is a useful and less invasive surgical procedure for resolution of intractable aspiration. Eur Arch Otorhinolaryngol. 2014; 271:1149-1155.

107. Murer K, Soyka MB, Broglie MA, Huber GF, Stoeckli SJ. Zenker's diverticulum: Outcome of endoscopic surgery is dependent on the intraoperative exposure. Eur Arch Otorhinolaryngol. 2015; 272:167-173.

108. Verdonck J, Morton RP. Systematic review on treatment of Zenker's diverticulum. Eur Arch Otorhinolaryngol. 2015; 272:3095-3107.

109. Papaspyrou G, Schick B, Papaspyrou S, Wiegand S, Al Kadah B. Laser surgery for Zenker's diverticulum: European combined study. Eur Arch Otorhinolaryngol. 2016; 273:183-188.

110. Volkert D, Berner YN, Berry E, *et al.* ESPEN Guidelines on Enteral Nutrition: Geriatrics. Clin Nutr. 2006; 25:330-360.

111. Lin TH, Yang CW, Chang WK. Evaluation of oropharyngeal dysphagia in older patients for risk stratification of pneumonia. Front Immunol. 2021; 12:800029.

112. Starmer HM, Dewan K, Kamal AN, Khan A, Maclean J, Randall DR. Building an integrated multidisciplinary

swallowing disorder clinic: Considerations, challenges, and opportunities. Ann NY Acad Sci. 2020; 1481:11-19.

113. Brodsky MB, Pandian V, Needham DM. Post-extubation dysphagia: A problem needing multidisciplinary efforts. Intensive Care Med. 2020; 46:93-96.

114. Umay E, Eyigor S, Giray E, *et al.* Pediatric dysphagia overview: Best practice recommendation study by multidisciplinary experts. World J Pediatr. 2022; 18:715-724.

115. Duval M, Black MA, Gesser R, Krug M, Ayotte D. Multidisciplinary evaluation and management of dysphagia: The role for otolaryngologists. J Otolaryngol Head Neck Surg. 2009; 38:227-232.

116. Moliadze V, Antal A, Paulus W. Electrode-distance dependent after-effects of transcranial direct and random noise stimulation with extracephalic reference electrodes. Clin Neurophysiol. 2010; 121:2165-2171.

117. Jayasekeran V, Rothwell J, Hamdy S. Non-invasive magnetic stimulation of the human cerebellum facilitates cortico-bulbar projections in the swallowing motor system. Neurogastroenterol Motil. 2011; 23:831-e341.

118. Cabib C, Nascimento W, Rofes L, Arreola V, Tomsen N, Mundet L, Palomeras E, Michou E, Clave P, Ortega O. Short-term neurophysiological effects of sensory pathway neurorehabilitation strategies on chronic poststroke oropharyngeal dysphagia. Neurogastroenterol Motil. 2020; 32:e13887.

119. Zhang C, Zheng X, Lu R, Yun W, Yun H, Zhou X. Repetitive transcranial magnetic stimulation in combination with neuromuscular electrical stimulation for treatment of post-stroke dysphagia. J Int Med Res. 2019; 47:662-672.

120. Khedr EM, Abo-Elfetoh N, Rothwell JC. Treatment of post-stroke dysphagia with repetitive transcranial magnetic stimulation. Acta Neurol Scand. 2009; 119:155-161.

121. Zhong L, Rao J, Wang J, Li F, Peng Y, Liu H, Zhang Y, Wang P. Repetitive transcranial magnetic stimulation at different sites for dysphagia after stroke: A randomized, observer-blind clinical trial. Front Neurol. 2021; 12:625683.

122. Kumar S, Wagner CW, Frayne C, Zhu L, Selim M, Feng W, Schlaug G. Noninvasive brain stimulation may improve stroke-related dysphagia: A pilot study. Stroke. 2011; 42:1035-1040.

123. Li CM, Wang TG, Lee HY, Wang HP, Hsieh SH, Chou M, Jason Chen JJ. Swallowing training combined with game-based biofeedback in poststroke dysphagia. PM R. 2016; 8:773-779.

124. Archer SK, Smith CH, Newham DJ. Surface electromyographic biofeedback and the effortful swallow exercise for stroke-related dysphagia and in healthy ageing. Dysphagia. 2021; 36:281-292.

125. Park JS, Hwang NK, Kim HH, Lee G, Jung YJ. Effect of neuromuscular electrical stimulation combined with effortful swallowing using electromyographic biofeedback on oropharyngeal swallowing function in stroke patients with dysphagia: A pilot study. Medicine (Baltimore). 2019; 98:e17702.

126. Benfield JK, Everton LF, Bath PM, England TJ. Does therapy with biofeedback improve swallowing in adults with dysphagia? A systematic review and meta-analysis. Arch Phys Med Rehabil. 2019; 100:551-561.

127. Dianna Burchell SHMK, Kathy S. Skill-based swallowing therapy using a computer-based training program improves swallowing-related quality of life and swallowing function for adults with dysphagia: A pilot study. J Clin Practice Speech-Lang Pathol. 2022; 24:130-137.

128. Perry SE, Sevitz JS, Curtis JA, Kuo SH, Troche MS. Skill training resulted in improved swallowing in a person with multiple system atrophy: An endoscopy study. Mov Disord Clin Pract. 2018; 5:451-452.

129. Athukorala RP, Jones RD, Sella O, Huckabee ML. Skill training for swallowing rehabilitation in patients with Parkinson's disease. Arch Phys Med Rehabil. 2014; 95:1374-1382.

130. Perie S, Trollet C, Mouly V, Vanneaux V, Mamchaoui K, Bouazza B, Marolleau JP, Laforet P, Chapon F, Eymard B, Butler-Browne G, Larghero J, St Guily JL. Autologous myoblast transplantation for oculopharyngeal muscular dystrophy: A phase I/IIa clinical study. Mol Ther. 2014; 22:219-225.

131. Gronhoj C, Jensen DH, Vester-Glowinski P, *et al.* Safety and efficacy of mesenchymal stem cells for radiation-induced xerostomia: A randomized, placebo-controlled phase 1/2 trial (MESRIX). Int J Radiat Oncol Biol Phys. 2018; 101:581-592.

Address correspondence to:
Ying Xia, Department of Neurosurgery, Haikou Affiliated Hospital of Central South University Xiangya School of Medicine, Haikou 570208, China.
E-mail: xiaying008@163.com

Peipei Song, National Center for Global Health and Medicine, Tokyo 162-8655, Japan.
E-mail: psong@it.ncgm.go.jp

Review

Considering traditional Chinese medicine as adjunct therapy in the management of chronic constipation by regulating intestinal flora

Ke Wang[1,2], Hua Qiu[3], Fang Chen[2], Pingping Cai[2], Fanghua Qi[2,*]

[1] The First Clinical Medical College, Shandong University of Traditional Chinese Medicine, Ji'nan, China;
[2] Traditional Chinese Medicine, Shandong Provincial Hospital affiliated with Shandong First Medical University, Ji'nan, China;
[3] Gynecology, Jinan Municipal Hospital of Traditional Chinese Medicine, Ji'nan, China.

SUMMARY   Chronic constipation is one of the most common gastrointestinal disorders worldwide. Due to changes in diet, lifestyle, and the aging population, the incidence of chronic constipation has increased year by year. It has had an impact on daily life and poses a considerable economic burden. Nowadays, many patients with chronic constipation try to seek help from complementary and alternative therapies, and traditional Chinese medicine (TCM) is often their choice. The intestinal flora play an important role in the pathogenesis of constipation by affecting the body's metabolism, secretion, and immunity. Regulating the intestinal flora and optimizing its composition might become an important prevention and treatment for chronic constipation. TCM has unique advantages in regulating the imbalance of intestinal flora, and its curative effect is precise. Therefore, we reviewed the relationship between intestinal flora and chronic constipation as well as advances in research on TCM as adjunct therapy in the management of chronic constipation by regulating intestinal flora. Some single Chinese herbs and their active ingredients (*e.g.*, *Rheum palmatum*, *Radix Astragalus*, and *Cistanche deserticola*), some traditional herbal formulations (*e.g.*, Jichuan decoction, Zengye decoction, and Zhizhu decoction) and some Chinese patent medicines (*e.g.*, Maren pills and Shouhui Tongbian capsules) that are commonly used to treat chronic constipation by regulating intestinal flora are highlighted and summarized. Moreover, some external forms of TCM, and especially acupuncture, have also been found to improve intestinal movement and alleviate constipation symptoms by regulating intestinal flora. We hope this review can contribute to an understanding of TCM as an adjunct therapy for chronic constipation and that it can provide useful information for the development of more effective constipation therapies.

Keywords   chronic constipation, traditional Chinese medicine, adjunct therapy, intestinal flora

1. Introduction

Chronic constipation is one of the most common gastrointestinal disorders worldwide. According to the Rome IV standard, chronic constipation is divided into four sub-types: functional constipation, irritable bowel syndrome with constipation, opioid-induced constipation, and functional defecation disorder, which includes insufficient propulsion of stools and coordination disorders during defecation (*1*). In recent years, due to changes in diet, lifestyle, and the aging population, the incidence of chronic constipation has increased year by year with a global prevalence of around 10-15% of the population (*2*). Although chronic constipation is not a life-threatening condition, it detrimentally impacts quality of life. It leads to mental and psychological disorders

and even increases the mortality rate of cardiovascular and cerebrovascular diseases (*3,4*). In addition, chronic constipation poses a substantial health care burden. Direct costs attributed to constipation-related health care in the US are estimated to be more than US$230 million per year (*5*). Therefore, investigate the pathogenesis of and effective therapies for chronic constipation is crucial.

Currently, the main therapies for chronic constipation involve lifestyle changes such as a high fiber diet and exercise, prescription laxatives, and surgery if indicated (*6*). Unfortunately, more than 50% of patients fail to respond to these standard treatments mainly due to dissatisfaction with efficacy, safety, adverse reactions, and cost (*7*). That is to say, the treatment of chronic constipation remains challenging. Therefore, a safe and cost-effective treatment for chronic constipation is

urgently needed. Nowadays, many patients with chronic constipation try to seek help from complementary and alternative therapies, and traditional Chinese medicine (TCM) is often their choice (*8*).

Increasing evidence suggests that the intestinal flora are involved in the development and progression of constipation (*9*). The intestinal flora maintain intestinal homeostasis through various complex mechanisms. Regulating the intestinal flora and optimizing its composition may become an important prevention and treatment for chronic constipation. TCM can prevent and treat chronic diseases through multiple targets, channels, and mechanisms, and it has a certain regulatory effect on the intestinal flora. Therefore, this paper has analyzed the relationship between intestinal flora and chronic constipation as well as the advances in research on TCM in regulating the intestinal flora of chronically constipated patients. It also summarizes the efficacy and mechanism of TCM in preventing and treating chronic constipation by regulating intestinal flora in order to provide new ideas for the prevention and treatment of chronic constipation using TCM.

2. The relationship between chronic constipation and intestinal flora

Constipation is a common intestinal problem, and its development is closely related to a disorder of intestinal micro-flora. There are a large number of diverse microbial groups in the human intestine that are mutually inhibited and interdependent, maintaining the steady state of the intestinal environment. This steady state is mainly a dynamic balance that affects the life and health of the host by regulating the composition of flora, metabolites, neurotransmitters, and participating in immune response. When the homeostasis of the intestinal environment is disrupted, the human body is more susceptible to neurological diseases, cardiovascular diseases, and metabolic diseases, and particularly functional gastrointestinal diseases. The link between chronic constipation and an intestinal microbial imbalance has been corroborated by numerous studies (*10*).

2.1. Constipation and an imbalance of the intestinal flora

Constipation will not only lead to a disorder of intestinal microbes but also affect the metabolism of flora, further aggravating constipation symptoms (*11*). The feces of patients with constipation accumulate in the intestine for a prolonged period, leading to an increase in pathogenic bacteria and a decrease in beneficial bacteria. This, in turn, increases harmful metabolites, damages the intestinal barrier, disrupts the stable balance of the intestinal environment, and creates a vicious cycle. Clinical studies have indicated that constipated patients have a significantly altered abundance and diversity of intestinal flora compared to healthy individuals.

In addition, certain metabolites, and particularly chenodeoxycholic acid and biliverdin, have been found to be significantly enriched (*12*). This indicates that the intestinal microbial community of chronically constipated patients is clearly abnormal.

Animal experiments further revealed the key role of intestinal flora in the pathogenesis of constipation (*13*). The researchers analyzed the colon movement pattern and fecal pellet transport in perfusion experiments and found that compared to healthy control mice, the ratio of intestinal motility and contraction, outflow/contraction volume, contraction speed, and the speed of fecal pellet propulsion in pseudo-sterile mice decreased. To further verify the key role of gut microbiota in the development of constipation, Ge *et al*. extracted gut microbiota from constipated patients and transplanted it into germ-free mice and then measuring their intestinal motility. Results indicated that these mice had significantly worse bowel movements, with fewer and smaller fecal pellets, lower fecal water content, delayed gastrointestinal transit time, and weaker spontaneous contractions of the colon smooth muscle (*14*).

Taken together, these studies fully demonstrate the impact of intestinal micro-flora on intestinal motility and its crucial role in constipation. Therefore, maintaining a stable state of intestinal micro-flora is highly significant in preventing and treating chronic constipation.

2.2. Correcting the imbalanced intestinal flora can alleviate chronic constipation

Disordered intestinal micro-flora is closely related to chronic constipation, so restoring the balance of intestinal micro-flora has become an effective method for treating chronic constipation. In this context, fecal microbiota transplantation (FMT), as a treatment to restore the balance of intestinal flora, shows great potential in relieving chronic constipation symptoms (*15*). First of all, FMT treatment has a significant effect on relieving chronic constipation. According to a clinical study, the cure rate of 34 patients who did not respond to conventional laxative drugs was as high as 73.5% after three rounds of FMT. FMT is more effective than traditional laxatives. During the treatment, the composition of intestinal flora improved, the levels of NO and 5-hydroxytryptamine (5-HT) in the serum increased, and intestinal peristalsis was enhanced (*16*). Secondly, FMT treatment can significantly increase the α diversity of intestinal flora. In a retrospective clinical trial, researchers compared the changes in fecal microbial composition in patients with functional constipation before and after FMT treatment. Results indicated that the abundance of *Clostridiales*, *Fusicatenibacter*, and *Paraprevotella* increased, while the abundance of some flora, including *Lactobacillus*, decreased. These changes in flora abundance may be related to the relief of patients' clinical symptoms (*17*).

In addition, probiotics, as a beneficial ingredient, also have a positive effect on alleviating chronic constipation symptoms. Systematic reviews and meta-analyses have indicated that probiotics can increase the frequency of bowel movements and improve overall chronic constipation symptom scores (*18*). For instance, the findings of a double-blind, randomized, placebo-controlled trial revealed that an intervention in the form of *Lactobacillus* HN019 + *Lactobacillus rhamnosus* HN001 in patients with functional constipation for 4 weeks effectively increased the frequency of bowel movements and relieved symptoms of hard stool by optimizing the intestinal micro-flora (*19*). In addition, an intervention in the form of a bacterial mixture in loperamide-induced constipated rats improved the intestinal transport capacity and fecal water content in constipated rats, and at the same time it up-regulated the biosynthesis of 5-HT (*20*). *Bifidobacterium lactis* TY-S01 acts to prevent constipation. It can accelerate intestinal peristalsis in constipated mice, maintain the water content of feces, and prevent the intestinal barrier from being destroyed. At the same time, TY-S01 can also maintain normal levels of 5-HT, motilin (MTL) and substance P (SP) in constipated mice, preventing an intestinal microbial imbalance in constipated mice and increasing the level of short-chain fatty acids (SCFAs) in feces of constipated mice (*21*).

To sum up, these studies further suggest that an imbalance in intestinal flora is closely related to chronic constipation. Therefore, regulating the production of intestinal micro-flora and intestinal metabolites can effectively treat chronic constipation.

2.3. Potential mechanisms by which the intestinal flora modulate constipation

The "intestinal-brain axis" is a neuroendocrine network that dynamically communicates between intestinal flora and brain (*22*). It mainly consists of the central nervous system (CNS), enteric nervous system (ENS), autonomic nervous system (ANS), intestinal flora, and its metabolites (*23*). The intestinal flora play a vital role in the gut-brain axis, which maintains homeostasis among the gastrointestinal tract, CNS, and microbial systems (*24*). The intestinal flora regulate intestinal function through its fermentation metabolites, including SCFAs, secondary bile salts (BAs), and methane, which play a key role. These substances can activate the corresponding receptors in enteroendocrine cells (ECs), enterochromaffin cells (ECCs), and neuron cells to synthesize biological compounds, thereby regulating intestinal movement (*25*). In addition, the intestinal flora can also synthesize and release a variety of neurotransmitters, such as tryptophan, 5-HT, SP, vasoactive intestinal polypeptide (VIP), acetylcholine (Ach), and gastrin (GAS). These neurotransmitters can regulate the contraction and relaxation of intestinal smooth muscle, thereby affecting intestinal peristalsis and defecation (*26*). In general, the intestinal flora play a key regulatory role in the gastrointestinal tract (Figure 1).

2.4. Intestinal flora, metabolites, and chronic constipation

SCFAs are beneficial metabolites produced by the decomposition of indigestible carbohydrates by intestinal flora. They play an important role in maintaining intestinal health and have functions such as stimulating intestinal peristalsis and retaining water in the intestine. The types of SCFAs include acetic acid, propionic acid, and butyric acid, which play various physiological roles in the human body. In a recent study, fecal samples from 30 patients with severe chronic constipation were examined and their levels of SCFAs were found to be significantly lower than those of the control group (*27*). This may be due to the feces remaining in the distal colon for too long, leading to an increase in harmful bacteria such as Desulfovibrio, Enterobacter faecalis, Lactococcus, and Rosea, which can affect the fermentation of intestinal microorganisms and decrease the concentration of SCFAs in feces. To alleviate symptoms in chronically constipated patients, researchers suggested supplementing their diet with fiber. After fiber supplementation, there was an increase in the level of SCFAs rich in butyrate in the intestine, acceleration of gastrointestinal transit, and an increase in the thickness of the mucosal layer. This may be because dietary fiber intake stimulates the secretion of colon hormones and enhances the expression of tight junction proteins, thereby maintaining the integrity of the intestinal barrier (*28,29*). Animal experiments indicated that the ratio of intestinal propulsive contractions to non-propulsive contractions, the speed of intestinal contractions, and the speed of fecal pellet propulsion increased after SCFAs were injected into GF mice. This indicates that SCFAs can effectively restore intestinal contractility (*13*). In addition, the symptoms of constipation were relieved and the level of SCFAs in the intestine increased after a Bifidobacterium intervention was implemented in mice with loperamide-induced constipation. The specific mechanism involves decreasing the pH level in the colon by increasing the level of butyric acid and propionic acid in the intestine. A lower pH level helps enhance the peristalsis of intestinal smooth muscle, thus alleviating constipation symptoms. At the same time, a low intestinal pH can also increase the number of Lactobacillus and Bifidobacterium and decrease the number of Clostridium, further maintaining the balance of the intestinal microecology (*30*). In a word, SCFAs are of great significance in relieving constipation symptoms.

Bile acids (BAs) are not only involved in the digestion and absorption of fat but also serve as important signaling molecules in the intestine. They regulate intestinal movement and colonic fluid secretion by stimulating intestinal chromaffin cells to release 5-HT.
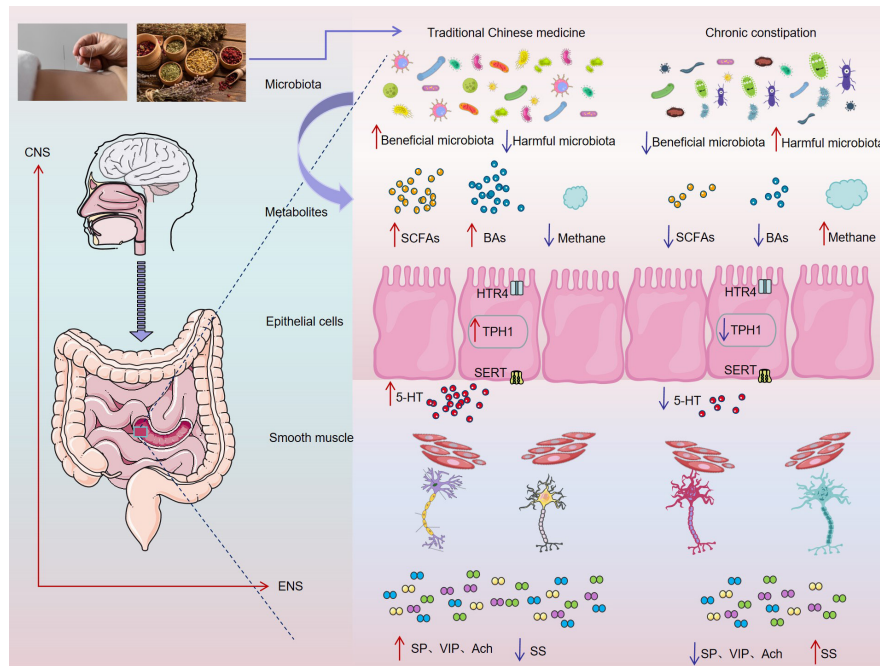
Figure 1. The potential mechanisms by which the intestinal flora modulate constipation when treated with traditional Chinese medicine. *Abbreviations*: CNS: central nervous system; ENS: enteric nervous system; SCFAs: short-chain fatty acids; BAs: secondary bile salts; 5-HT: 5-hydroxytryptamine; HTR4: 5-HT4 receptor; TPH1: Tryptophan hydroxylase 1; SERT: serotonin transporter; SP: substance P; VIP: vasoactive intestinal polypeptide, Ach: acetylcholine; SS: somatostatin.

This mechanism is helpful in maintaining the normal physiological function of the intestine and ensuring the full absorption of nutrients and smooth discharge of waste (*31,32*). In addition, BAs also play a key role in maintaining a balanced intestinal flora. They can promote the growth of beneficial bacteria and inhibit the reproduction of harmful bacteria. When the level of BA is insufficient, an imbalance in intestinal flora may result in slow intestinal peristalsis, leading to issues such as constipation (*33*). After an intervention in the form of Bacillus subtilis in a mouse model of constipation, the constipation symptoms of mice were markedly alleviated. Metabonomic results indicated that the BA content of mice increased significantly, and the 5-HT released by ECs cells through the BA receptor TGR5/TRPA1 pathway also increased significantly (*34*). Elobixibat is a new laxative for constipation that increases BA flow to the colon by inhibiting the ileal BA transporter. This action promotes the secretion of more water in the intestinal tract and stimulates intestinal peristalsis, effectively treating chronic constipation (*35*). Moreover, studies have found that apple juice (AJ) has the potential to relieve constipation. AJ can reduce BA reabsorption in the intestine, promote intestinal peristalsis, and alleviate constipation symptoms by down-regulating the expression of the BA transporter (*36*).

Methane is a gas produced by the fermentation of carbohydrates by intestinal flora in an anaerobic environment. Under normal circumstances, the generation and excretion of methane has no negative impact on human health. When the intestinal flora is unbalanced and too much methane is produced, however, it can affect the intestinal environment and cause a series of digestive system problems (*37*). The number of beneficial Bifidobacterium and Lactobacillus bacteria in stool samples of patients with functional constipation significantly reduced compared to that in healthy individuals. In addition, their methane respiratory emissions are also higher. These beneficial bacteria are crucial to maintaining intestinal health, and their decrease suggests an imbalance in the intestinal flora, which may result in intestinal dysfunction (*38*). Methane is a gas that cannot be used by the human body, so the methane breath test is widely used to detect methane production. In an experiment, researchers found that the number of methane-producing bacteria and methane production in patients with chronic constipation is higher than in healthy individuals (*39*). This further confirms the relationship between an imbalance in intestinal flora, methane, and constipation. In addition, when the researchers studied subjects with constipation-dominant IBS, they found that their respiratory methane level was also high. This may be related to the relative abundance of methanogenic bacteria (mainly *Methanobrevibacter*) in their feces and the absolute abundance of *Methanobrevibacter smithii* in their feces. These findings provide further evidence for the role of methane in intestinal diseases (*40*).

2.5. Intestinal flora, neurotransmitters and chronic constipation

Studies have confirmed that intestinal flora can stimulate

the release of 5-HT from intestinal chromaffin cells (EC) through metabolites of SCFAs and BAs, thus promoting intestinal peristalsis (*32*). 5-HT needs to bind with the 5-HT4 receptor (HTR4) to stimulate secretion and peristalsis reflex and promote intestinal peristalsis (*41*). Selective HTR4 agonists, such as procarbide, can be used to treat constipation (*42*). Tryptophan hydroxylase 1 (TPH1) is the key enzyme for 5-HT synthesis. Increasing its activity significantly improves the synthesis of 5-HT in the intestine and further promotes intestinal peristalsis. Colon transport was found to improve significantly after oral administration of butyrate to GM mice, but this change was not observed in TPH1 KO mice, which may be related to the role of 5-HT in the intestine. This demonstrates that increasing the production of 5-HT-producing bacteria in the intestine can help alleviate constipation (*13*). MTL is a gastrointestinal hormone that can not only secrete gastric acid but also increase intestinal peristalsis. A study found that the serum MTL level in children with constipation was significantly lower than that in the healthy control group, suggesting that the decrease in MTL levels may be related to the pathogenesis of constipation (*43*). The neurotransmitters SP and VIP were found to be decreased in the colon of patients with constipation compared to their levels in healthy individuals (*44*). SP has the ability to inhibit the release of inflammatory factors, reduce inflammatory reactions, strengthen the tight connections between intestinal mucosal epithelial cells, improve the integrity of the intestinal barrier, and ultimately reduce intestinal injury (*45*). VIP can promote intestinal peristalsis and fluid secretion when it acts on the intestinal mucosa and submucosal neurons (*46*). In addition, VIP, as an effective anti-inflammatory mediator, can maintain the homeostasis of intestinal flora by protecting the intestinal epithelial barrier (*47*). Somatostatin (SS), an inhibitory neurotransmitter, can relax gastrointestinal smooth muscle, reduce gastrointestinal peristalsis, and increase gastrointestinal transit time (*48*). The excitatory neurotransmitter ACh is involved in regulating intestinal peristalsis and secretion (*49*). A new type of lactic acid bacteria was found to significantly increase the defecation volume and fecal moisture content in constipated mice. At the same time, it increased the serum levels of MTL, SP, Ach, and VIP in mice while decreasing the level of SS (*50*).

To summarize, the intestinal flora, metabolites, and neurotransmitters are closely related to constipation. By regulating SCFAs, BAs, methane, 5-HT, and other substances, they help to maintain the balance of intestinal flora and alleviate constipation symptoms. Therefore, attention must be paid to the intestinal flora and its metabolites in the process of preventing and treating chronic constipation.

3. TCM for chronic constipation based on intestinal flora

According to the theory of TCM, constipation is located in the large intestine. Its pathogenesis mainly lies in the disorder of the *zang-fu* organs, dysfunction of the spleen and stomach, an imbalance of the liver and kidney, and a deficiency of *Qi* in the lungs and a deficiency of *Qi* and blood. These factors can affect the conducting function of the large intestine and lead to constipation. Therefore, regulating the function of the *zang-fu* organs is key to treating constipation. TCM treatment involves formulating an individualized treatment plan based on the type of syndrome. This approach can effectively regulate the functions of the *zang-fu* organs and alleviate symptoms, providing unique advantages. Chinese medicine treatments mainly include internal and external treatments. Internal treatments include Chinese medicine decoctions, Chinese patent medicine preparations, and single Chinese medicine remedies. External treatments include acupuncture, use of acupoints, acupoint catgut embedding, and massage. TCM causes minimal adverse reactions and has a marked curative effect, making it an important supplementary and alternative therapy for constipation. Numerous scientific studies have confirmed that TCM can treat constipation by improving the composition of intestinal flora, regulating the level of microbial metabolites, protecting the function of the intestinal mucosal barrier, and balancing the intestinal microecosystem.

3.1. Single Chinese herbs and their active ingredients

Several single Chinese herbs and their active compounds have been found to have a potentially beneficial effect at treating chronic constipation by regulating intestinal flora. Therefore, a brief overview of the pharmacology of the most commonly used ingredients and their effects on constipation is presented below (Table 1).

Rheum palmatum (Da-Huang in Chinese) is a drug commonly used to treat constipation. It can significantly reduce the time food takes to pass through the digestive system, increase the amount of water in feces, and improve the hormonal balance of the digestive tract. It also helps protect the mucous layer of the colon by regulating the intestinal flora and its byproducts (*51*). In addition, rhubarb contains sennoside A, a natural anthraquinone compound. Studies have found that a conventional dose of sennoside A for less than a week can effectively alleviate constipation symptoms in mouse models. This is mainly achieved by increasing the abundance of beneficial intestinal bacteria such as Lactobacillus and Romboutsia while reducing the abundance of harmful bacteria like *Akkermansia* and UCG_005. It also regulates the expression of the colonic aquaporins AQP1 and AQP3. However, a point worth noting is that sennoside A should not be used for extended periods of time as its laxative action can weaken and potentially damage the colon (*52*).

Radix Astragalus (Huang-Qi in Chinese) is a well-

Table 1. Most commonly used herbs to treat chronic constipation by regulating intestinal flora and their active ingredients

Herbs or active ingredients	Source	Subjects	Type of model	Changes in intestinal flora	Mechanisms	Ref.
Rheum palmatum	Rheum palmatum	Rats	Loperamide	Ligilactobacillus↑; Prevotellaceae↑; Limosilactobacillus↑; UCG-001↑	Regulating the intestinal flora and its metabolites.	51
Sennoside A	Rheum palmatum	Mice	Loperamide	Lactobacillus↑; Romboutsia↑; Akkermansia↓; UCG_005↓	Regulating the abundance of intestinal flora and aquaporin.	52
Astragaloside IV	Radix Astragalus	Rats	Loperamide	Firmicutes↑; Lactobacillales↑; Lactobacillus↑; Lactobacillus reuteri↑	Regulating the composition of the intestinal flora and producing butyric acid.	55
Astragalus polysaccharide	Radix Astragalus	Rats	D-galactose and mixture	Blautia↑; Lactobacillus↓	Altering gut microbiota and improving the gut environment to alleviate constipation.	56
Platycodon grandiflorum polysaccharides	Platycodon grandiflorum	Rats	Loperamide	Bacteroidetes↑; Firmicutes↓; Roseburia↑; Butyricimonas↑; Ruminiclostridium↑; Clostridia_UCG-014↓; Lactobacillus↓; Enterococcus↓	Adjusting the composition of flora and the number of bacteria producing butyrate increases, leading to increased levels of neurotransmitters and promoting intestinal peristalsis.	58
Chrysanthemum morifolium polysaccharide	Chrysanthemum morifolium	Rats	Loperamide	Lactobacillus↑; Romboutsia↑; Lachnospiraceae_NK4A136_group↓; Roseburia↓	Increasing species abundance and flora diversity, improving the composition of flora, regulating neurotransmitter levels, promoting intestinal peristalsis, and relieving constipation.	60
Cistanche deserticola polysaccharides	Cistanche deserticola	Rats	D-galactose and mixture	Ruminococcus↑	Regulating the composition of the microbiota and the metabolites of the microbiota.	64
Cinnamic acid	Radix Scrophulariae	Mice	Loperamide	Rikenella↑; Monoglobus↑; Lachnospiraceae_NK4A136_group↑; Akkermansia↑; Desulfovibrionaceae↑; Lachnoclostridium↑; Monoglobus↑; Acinetobacter↑; Anaerofustis↑;	Improving the composition and abundance of intestinal microflora and regulating the production of SCFAs.	66
Volatile oil	Citrus aurantium; Rhizoma Atractylodis	Rats	Diphenoxylate	Proteobacteria↑; Allobaculum↑; Ruminococcaceae↑; Romboutsia↓	Improving the composition and metabolites of the microbiota, regulating neurotransmitters, and promoting intestinal motility.	68

Note: Abbreviations: SCFAs: short-chain fatty acids.

known herbal medicine with purported tonic properties that has been widely used to treat a variety of diseases in China and Southeast Asia for thousands of years (*53*). The long-term administration of *Radix Astragalus* has been found to significantly modulate the intestinal flora of hens by increasing the abundance of *Romboutsia* and *Lactobacillus* (*54*). Astragaloside IV, one of the active ingredients of *Radix Astragalus*, has been found to effectively promote intestinal transit in mice with loperamide-induced slow transit constipation by inhibiting the loss of ICCs, mediating the regulation of the gut microbiota composition, and enhancing butyric acid generation (*55*). Astragalus polysaccharide is also one of active ingredients of *Radix Astragalus*. It has been reported to be effective against constipation by altering gut microbiota and improving the gut environment (56). Microbiome analysis revealed that Astragalus polysaccharide increased the relative abundance of *Blautia* while decreasing the relative abundance of *Lactobacillus* in elderly rats with constipation. In addition, Astragalus polysaccharide reduced the levels of acetate, butyrate, and propionate in fecal samples, correspondingly regulating glycolysis/gluconeogenesis metabolism and pyruvate metabolism.

Platycodon grandiflorum (Jie-Geng in Chinese), a traditional Chinese medicinal herb acting on the lung meridian, has been widely used to treat pulmonary and respiratory disorders (*57*). According to the theory of TCM, the lungs and large intestine are connected. Therefore, after regulating the function of the lungs, the conductive function of the large intestine can be restored, which is helpful in relieving constipation. Notably, *Platycodon grandiflorum* polysaccharides are the main active ingredients isolated from *Platycodon grandiflorum*. An animal study indicated that it promoted intestinal peristalsis by increasing the levels of expression of 5-HT-related proteins and mediated the composition of the intestinal flora, thereby alleviating constipation (*58*). 16S rRNA gene sequencing indicated that *Platycodon grandiflorum* polysaccharides significantly enriched the relative abundance of butyrate-producing bacteria, including *Roseburia*, *Butyricimonas*, and *Ruminiclostridium*, while suppressed several pernicious bacteria, such as *Clostridia* UCG-014, *Enterococcus*, and *Lactobacillus*.

Chrysanthemum morifolium (Ju-Hua in Chinese) is a well-known edible medicinal plant that is widely consumed as herbal tea in Asia and some other regions (*59*). It has been reported to have various physiological effects, such as anti-inflammatory and free radical scavenging activity. The bioactive components of *Chrysanthemum morifolium* are mainly flavonoids, polysaccharides, volatile oils, terpenoids and organic acids. Recently, Wang *et al*. suggested that *Chrysanthemum morifolium* polysaccharide has potential regulatory effects on functional constipation (*60*). By increasing the abundance of beneficial bacteria and

decreasing the abundance of pathogenic bacteria, it may improve the composition of intestinal microorganisms and thus promote intestinal motility.

Cistanche deserticola (Rou-Cong-Rong in Chinese), known as "desert Ginseng," is a traditional and precious Chinese herbal medicine (*61*). According to the theory of TCM, *Cistanche deserticola* can supplement the kidney, boost the essence of blood, and moisten the intestines to free stool. It is commonly used to treat conditions such as impotence, seminal emission, infertility, general weakness with lassitude of the loins and knees, and chronic constipation (*62*). The bioactive components of *Cistanche deserticola* mainly include phenyl ethanol glycosides, polysaccharides, flavonoids, and so on. Polysaccharides are a principal component that has significant effects on constipation (*63*). Liu *et al*. found that *Cistanche deserticola* polysaccharides significantly regulated the abnormalities of behavioral indices, microbial richness and diversity, and metabolite profiles that were induced by constipation in aged rats (*64*). From an intestinal microbiological point of view, *Cistanche deserticola* polysaccharides significantly increased the prevalence of beneficial bacteria while reducing the potentially pathogenic bacterial population.

Scrophulariae Radix (Xuan-Shen in Chinese) is one of the most popular traditional Chinese herbs that serves to cool the blood, nourish yin, purge fire, and remove toxins according to the Pharmacopoeia of the People's Republic of China (2020 Edition). It is usually used to treat rheumatism, pharyngalgia, arthritis, constipation and conjunctival congestion (*65*). Cinnamic acid is an organic acid isolated from *Scrophulariae Radix* that can effectively regulate the biological activity of intestinal flora. Jiang *et al*. found that cinnamic acid effectively treated slow transit constipation by ameliorating the composition and abundance of the intestinal microbiome to regulate the production of SCFAs (*66*). It significantly improved the diversity and abundance of the beneficial microbiome. Moreover, the production of SCFAs, including acetic acid, butyric acid, propionic acid and valeric acid, was significantly promoted by cinnamic acid.

Citrus aurantium (Zhi-Shi in Chinese) and *Rhizoma Atractylodis Macrocephalae* (Bai-Zhu in Chinese) are a classical drug pair that have been widely used to treat gastrointestinal motility disorders for thousands of years, and they display a definite advantage in the treatment of chronic constipation (*67*). According to the Pharmacopoeia of the People's Republic of China (2020 Edition), *Citrus aurantium*, commonly known as bitter orange, can treat stool obstruction and it has the ability to break up *Qi* and eliminate stagnation and dissolve and disperse phlegm, while *Rhizoma Atractylodis Macrocephalae* replenishes *Qi* and it tonifies the spleen, removes water from the intestinal track, and promotes water circulation. Volatile oil is an active ingredient of *Citrus aurantium* and *Rhizoma*

Atractylodis Macrocephalae that has been reported to alleviate constipation in rats by altering the host metabolome and intestinal microbiota composition (*68*). It promotes intestinal peristalsis, increases fecal water content, regulates the levels of gastrointestinal hormones (GAS and SP), reduces the inflammatory response (IL-6 and TNF-α), and regulates brain-intestinal peptides (5-HT and VIP). In addition, volatile oil improves the composition of the intestinal microbiota by reducing harmful bacteria and promoting beneficial bacteria.

3.2. Traditional herbal formulations

Traditional herbal formulations (or Kampo in Japanese) are compound formulations that mostly have been used for thousands of years (*69*). Several traditional herbal formulations have been found to have a potentially beneficial effect at treating chronic constipation by regulating intestinal flora. Therefore, a brief overview of the pharmacology of the most commonly used traditional herbal formulations and their effects on constipation is presented below (Table 2).

A Jichuan decoction is a classical and famous traditional herbal formula that has been extensively used for chronic constipation and other gastroenteric disorders for hundreds of years. It consists of six herbs including *Angelica sinensis* (Dang-Gui in Chinese), *Achyranthes bidentata* (Niu-Xi in Chinese), *Alisma orientalis* (Ze-Xie in Chinese), *Cistanche deserticola* (Rou-Cong-Rong in Chinese), *Cimicifuga foetida* (Sheng-Ma in Chinese), and *Citrus aurantium* (Zhi-Shi in Chinese). Lin *et al.* found that the Jichuan decoction exhibited excellent activity against loperamide-induced chronic constipation in rats (70). It alleviated chronic constipation by inhibiting the cAMP/PKA/AQPs signaling pathway and maintaining inflammatory/intestinal flora homeostasis. In addition, the Jichuan decoction also maintained intestinal health by reducing the apoptosis rate of enteric glial cells (*71*).

A Zengye decoction, a well-known traditional herbal formulation, consists of three herbs including *Radix Scrophulariae* (Xuan-Shen in Chinese), *Radix Rehmanniae* (Sheng-Di in Chinese) and *Radix Ophiopogonis* (Mai-Dong in Chinese). It has been widely used in many Asian countries for thousands of years to treat constipation and diseases related to a *yin* deficiency. Liu *et al.* found that the Zengye decoction regulated the intestinal microbiota of constipated rats to normal levels and it changed the endogenous metabolites of the host through the intestinal microbiota, resulting in therapeutic action (*72*). It reduced the level of harmful bacteria, such as *Desulfovibrio*, *Ruminococcus*, *Prevotella* and *Dorea*, and increased the abundance of *Oxalobacter*, *Clostridium*, and *Roseburia*.

A Simo decoction is a famous traditional herbal formula that has been used to treat gastrointestinal diseases for hundreds of years. It consists of four herbs,

Table 2. Most commonly used traditional herbal formulations to treat chronic constipation by regulating intestinal flora

Herbal formulations	Composition	Subjects	Type of model	Changes in intestinal flora	Mechanisms	Ref.
Jichuan decoction	Six herbs: Angelica sinensis, Achyranthes bidentata, Alisma orientalis, Cistanche deserticola, Cimicifuga foetida, and Citrus aurantium	Rats	Loperamide	Bacteroidetes↑; Lactobacillus↑; Erysipelas↑; Lachnospira↓; Verrucobacterium↓; Helicobacter↓	Promoting intestinal movement by inhibiting the cAMP/PKA/AQPs signaling pathway, reducing inflammation, and maintaining intestinal flora homeostasis.	70
Zengye decoction	Three herbs: Radix Scrophulariae, Radix Rehmanniae and Radix Ophiopogonis	Rats	Restricted water, loperamide, and D-galactose	Oxalobacter↑; Clostridium↑; Roseburia↑; Desulfovibrio↓; Ruminococcus↓; Prevotella↓; Dorea↓	Regulating intestinal microbiota to normal levels and changing the endogenous metabolites of the host.	72
Simo decoction	Four herbs: Fructus aurantii, Aucklandiae Radix, Semen arecae, and Linderae Radix	Mice	Sennae Folium and controlling the diet and water intake	Bacteroides↑; Alistipes↑; Faecalibacterium↑; Subdoligranulum↑; Lactiplantibacillus↑; Phascolarctobacterium↑	Increasing the abundance of beneficial bacteria via the brain-bacteria-gut axis, promoting a healthy intestinal environment, and reducing oxidative stress.	73
Xiao Chengqi formula	Three herbs: Rheum palmatum, Citrus aurantium, and Magnolia officinalis	Rats	Loperamide	Roseburia spp.↑	Promoting the colonization of beneficial bacteria and increasing the butyl aminobenzene level after metabolism.	74
Zhizhu decoction	Two herbs: Citrus aurantium and Rhizoma Atractylodis Macrocephalae	Mice	Diphenoxylate	Bifidobacteriaceae↓; Pseudomonadaceae↓; Rikenella↓; Shigella↑; Bifidobacterium↓; Pseudomonas↓; Clostridium↑	Regulating the intestinal microflora, activating the AHR signaling pathway, and promoting neuronal excitability.	76

Note: Abbreviations: AHR: aryl hydrocarbon receptor.

Fructus aurantii (Zhi-Ke in Chinese), *Aucklandiae Radix* (Mu-Xiang in Chinese), *Semen arecae* (Bin-Lang in Chinese), and *Linderae Radix* (Wu-Yao in Chinese). Mounting evidence proves that the Simo decoction can treat constipation by regulating intestinal microbiota and related oxidative stress indicators. It can increase the abundance of beneficial bacteria through the brain-bacteria-gut axis in association with intestinal mucosal microbiota, promote a healthy intestinal environment, and reduce oxidative stress (*73*).

Xiao-Cheng-Qi-Tang, an ancient traditional herbal formula, has been used as a heat-clearing, intestine movement, and cathartic herb for thousands of years. It consists of three herbs, *Rheum palmatum* (Da-Huang in Chinese), *Citrus aurantium* (Zhi-Shi in Chinese), and *Magnolia officinalis* (Hou-Pu in Chinese). Zhou *et al.* found that Xiao-Cheng-Qi-Tang improved the defecation of patients with slow transit constipation by protecting ICC activity, promoting the colonization of *Roseburia* spp. to promote peristalsis, and increasing the butyl aminobenzene level after metabolism (*74*). In addition, Liu *et al.* suggested that the anti-inflammatory activity of Xiao-Cheng-Qi-Tang was at least partially mediated by intestinal bacterial metabolism (*75*).

A Zhizhu decoction, consisting of *Citrus aurantium* (Zhi-Shi in Chinese) and *Rhizoma Atractylodis Macrocephalae* (Bai-Zhu in Chinese), is widely used in the treatment of functional gastrointestinal diseases caused by a spleen deficiency and *Qi* stagnation syndrome. The Zhizhu decoction has been reported to have beneficial laxative action on constipation in mouse models, which may be attributed to its ability to alter the composition of intestinal flora and activate the aryl hydrocarbon receptor (AHR) signaling pathway (*76*). In addition, the Zhizhu decoction increases the expression of Ach, SP, and 5-HT in the colon while decreasing the expression of VIP.

3.3. Chinese patent medicines

Chinese patent medicines are a form of Chinese herbal medicine that are isolated from single herbs or traditional herbal formulations and that are prepared using modern advanced pharmaceutical technology. There are various dosage forms including injections, tablets, pills, capsules, and liquids. Compared to traditional decoctions, Chinese patent medicines are safer, more effective, and easier to use (*69*). Thus, Chinese patent medicines are becoming increasingly popular in China and are attracting attention worldwide. A brief overview of the pharmacology of the most commonly used Chinese patent medicines that have been approved by the State Food and Drug Administration (FDA) of China and their effects on constipation is briefly presented below (Table 3).

Maren pills are a well-known Chinese patent medicine consisting of six medicinal herbs including *Rheum palmatum* (Da-Huang in Chinese), *Magnolia*

Table 3. Most commonly used Chinese patent medicines to treat chronic constipation by regulating intestinal flora

Chinese patent medicines	Composition	Subjects	Type of model	Changes in intestinal flora	Mechanisms	Ref.
Maziren pills	Six herbs: Rheum palmatum, Magnolia officinalis, Fructus aurantii, Amygdalus communis, Cannabis sativa, and Paeonia lactiflora	Mice	Senna leaf and food restriction	Bacteroides↑; Firmicutes↓	Alleviating symptoms and colon inflammation in constipated mice, reducing the level of VIP in the colon, increasing the level of SP, regulating the composition of flora.	77
		Rats	Loperamide	Lactobacillus↑; Prevotella↓	Activating 5-HT pathway, regulating SCFAs metabolism and regulating the composition of intestinal flora.	78
Shouhui Tongbian capsules	Eight herbs: Fallopia multiflora, Cassiae Semen, Lycii Fructus, Panax ginseng, Aloe vera, Colla corii asini, Citrus aurantium and Rhizoma Atractylodis Macrocephalae	Mice	Loperamide	Lactobacillus↑; Firmicutes/Bacteroides↑	Remodeling the composition of gut microbes and regulating production of intestinal metabolites.	79
		Mice	Loperamide	Verrucomicrobiota↑; Firmicutes/Bacteroides↑	Correcting gut microbiota dysbiosis and activating bacterial metabolite-mediated intraintestinal 5-HT synthesis.	80

Note: Abbreviations: VIP: vasoactive intestinal polypeptide; SP: substance P; 5-HT: 5-hydroxytryptamine; SCFAs: short-chain fatty acids.

officinalis (Hou-Pu in Chinese), *Fructus aurantii* (Zhi-Ke in Chinese), *Amygdalus communis* (Xing-Ren in Chinese), *Cannabis sativa* (Huo-Ma-Ren in Chinese), and *Paeonia lactiflora* (Bai-Shao in Chinese). Widely used in clinical practice, Maren pills have been proven to increase the frequency of defecation and alleviate clinical symptoms of patients with constipation. Yu *et al.* found that Maren pills effectively alleviated symptoms and colon inflammation in mice with slow transit constipation, they reduced the level of VIP in the colon, they increased the level of SP, they regulated the composition of flora, and they relieved constipation (*77*). In addition, Maren pills increased the levels of acetic acid, propionic acid, and butyric acid, activated the 5-HT pathway, and promoted intestinal movement by regulating the composition of intestinal flora (*78*).

Shouhui Tongbian capsules are a Chinese patent medicine widely used to treat constipation. The prescription of Shouhui Tongbian Capsule consists of 8 Chinese herbs, *Fallopia multiflora* (He-Shou-Wu in Chinese), *Cassiae Semen* (Jue-Ming-Zi in Chinese), *Lycii Fructus* (Gou-Qi-Zi in Chinese), *Panax ginseng* (Ren-Shen in Chinese), *Aloe vera* (Lu-Hui in Chinese), *Colla corii asini* (E-Jiao in Chinese), *Citrus aurantium* (Zhi-Shi in Chinese), and *Rhizoma Atractylodis Macrocephalae* (Bai-Zhu in Chinese). Lin *et al.* found that Shouhui Tongbian capsules ameliorated the development of loperamide-induced constipation in rats by remodeling the composition of gut microbial and regulating production of intestinal metabolites (*79*). Notably, they increased the relative abundance of *Lactobacillus* and the ratio of *Firmicutes* to *Bacteroides* (F/B). In addition, Shouhui Tongbian capsules alleviated constipation by regulating the intestinal flora imbalance, altering microbial metabolites, stimulating the release of intestinal 5-HT, and protecting intestinal neuron differentiation (*80*).

3.4. External treatment with TCM

External forms of TCM, a unique traditional treatment with a long history in China, refer to treatments including acupuncture, moxibustion, massage, and use of acupoints. These external treatments were reported to be effective and also able to avoid adverse consequences such as abdominal pain, an electrolyte disturbance, melanosis coli, and severe drug dependence after long-term use of laxatives (*81*). Therefore, a brief outline of the most commonly used TCM external treatments and their effects on constipation is presented below (Table 4).

Acupuncture has been markedly effective in treating functional constipation. A study revealed the mechanism of action of acupuncture at three acupoints (Tianshu (ST25), Shangjuxu (ST37), and Fujie (SP14)) in alleviating the clinical symptoms of patients. It helped to reconfigure the intestinal flora and increase the level of butyric acid, an SCFA that is crucial for maintaining

Table 4. Most commonly used TCM external treatments for chronic constipation by regulating intestinal flora

External treatment	Acupuncture point	Subjects	Changes in intestinal flora	Mechanisms	Ref.
Acupuncture	Tianshu (ST25); Shangjuxu (ST37); Fujie (SP14)	Functionally constipated patients(*n* = 80)	Bifidobacterium↑; g_Lactobacillus↑; Pseudomonas↓; g_Pseudomonas↓; f_Peptostreptococcaceae↓; g_Eubacterium_corprostanoligenes_group↓	Adjusting the composition of intestinal flora and increasing the level of butyric acid	82
Electro-acupuncture	Tianshu (ST25); Shangjuxu (ST37)	Functionally constipated mice	Staphylococcaceae↑; Muribaculaceae↓; Enterobacteriaceae↓	Re-balancing the gut microbiota and promoting the generation of butyric acid	83
Electro-acupuncture	Bilateral Zusanli	Spinal cord injury rats	Proteobacteria↓; Clostridia↓; Gammaproteobacteria↓; Erysipelotrichia↓	Modulating microbiota and metabolites and regulating the 5-HT system.	84
Acupoint massage	-	Chronic function patients (*n* = 104)	Pseudobutyrivibrio↑; Ruminiclostridium↑; Fusicatenibacter↓	Improving the microbial composition	85

intestinal health. The specific microorganisms affected by acupuncture can be predicted using 16S rRNA technology, providing a new method with which to evaluate the effectiveness of acupuncture (*82*).

Electroacupuncture (EA) can increase the frequency and intensity of acupoint stimulation based on common acupuncture techniques, allowing for more effective treatment on the meridians. In experimental studies, EA has been found to significantly improve intestinal movement in constipated mice and alleviate constipation symptoms. However, EA did not reverse slow colonic transit in pseudosterile (PGF) mice, indicating that intestinal microflora play a crucial role in the treatment of constipation with EA. To further explore this mechanism, researchers used 16S rRNA sequencing technology to quantify intestinal microorganisms and found that EA treatment restored the ratio of Firmicutes to Bacteroides and increased the production of butyric acid in constipated mice by increasing the abundance of Staphylococcus, which helps alleviate constipation (*83*). In addition, EA has also been found to regulate the 5-HT system by regulating microorganisms and metabolites, thereby alleviating constipation symptoms caused by spinal cord injury. 5-HT is a neurotransmitter that plays a significant role in regulating intestinal movement (*84*).

Acupoint sticking therapy for constipation involves laxative action as well as the use of acupoints. A clinical study confirmed that acupoint therapy changed the composition of intestinal microflora related to cytokines in constipated patients and relieved constipation symptoms (*85*).

4. Conclusion

Overall, Chinese medicine has a marked curative effect on chronic constipation. It alleviates constipation symptoms and also regulates intestinal flora and metabolites, reduces inflammatory reactions, and protects the intestinal mucosal barrier. This provides various options for treating constipated patients. When using TCM to treat constipation, however, we must follow the principle of syndrome differentiation and treatment. This study summarizes several TCM medicines and external treatments for chronic constipation by regulating intestinal flora. The hope is that this study will provide valuable information for further research on the mechanism of TCM in treating chronic constipation by regulating intestinal flora.

Conflict of Interest: The authors have no conflicts of interest to disclose.

References

1. Barbara G, Barbaro MR, Marasco G, Cremon C. Chronic constipation: From pathophysiology to management. Minerva Gastroenterol (Torino). 2023; 69:277-290.
2. Aziz I, Whitehead WE, Palsson OS, Törnblom H, Simrén M. An approach to the diagnosis and management of Rome IV functional disorders of chronic constipation. Expert Rev Gastroenterol Hepatol. 2020; 14:39-46.
3. Belsey J, Greenfield S, Candy D, Geraint M. Systematic review: Impact of constipation on quality of life in adults and children. Aliment Pharmacol Ther. 2010; 31:938-949.
4. Sumida K, Molnar MZ, Potukuchi PK, Thomas F, Lu JL, Yamagata K, Kalantar-Zadeh K, Kovesdy CP. Constipation and risk of death and cardiovascular events. Atherosclerosis. 2019; 281:114-120.
5. Harris LA, Chang CH. Burden of constipation: Looking beyond bowel movements. Am J Gastroenterol. 2022; 117:S2-S5.
6. Chang L, Chey WD, Imdad A, Almario CV, Bharucha AE, Diem S, Greer KB, Hanson B, Harris LA, Ko C, Murad MH, Patel A, Shah ED, Lembo AJ, Sultan S. American Gastroenterological Association-American College of Gastroenterology Clinical Practice Guideline: Pharmacological Management of Chronic Idiopathic Constipation. Am J Gastroenterol. 2023; 118:936-954.
7. Shah ED, Staller K, Nee J, Ahuja NK, Chan WW, Lembo A, Brenner DM, Siegel CA, Chey WD. Evaluating the impact of cost on the treatment algorithm for chronic idiopathic constipation: Cost-effectiveness analysis. Am J Gastroenterol. 2021; 116:2118-2127.
8. Wang X, Yin J. Complementary and alternative therapies for chronic constipation. Evid Based Complement Alternat Med. 2015; 2015:396396.
9. Iancu MA, Profir M, Roşu OA, Ionescu RF, Cretoiu SM, Gaspar BS. Revisiting the intestinal microbiome and its role in diarrhea and constipation. Microorganisms. 2023; 11:2177.
10. Chen Y, Zhou J, Wang L. Role and mechanism of gut microbiota in human disease. Front Cell Infect Microbiol. 2021; 11:625913.
11. Zhao Y, Yu YB. Intestinal microbiota and chronic constipation. Springerplus. 2016; 5:1130.
12. Li YQ, Yan XY, Xiao XJ, Ma PT, Wang SQ, Liu HL, Zhang W, Chen M, Yao JP, Li Y. The gut microbiome and metabolites are altered and interrelated in patients with functional constipation. Front Microbiol. 2023; 14:1320567.
13. Vincent AD, Wang XY, Parsons SP, Khan WI, Huizinga JD. Abnormal absorptive colonic motor activity in germ-free mice is rectified by butyrate, an effect possibly mediated by mucosal serotonin. Am J Physiol Gastrointest Liver Physiol. 2018; 315:G896-G907.
14. Ge X, Zhao W, Ding C, Tian H, Xu L, Wang H, Ni L, Jiang J, Gong J, Zhu W, Zhu M, Li N. Potential role of fecal microbiota from patients with slow transit constipation in the regulation of gastrointestinal motility. Sci Rep. 2017; 7:441.
15. Liu QH, Ke X, Xiao C. Current applications of fecal microbiota transplantation in functional constipation. Evid Based Complement Alternat Med. 2022; 2022:7931730.
16. Tian Y, Zuo L, Guo Q, Li J, Hu Z, Zhao K, Li C, Li X, Zhou J, Zhou Y, Li XA. Potential role of fecal microbiota in patients with constipation. Therap Adv Gastroenterol.

2020; 13:1756284820968423.

17. Zhang X, Li N, Chen Q, Qin H. Fecal microbiota transplantation modulates the gut flora favoring patients with functional constipation. Front Microbiol. 2021; 12:700718.

18. van der Schoot A, Helander C, Whelan K, Dimidi E. Probiotics and synbiotics in chronic constipation in adults: A systematic review and meta-analysis of randomized controlled trials. Clin Nutr. 2022; 41:2759-2777.

19. Lai H, Li Y, He Y, *et al*. Effects of dietary fibers or probiotics on functional constipation symptoms and roles of gut microbiota: A double-blinded randomized placebo trial. Gut Microbes. 2023; 15:2197837.

20. Deng Y, Li M, Mei L, Cong LM, Liu Y, Zhang BB, He CY, Zheng PY, Yuan JL. Manipulation of intestinal dysbiosis by a bacterial mixture ameliorates loperamide-induced constipation in rats. Benef Microbes. 2018; 9(3):453-464.

21. Tang T, Wang J, Jiang Y, Zhu X, Zhang Z, Wang Y, Shu X, Deng Y, Zhang F. Bifidobacterium lactis TY-S01 prevents loperamide-induced constipation by modulating gut microbiota and its metabolites in Mice. Front Nutr. 2022; 9:890314.

22. Cryan JF, O'Riordan KJ, Cowan CSM, *et al*. The microbiota-gut-brain axis. Physiol Rev. 2019; 99:1877-2013.

23. Zhao Q, Chen YY, Xu DQ, Yue SJ, Fu RJ, Yang J, Xing LM, Tang YP. Action mode of gut motility, fluid and electrolyte transport in chronic constipation. Front Pharmacol. 2021; 12:630249.

24. Martin CR, Osadchiy V, Kalani A, Mayer EA. The brain-gut-microbiome axis. Cell Mol Gastroenterol Hepatol. 2018; 6:133-148.

25. Wang JK, Yao SK. Roles of gut microbiota and metabolites in pathogenesis of functional constipation. Evid Based Complement Alternat Med. 2021; 2021:5560310.

26. Heiss CN, Olofsson LE. Gut microbiota-dependent modulation of energy metabolism. J Innate Immun. 2018; 10:163-171.

27. Shi Y, Chen Q, Huang Y, Ni L, Liu J, Jiang J, Li N. Function and clinical implications of short-chain fatty acids in patients with mixed refractory constipation. Colorectal Dis. 2016; 18:803-810.

28. Zhuang M, Shang W, Ma Q, Strappe P, Zhou Z. Abundance of probiotics and butyrate-production microbiome manages constipation *via* short-chain fatty acids production and hormones secretion. Mol Nutr Food Res. 2019; 63:e1801187.

29. Müller M, Hermes GDA, Canfora EE, Smidt H, Masclee AAM, Zoetendal EG, Blaak EE. Distal colonic transit is linked to gut microbiota diversity and microbial fermentation in humans with slow colonic transit. Am J Physiol Gastrointest Liver Physiol. 2020; 318:G361-G369.

30. Wang L, Hu L, Xu Q, Yin B, Fang D, Wang G, Zhao J, Zhang H, Chen W. Bifidobacterium adolescentis exerts strain-specific effects on constipation induced by loperamide in BALB/c mice. Int J Mol Sci. 2017; 18:318.

31. Bajor A, Gillberg PG, Abrahamsson H. Bile acids: Short and long term effects in the intestine. Scand J Gastroenterol. 2010; 45:645-664.

32. Kidd M, Modlin IM, Gustafsson BI, Drozdov I, Hauso O, Pfragner R. Luminal regulation of normal and neoplastic human EC cell serotonin release is mediated by bile salts, amines, tastants, and olfactants. Am J Physiol Gastrointest Liver Physiol. 2008; 295:G260-G272.

33. Quigley EM, Spiller RC. Constipation and the microbiome: Lumen versus mucosa! Gastroenterology. 2016; 150:300-303.

34. Chen Z, Feng J, Hu S, Hua Y, Ma S, Fu W, Yang Q, Zhang X. Bacillus subtilis promotes the release of 5-HT to regulate intestinal peristalsis in STC mice *via* bile acid and its receptor TGR5 pathway. Dig Dis Sci. 2022; 67:4410-4421.

35. Nakajima A, Seki M, Taniguchi S. Determining an optimal clinical dose of elobixibat, a novel inhibitor of the ileal bile acid transporter, in Japanese patients with chronic constipation: A phase II, multicenter, double-blind, placebo-controlled randomized clinical trial. J Gastroenterol. 2018; 53:525-534.

36. Zhu Q, Iwai R, Okaguchi T, Shirasaka Y, Tamai I. Apple juice relieves loperamide-induced constipation in rats by downregulating the intestinal apical sodium-dependent bile acid transporter ASBT. Food Funct. 2023; 14:4836-4846.

37. Sahakian AB, Jee SR, Pimentel M. Methane and the gastrointestinal tract. Dig Dis Sci. 2010; 55:2135-2143.

38. Dimidi E, Christodoulides S, Scott SM, Whelan K. Mechanisms of action of probiotics and the gastrointestinal microbiota on gut motility and constipation. Adv Nutr. 2017; 8:484-494.

39. Vega AB, Perelló A, Martos L, García Bayo I, García M, Andreu V, Abad A, Barenys M. Breath methane in functional constipation: Response to treatment with Ispaghula husk. Neurogastroenterol Motil. 2015; 27:945-953.

40. Villanueva-Millan MJ, Leite G, Wang J, *et al*. Methanogens and hydrogen sulfide producing bacteria guide distinct gut microbe profiles and irritable bowel syndrome subtypes. Am J Gastroenterol. 2022; 117:2055-2066.

41. Hoffman JM, Tyler K, MacEachern SJ, Balemba OB, Johnson AC, Brooks EM, Zhao H, Swain GM, Moses PL, Galligan JJ, Sharkey KA, Greenwood-Van Meerveld B, Mawe GM. Activation of colonic mucosal 5-HT(4) receptors accelerates propulsive motility and inhibits visceral hypersensitivity. Gastroenterology. 2012; 142:844-854.e4.

42. Daniali M, Nikfar S, Abdollahi M. An overview of the efficacy and safety of prucalopride for the treatment of chronic idiopathic constipation. Expert Opin Pharmacother. 2019; 20:2073-2080.

43. Ulusoy E, Arslan N, Küme T, Ülgenalp A, Çirali C, Bozkaya Ö, Ercal D. Serum motilin levels and motilin gene polymorphisms in children with functional constipation. Minerva Pediatr (Torino). 2021; 73:420-425.

44. King SK, Sutcliffe JR, Ong SY, Lee M, Koh TL, Wong SQ, Farmer PJ, Peck CJ, Stanton MP, Keck J, Cook DJ, Chow CW, Hutson JM, Southwell BR. Substance P and vasoactive intestinal peptide are reduced in right transverse colon in pediatric slow-transit constipation. Neurogastroenterol Motil. 2010; 22:883-892, e234.

45. Hwang DY, Kim S, Hong HS. Substance-P ameliorates dextran sodium sulfate-induced intestinal damage by preserving tissue barrier function. Tissue Eng Regen Med. 2017; 15:63-73.

46. Fung C, Unterweger P, Parry LJ, Bornstein JC, Foong JP. VPAC1 receptors regulate intestinal secretion and muscle contractility by activating cholinergic neurons in guinea pig jejunum. Am J Physiol Gastrointest Liver Physiol. 2014; 306:G748-G758.

47. Bains M, Laney C, Wolfe AE, Orr M, Waschek JA, Ericsson AC, Dorsam GP. Vasoactive intestinal peptide deficiency is associated with altered gut microbiota communities in male and female C57BL/6 mice. Front Microbiol. 2019; 10:2689.

48. Corleto VD. Somatostatin and the gastrointestinal tract. Curr Opin Endocrinol Diabetes Obes. 2010; 17:63-68.

49. Sam C, Bordoni B. Physiology, Acetylcholine. 2023 Apr 10. In: StatPearls [Internet]. Treasure Island (FL): StatPearls Publishing; 2024 Jan. PMID: 32491757.

50. Tan Q, Hu J, Zhou Y, Wan Y, Zhang C, Liu X, Long X, Tan F, Zhao X. Inhibitory effect of Lactococus lactis subsp. lactis HFY14 on diphenoxylate-induced constipation in mice by regulating the VIP-cAMP-PKA-AQP3 signaling pathway. Drug Des Devel Ther. 2021; 15:1971-1980.

51. Yang L, Wan Y, Li W, Liu C, Li HF, Dong Z, Zhu K, Jiang S, Shang E, Qian D, Duan J. Targeting intestinal flora and its metabolism to explore the laxative effects of rhubarb. Appl Microbiol Biotechnol. 2022; 106:1615-1631.

52. Zhang MM, Gong ZC, Zhao Q, Xu DQ, Fu RJ, Tang YP, Chen YY. Time-dependent laxative effect of sennoside A, the core functional component of rhubarb, is attributed to gut microbiota and aquaporins. J Ethnopharmacol. 2023; 311:116431.

53. Zhang X, Qiu H, Li C, Cai P, Qi F. The positive role of traditional Chinese medicine as an adjunctive therapy for cancer. Biosci Trends. 2021; 15:283-298.

54. Qiao H, Zhang L, Shi H, Song Y, Bian C. Astragalus affects fecal microbial composition of young hens as determined by 16S rRNA sequencing. AMB Express. 2018; 8:70.

55. He Q, Han C, Huang L, Yang H, Hu J, Chen H, Dou R, Ren D, Lin H. Astragaloside IV alleviates mouse slow transit constipation by modulating gut microbiota profile and promoting butyric acid generation. J Cell Mol Med. 2020; 24:9349-9361.

56. Liu X, Li M, Jian C, Wei F, Liu H, Li K, Qin X. Astragalus polysaccharide alleviates constipation in the elderly *via* modification of gut microbiota and fecal metabolism. Rejuvenation Res. 2022; 25:275-290.

57. Zhang L, Wang Y, Yang D, Zhang C, Zhang N, Li M, Liu Y. Platycodon grandiflorus - An ethnopharmacological, phytochemical and pharmacological review. J Ethnopharmacol. 2015; 164:147-161.

58. Hao M, Song J, Zhai X, Cheng N, Xu C, Gui S, Chen J. Improvement of loperamide-hydrochloride-induced intestinal motility disturbance by Platycodon grandiflorum polysaccharides through effects on gut microbes and colonic serotonin. Front Cell Infect Microbiol. 2023; 13:1105272.

59. Cheng W, Li J, You T, Hu C. Anti-inflammatory and immunomodulatory activities of the extracts from the inflorescence of Chrysanthemum indicum Linné. J Ethnopharmacol. 2005; 101:334-337.

60. Wang J, Liang Q, Zhao Q, Tang Q, Ahmed AF, Zhang Y, Kang W. The effect of microbial composition and proteomic on improvement of functional constipation by Chrysanthemum morifolium polysaccharide. Food Chem Toxicol. 2021 Jul;153:112305.

61. Cheng N, Wang H, Hao H, Rahman FU, Zhang Y. Research progress on polysaccharide components of Cistanche deserticola as potential pharmaceutical agents. Eur J Med Chem. 2023; 245:114892.

62. Wang T, Zhang X, Xie W. Cistanche deserticola Y. C. Ma, "Desert ginseng": A review. Am J Chin Med. 2012; 40:1123-1141.

63. Jia Y, Guan Q, Guo Y, Du C. Reduction of inflammatory hyperplasia in the intestine in colon cancer-prone mice by water-extract of Cistanche deserticola. Phytother Res. 2012; 26:812-819.

64. Liu X, Jian C, Li M, Wei F, Liu H, Qin X. Microbiome-metabolomics deciphers the effects of Cistanche deserticola polysaccharides on aged constipated rats. Food Funct. 2022; 13:3993-4008.

65. Wang S, Wang Q, Yin X, Chen B, Liu X. Simultaneous determination of iridoid glycosides, phenylpropanoid glycosides, organic acids, nucleosides and amino acids in Scrophulariae Radix processed by different processing methods by HPLC-QTRAP-MS/MS. J Chromatogr Sci. 2022; 60:232-242.

66. Jiang JG, Luo Q, Li SS, Tan TY, Xiong K, Yang T, Xiao TB. Cinnamic acid regulates the intestinal microbiome and short-chain fatty acids to treat slow transit constipation. World J Gastrointest Pharmacol Ther. 2023; 14(2):4-21.

67. Yan S, Hao M, Yang H, Sun M, Wu B, Yue Y, Wang X. Metabolomics study on the therapeutic effect of the Chinese herb pair Fructus Aurantii Immaturus and Rhizoma Atractylodis Macrocephalae in constipated rats based on UPLC-Q/TOF-MS analysis. Ann Palliat Med. 2020; 9:2837-2852.

68. Wang L, Wang F, Zhang X, Chen Q, Xu J, Li H, Li F, Yang M. Transdermal administration of volatile oil from Citrus aurantium-Rhizoma Atractylodis macrocephalae alleviates constipation in rats by altering host metabolome and intestinal microbiota composition. Oxid Med Cell Longev. 2022; 2022:9965334.

69. Qi F, Li A, Inagaki Y, Gao J, Li J, Kokudo N, Li XK, Tang W. Chinese herbal medicines as adjuvant treatment during chemo- or radio-therapy for cancer. Biosci Trends. 2010; 4:297-307.

70. Lin L, Jiang Y, Lin P, Ge L, Wan H, Dai S, Zhang R, Yao J, Zeng X, Peng Y. Classical famous prescription of Jichuan decoction improved loperamide-induced slow transit constipation in rats through the cAMP/PKA/AQPs signaling pathway and maintained inflammatory/intestinal flora homeostasis. Heliyon. 2023; 10:e21870.

71. Wang XM, Lv LX, Qin YS, Zhang YZ, Yang N, Wu S, Xia XW, Yang H, Xu H, Liu Y, Ding WJ. Ji-Chuan decoction ameliorates slow transit constipation *via* regulation of intestinal glial cell apoptosis. World J Gastroenterol. 2022; 28:5007-5022.

72. Liu D, Lin L, Lin Y, Zhong Y, Zhang S, Liu W, Zou B, Liao Q, Xie Z. Zengye decoction induces alterations to metabolically active gut microbiota in aged constipated rats. Biomed Pharmacother. 2019; 109:1361-1371.

73. Yi X, Zhou K, Deng N, Cai Y, Peng X, Tan Z. Simo decoction curing spleen deficiency constipation was associated with brain-bacteria-gut axis by intestinal mucosal microbiota. Front Microbiol. 2023; 14:1090302.

74. Zhou Q, Zhang D, Zhang H, Wan X, Hu B, Zou Q, Su D, Peng H, Huang D, Ren D. Effects of Xiao Chengqi formula on slow transit constipation by assessing gut microbiota and metabolomics analysis *in vitro* and *in vivo*. Front Pharmacol. 2022; 13:864598. Erratum in: Front Pharmacol. 2023; 14:1256600.

75. Liu XY, Li L, Li XQ, Yu BY, Liu JH. Identification of active compound combination contributing to anti-inflammatory activity of Xiao-Cheng-Qi Decoction *via* human intestinal bacterial metabolism. Chin J Nat Med.

2018; 16:513-524.

76. Wen Y, Zhan Y, Tang S, Liu F, Wu R, Kong P, Li Q, Tang X. Zhizhu decoction alleviates slow transit constipation by regulating aryl hydrocarbon receptor through gut microbiota. Pharm Biol. 2023; 61:111-124.

77. Yu Z, Hao L, Li Z, Sun J, Chen H, Huo H, Li X, Shan Z, Li H. Correlation between slow transit constipation and spleen deficiency, and gut microbiota: A pilot study. J Tradit Chin Med. 2022; 42:353-363.

78. Zhan Y, Wen Y, Du LJ, Wang XX, Tang SY, Kong PF, Huang WG, Tang XG. Effects of Maren pills on the intestinal microflora and short-chain fatty acid profile in drug-induced slow transit constipation model rats. Front Pharmacol. 2022; 13:804723.

79. Lin Q, Liu M, Erhunmwunsee F, Li B, Mou Y, Wang S, Zhang G, Tian J. Chinese patent medicine Shouhui Tongbian capsule attenuated loperamide-induced constipation through modulating the gut microbiota in rat. J Ethnopharmacol. 2022; 298:115575.

80. Bai J, Cai Y, Huang Z, Gu Y, Huang N, Sun R, Zhang G, Liu R. Shouhui Tongbian capsule ameliorates constipation *via* gut microbiota-5-HT-intestinal motility axis. Biomed Pharmacother. 2022; 154:113627.

81. Wu Y, Ying Q, He Y, Xie X, Yuan X, Wang M, Fei X, Yang X. Effect of external therapies of traditional Chinese medicine on constipation in patients with CRF: A meta-analysis. PLoS One. 2023; 18:e0291968.

82. Yan XY, Yao JP, Li YQ, Xiao XJ, Yang WQ, Chen SJ, Tang TC, Yang YQ, Qu L, Hou YJ, Chen M, Li Y. Effects of acupuncture on gut microbiota and short-chain fatty acids in patients with functional constipation: A randomized placebo-controlled trial. Front Pharmacol. 2023; 14:1223742.

83. Xu MM, Guo Y, Chen Y, Zhang W, Wang L, Li Y. Electro-acupuncture promotes gut motility and alleviates functional constipation by regulating gut microbiota and increasing butyric acid generation in mice. J Integr Med. 2023; 21:397-406.

84. Cheng J, Li W, Wang Y, Cao Q, Ni Y, Zhang W, Guo J, Chen B, Zang Y, Zhu Y. Electroacupuncture modulates the intestinal microecology to improve intestinal motility in spinal cord injury rats. Microb Biotechnol. 2022; 15:862-873.

85. Chen H, Tan PS, Li CP, Chen BZ, Xu YQ, He YQ, Ke X. Acupoint massage therapy alters the composition of gut microbiome in functional constipation patients. Evid Based Complement Alternat Med. 2021; 2021:1416236.

Address correspondence to:
Fanghua Qi, Traditional Chinese Medicine, Shandong Provincial Hospital affiliated with Shandong First Medical University, No. 324 Jingwuweiqi Road, Ji'nan, Shandong, China 250021.
E-mail: qifanghua2006@126.com

Mini-Review

Renal safety of tenofovir alafenamide-based antiretroviral therapy in people with HIV: A mini-review

Fang Zhao, Hongzhou Lu[*]

National Clinical Research Centre for Infectious Diseases, The Third People's Hospital of Shenzhen and The Second Affiliated Hospital of Southern University of Science and Technology, Shenzhen, Guangdong, China.

SUMMARY　　Antiretroviral therapy (ART) has significantly enhanced the outlook for people with HIV(PWH), yet certain ART medications can adversely affect the renal function of these patients. Of particular concern is the nephrotoxicity associated with tenofovir disoproxil fumarate (TDF). Compared to TDF, tenofovir alafenamide (TAF), another prodrug of tenofovir (TFV), results in lower TFV plasma levels, thereby alleviating the TFV-associated mitochondrial toxicity on proximal renal tubular cells. Currently, numerous clinical trials and real-world studies have demonstrated the favorable renal safety profile of ART regimens incorporating TAF for PWH. This paper seeks to consolidate the available evidence regarding the renal safety of TAF-based regimens in PWH, encompassing both the general PWH and those with renal impairment or predisposing factors, in order to offer recommendations and insights for TAF clinical application.

Keywords　　people with HIV (PWH), tenofovir alafenamide (TAF), renal safety

1. Introduction

Kidney disease is a common complication of HIV infection and its treatment, affecting quality of life and life expectancy of patients (*1,2*). Across different countries and populations, the global prevalence of chronic kidney disease (CKD) among patients with HIV varies significantly, ranging from 1% to 49%. The highest prevalence is observed in Africa (*3-9*) (Figure 1).

Various definitions of kidney disease have been utilized in previous studies on renal disease in PWH. Despite the variations in definition, a significant percentage of PWH exhibit signs of renal impairment (*10*). For instance, a cross-sectional study defined kidney disease as meeting at least one of the following criteria: estimated glomerular filtration rate (eGFR) < 60 mL/min/1.73 m^2, hematuria, proteinuria, or microalbuminuria. According to this definition, 19.0% of HIV-infected individuals in the study were found to have kidney disease (*10*). Kidney disease in PWH is associated with multiple risk factors, in addition to factors related to the patients themselves, such as HIV infection, genetic susceptibility, comorbidities and co-infections. Renal toxicity of some antiretroviral drugs (ARVs) is also an important risk factor (*11*).

Nephrotoxicity is a prevalent adverse effect among some ARVs, particularly observed with TDF and certain protease inhibitors (such as Atazanavir and Lopinavir/ritonavir). TDF is still included in several first-line antiretroviral regimens due to its potent antiviral activity. However, extensive researches have consistently demonstrated that the risk of acute kidney injury (AKI), chronic kidney disease (CKD), nephrogenic diabetes insipidus, and proteinuria associated with TDF use are increased (*12*). Therefore, the nephrotoxicity of TDF has long been a matter of concern. TDF, a prodrug of tenofovir (TFV), exhibits limited plasma stability and an exceptionally short half-life of 0.4 minutes. In plasma, most TDF undergoes conversion to TFV (*13,14*), which is subsequently excreted *via* glomerular passive filtration and tubular active secretion (*11,15*). A prevailing hypothesis suggests that TFV accumulation inhibits mitochondrial DNA polymerase γ, resulting in reduced mitochondrial DNA content and oxidative respiratory chain dysfunction. This cascade ultimately leads to mitochondrial toxicity in proximal tubular cells, potentially explaining TDF-induced nephrotoxicity (*15-17*). Additionally, observations indicate that single nucleotide polymorphisms (SNPs) within the adenosine triphosphate-binding cassette transporters C2 (ABCC2) gene may be associated with tubular dysfunction induced by TDF. Although the precise underlying mechanism remains unclear, this link may be attributed to ABCC2's impact on the transport of various substances within
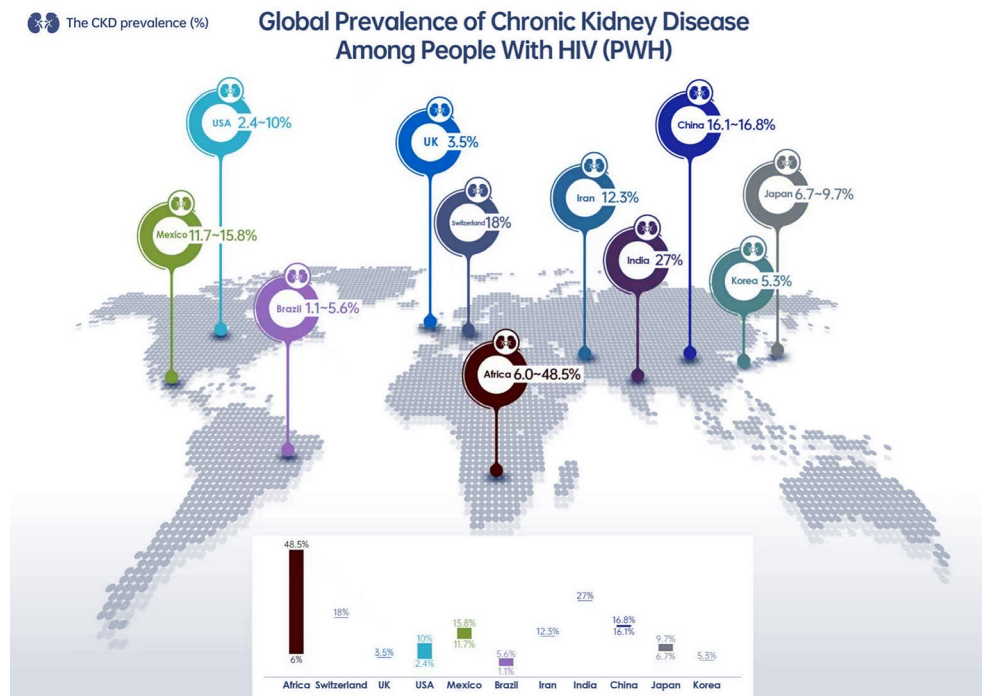
Figure1. Global prevalence of chronic kidney disease among people with HIV (PWH). The incidence of HIV-associated chronic kidney disease (CKD) varies significantly across different time periods, populations, and contexts. The highest prevalence is seen in Africa.
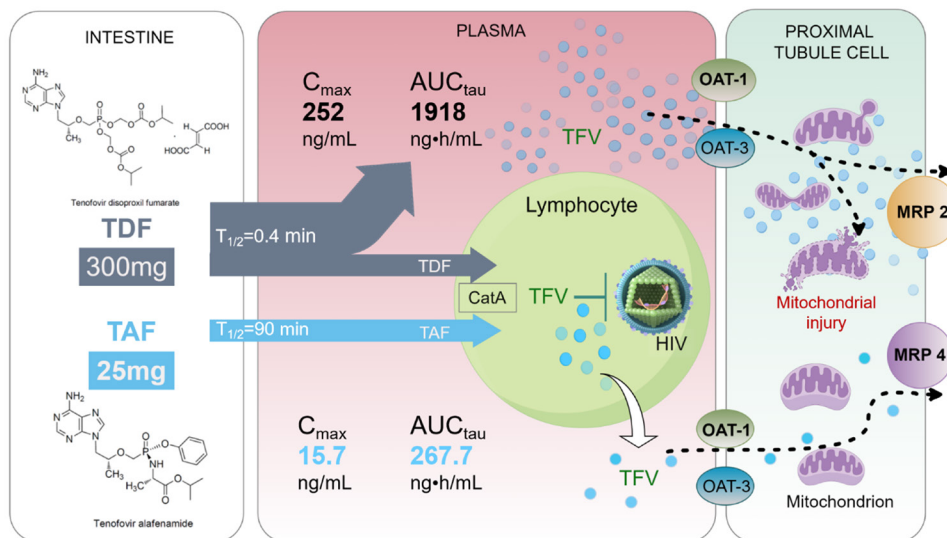
Figure 2. The differences in renal metabolism mechanisms between TAF and TDF. Compared to TDF, TAF exhibits better plasma stability (with a half-life of 90 minutes). After oral administration, TAF efficiently enters target cells and undergoes hydrolysis by the lysosomal carboxypeptidase cathepsin A (CatA) to form TFV. In contrast, TDF is readily hydrolyzed to TFV in the plasma. Large amounts of TFV enter proximal renal tubular cells vie organic anion transporter (OAT)-1 and OAT-3. Intracellular accumulation of tenofovir can cause mitochondrial toxicity and proximal tubular injury. TAF is not a substrate for OAT 1 and 3 and thus does not accumulate in proximal tubular cells, which may be the reason for the better renal safety of TAF (*78*).MRP: multidrug resistance-related protein.

tubular cells (*18,19*). Previous research underscores that tenofovir-related kidney injury is dose-dependent, with elevated TFV plasma concentrations correlating with an increased risk of renal damage (*15,20,21*).

Tenofovir alafenamide (TAF) is a novel prodrug of tenofovir (TFV), a nucleotide reverse transcriptase inhibitor. TAF has greater plasma stability and higher intracellular metabolism to TFV than its predecessor, tenofovir disoproxil fumarate (TDF). Therefore, 25 mg of TAF achieves higher concentrations of the active metabolite, tenofovir-diphosphate (TFV-DP), in target cells than 300 mg of TDF, while reducing the average systemic exposure to TFV in plasma by approximately 90% (*22,23*) (Figure 2). Pharmakinetic data from pivotal

Phase 3 studies show that HIV-infected individuals receiving elvitegravir/cobicistat/emtricitabine/TAF (E/c/F/TAF) have 91% (*24*) lower plasma TFV exposure than those receiving E/c/F/TDF. As a result, TAF improves renal safety and has been confirmed in numerous clinical trials (*25*). This review synthesizes existing evidence on the renal safety of TAF-containing regimens in HIV-infected patients, both in general and in those with concurrent kidney injury or related risk factors, aiming to provide guidance and reference for the clinical use of TAF-based regimens.

2. Renal safety data for the use of TAF-containing regimens in general PWH

Numerous studies have shown that TAF-containing regimens are safer for the kidneys than TDF-containing regimens in in general PWL. Several Phase 3 clinical trials have demonstrated that TAF-containing regimens improved renal function more than TDF-containing regimens in HIV-infected patients with a median baseline eGFR of 99.4 to 117 mL/min (*24,26-29*). No HIV-infected patients receiving TAF-containing regimens developed proximal renal tubulopathy or Fanconi syndrome. Substantial evidence supports the renal safety advantage of TAF-containing regimens over TDF-containing regimens. A meta-analysis of 26 clinical trials involving 9,322 HIV-infected patients with a median (IQR) baseline creatinine clearance (CrCl) of 108.6 (91.1, 129.3) mL/min showed that the TAF-containing regimen group had significantly fewer cases of proximal renal tubulopathy (0 case *vs.* 10 cases, $p < 0.0001$) and treatment discontinuation due to renal adverse events (3 cases *vs.* 14 cases, $p < 0.001$) than the TDF-containing regimen group; the TAF-containing regimen group also had a higher proportion of improvement in renal biomarkers during the 96-week treatment period (*30*). Furthermore, several Phase 3 clinical trials (*31-33*) have shown that TAF-containing regimens have similar renal safety as abacavir (ABC) and lamivudine (3TC)-based regimens in HIV-infected patients with a median baseline CrCl or eGFR > 100 mL/min; HIV-infected patients who switched from these regimens to TAF-containing regimens maintained stable CrCl, retinol binding protein to creatinine ratio (RBP/Cr), urine β2-microglobulin to creatinine ratio (β2-MG/Cr), urine protein to creatinine ratio (UPCR), and urine albumin to creatinine ratio (UACR), without developing proximal renal tubulopathy or Fanconi syndrome.

In addition to these clinical trials, long-term follow-up data and real-world studies confirm the favorable renal safety of TAF. Long-term follow-up results from two large Phase 3 clinical trials found that treatment-naïve HIV-infected patients receiving bictegravir (BIC)/emtricitabine (FTC)/TAF (B/F/TAF) therapy (with a median [IQR] baseline eGFR of 122 [104-143] mL/min) did not discontinue treatment due to renal-related adverse

events or develop proximal renal tubulopathy during 5 years of treatment (*34*). The eGFR in HIV-infected patients declined slightly in the first four weeks and then stabilized, this decline is consistent with the inhibitory effect of BIC on the renal tubular secretion of creatinine *via* organic cation transporter-2 (*34,35*) . Moreover, a retrospective real-world study conducted in HIV-infected patients with normal baseline renal function (eGFR ≥ 90 mL/min/1.73 m²) showed that the median annual eGFR change improved significantly from -2.79 mL/min/1.73 m²/year to -0.28 mL/min/1.73 m²/year ($p < 0.01$) when HIV-infected patients switched from TDF-containing regimens to TAF-containing regimens (*36*).

3. Renal safety data of TAF-containing regimens in PWH with renal impairment (Table 1)

3.1 PWH with mild renal impairment (60 ≤ eGFR < 90 mL/min/1.73 m²)

Clinical trials and real-world studies have shown that switching from TDF-containing regimens to TAF-containing regimens improved renal function in HIV-infected patients with mild renal impairment. A prospective cohort study of 38 HIV-infected patients with a median (IQR) baseline eGFR of 77.0 (67.9, 83.3) mL/min/1.73 m² switched from TDF-containing regimens to TAF-containing regimens. After 12 months, the median (IQR) eGFR increased significantly to 84.3 (74.07, 95.0) mL/min/1.73 m² ($p = 0.001$) (*37*). A pooled analysis of a prospective randomized study and a retrospective cohort study involved 250 HIV-infected patients who had virological suppression on TDF-containing regimens and switched to TAF ($n = 130$) or ABC ($n = 120$) regimens due to significant eGFR decline. Significant eGFR decline was defined as an eGFR decline rate > 3 mL/min/year for > 5 years, an eGFR decline > 25%, or an eGFR > 90 mL/min at baseline and < 70 mL/min at the end of TDF-containing regimen treatment. At baseline, the mean eGFR for the TAF and ABC regimen groups was 73 and 68 mL/min, respectively, and 80% and 72% of patients, respectively, had an eGFR ≥ 60 mL/min. The results showed that at 48 weeks of treatment, both groups had a significant median eGFR increase from baseline, with 5.0 and 6.0 mL/min, respectively ($p > 0.1$ between the two groups); 23% and 26% of patients, respectively, had an eGFR increase >50% ($p > 0.1$ between the two groups). At 96 weeks of treatment, both groups had a similar median eGFR increase from baseline, with 6.0 and 8.5 mL/min, respectively ($p > 0.1$ between the two groups); 18% and 27% of patients, respectively, had an eGFR increase > 50% ($p > 0.1$ between the two groups) (*38*). Another cohort study of 309 HIV-infected patients who switched from TDF-containing regimens to TAF-containing regimens had a median (IQR) baseline eGFR of 78.6 (63.3, 96.4) mL/min/1.73 m². During TDF-containing regimen treatment, 40.8% and 22.7% of

Table 1. Renal safety data for the use of TAF-containing regimens in HIV-infected people with normal renal function and in those with concurrent kidney injury

HIV-infected people with normal renal function (eGFR > 90 mL/min/1.73 m²)

Author Reference	Study design	Regimen	Sample (n)	Study period	Outcomes of eGFR	Outcomes of renal biomarkers
Gupta *et al.* Aids.2019 (*30*)	Pooled analysis	TAF-based regimen *vs.* TDF-based regimen	9,322	96 weeks	Naive patients: Median CrCl had declined less in the TAF group compared with the TDF group (difference in LSM 6.0 mL/min, $P < 0.001$ for week 96); Switch patients: Median CrCl increased in the TAF group while no change was seen in the TDF group (difference in LSM 5.2 mL/min, $P < 0.001$ for week 96).	Naive patients: Median UACR decreased by 5.2% with TAF *vs.* an increase of 4.9% with TDF ($P < 0.001$). Median RBP:Cr increased by 13.8% with TAF compared with an increase of 74.2% on TDF($P < 0.001$). Median β2M:Cr declined by32.1% with TAF compared with an increase of 33.5% on TDF ($p < 0.001$); Switch patients: Median UACR decreased by 5.4% on TAF and increased by 27.0% on TDF ($p < 0.001$). Median RBP:Cr decreased by 2.3% on TAF and increased 61.2% on TDF ($p < 0.001$). Median b2M:Cr decreased by 25.8% with TAF and increased by 53.0% on TDF ($p < 0.001$).
Orkin *et al.* Lancet HIV.2020 (*32*)	Phase III RCT	BIC/TAF/FTC *vs.* DTG/ABC/3TC	631	144 weeks	Median eGFR: -9.6 mL/min in the BIC/TAF/FTC group *vs.* -11.7 mL/min in the DTG/ABC/3TC group ($p = 0.34$).	Median UACR:2.6 mg/g in the BIC/TAF/FTC group *vs.* -1.6 mg/g in the DTG/ABC/3TC group ($p = 0.94$) ; Median β2M:Cr:-26.4 μg/g in the BIC/TAF/FTC group *vs.* -34.2μg/g in the DTG/ABC/3TC group ($p = 0.41$); Median RBP:Cr:19.6 μg/g in the BIC/TAF/FTC group *vs.* 15.4μg/g in the DTG/ABC/3TC group ($p = 0.83$).
Sax *et al.* eClinicalMedicine. 2023 (*34*)	Phase III RCT	B/F/TAF	634	5 years	The median change at Week 240 in eGFR_CG was -8.4 mL/min, consistent with BIC inhibition of organic cation transporter-2 and tubular creatinine secretion.	

HIV-infected people with mild renal impairment (60 ≤eGFR < 90 mL/min/1.73 m²)

Author Reference	Study design	Regimen	Sample (n)	Study period	Outcomes of eGFR	Outcomes of renal biomarkers
Rieke *et al.* HIV Glasgow.2018 (*37*)	Observational clinical cohort	FTC/TAF-based regimens *vs.* FTC/TDF-based regimens	38	48 weeks	Median eGFR increased significantly from time of switch to month 12 (from 77.0 to 84.3 mL/min/1.73m², $p = 0.001$).	

HIV-infected people with rapid or sharp decline in eGFR.
Sharp eGFR defined as: eGFR decline of > 3 mL/min/yr during ≥ 5yrs of TDF use or > 25% eGFR decline or eGFR < 70 mL/min with eGFR > 90mL/min at TDF initiation

Author Reference	Study design	Regimen	Sample (n)	Study period	Outcomes of eGFR	Outcomes of renal biomarkers
Verwijset *et al.* CROI.2020 (*38*)	Observational clinical cohort	TAF based regimen *vs.* ABC-based regimen	250	96 weeks	50% eGFR recovery observed in 18% with TAF and 26% with ABC ($p > 0.1$); Median eGFR increase in TAF group is 6.0 mL/min, in ABC group is 8.5 mL/min, ($P > 0.1$).	

Table 1. Renal safety data for the use of TAF-containing regimens in HIV-infected people with normal renal function and in those with concurrent kidney injury (continued)

Author Reference	Study design	Regimen	Sample (n)	Study period	Outcomes of eGFR	Outcomes of renal biomarkers
HIV patients with moderate renal impairment (30 ≤ eGFR < 60 mL/min/1.73 m²)						
Podzamczer et al. IAS.2017 (41)	Phase III single-arm study	E/C/F/TAF	242	144 weeks	Median changes from baseline at Week 144 with prestwich TDF use: eGFR$_{CKD-EPI}$ sCr: 3.6 mL/min/1.73 m² eGFR$_{CKD-EPI}$ cysC: 3.7 mL/min/1.73 m²	Of those participants with clinically significant albuminuria (UACR ≥ 30 mg/g) at baseline, 47% had resolution by Week 144; The median UACR decreased from 41 mg/g at baseline to 10 mg/g at the 144 weeks.
HIV patients with severe renal impairment (15 ≤ eGFR < 30 mL/min/1.73 m²)						
Custodio et al. Antimicrobial agents and chemotherapy.2016 (43)	Phase I single-dose study	TAF	14	14 days	No clinically relevant changes in the median serum creatinine level, eGFR, or phosphate level were observed in any subject in either group.	

patients had an eGFR decline rate > 3 and 5 mL/min/1.73 m²/year, respectively. These patients had a significant eGFR improvement after switching to TAF-containing regimens, with mean annual increases of 2.72 and 2.78 mL/min/1.73 m², respectively (both $p < 0.001$) (39).

3.2 PWH with moderate renal impairment (30 ≤ eGFR < 60 mL/min/1.73 m²).

TAF-containing regimens are safe for the kidneys in HIV-infected patients with moderate renal impairment (30 ≤ eGFR < 60 mL/min/1.73 m²), according to clinical trials and real-world studies. A Phase 3 clinical trial switched 242 HIV-infected patients with viral suppression and baseline eGFR of 30-69 mL/min to TAF-containing regimens, and 42% and 49% of them had significant proteinuria and albuminuria at baseline (40). In this study, 158 patients (65%) who had used TDF-containing regimens at baseline improved their median eGFR significantly at 144 weeks after switching to TAF-containing regimens; while 84 patients (35%) who had used non-TDF regimens at baseline did not change their median eGFR significantly at 144 weeks after switching to TAF-containing regimens. The urine RBP/Cr ratio and β2-MG/Cr ratio improved significantly at 1 week and remained stable for 144 weeks in patients who switched from TDF-containing regimens to TAF-containing regimens(40-42). The median UACR decreased from 41 mg/g at baseline to 10 mg/g at week 144. Patients did not develop proximal tubular dysfunction or Fanconi syndrome (41). Another prospective cohort study showed that the proportion of patients with moderate renal impairment decreased from 9.1% at baseline to 3.0% after 12 months of switching from TDF-containing regimens to TAF-containing regimens (37).

3.3 PWH with severe renal impairment (eGFR < 30 mL/min/1.73 m²)

Few studies have explored the application of TAF-containing regimens in HIV-infected patients with severe renal impairment, but they suggest that these patients can use TAF-containing regimens based on their clinical needs. A Phase 1 clinical trial tested the safety of TAF in non-HIV-infected patients with severe renal impairment who did not receive hemodialysis. The study involved 14 non-HIV-infected patients with severe renal impairment (mean eGFR of 24.0 mL/min) and 13 non-HIV-infected patients with eGFR ≥ 90 mL/min as a control group. They received a single dose of TAF 25 mg and had a 14-day follow-up. The results showed that the patients with severe renal impairment had higher TAF exposure than the control group, but the difference was not clinically significant. The patients with severe renal impairment also had higher TFV exposure than the control group, but lower than the levels in previously studied subjects without renal impairment who received a single dose

of TDF 300 mg. The adverse event rates were similar between the two groups (6 events in the severe renal impairment group and 7 events in the control group), and no clinically significant changes occurred in serum creatinine or eGFR (*43*) . Although this study showed preliminary safety of TAF in non-HIV-infected patients with severe renal impairment who did not receive hemodialysis, Phase 3 clinical trial data are lacking on the use of TAF-containing regimens in HIV-infected patients with severe renal impairment who did not receive hemodialysis. Therefore, TAF-containing regimens are not approved for use in HIV-infected patients with estimated creatinine clearance (CrCl) of 15-30 mL/min or with end-stage renal disease (ESRD, CrCl < 15 mL/min) who did not receive long-term hemodialysis (*44-46*). The safety of TAF-containing regimens in this subgroup of HIV-infected patients requires further validation.

Phase 3 clinical trials and real-world studies show that switching to TAF-containing regimens is safe and tolerable for HIV-infected patients with ESRD who receive hemodialysis, and maintains high virologic suppression rates (*47-51*). A multicenter Phase 3b study switched 55 HIV-infected patients with virologic suppression and ESRD undergoing hemodialysis to E/c/F/TAF, and during a 2-year period, only 4 patients (7.3%) discontinued the treatment due to adverse events, with 2 cases related to the study drug. The patients had virologic suppression rates of 81.8% at 1 year and 55% at 2 years (*47,48*). In this study, 10 patients who completed 2 years of E/c/F/TAF treatment entered an open-label extension phase and switched to B/F/TAF treatment. At 1 year of treatment, no patients discontinued the treatment due to adverse events, and all patients had virologic suppression (*49*). Another retrospective study of 17 HIV-infected patients with ESRD undergoing hemodialysis who switched ART regimens, with 15 patients switching to TAF-containing regimens (12 of them to B/F/TAF), showed that only 1 patient discontinued the treatment due to adverse events, and the overall virologic suppression rate was 82% at 1 year (*50*). Case reports also showed that 6 HIV-infected patients with ESRD undergoing hemodialysis who switched to B/F/TAF had no adverse events, and the virologic suppression rate was 100% at 1 year (*51*). Based on these data, HIV-infected patients with ESRD who undergo long-term hemodialysis can use TAF-containing regimens; E/c/F/TAF, B/F/TAF, and dolutegravir/rilpivirine (DTG/RPV) are the only approved complete single-tablet regimens for HIV-infected patients with ESRD who receive hemodialysis (*44,46,52*).

4. Renal Safety Data of TAF-Containing Regimens in PWH at Risk of Kidney Injury (Table 2)

4.1. Elderly PWH

Kidney disease is more likely in HIV-infected individuals with advanced age(*53,54*), so renal safety of antiretroviral drugs is crucial for elderly HIV-infected patients on antiretroviral therapy. Subgroup analyses of two large multicenter Phase 3 clinical trials showed good renal safety of TAF-containing regimens in elderly HIV-infected patients with normal renal function. The studies involved 196 HIV-infected patients aged ≥50 years who received B/F/TAF (*n* = 96), DTG+FTC/TAF (*n* = 59), or DTG/ABC/3TC (*n* = 41). The baseline median (IQR) eGFR values were 99.0 (83.7–114.0), 104.0 (84.2–121.8), and 101.9 (83.2–130.5) mL/min, respectively. The 144-week treatment results showed that no patients in the B/F/TAF or DTG+FTC/TAF group discontinued the treatment or developed proximal renal tubulopathy due to renal adverse events, while one patient in the DTG/ABC/3TC group discontinued the treatment due to renal failure, which was not related to the study drugs. The median eGFR changes at week 144 from baseline were -9, -9, and -11 mL/min in the three HIV-infected groups, which matched the effect of BIC and DTG inhibiting creatinine secretion by inhibiting organic cation transporter 2 (*55*).

Clinical trials and real-world studies show good renal safety of TAF-containing regimens in elderly HIV-infected patients with mild renal impairment. A multicenter Phase 3 clinical trial switched 167 HIV-infected patients aged ≥ 60 years who had virologic suppression and received TDF-containing regimens to E/c/F/TAF (*n* = 111) or continued with TDF-containing regimens (*n* = 56). The baseline median (IQR) eGFR was 80 (68–91) mL/min. The 48-week treatment results showed that both groups maintained stable eGFR and serum creatinine levels. The E/c/F/TAF group improved significantly in UACR, UPCR, RBP/Cr, and β2-MG/Cr than the TDF-containing regimen group at week 48 (percentage change from baseline): UACR (-27.8% *vs*. -7.7%, *p* = 0.0042), UPCR (-49.8% *vs*. -3.8%, *p* = 0.00027), RBP/Cr (-41.5% *vs*. 15.2%, *p* < 0.0001), and β2-MG/Cr (-58.7% *vs*. 13.6%, *p* < 0.0001) (*56*). Another retrospective Italian cohort study of 93 HIV-infected patients aged ≥ 55 years who switched to B/F/TAF-containing regimens had a baseline median (IQR) eGFR of 83 (74–91) mL/min/1.73 m^2. After 48 weeks of switching, serum creatinine and eGFR levels did not change significantly, and the median change compared with baseline at 48 weeks was 0. (*P*-values were 0.073 and 0.737, respectively) (*57*).

TAF-containing regimens also keep renal function stable in elderly HIV-infected patients with moderate renal impairment. A Phase 3b clinical trial switched 86 HIV-infected patients aged ≥ 65 years who had virologic suppression and received E/c/F/TAF or TDF-containing regimens to B/F/TAF treatment. The baseline median (IQR) eGFR was 76.2 (39.6–130.2) mL/min (*58*). The 96-week treatment results showed that there were no renal adverse events, treatment discontinuations, proximal renal tubulopathy, or Fanconi syndrome (*58,59*).

Table 2. Renal safety data of TAF-containing regimens in PWH at risk of kidney injury

Author Reference	Study design	Regimen	Sample (n)	Study period	Outcomes of eGFR	Outcomes of renal biomarkers
HIV/HBV coinfection						
Surial *et al.* J Acquir Immune Defic Syndr.2020 (62)	Observational clinical cohort	Switched from TDF-based regimen to TAF-based regimen	106	14.1 months-14.6 months	60 mL/min/1.73 m^2 < baseline eGFR < 89 mL/min/1.73 m^2:eGFR increased by 3.2 mL/min/1.73 m^2 1 year (95% CI 1.2 to 5.2) after switching to TAF (*P*-value for slope difference 0.001). Baseline eGFR < 60 mL/min/1.73 m^2 :eGFR increased by 6.2 mL/min/1.73 m^2 1 year after the switch (95% CI 2.4 to 10.0, *P*-value for slope difference, 0.001).	Switching to TAF led to a change in urine protein-to-creatinine ratio of -6.3 mg/mmol 1 year after the switch (95% CI -10.0 to -2.7, *P*-value for slope difference 0.01).
HIV/HCV coinfection						
Huhn *et al.* PLoS One. 2020 (63)	Phase IIIb RCT	E/C/F/TAF or R/F/TAF	148	36 weeks	Median baseline eGFR$_{CG}$ was 99.8 mL/min, with the median change 2.2 mL/min at W8, 0.9 mL/min at Post-HCV W4, and 0.1 mL/min at Post-HCV W12.	Quantitative measures of urine protein (urine ratios of albumin, retinol binding protein, and beta-2-microglobulin to creatinine) were reduced after switch to an F/TAF-based regimen; these reductions were maintained after the addition of LDV/SOF and for the duration of the study.
Elderly PWH						
Mills *et al.* CROI. 2020 (55)	Pooled analysis	BIC/TAF/FTC *vs.* DTG/ABC/3TC *vs.* DTG+F/TAF	196	144 weeks	At the 144 weeks, the changes of median eGFR in the three groups (BIC/TAF/FTC, DTG/ABC/3TC, DTG+F/TAF) were -9, -9 and -11 mL/min, respectively.	Median UACR decreased by 23% with B/F/TAF *vs.* an increase of 34% with DTG/ABC/3TC. Median RBP:Cr increased by 1% with B/F/TAF compared with an increase of 11% with DTG/ABC/3TC. Median β2M:Cr declined by 54% with B/F/TAF compared with an decrease of 39% with DTG/ABC/3TC.
Maggiolo *et al.* The Lancet HIV. 2019 (56)	Phase III RCT	Regimen containing TDF *vs.* EVG/c/FTC/TAF	167	48 weeks	Change from baseline in eGFR: EVG/c/TAF/FTC group (median change -2·4 mL/min [IQR -7·2 to 6·6]) *vs.* TDF group (median change 0·6 mL/min [-5·7 to 5·4]), (*p* = 0.44).	Median UACR decreased by 27.8% with EVG/c/TAF/FTC *vs.* an decrease of 7.7% with TDF-based regimen (*p* = 0·0042). Median urine protein to creatinine ratio(UPCR) decreased by 49.8% with EVG/c/TAF/FTC *vs.* an decrease of 3.8% with TDF-based regimen (*p* = 0.00027). Median β2 microglobulin to creatinine ratio decreased by 58.7% with EVG/c/TAF/FTC *vs.* an increase of 13.6% with TDF-based regimen (*p* < 0·0001) Median retinol-binding protein to creatinine ratio decreased by 41.5% with EVG/c/TAF/FTC *vs.* an increase of 15.2% with TDF-based regimen (*p* < 0·0001).
HIV patients with diabetes						
Stein *et al.* ASM/ ICAA. 2016 (68)	Phase III RCT	EVG/c/FTC/TAF	33	96 weeks	eGFR remained stable, and the change of median eGFR from baseline was 0.0 mL/min (*p* = 0.86).	The following markers of proteinuria and proximal tubular lesions improved (baseline *vs.* median at the 96 weeks): UPCR (269 *vs.* 135 mg/g), UACR (58 *vs.* 35 mg/g), RBP/Cr ratio (2,119 *vs.* 247 g/g) and β2-MG/Cr ratio (2,449 *vs.*328g/g) (except UACR, all other improvements were statistically significant).

A pooled analysis of four international clinical trials switched 140 virologically suppressed HIV-infected patients aged ≥ 65 years from other regimens to B/F/TAF treatment. The baseline median (range) eGFR was 74 (38–130) mL/min. The 48-week results showed a slight and stable median eGFR decline (a decrease of 2.7 mL/min from baseline at week 48), and no renal adverse events, treatment discontinuations, or proximal renal tubulopathy occurred in the patients (*60*).

4.2. People with HIV and hepatitis B virus (HBV) or hepatitis C virus (HCV) co-infection

HBV and HCV co-infection is an independent risk factor for kidney disease in HIV-infected individuals (*61*) . Studies show that TAF-containing regimens are safe for the kidneys in two subgroups of patients. A prospective cohort study switched 106 HIV/HBV co-infected patients to TAF-containing regimens after receiving TDF treatment and achieving HIV virologic suppression. At baseline, 79.2% of the patients had eGFR levels of 60-89 mL/min/1.73 m², and 20.8% had eGFR < 60 mL/min/1.73m². After one year of TAF-containing regimens, the mean (95% CI) eGFR levels increased from baseline by 3.2 (1.2-5.2) mL/min/1.73m² and 6.2 (2.4-10.0) mL/min/1.73 m² in the two groups of patients, respectively. Additionally, the overall population had a mean decrease of 6.3 mg/mmol in UPCR compared to baseline. TAF-containing regimens reversed the worsening trend in eGFR and UPCR in the study patients during the year before baseline when they received TDF-containing regimens (all *P*-values< 0.05) (*62*). Another Phase 3b clinical trial included 148 HIV-infected patients with HCV co-infection and HIV virologic suppression who were randomly assigned to rilpivirine(R)/F/TAF (*n* = 74) or E/c/F/TAF (*n* = 74) treatment. After 8 weeks, they started a 12-week course of HCV antiviral therapy while continuing with TAF-containing regimens. The median (IQR) baseline eGFR in the two groups of patients was 100 (75-118) mL/min/1.73 m² and 99 (79-115) mL/min/1.73m², respectively. The results showed that the eGFR was stable during the study period, and the median eGFR change for the overall patients after 12 weeks of HCV antiviral therapy was 0.1 mL/min/1.73m². Furthermore, the R/F/TAF group showed improvement in renal function including UACR, RBP/Cr, and β2-MG/Cr, with median changes from baseline of -6.9%, -27.6%, and -70.0%, respectively. In the E/c/F/TAF group, the median changes were -1.2%, -18.2%, and -52.7% (*63*). In China, a multicenter study switched 243 HIV-infected patients with concurrent HCV infection and HIV virologic suppression to TAF-containing regimens and started a 12-week course of HCV treatment after 4 weeks. The results showed good safety and tolerability, and no patients discontinued treatment due to adverse events (*64*).

4.3. PWH with comorbidities

Comorbidities such as diabetes and hypertension, or a history of kidney disease, can increase the risk of kidney disease in HIV-infected individuals (*65,66*). Several studies suggest that TAF-containing regimens maintain stable kidney function in HIV-infected patients with these comorbidities(*40,42,59,67,68*). For example, in the Phase 3b clinical trial mentioned above, 86 HIV-infected patients aged ≥ 65 years with a baseline median (IQR) eGFR of 76.2 (39.6-130.2) mL/min (51.2% with a history of hypertension) received TAF-containing regimens for 96 weeks without renal adverse events, treatment discontinuation, proximal renal tubulopathy, or Fanconi syndrome (*58,59*) . In another Phase 3 study, 33 HIV-infected patients with moderate renal impairment (baseline eGFR of 30-69 mL/min) and diabetes received TAF-containing regimens for 96 weeks, resulting in stable eGFR and improvements in UPCR, UACR, RBP/Cr, and β2-MG/Cr (median values at baseline *vs.* week 96): UPCR (269 *vs.* 135 mg/g), UACR (58 *vs.* 35 mg/g), RBP/Cr ratio (2,119 *vs.* 247 µg/g), and β2-MG/Cr ratio (2,449 *vs.* 328 µg/g). Except for UACR, all improvements were statistically significant(*68*). In a multicenter, single-arm, open-label, Phase 4 clinical trial, 31 HIV-infected patients with a history of TDF-related proximal renal tubulopathy and eGFR >30 mL/min/1.73 m² received F/TAF-containing regimens. The baseline median eGFR (IQR) calculated using the serum creatinine formula and cystatin C formula was 75 (69-92) mL/min/1.73 m² and 60 (52-69) mL/min/1.73 m², respectively. The 96-week results showed no recurrence of glycosuria or proximal renal tubulopathy. The eGFR calculated using the creatinine formula declined slightly (-1.9 mL/min/1.73 m²/year, *p* = 0.024), but the eGFR calculated using the cystatin C formula did not decline significantly (-0.9 mL/min/1.73 m²/year, *p* = 0.16). Ten and five cases of rapid eGFR decline (> 5 mL/min/1.73 m²/year) occurred based on the creatinine and cystatin C formulas, respectively, but the relation to TAF was unclear. The patients did not change significantly in UACR, RBP/Cr, and phosphate excretion fraction (all *P*-values > 0.2) (*67*).

In summary, clinical trials and real-world studies show the renal safety of TAF-containing regimens for HIV-infected patients, including those with renal insufficiency or at risk of kidney injury. Individual case reports of renal safety events in HIV-infected patients treated with TAF-containing regimens exist, but most of these patients had risk factors for kidney disease (such as HCV co-infection, diabetes, hypertension, history of kidney disease, or long-term use of antiretroviral drugs with renal injury risk, such as TDF) (*69-74*). These reports do not prove that TAF causes renal safety issues. International guidelines recommend TAF-containing regimens for most HIV-infected patients (*75-77*). HIV-infected patients with renal impairment, including TDF-

related renal injury, can also consider TAF-containing regimens as a safe alternative.

Conflict of Interest: The authors have no conflicts of interest to disclose.

References

1. Cohen SD, Ingelfinger JR, Kopp JB, Kimmel PL. Kidney Diseases Associated with Human Immunodeficiency Virus Infection. N Engl J Med. 2017; 377:2363-2374.
2. Shi R, Chen X, Lin H, Ding Y, He N. Incidence of impaired kidney function among people with HIV: A systematic review and meta-analysis. BMC Nephrol. 2022; 23:107.
3. Rosenberg AZ, Naicker S, Winkler CA, Kopp JB. HIV-associated nephropathies: epidemiology, pathology, mechanisms and treatment. Nat Rev Nephrol. 2015; 11:150-160.
4. Mocroft A, Kirk O, Gatell J, Reiss P, Gargalianos P, Zilmer K, Beniowski M, Viard JP, Staszewski S, Lundgren JD. Chronic renal failure among HIV-1-infected patients. AIDS. 2007; 21:1119-1127.
5. Estrella MM, Fine DM. Screening for chronic kidney disease in HIV-infected patients. Adv Chronic Kidney Dis. 2010; 17:26-35.
6. Valdivia-Cerda V, Alvarez-Zavala M, Sanchez-Reyes K, Cabrera-Silva RI, Ruiz-Herrera VV, Loza-Salazar AD, Martinez-Ayala P, Vazquez-Limon JC, Garcia-Garcia G, Andrade-Villanueva JF, Gonzalez-Hernandez LA. Prevalence and risk factors of chronic kidney disease in an HIV positive Mexican cohort. BMC Nephrol. 2021; 22:317.
7. Cao Y, Gong M, Han Y, Xie J, Li X, Zhang L, Li Y, Song X, Zhu T, Li T. Prevalence and risk factors for chronic kidney disease among HIV-infected antiretroviral therapy-naive patients in mainland China: A multicenter cross-sectional study. Nephrology (Carlton). 2013; 18:307-312.
8. Yanagisawa N, Ando M, Ajisawa A, Imamura A, Suganuma A, Tsuchiya K, Nitta K. Clinical characteristics of kidney disease in Japanese HIV-infected patients. Nephron Clin Pract. 2011; 118:c285-291.
9. Kim EJ, Ahn JY, Kim YJ, *et al*. The Prevalence and Risk Factors of Renal Insufficiency among Korean HIV-Infected Patients: The Korea HIV/AIDS Cohort Study. Infect Chemother. 2017; 49:194-204.
10. Zhao N, Xiang P, Zeng Z, Liang H, Wang F, Xiao J, Yang D, Wang S, Chen M, Gao G. Prevalence and risk factors for kidney disease among hospitalized PLWH in China. AIDS Res Ther. 2023; 20:49.
11. Lucas A, Wyatt CM. HIV at 40: kidney disease in HIV treatment, prevention, and cure. Kidney Int. 2022; 102:740-749.
12. Jotwani V, Atta MG, Estrella MM. Kidney Disease in HIV: Moving beyond HIV-Associated Nephropathy. J Am Soc Nephrol. 2017; 28:3142-3154.
13. Ma Q, Ocque AJ, Morse GD, Sanders C, Burgi A, Little SJ, Letendre SL. Switching to Tenofovir Alafenamide in Elvitegravir-Based Regimens: Pharmacokinetics and Antiviral Activity in Cerebrospinal Fluid. Clin Infect Dis. 2020; 71:982-988.
14. Aloy B, Tazi I, Bagnis CI, Gauthier M, Janus N, Launay-Vacher V, Deray G, Tourret J. Is Tenofovir Alafenamide Safer than Tenofovir Disoproxil Fumarate for the Kidneys? AIDS Rev. 2016; 18:184-192.
15. Nishijima T, Gatanaga H, Oka S. Tenofovir nephrotoxicity among Asians living with HIV: review of the literature. Glob Health Med. 2019; 1:88-94.
16. Tourret J, Deray G, Isnard-Bagnis C. Tenofovir Effect on the Kidneys of HIV-Infected Patients. J Am Soc Nephrol. 2013; 24:1519-1527.
17. Tsai WS, Wang LS, Hsu YH, Lin YL, Fang TC, Hsu BG. Tenofovir nephropathy in a patient with human immunodeficiency virus. Tzu Chi Medical Journal. 2015; 27:83-86.
18. Sano T, Kawaguchi T, Ide T, Amano K, Kuwahara R, Arinaga-Hino T, Torimura T. Tenofovir Alafenamide Rescues Renal Tubules in Patients with Chronic Hepatitis B. Life (Basel). 2021; 11:263.
19. Nishijima T, Komatsu H, Higasa K, Takano M, Tsuchiya K, Hayashida T, Oka S, Gatanaga H. Single Nucleotide Polymorphisms in ABCC2 Associate With Tenofovir-Induced Kidney Tubular Dysfunction in Japanese Patients With HIV-1 Infection: A Pharmacogenetic Study. Clin Infect Dis. 2012; 55:1558-1567.
20. Avihingsanon A, Sophonphan J, Thammajaruk N, Chaihong P, Burger DM, Cressey TR, Ramautarsing RA, Praditornsilpa K, Avihingsanon Y, Ruxrungtham K, HIV-NAT 114 study team. Plasma tenofovir concentrations and proximal tubular dysfunction in HIV-Infected adults receiving tenofovir in Thailand. J AIDS Clin Res. 2015; 6:477-483.
21. Rodríguez-Nóvoa S, Labarga P, D'Avolio A, Barreiro P, Albalate M, Vispo E, Solera C, Siccardi M, Bonora S, Di Perri G, Soriano V. Impairment in kidney tubular function in patients receiving tenofovir is associated with higher tenofovir plasma concentrations. AIDS. 2010; 24:1064-1066.
22. Ray AS, Fordyce MW, Hitchcock MJM. Tenofovir alafenamide: A novel prodrug of tenofovir for the treatment of Human Immunodeficiency Virus. Antiviral Res. 2016; 125:63-70.
23. Ruane PJ, DeJesus E, Berger D, Markowitz M, Bredeek UF, Callebaut C, Zhong L, Ramanathan S, Rhee MS, Fordyce MW, Yale K. Antiviral activity, safety, and pharmacokinetics/pharmacodynamics of tenofovir alafenamide as 10-day monotherapy in HIV-1-positive adults. J Acquir Immune Defic Syndr. 2013; 63:449-455.
24. Sax PE, Wohl D, Yin MT, *et al*. Tenofovir alafenamide versus tenofovir disoproxil fumarate, coformulated with elvitegravir, cobicistat, and emtricitabine, for initial treatment of HIV-1 infection: Two randomised, double-blind, phase 3, non-inferiority trials. The Lancet. 2015; 385:2606-2615.
25. Wassner C, Bradley N, Lee Y. A Review and Clinical Understanding of Tenofovir: Tenofovir Disoproxil Fumarate versus Tenofovir Alafenamide. J Int Assoc Provid AIDS Care. 2020; 19:2325958220919231.
26. Gallant JE, Daar ES, Raffi F, *et al*. Efficacy and safety of tenofovir alafenamide versus tenofovir disoproxil fumarate given as fixed-dose combinations containing emtricitabine as backbones for treatment of HIV-1 infection in virologically suppressed adults: A randomised, double-blind, active-controlled phase 3 trial. Lancet HIV. 2016; 3:e158-165.

27. Raffi F, Orkin C, Clarke A, Slama L, Gallant J, Daar E, Henry K, Santana-Bagur J, Stein DK, Bellos N, Scarsella A, Yan M, Abram ME, Cheng A, Rhee MS. Brief Report: Long-Term (96-Week) Efficacy and Safety After Switching From Tenofovir Disoproxil Fumarate to Tenofovir Alafenamide in HIV-Infected, Virologically Suppressed Adults. J Acquir Immune Defic Syndr. 2017; 75:226-231.

28. Arribas JR, Thompson M, Sax PE, Haas B, McDonald C, Wohl DA, DeJesus E, Clarke AE, Guo S, Wang H, Callebaut C, Plummer A, Cheng A, Das M, McCallister S. Brief Report: Randomized, Double-Blind Comparison of Tenofovir Alafenamide (TAF) *vs* Tenofovir Disoproxil Fumarate (TDF), Each Coformulated With Elvitegravir, Cobicistat, and Emtricitabine (E/C/F) for Initial HIV-1 Treatment: Week 144 Results. J Acquir Immune Defic Syndr. 2017; 75:211-218.

29. Mills A, Arribas JR, Andrade-Villanueva J, *et al.* Switching from tenofovir disoproxil fumarate to tenofovir alafenamide in antiretroviral regimens for virologically suppressed adults with HIV-1 infection: a randomised, active-controlled, multicentre, open-label, phase 3, non-inferiority study. Lancet Infect Dis. 2016; 16:43-52.

30. Gupta SK, Post FA, Arribas JR, *et al.* Renal safety of tenofovir alafenamide *vs.* tenofovir disoproxil fumarate: a pooled analysis of 26 clinical trials. AIDS. 2019; 33:1455-1465.

31. Molina JM, Ward D, Brar I, Mills A, Stellbrink HJ, López-Cortés L, Ruane P, Podzamczer D, Brinson C, Custodio J, Liu H, Andreatta K, Martin H, Cheng A, Quirk E. Switching to fixed-dose bictegravir, emtricitabine, and tenofovir alafenamide from dolutegravir plus abacavir and lamivudine in virologically suppressed adults with HIV-1: 48 week results of a randomised, double-blind, multicentre, active-controlled, phase 3, non-inferiority trial. Lancet HIV. 2018; 5:e357-e365.

32. Orkin C, DeJesus E, Sax PE, *et al.* Fixed-dose combination bictegravir, emtricitabine, and tenofovir alafenamide versus dolutegravir-containing regimens for initial treatment of HIV-1 infection: Week 144 results from two randomised, double-blind, multicentre, phase 3, non-inferiority trials. Lancet HIV. 2020; 7:e389-e400.

33. Winston A, Post FA, DeJesus E, *et al.* Tenofovir alafenamide plus emtricitabine versus abacavir plus lamivudine for treatment of virologically suppressed HIV-1-infected adults: a randomised, double-blind, active-controlled, non-inferiority phase 3 trial. Lancet HIV. 2018; 5:e162-e171.

34. Sax PE, Arribas JR, Orkin C, Lazzarin A, Pozniak A, DeJesus E, Maggiolo F, Stellbrink HJ, Yazdanpanah Y, Acosta R, Huang H, Hindman JT, Martin H, Baeten JM, Wohl D. Bictegravir/emtricitabine/tenofovir alafenamide as initial treatment for HIV-1: five-year follow-up from two randomized trials. EClinicalMedicine. 2023; 59:101991.

35. Deeks ED. Bictegravir/emtricitabine/tenofovir alafenamide: a review in HIV-1 infection. Drugs. 2018; 78:1817-1828.

36. Teira R, Diaz-Cuervo H, Aragão F, *et al.* eGFR-EPI changes among HIV patients who switch from F/TDF to F/TAF while maintaining the same third agent in the Spanish VACH cohort. HIV Res Clin Pract. 2021; 22:78-85.

37. Rieke A, Jessen H, Pauli R, Waizmann M, Heuchel T, Postel N, Lymperopoulou C, Faghmous I, Diaz-Cuervo H, Ramroth H. Real-world effects of treatment with emtricitabine/tenofovir alafenamide versus emtricitabine/tenofovir disoproxil fumarate-based regimens in people living with HIV in a clinical cohort in Germany. *https://hivglasgow.org/wp-content/uploads/2018/11/P206-1.pdf* (accessed March 23, 2024).

38. Verwijs R, Wijting I, Kasteren Mv, Hollander JGd, Derdelinckx I, Berk Gvd, Vrouenraets S, Claassen M, Bierman W, Rokx C, Rijnders B. BACTAF-Prospective Randomized Study & BACTAF-Retrospective Cohort Study: eGFR Recovery 96 Weeks After a TDF toTAF or ABC Switch for TDF-Associated EGFR Decline. *https://www.croiconference.org/wp-content/uploads/sites/2/posters/2020/1430_2_Verwijs_00689.pdf* (accessed March 23, 2024).

39. Ibrahim F, Campbell L, Bailey AC, Stockwell S, Waters L, Orkin C, Johnson M, Gompels M, De Burgh-Thomas A, Jones R, Schembri G, Mallon PW, Post FA. Estimated glomerular filtration rate slopes on tenofovir alafenamide. HIV Med. 2020; 21:607-612.

40. Pozniak A, Arribas JR, Gathe J, *et al.* Switching to tenofovir alafenamide, coformulated with elvitegravir, cobicistat, and emtricitabine, in HIV-infected patients with renal impairment: 48-week results from a single-arm, multicenter, open-label phase 3 study. J Acquir Immune Defic Syndr. 2016; 71:530-537.

41. Podzamczer D, Arriba J, Clarke A, Cotte L, Mudrikova T, Negredo E, Short WR, Jiang S, Cheng Am Das M. Adults with renal impairment switching from tenofovir disoproxil fumarate to tenofovir alafenamide have improved renal and bone safety through 144 weeks. *https://www.natap.org/2017/IAS/IAS_65.htm* (accessed March 23, 2024).

42. Post FA, Tebas P, Clarke A, Cotte L, Short WR, Abram ME, Jiang S, Cheng A, Das M, Fordyce MW. Brief report: Switching to tenofovir alafenamide, coformulat.ed with elvitegravir, cobicistat, and emtricitabine, in HIV-infected adults with renal impairment: 96-week results from a single-arm, multicenter, open-label phase 3 study. J Acquir Immune Defic Syndr. 2017; 74:180-184.

43. Custodio JM, Fordyce M, Garner W, Vimal M, Ling KHJ, Kearney BP, Ramanathan S. Pharmacokinetics and safety of tenofovir alafenamide in HIV-uninfected subjects with severe renal impairment. Antimicrob Agents Chemother. 2016; 60:5135-5140.

44. Gilead Sciences. Full prescribing information for BIKTARVY. *https://www.accessdata.fda.gov/drugsatfda_docs/label/2018/210251s000lbl.pdf* (accessed March 23, 2024).

45. Gilead Sciences. Full prescribing information for DESCOVY. *https://www.accessdata.fda.gov/drugsatfda_docs/label/2021/208215s017lbl.pdf* (accessed March 23, 2024).

46. Gilead Sciences. Full prescribing information for GENVOYA. *https://www.accessdata.fda.gov/drugsatfda_docs/label/2016/207561s002lbl.pdf* (accessed March 23, 2024).

47. Eron JJ, Lelievre J-D, Kalayjian R, *et al.* Longer-Term Safety and Efficacy of Elvitegravir/Cobicistat/Emtricitabine/Tenofovir Alafenamide in Virologically Suppressed Adults Living With HIV and End-Stage Renal Disease on Chronic Hemodialysis. Open Forum Infect Dis. 2019 Oct 23; 6(Suppl 2):S864.

48. Eron JJ, Lelievre J-D, Kalayjian R, *et al.* Safety of elvitegravir, cobicistat, emtricitabine, and tenofovir alafenamide in HIV-1-infected adults with end-stage renal

disease on chronic haemodialysis: an open-label, single-arm, multicentre, phase 3b trial. Lancet HIV. 2018 Dec; 13:S2352-3018(18)30296-0.

49. Eron JJ, Wilkin A, Ramgopal M, *et al*. A Daily Single-Tablet Regimen of Bictegravir/Emtricitabine/Tenofovir Alafenamide in Virologically Suppressed Adults Living With HIV and End-stage Renal Disease on Chronic Hemodialysis. Open Forum Infect Dis. 2020 Dec 31; 7(Suppl 1):S529-530.

50. Otto A, Pecora Fulco *p*. A retrospective evaluation of highly active antiretroviral therapy simplification in patients with end-stage renal disease receiving hemodialysis. Int J STD AIDS. 2021; 32:963-967.

51. Sidman EF, Ondrush NM. Utilization of bictegravir/emtricitabine/tenofovir alafenamide in patients with end-stage renal disease on hemodialysis. Am J Health Syst Pharm. 2023; 80:e92-e97.

52. GlaxoSmithKline. Full prescribing information for JULUCA. *https://www.accessdata.fda.gov/drugsatfda_docs/label/2017/210192s000lbl.pdf* (accessed March 23, 2024).

53. Alfano G, Cappelli G, Fontana F, Di Lullo L, Di Iorio B, Bellasi A, Guaraldi G. Kidney Disease in HIV Infection. J Clin Med. 2019; 8:1254 :1254.

54. Ando M, Ando Y. A high likelihood of increase in end-stage renal disease among the Japanese HIV-infected population. Renal Replacement Therapy. 2019; 5:1-9.

55. Mills A, Gupta SK, Brinson C, Workowski K, Clarke A, Antinori A, Stephens JL, Koenig E, Arribas JR, Asmuth DM, Ward D, Rockstroh JK, Huang H, Martin H, Brainar DM. 144-Week Efficacy and Safety of B/F/TAF in Treatment-Naive Adults Age ≥50 Years.*https://www.natap.org/2020/CROI/croi_50.htm* (accessed March 23, 2024).

56. Maggiolo F, Rizzardini G, Raffi F, Pulido F, Mateo-Garcia MG, Molina J-M, Ong E, Shao Y, Piontkowsky D, Das M. Bone mineral density in virologically suppressed people aged 60 years or older with HIV-1 switching from a regimen containing tenofovir disoproxil fumarate to an elvitegravir, cobicistat, emtricitabine, and tenofovir alafenamide single-tablet regimen: a multicentre, open-label, phase 3b, randomised trial. Lancet HIV. 2019; 6:e655-e666.

57. Lazzaro A, Cacciola EG, Borrazzo C, Innocenti GP, Cavallari EN, Mezzaroma I, Falciano M, Fimiani C, Mastroianni CM, Ceccarelli G. Switching to a bictegravir single tablet regimen in elderly people living with HIV-1: data analysis from the BICTEL cohort. Diagnostics. 2021; 12:76.

58. Maggiolo F, Rizzardini G, Molina J-M, *et al*. Bictegravir/emtricitabine/tenofovir alafenamide in virologically suppressed people with HIV aged≥ 65 years: week 48 results of a phase 3b, open-label trial. Infect Dis Ther. 2021; 10:775-788.

59. Maggiolo F, Rizzardini G, Molina JM, *et al*. Bictegravir/emtricitabine/tenofovir alafenamide in older individuals with HIV: Results of a 96-week, phase 3b, open-label, switch trial in virologically suppressed people≥ 65 years of age. HIV Med. 2023; 24:27-36.

60. Ramgopal M, Maggiolo F, Ward D, Lebouche B, Rizzardini G, Molina JM, Brinson C, Wang H, Gallant J, Collins SE, McNichollR, Martin H. Pooled analysis of 4 international trials of bictegravir/emtricitabine/tenofovir alafenamide (B/F/TAF) in adults aged > 65 or older demonstrating safety and efficacy: week 48 results. *https://*

www.hivandmore.de/kongresse/iac2020/Ramgopal_Pooled-BVY-W48-in-65yo-and-older_AIDS-2020_OAB0403_Submitted.pdf (accessed March 23, 2024).

61. Mocroft A, Neuhaus J, Peters L, Ryom L, Bickel M, Grint D, Koirala J, Szymczak A, Lundgren J, Ross MJ, Wyatt CM, INSIGHT SMART Study Group; ESPRIT Study Group. Hepatitis B and C co-infection are independent predictors of progressive kidney disease in HIV-positive, antiretroviral-treated adults. PLoS One. 2012; 7:e40245.

62. Surial B, Béguelin C, Chave J-P, Stöckle M, Boillat-Blanco N, Doco-Lecompte T, Bernasconi E, Fehr J, Günthard HF, Schmid P, Walti LN, Furrer H, Rauch A, Wandeler G; and the Swiss HIV Cohort Study. Brief report: switching from TDF to TAF in HIV/HBV-Coinfected individuals with renal dysfunction—a prospective cohort study. J Acquir Immune Defic Syndr. 2020; 85:227-232.

63. Huhn GD, Ramgopal M, Jain MK, *et al*. HIV/HCV therapy with ledipasvir/sofosbuvir after randomized switch to emtricitabine-tenofovir alafenamide-based single-tablet regimens. PLoS One. 2020; 15:e0224875.

64. Lin W, Wang X, Zhang J, *et al*. A simple, feasible, efficient and safe treatment strategy of sofosbuvir/velpatasvir for chronic HCV/HIV-1 coinfected patients regardless of HCV genotypes: a multicenter, open-label study in China. Lancet Reg Health West Pac. 2023; 36:100749.

65. Wyatt CM. Kidney disease and HIV infection. Top Antivir Med. 2017; 25:13-16.

66. Mwemezi O, Ruggajo P, Mngumi J, Furia FF. Renal Dysfunction among HIV-Infected Patients on Antiretroviral Therapy in Dar es Salaam, Tanzania: A Cross-Sectional Study. Int J Nephrol. 2020; 2020:8378947.

67. Campbell L, Barbini B, Burling K, Cromarty B, Hamzah L, Johnson M, Jones R, Samarawickrama A, Williams D, Winston A, Post FA; FANTA trial team. Safety of tenofovir alafenamide in people with HIV who experienced proximal renal tubulopathy on tenofovir disoproxil fumarate. J Acquir Immune Defic Syndr. 2021; 88:214-219.

68. Stein DK, Pozniak A, Gupta S, Post F, Arribas J, Bloch M, Benson P, Crofoot G, Jiang S, Das M, Fordyce MW. Tenofovir Alafenamide in Participants with Diabetes and Renal Impairment: Renal Safety Through 96 Weeks. *https://www.natap.org/2016/HIV/062116_03.htm* (accessed March 23, 2024).

69. Abbasi AA, Patti R, Ghatak A, Seneviratne C, Kupfer Y, Kamholz S. Tenofovir alafenamide-induced renal tubular acidosis. Am J Ther. 2019; 26:e627-e628.

70. Bahr NC, Yarlagadda SG. Fanconi syndrome and tenofovir alafenamide: A case report. Ann Intern Med. 2019; 170:814-815.

71. Lamarche J, Ibrahim BB, Velez AP, Peguero A, Courville C, Antar M, Taha M. Tenofovir alafenamide and proximal tubule mitochondrial toxicity. *https://cme.kidney.org/spa/nkf2018scm/gallery/abstracts?abstractId=3957bdea-6178-4e56-81f5-f7130c1eefbe* (accessed March 23, 2024).

72. Novick TK, Choi MJ, Rosenberg AZ, McMahon BA, Fine D, Atta MG. Tenofovir alafenamide nephrotoxicity in an HIV-positive patient: A case report. Medicine. 2017; 96:e8046.

73. Serota DP, Franch HA, Cartwright EJ. Acute Kidney Injury in a Patient on Tenofovir Alafenamide Fumarate After Initiation of Treatment for Hepatitis C Virus Infection. Open Forum Infect Dis. 2018; 5:ofy189.

74. Ueaphongsukkit T, Gatechompol S, Avihingsanon A, Surintrspanont J, Iampenkhae K, Avihingsanon Y, Udomkarnjananun S. Tenofovir alafenamide nephrotoxicity: A case report and literature review. AIDS Res Ther. 2021; 18:53.

75. European AIDS Clinical Society. the EACS Guidelines Version 12.0. *https://www.eacsociety.org/media/guidelines-12.0.pdf* (accessed March 23, 2024).

76. Panel on Antiretroviral Guidelines for Adults and Adolescents. Guidelines for the Use of Antiretroviral Agents in Adults and Adolescents with HIV. *https://clinicalinfo.hiv.gov/en/guidelines/hiv-clinical-guidelines-adult-and-adolescent-arv/whats-new* (accessed March 23, 2024).

77. World Health Organization. Consolidated guidelines on HIV prevention, testing, treatment, service delivery and monitoring: Recommendations for a public health approach. *https://www.who.int/publications/i/item/9789240031593* (accessed March 23, 2024)

78. Ray AS, Fordyce MW, Hitchcock MJ. Tenofovir alafenamide: A novel prodrug of tenofovir for the treatment of Human Immunodeficiency Virus. Antiviral Res. 2016; 125:63-70.

*Address correspondence to:
Hongzhou Lu, Department of Infectious Diseases, National Clinical Research Center for Infectious Diseases, Shenzhen Third People's Hospital, Shenzhen 518112, Guangdong Province, China.
E-mail: luhongzhou@fudan.edu.cn

Original Article

NAD(P)H-quinone oxidoreductase 1 induces complicated effects on mitochondrial dysfunction and ferroptosis in an expression level-dependent manner

Jaewang Lee[#], Dong-Hoon Hyun[*]

Department of Life Science, Ewha Womans University, Seoul, South Korea.

SUMMARY NAD(P)H-quinone oxidoreductase 1 (NQO1) is an essential redox enzyme responsible for redox balance and energy metabolism. Despite of its importance, the brain contains high capacity of polyunsaturated fatty acids and maintains low levels of NQO1 expression. In this study, we examined how levels of NQO1 expression affects cell survival in response to toxic insults causing mitochondrial dysfunction and ferroptosis, and whether NQO1 has a potential as a biomarker in different stressed conditions. Following treatment with rotenone, overexpressed NQO1 in SH-SY5Y cells improved cell survival by reducing mitochondrial reductive stress *via* increased NAD$^+$ supply without mitochondrial biogenesis. However, NQO1 overexpression boosted lipid peroxidation following treatment with RSL3 and erastin. A lipid droplet staining assay showed increased lipid droplets in cells overexpressing NQO1. In contrast, NQO1 knockdown protected cells against ferroptosis by increasing GPX4, xCT, and the GSH/GSSG system. Also, NQO1 knockdown showed lower iron contents and lipid droplets than non-transfectants and cells overexpressing NQO1, even though it could not attenuate cell death when exposed to rotenone. In summary, our study suggests that different NQO1 levels may have advantages and disadvantages depending on the surrounding environments. Thus, regulating NQO1 expression could be a potential supplementary tool when treating neuronal diseases.

Keywords NQO1, mitochondrial biogenesis, NAD$^+$, lipid peroxidation, ferroptosis, reductive stress

1. Introduction

Energy metabolism is a vital process for cell survival. Cells generate adenosine triphosphate (ATP) mainly *via* mitochondrial respiration requiring carbon sources and electron donors. Primarily, cells break glucose and glutamine into small molecules, and provide with carbons and transfer electrons in forms of nicotinamide adenine dinucleotide (NADH) or flavin adenine dinucleotide (FADH$_2$), resulting in ATP production in the mitochondria. In rapidly proliferating cells, energy demands are increased to meet growing cellular biomass. Nicotinamide adenine dinucleotide (NAD$^+$) is an important electron carrier for activating energy metabolism, and converted to NADH by acquiring electrons during metabolic processes (*1*). NADH transfers electrons to biomolecules for their activation. NAD$^+$ is a coenzyme for the redox balance and activates non-redox NAD$^+$-dependent enzymes such as sirtuins and poly(ADP-ribose) polymerase (PARP) (*2*). Furthermore, nicotinamide adenine dinucleotide phosphate (NADP$^+$) plays a significant role in cell metabolism such as

oxidative stress (*e.g.*, the GSH/GSSG system) and anabolic pathways (*e.g.*, fatty acid synthesis). Low NAD(P)$^+$ levels are linked to many diseases including metabolic dysfunction and neurodegenerative diseases. Also, mitochondrial dysfunction promoted by metabolic stress exacerbates progressive oxidative damage, resulting in neurodegenerative diseases. A recent study showed that de novo NAD$^+$ synthesis fortified mitochondrial functions and improved health, suggesting that restoring NAD$^+$ levels is a potential therapeutic target for some diseases. These characteristics make NAD$^+$ central to energy metabolism.

NAD(P)H-quinone oxidoreductase 1 (NQO1) is a phase II antioxidant enzyme capable of detoxification and NAD$^+$ supply through two electron transfer without semiquinone radical production (*3*). Increased NQO1 could boost mitochondrial functions (*4,5*). By contrast, NQO1-mediated futile redox cycling of β-lapachone causes oxidative stress by damaging DNA, hyperactivating PARP, and depleting NAD$^+$ and ATP (*6*). β-Lapachone could decrease inositol pyrophosphates by NQO1 (*7*). These results suggest that understanding

two-sided effects of NQO1 is essential to regulate cellular environments properly. However, most studies for a disease therapy are focused on attenuating reactive oxygen species (ROS) levels by increasing NQO1 activity or expression levels.

Ferroptosis is a regulated cell death induced by iron-dependent lipid peroxidation (*8*). Ferroptosis can be caused by inhibiting glutathione peroxidase 4 (GPX4) or system xc⁻ cystine/glutamate antiporter (xCT) (*9*). GPX4 oxidizes glutathione (GSH) and converts lipid peroxyl radicals to lipid alcohols. GPX4 inhibition cannot protect cells against lipid peroxidation following (1S,3R)-RSL3 (RSL3) treatment (*10*). xCT involved in GSH synthesis is another central ferroptosis regulator. Inhibited xCT depletes GSH synthesis in the presence of erastin. GSH deficiency hinders the redox cycle *via* GPX4, and ultimately promotes ferroptosis by decreasing neutralization of lipid peroxyl radicals (*11*). xCT inhibition also attenuates glutamine metabolism and lowers nutrient flexibility (*12*). Acyl-CoA synthetase long-chain family member 4 (ACSL4) increases levels of polyunsaturated fatty acids (PUFAs), raising sensitivity to ferroptosis by increasing lipid peroxidation (*13*). Moreover, high levels of lipid droplets could proportionally elevate susceptibility to ferroptosis because of elevated PUFAs and lipophagy activation (*14*). Meanwhile, epithelial-mesenchymal transition (EMT) shifted glucose-dependent metabolism to lipid-dependent metabolism and increased ferroptosis sensitivity (*14,15*). Increased cellular density in cancers reduced ferroptosis, but cells with mesenchymal traits had enhanced ferroptosis sensitivity (*14,15*). These reports indicate that differentiated or undifferentiated neuronal cells may have different responses to ferroptosis inducers, considering that their morphologies are different, similar to cells with epithelial or mesenchymal characteristics (*16*).

NQO1 as a NAD⁺ supplier or an antioxidant is an important factor in attenuating cellular stress. Still, little has been studied on its adverse effects on neural cells. In this study, effects of NQO1 expression on different environments and its potential as biomarker were examined.

2. Materials and Methods

2.1. Cell culture and reagents

SH-SY5Y cells (ATCC, Manassas, VA, USA) were cultured in Dulbecco's Modified Eagle's Medium supplemented with 10% fetal bovine serum, 1% antibiotic-antimycotic including 100 IU/ml penicillin, 100 μg/ml streptomycin and 0.25 μg/ml amphotericin B in a humidified 5% CO_2/95% air atmosphere. All materials required for cell culture were purchased from Thermo Fisher Scientific (Waltham, MA, USA). Cells were treated with rotenone (Sigma Aldrich, St. Louis,

MO, USA), (1S, 3R)-RSL3 (Cayman Chemical Co., Ann Arbor, MI, USA), or erastin (Selleckchem, Houston, TX, USA). The following is a diagram to show the protocol of the present study (Figure S1, *https://www.biosciencetrends.com/supplementaldata/196*).

2.2. Cell viability and death assays

Cell viability was assessed using the Cell Counting Kit-8 (CCK-8; Dojindo Laboratories, Tokyo, Japan), as described by the manufacturer's protocol. Cells ($1x10^4$ cell/well) were seeded in a 12-well culture plate. Cells at 70% confluency were pretreated with dicoumarol for 2 h, and then exposed to rotenone, RSL3, or erastin. The equivalent amount of dimethyl sulfoxide (DMSO) was used as controls. Cells were incubated with CCK-8 solution for 1 h at 37°C, and absorbance was measured at 450 nm using the SpectraMax M3 microplate reader (Molecular Devices, Sunnyvale, CA, USA). LDH assay was performed using the Cytotoxicity LDH Assay Kit-WST (Dojindo Laboratories), according to the manufacturer's protocol. After treatment for 24 h, the lysis buffer was added to samples, and incubated for 30 min at 37°C. The working solution was treated for 30 min at room temperature (RT), and then the stop solution was added to the mixtures. Absorbance was read at 490 nm. ATP-based cell viability was measured using CellTiter-Glo 2.0 (Promega, Pittsburg, WI, USA). After exposure to rotenone, N-acetyl-L cysteine (NAC; Sigma-Aldrich), or nicotinamide mononucleotide (NMN; Sigma-Aldrich) for 24 h at 37°C, cells were incubated with CellTiter-Glo 2.0 solution for 30 min at RT. Luminescence was measured using the SpectraMax M3 microplate reader. Cell death after rotenone treatment was examined using 5 μM SYTOX Green (Thermo Fisher Scientific). Stained cells were observed using the ECLIPSE Ts2R fluorescent microscope (Nikon, Tokyo, Japan). Dead cells were quantified by counting SYTOX Green-positive cells. For the colony formation assay, cells were seeded 500 cells/well into a 6-well plate. After 14 days in culture, cells were stained with a 0.5% crystal violet solution, and the number of colonies was counted.

2.3. Measurement of GSH, ROS production, lipid ROS, mitochondrial superoxide, and mitochondrial membrane potential

GSH levels were measured using the EnzyChrom GSG/GSSG Assay Kit (BioAssay System, Hayward, CA, USA), according to the manufacturer's procedure. ROS generation was assessed using 10 μM 2′,7′-dichlorofluorescein diacetate (DCFDA; Abcam, Cambridge, UK) following culturing cells with or without rotenone for 8 h. Stained cells were incubated for 30 min at 37°C. Fluorescence was measured using the SpectraMax M3 microplate reader and the CytoFLEX

flow cytometer (Beckman Coulter, Chaska, MN, USA). Lipid ROS was determined by staining cells with 5 μM BODIPY 581/591 C11 (Thermo Fisher Scientific, Waltham, MA, USA). After 30 min at 37°C, intensity was measured by the CytoFLEX flow cytometer. Mitochondrial superoxide was examined using 1 μM MitoSOX (Thermo Fisher Scientific). After 30 min at 37 °C, stained cells were analyzed by the CytoFLEX flow cytometer and ECLIPSE Ts2R fluorescent microscope at 612 nm. Images were quantified using the Image J software. Mitochondria membrane potentials were measured by staining cells with 200 nM tetramethyl rhodamine ethyl ester (Thermo Fisher Scientific) for 20 min. Fluorescence was measured every 2 h using the SpectraMax M3 microplate reader. Mean fluorescent intensity of each group was normalized to that of the control group for quantification.

2.4. Iron measurements

Intracellular iron contents were also quantified using the Iron Assay Kit (Sigma-Aldrich) according to the manufacturer's guide. Intracellular ferrous iron was stained with FerroOrange (Dojindo Laboratories), and mitochondrial ferrous iron levels were assayed using 5 μM Mito-FerroGreen (Dojindo Laboratories). Stained cells were observed by the ECLIPSE Ts2R fluorescent microscope at 546 nm and 455 nm, respectively. Images were quantified using the Image J software.

2.5. RNA interference, transfection, gene overexpression and gene mutation

For NQO1 knockdown, cells were stably transfected with four short hairpin RNAs (shRNAs) targeting *NQO1* mRNA (pGPU6/Neo, GenePharma, Shanghai, China) using Lipofectamine 3000 reagent (Thermo Fisher Scientific). NQO1 expression levels were confirmed by immunoblot analysis, and the #4 construct was chosen (Table 1 and Figure S2D, *https://www.biosciencetrends. com/supplementaldata/196*). For NQO1 overexpression, pUCIDT(Amp)-NQO1 (Integrated DNA Technologies, Coralville, IA, USA) was digested by Hind III and Not I, and NQO1 fragment was inserted into pcDNA3.1(+) mammalian expression vector (Thermo Fisher Scientific). Cells were seeded and stably transfected with a control plasmid (Thermo Fisher Scientific) or pcDNA3.1-NQO1 plasmid using Lipofectamine 3000 reagent. For designing the mutant form, the mutation site was determined according to a previous report (*17*). The NQO1^{Y128F} mutant construct was designed using EZchange Site-Directed Mutagenesis Kit (Enzynomics, Daejeon, South Korea) according to the manufacturer's procedure. The mutation was ordered and confirmed by DNA sequencing (Macrogen, Seoul, South Korea). NQO1 expression levels were confirmed by immunoblot analysis.

Table 1. The sequences of RT-qPCR primers and shRNAs targeting *NQO1*

Name	Sequences
MDH1	F: 5'-CCAGGGTGCAGCCTTAGATA-3
	R: 5'-TGAAGTTCTCCTTGGGGATG-3'
MDH2	F: 5'-GGTTTCCATCAGTGGCCTAA-3'
	R: 5'-TTCAGAGGCCACAGTGTCTG-3'
NQO1	F: 5'-GTTGCCTGAAAAATGGGAGA-3'
	R: 5'-AAAAACCACCAGTGCCAGTC-3'
ACTB	F: 5'-CTCTTCCAGCCTTCCTTCCT-3'
	R: 5'-AGCACTGTGTTGGCGTACAG-3'
LDHA	F: 5'-TGGCAGCCTTTTCCTTAGAA-3'
	R: 5'-CTTTCTCCCTCTTGCTGACG-3'
LDHB	F: 5'-TGTGAATGTGGCAGGTGTTT-3'
	R: 5'-GGCACTTTCAACCACCATCT-3'
GOT2	F: 5'-GTCCTCCCATCTTGGAACAA-3'
	R: 5'-GCATTATTTCCCTTGCTGGA-3'
FH	F: 5'-TGACAAGGCAGCAAAGATTG-3'
	R: 5'-ACCCATTCGTCAAACTGCTC-3'
SDHA	F: 5'-GATTACTCCAAGCCCATCCA-3'
	R: 5'-GTTTTGTCGATCACGGGTCT-3'
SDHB	F: 5'-CAATGAACATCAATGGAGGC-3'
	R: 5'-CTTGCCTTCCTGAGATTCAT-3'
OGDH	F: 5'-ACTGGCTGCTCTGTCTTGGT-3'
	R: 5'-CCCTCTTCTGACCTGCTTTG-3'
ACO2	F: 5'-GAAATTGAGCGAGGCAAGTC-3'
	R: 5'-CAGATGGTCACAGTGGATGG-3'
CPT1A	F: 5'-TCGTCACCTCTTCTGCCTTT-3'
	R: 5'-GGGGTCTGGCTTGTTGATAA-3'
GLS2	F: 5'-GTGCACTGTGGATGGTCAAC-3'
	R: 5'-GTGCCTAGGGTGCTTATGGA-3'

shRNA sequences

#1	S: 5'-CACCGGTTTGAGCGAGTGTTCATAGTTCAAGA GACTATGAACACTCGCTCAAACCTTTTTTG-3'
	A: 5'-GATCCAAAAAAGGTTTGAGCGAGTGTTCATA GTCTCTTGAACTATGAACACTCGCTCAAACC-3'
#2	S: 5'-CACCGCAGACGCCCGAATTCAAATCTTCAAGA GAGATTTGAATTCGGGCGTCTGCTTTTTTG-3'
	A: 5'-GATCCAAAAAAGCAGACGCCCGAATTCAAAT CTCTCTTGAAGATTTGAATTCGGGCGTCTGC-3'
#3	S: 5'-CACCGCAGCCTCTTTGACCTAAACTTTCAAGA GAAGTTTAGGTCAAAGAGGCTGCTTTTTTG-3'
	A: 5'-GATCCAAAAAAGCAGCCTCTTTGACCTAAACT TCTCTTGAAAGTTTAGGTCAAAGAGGCTGC-3'
#4	S: 5'-CACCGGCCAATTCAGAGTGGCATTCTTCAAGA GAGAATGCCACTCTGAATTGGCCTTTTTTG-3'
	A: 5'-GATCCAAAAAAGGCCAATTCAGAGTCGCATT CTCTCTTGAAGAATGCCACTCTGAATTGGCC-3'

2.6. Reverse transcription-quantitative PCR and immunoblot analysis

When cells were 70% confluent, they were treated with indicated drugs. According to the manufacturer's instructions, total RNA from treated cells were extracted using QIAwave RNA Mini Kit (Qiagen, Venlo, Netherlands). Reverse transcription-quantitative polymerase chain reaction (RT-qPCR) was conducted using AccuPower 2X GreenStar^{TM} qPCR Master Mix with 80X ROX (Bioneer, Daejeon, South Korea) after performing complementary DNA (cDNA) synthesis using AccuPower RT-PCR PreMix & Master Mix (Bioneer). *NQO1*, *LDHA*, *LDHB*, *CPT1A*, *MDH1*,

MDH2, *FH*, *SDHA*, *SDHB*, *OGDH*, *ACO2*, *GLS2*, *GOT2*, and *ACTB* (Table 1) were amplified. Relative target mRNA levels were determined using the $2^{-(\Delta\Delta Ct)}$ method, and normalized against *ACTB* mRNA levels. mRNAs levels were confirmed by the StepOnePlus (Applied Biosystems, Foster City, CA, USA). For immunoblot analysis, cells were lysed using Cell Lysis Buffer (Cell Signaling Technology, Danvers, MA, USA) containing a protease/phosphatase inhibitor cocktail (Cell Signaling Technology). Cell lysates were resolved using 6%–15% SDS gels, separated proteins were transferred to nitrocellulose membranes, and then probed with appropriate primary and secondary antibodies. Following primary antibodies were used: NQO1, Nrf2 and Keap1 were purchased from GeneTex (Irvine, CA, USA); PGC-1α, SIRT1, xCT, NDUFA9, SDHB, UQCRC2, COX IV, ATP5A, aconitase 2, MnSOD, FTH1, NCOA4 and GPX4 from Abcam (Cambridge, UK); SIRT3 and E-cadherin from Thermo Fisher Scientific; PARP from Cell Signaling; ACSL4 and vimentin from Santa Cruz Biotechnology (Dallas, TX, USA); and FPN and Tfr from Novus Biologicals (Littleton, CO, USA). Antibodies against α-tubulin (GeneTex, Irvine, CA, USA) or β-actin (BioWorld, Atlanta, GA, USA) were served as total loading controls. All antibodies were diluted to concentrations between 1:500 and 1:30,000.

2.7. Measurement of NAD⁺/NADH ratio

When cells had grown to 70% confluency, $NAD^+/NADH$ ratio was measured using $NAD^+/NADH$ Assay Kit (Abcam), according to the manufacturer's instructions. $NAD^+/NADH$ ratio was determined by subtracting NADH from total NAD followed by dividing the product by NADH. Relative quantities of the $NAD^+/NADH$ ratio among groups were normalized against the control.

2.8. Measurement of malondialdehyde (MDA)

When cells had grown to 70% confluency, cells were treated with rotenone, RSL3, or erastin with indicated doses for 12 h. Cells were lysed to measure levels of lipid peroxidation using Malondialdehyde (MDA) Assay Kit (Abcam), according to the manufacturer's procedures.

2.9. Measurement of mitochondria complex I activity

When cells had grown to 90% confluency, mitochondrial fractions were isolated using Mitochondria Isolation Kit for Cultured Cells (Abcam). The mitochondria complex I activity was measured using the Mitochondrial Complex I activity Assay Kit (Sigma Aldrich), according to the manufacturer's procedures.

2.10. Staining of the mitochondria and lipid droplets

Cells were stained with 5 µM MitoTracker Red CMXRos (Thermo Fisher Scientific) to confirm mitochondrial change and obtained images were quantified using Image J software. Cells were stained with BODIPY 493/503 (Thermo Fisher Scientific) to observe lipid droplets, and lipid droplets were counted for quantification.

2.11. Statistical analysis

Data were presented as average ± standard error of means (SEM) after Kolmogorov-Smirnov test. Statistically significant differences between treatment groups were assessed using the Mann-Whitney *U*-test or analysis of variance (ANOVA) with the Bonferroni post-hoc test. All statistical tests were two-sided, and a *P* value of < 0.05 was statistically significant. The statistical tests were performed using IBM SPSS Statistics version 22.0 (IBM, Armonk, NY, USA).

3. Results

3.1. NQO1 overexpression does not change cellular ROS levels and expression of metabolic enzymes

NQO1 plays a significant role in cell survival by providing $NAD(P)^+$ and maintenance of redox homeostasis (Figure 1A), but SH-SY5Y cells tend to express low NQO1 levels (*18*). NQO1 was stably
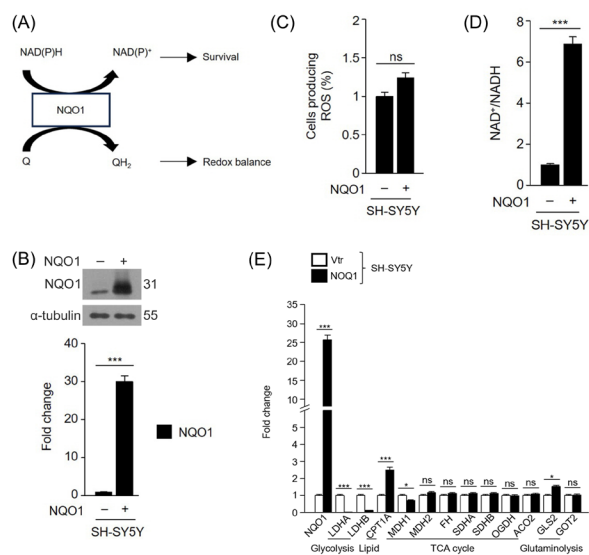
Figure 1. NQO1 overexpression increases NAD⁺ but decreases basal ROS levels. (A) A schematic image of NQO1 functions. **(B)** Expression levels of NQO1 mRNA in SH-SY5Y with or without NQO1 transfection were confirmed using RT-qPCR and immunoblot analysis. **(C)** NAD⁺/NADH ratio was measured by NAD⁺/NADH assay in SH-SY5Y in the presence or absence of NQO1 transfection. **(D)** Cellular basal ROS levels were measured vis FACS using DCFDA for 20 min and then quantified. **(E)** Basal mRNA levels of metabolic proteins in vector control and NQO1 transfectant were examined using RT-qPCR. The results were normalized to vector control. Values are average ± SEM from three independent experiments. ns; not significant. *$P < 0.05$, ***$P < 0.001$ relative to their parental cells.
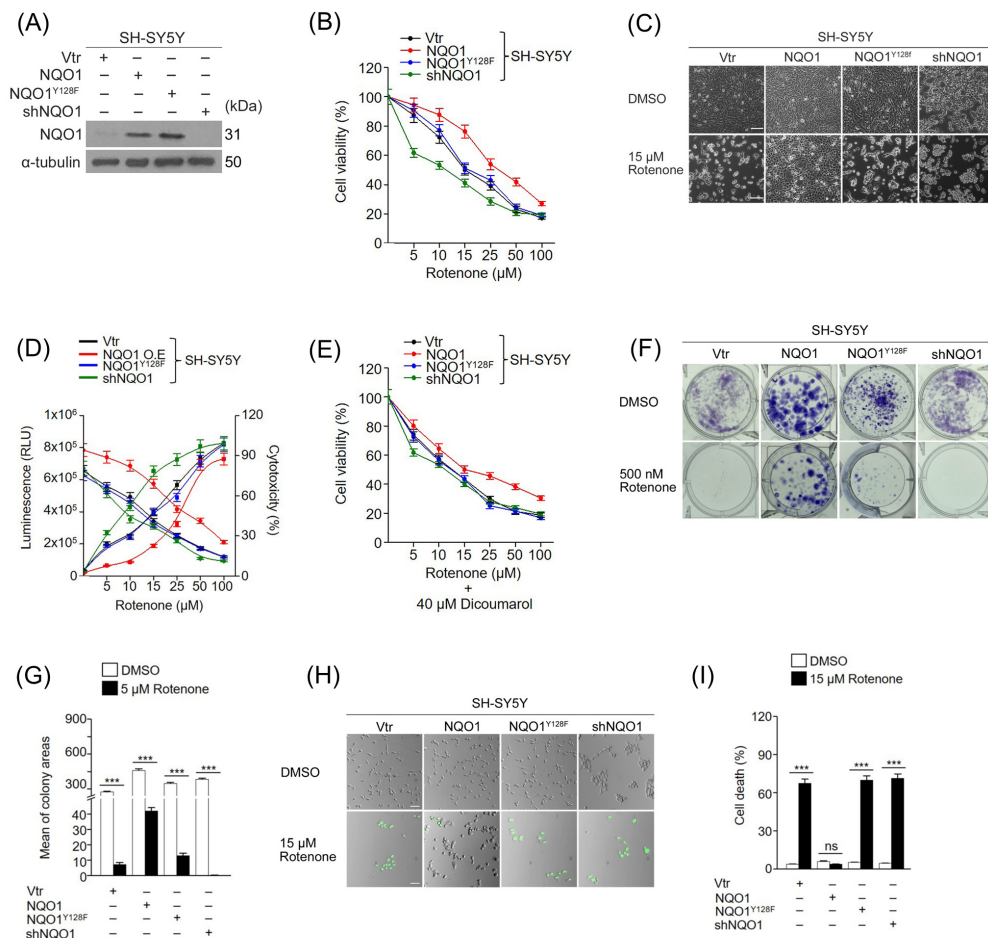
Figure 2. NQO1 protects cells from toxic insults. (A) NQO1 overexpression, NOQ1[Y128F] mutant form, and NOQ1 knockdown were confirmed by immunoblot analysis. **(B)** Cell viability was measured following exposure to rotenone with indicated doses for 24 h. **(C)** Cell morphological images were captured by a bright-field microscope after addition of 15 μM rotenone. Original magnification, x100. Scale bar size, 100 μm. **(D)** ATP-based cell viability assay was measured by CellTiter-Glo. Cytotoxicity was measured by LDH assay. **(E)** Cell viability change was determined after rotenone addition to cells pretreated with 40 μM dicoumarol. **(F, G)** The clonogenic assay using 0.5% crystal violet was assessed after cells cultured with or without 5 μM rotenone. Colony areas were quantified using the Image J software. **(H, I)** Cell death was assessed using 5 μM SYTOX green following treatment of cells were with 15 μM rotenone for 24 h. Stained cells show dead cells. Stained images were quantified using the Image J software. Original magnification, x100. Scale bar size, 100 μm. Data are average ± SEM from three independent experiments. ns; not significant. ***$P < 0.001$ relative to DMSO treatment.

overexpressed (Figure 1B). NAD$^+$/NADH ratio in cells overexpressing NQO1 was increased compared with that in non-transfectants ($P < 0.001$) (Figure 1C). Total ROS levels were increased in cells transfected with NQO1 compared with those in control cells (Figure 1D). RT-qPCR results showed that levels of *LDHA* and *LDHB* were decreased, but *GLS2* (a glutaminolysis-related protein) and *CPT1A* (a fatty acid oxidation-related protein) increased in cells with high NQO1 levels. However, levels of cycle-related proteins were not significantly changed ($P < 0.05$, Figure 1E).

3.2. NQO1 protects SH-SY5Y cells against rotenone

Cells transfected with NQO1[Y128F] or shNQO1 were designed to compare cell survival under conditions of interference with energy metabolism (Figure 2A). Cell viability results showed that NQO1 overexpression rendered cells more resistant to rotenone than control

cells (Figure 2B-D). Pretreatment with dicoumarol greatly affected viability of NQO1-overexpressing cells after exposure to rotenone (Figure 2E). To confirm long-term effects of low doses of rotenone on cells, the colony formation test was performed. Colony formation results showed that NQO1 overexpression made cells less susceptible to rotenone than controls ($P < 0.001$, Figure 2F-G). In parallel, cell death was significantly attenuated in NQO1-overexpressing cells when exposed to rotenone, compared with others ($P < 0.001$, Figure 2H-I).

3.3. NQO1 inhibition increases GSH/GSSG dependency

Because oxidative stress is caused when the mitochondria complex I is inhibited by rotenone (*19*), ROS levels were measured by DCFDA staining, total GSH and GSH levels were assessed. NQO1-knockdown cells showed higher DCFDA staining. On the contrary, NQO1-
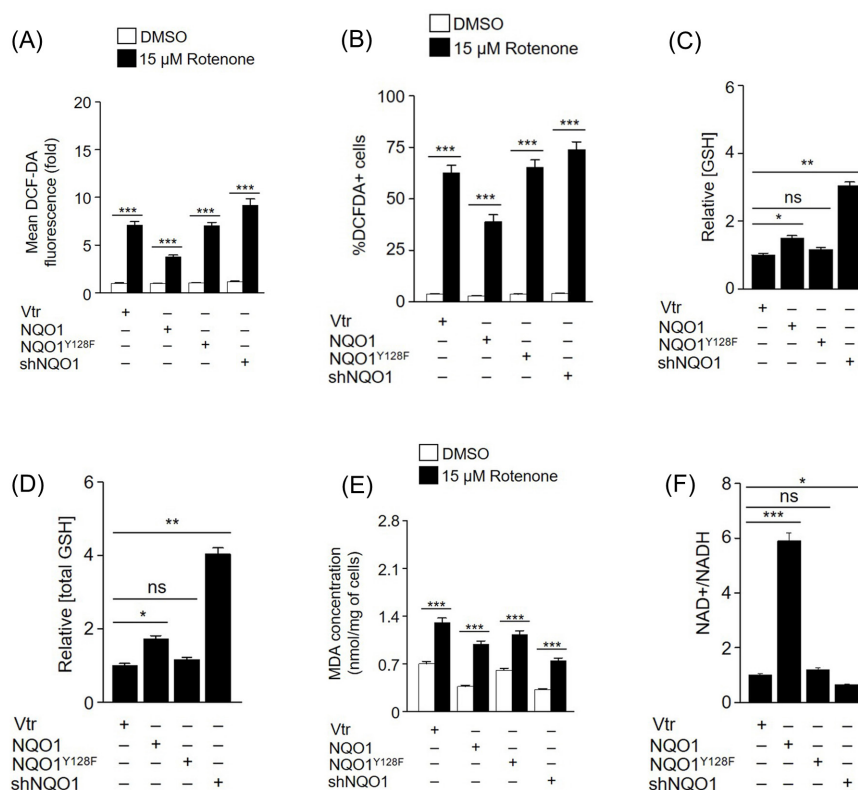
Figure 3. NQO1 knockdown increases GSG/GSSG dependency. **(A, B)** Cellular ROS levels were measured after cells were treated with 15 μM rotenone for 8 h and then were stained in 5 μM DCF-DA for 30 min. **(C, D)** GSH and total GSH levels under normal conditions were determined. **(E)** Cellular MDA contents were measured to determine lipid peroxidation after addition of 15 μM rotenone. **(F)** NAD$^+$/NADH ratio was measured by the NAD$^+$/NADH assay with no treatment. Values are average ± SEM from three independent experiments. ns; not significant; *$P < 0.05$, **$P < 0.01$, ***$P < 0.001$ relative to DMSO treatment or vector control.

overexpressing cells showed lower DCFDA staining ($P < 0.01$, Figure 3A-B). There was no significant difference among control, NQO1^{Y128F}, and NQO1 knockdown. Interestingly, both GSH levels were higher in NQO1-knockdown cells ($P < 0.05$, Figure 3C-D). Also, NQO1-knockdown cells showed lower MDA concentration when rotenone was added ($P < 0.001$, Figure 3E). NQO1 overexpression induced higher NAD$^+$/NADH ratio, but NQO1 knockdown lower ($P < 0.05$, Figure 3F).

3.4. NQO1 overexpression does not boost mitochondrial biogenesis but decreases reductive stress by supplying NAD$^+$

In order to confirm which of NQO1 functions (a NAD$^+$ provider and an antioxidant) is important for cell survival under conditions of rotenone treatment, ATP-based cell viability was performed using NAC (an antioxidant) and NMN (a NAD$^+$ precursor), respectively. Cell viability was higher in NMN-treated groups than in NAC-treated ones. Cell viability results implied that ATP production was higher after NMN addition compared to NAC treatment ($P < 0.05$, Figure 4A). This difference would be due to NAD$^+$ supply ($P < 0.05$, Figure 4B). The GSH-GSSG system can protect cells from ROS but cannot directly boost or maintain mitochondrial activity in the

presence of rotenone ($P < 0.05$, Figure 4C).

Considering previous studies showed that increasing NQO1 could increase mitochondrial activity (*20*) and NAD$^+$ produced by NQO1 could promote mitochondrial biogenesis by activating the PGC-1α-SIRT1 axis (*21*), the extent of mitochondrial biogenesis in cells with control, NQO1 overexpression, NQO1^{Y128F}, or shNQO1 were determined. Immunoblot results showed that levels of PGC-1α were increased in NQO1-overexpressing cells compared with others. Likewise, PGC-1α levels were decreased in NQO1 knockdown cells. SIRT3 (a critical molecule involved in mitochondrial biogenesis) levels were not significantly changed among all groups. SIRT1 was higher in NQO1 knockdown cells. PARP (a NAD$^+$-consuming protein) levels were also dramatically elevated in both NOQ1-overexpressing cells and NQO1-knockdown cells. Immunoblot analysis for confirming oxidative stress showed that Nrf2 levels were increased and Keap1 levels were decreased slightly in NOQ1-overexpressing cells and NQO1-knockdown cells. Levels of all NAD$^+$-consuming proteins were increased in both NQO1-overexpressing cells and NQO1-knockdown cells (Figure 4D).

Levels of ETC proteins among all groups were measured to observe whether expression levels of mitochondrial proteins involved in oxidative
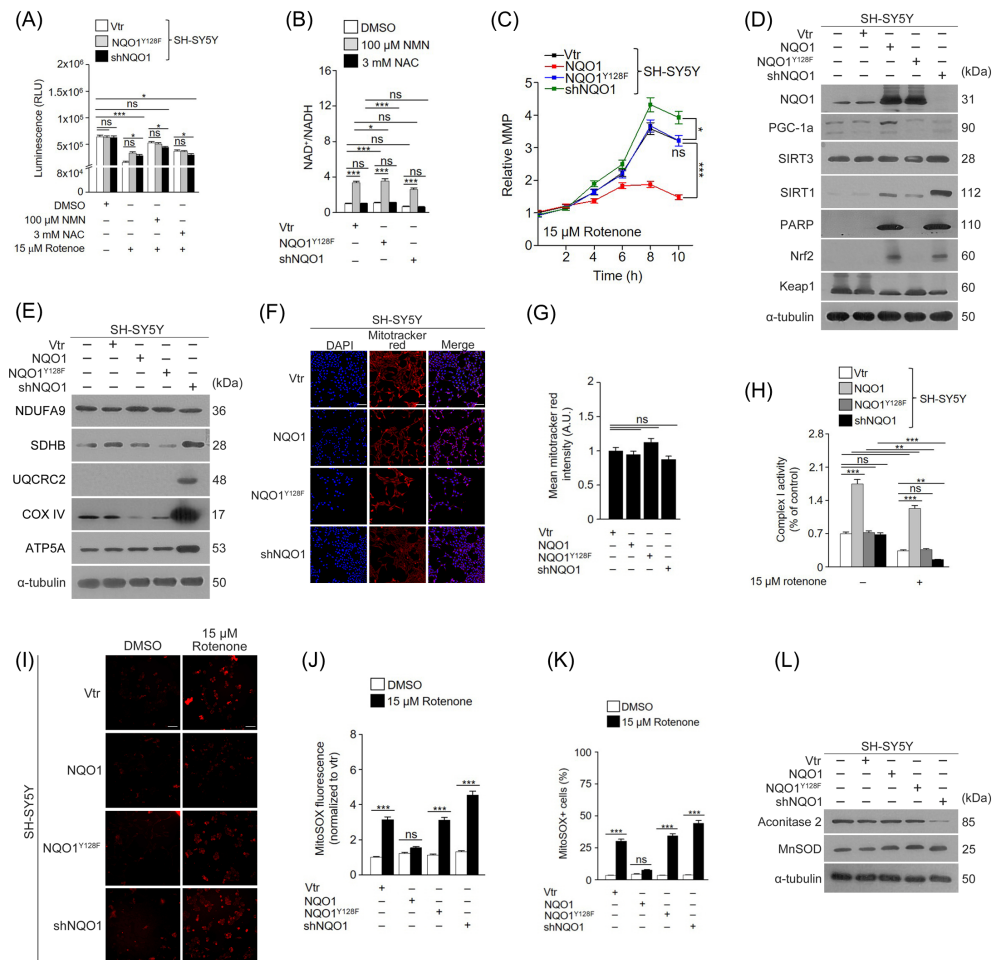
Figure 4. Biogenesis is not the main factor of cell survival under conditions of complex I inhibition. (A) ATP levels were indirectly measured using CellTiter-Glo after cells were subjected to 15 μM rotenone, 100 μM NMN, and 3 mM NAC for 24 h. **(B)** NAD$^+$/NADH ratio was measured after treatment with 15 μM rotenone, 200 μM NAM, and 3 mM NAC for 24 h. **(C)** Mitochondrial activity was determined using MMP following exposure of cells to 15 μM rotenone. **(D, E)** Levels of proteins responsible for mitochondrial biogenesis were assessed by immunoblot analysis. **(F, G)** The mitochondria were visualized by staining cell with 5 μM MitoTracker Red for 20 min, and their fluorescent images were quantified using the Image J software. Original magnification, x 200. Scale bar size, 50 μm. **(H)** The complex I activity was measured after being treated with 15 μM rotenone for 24 h to examine mitochondrial complex I efficiency. **(I, K)** Mitochondrial superoxide production was measured by FACS using 1 μM MitoSOX for 30 min after 15 μM rotenone treatment for 8 h. Intensity was quantified using the Image J software. Original magnification, x200. Scale bar size, 50 μm. **(L)** Mitochondrial stress was determined by immunoblot analysis. Data are average ± SEM from three independent experiments. ns; not significant. *$P < 0.05$, **$P < 0.01$, ***$P < 0.001$ relative to DMSO treatment or vector control group.

phosphorylation were changed. NDUFA9 levels were slightly increased in cells overexpressing NQO1 compared with control cells. Levels of SDHB, UQCRC2, and ATP5A in NQO1-overexpressing cells were not significantly changed compared with control cells (Figure 4E and Figure S3A, *https://www.biosciencetrends.com/ supplementaldata/196*). In contrast, levels of SDHB, UQCRC2, and ATP5A were significantly increased in NQO1-knockdown cells compared with others. NQO1 downregulation tended to decrease NDUFA levels. In particular, COX IV levels were greatly increased by NQO1 knockdown, but decreased by NQO1 overexpression (Figure 4E). Meanwhile, LDHA mRNA levels were increased in cells overexpressing NQO1 (Figure S3D, *https://www.biosciencetrends.com/ supplementaldata/196*).

Examination of mitochondrial iron (a gist molecule of the iron-sulfur cluster) contents showed that Mito-FerroGreen fluorescence intensity was not significantly changed between control cells and NQO1-overexpressing cells. However, Mito-FerroGreen fluorescence intensity was decreased in NQO1-knockdown cells ($P < 0.01$, Figure S3B-C, *https://www.biosciencetrends.com/ supplementaldata/196*). Furthermore, MitoTracker staining images indirectly showed that the number of mitochondria was not significantly different among all groups (Figure 4F-G). On the contrary, NQO1-overexpressing cells maintained highed complex I activity compared with other groups ($P < 0.01$, Figure 4H).

MitoSOX results indicated that mitochondrial ROS levels were lowered by NQO1 overexpression, but raised by NQO1 knockdown after exposure to rotenone ($P < 0.05$) (Figure 4I-K). Immunoblot analysis showed that
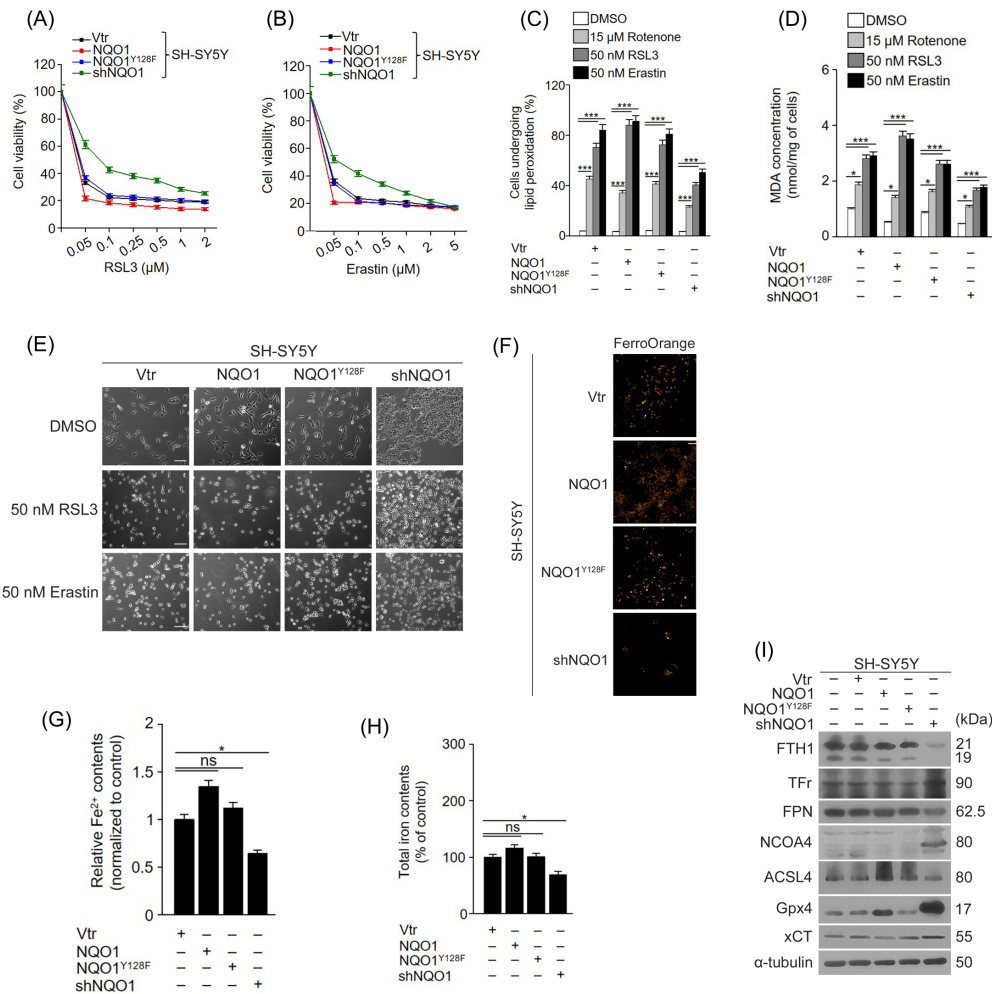
Figure 5. NQO1 knockdown reduces sensitivity to ferroptosis. (A, B) Cell viability change was assessed following treatment with RSL3 and erastin with indicated doses for 24 h. **(C)** Levels of lipid peroxyl were measured via FACS after cells were treated with 15 μM rotenone, 50 nM RSL3, and 50 nM erastin for 8 h and then stained with 5 μM BODIPY C-11 for 30 min. **(D)** Cellular MDA contents were measured following addition of 15 μM rotenone, 50 nM RSL3, or 50 nM erastin. **(E)** Bright-field microscope images after 50 nM RSL3 or 50 nM erastin treatment. Original magnification, x200. Scale bar size, 50 μm. **(F, G)** Cells were stained with 5 μM FerroOrange dye for 20 min to visualize relative ferrous iron levels, and fluorescent images were quantified by Image J software. Original magnification, x100. Scale bar size, 100 μm. **(H)** Cellular total iron contents were measured. **(I)** Expression of ferroptosis-related proteins under normal conditions was determined by immunoblot analysis were performed. Values are average ± SEM from three independent experiments. ns; not significant. *$P < 0.05$, **$P < 0.01$, ***$P < 0.001$ relative to DMSO treatment or vector control.

under normal culture conditions, aconitase 2 levels were decreased and MnSOD levels were increased in NQO1 knockdown. However, aconitase 2 levels were not changed, and MnSOD2 levels were increased by NQO1 overexpression.

3.5. NQO1 knockdown endows cells with resistance to ferroptosis

When treated with RSL3 or erastin, a GPX4 inhibitor and an xCT inhibitor, respectively, cell viability was the highest in NQO1-knockdown cells at all indicated doses (except for 5 μM erastin) compared with others (Figure 5A-B). In addition, levels of lipid ROS ($P < 0.001$) and MDA ($P < 0.05$) were lower in cells with downregulated NQO1 (Figure 5C-D). Bright-field images showed

responses to ferroptosis inducers (Figure 5E). Levels of ferrous iron (Fe^{2+}) and total iron were lower in NQO1-knockdown cells compared with others ($P < 0.05$, Figure 5F-H). Immunoblot analysis related to ferroptosis showed that expression levels of FTH1, ACSL4, and FPN were decreased in NQO1-knockdown cells compared with others (Figure 5I). However, Tfr, NCAO4, GPX4, and xCT levels were higher in cells with downregulated NQO1 than others. Moreover, NQO1-knockdown cells included a smaller number of lipid droplets compared with others ($P < 0.01$, Figure S4A-B, *https://www.biosciencetrends.com/supplementaldata/196*).

4. Discussion

Mitochondrial dysfunction is found at the early stage in

many neurodegenerative diseases. Under undesirable environments, cells can survive through metabolic shift and a compensatory mechanism such as activation of plasma membrane (PM) redox enzymes. Previous studies revealed that upregulated PM redox enzymes (*e.g.*, NQO1, cytochrome b5 reductase) promoted mitochondrial functions under conditions of metabolic and proteotoxic stresses (*22*). These results emphasize the importance of PM redox enzymes in response to various toxic conditions. However, previous studies were focused on boosting NQO1 without considering whether low NQO1 levels benefit cells or what are benefits NQO1 offers to cells despite its low expression in neuronal cells.

This study demonstrated that SH-SY5Y cells could respond differently to toxic insults depending on NQO1 levels (Figure S1, *https://www.biosciencetrends.com/supplementaldata/196*). As described at the previous study (*20*), increased NQO1 reduced susceptibility to inhibition of the mitochondrial complex I. Although the GSH/GSSG system was significantly increased in NQO1-knockdown cells, ROS levels were still higher in NQO1-knockdown cells following rotenone treatment, compared with others (Figure 3A-B). This means that an antioxidant function of NQO1 might not be the most crucial factor for survival under complex I inhibition. This result suggests to consider another function of NQO1 as a key factor for cell survival in response to complex I inhibition. In addition, dramatic decreased levels of cellular ROS were not observed in cells overexpressing NQO1. Instead, cellular ROS levels were increased in both NQO1-overexpressing cells and NQO1-knockdown cells compared to those in control cells, even though there was no significant difference between them, possibly due to mild cellular stress. Assessment of GSH levels and immunoblot analysis using antibodies against Nrf2 and Keap1 supported that mild oxidative stress was continuous in both NQO1-overexpressing cells and NQO1-knockdown cells (Figure 3C and Figure 4D). Considering that NAD^+ is a primary energy carrier in the mitochondria and NQO1 functions as an NAD^+ provider, increased cellular ROS is likely due to elevated electron transport in the mitochondria through increased NAD^+ levels in NQO1-overexpressing cells and due to reductive stress generated from decreased NAD^+/NADH ratio in NQO1-knockdown cells (Figure 3F) (*23*). It may be unusual that decreased NQO1 reduced NAD^+/NADH because high GSH contents mean increased $NAD(P)^+$ levels (*24*), but it can be assumed that an available and absolute amount of NAD^+ for the mitochondria may be diminished to maintain the GSH/GSSG cycle against increased ROS levels. Interestingly, highly increased NQO1 levels did not change expression levels of central metabolic proteins in the mitochondria. Instead, levels of glycolysis-related proteins were decreased and those of lipid metabolism-related proteins were increased. A meta-analysis of human metabolism showed that NAD^+ precursor supplementation activated lipid metabolism (*25*). This metabolic change seemed to be an action to prevent cell death and store energy sources because excessive ATP can induce apoptosis (*26*), consistent with increased levels of proteins responsible for lipid metabolism and lipid droplets (Figure 1E and Figure S4A-B, *https://www.biosciencetrends.com/supplementaldata/196*). By contrast, NQO1-knockdown cells exhibited increased aerobic glycolysis because increased demand for NAD^+ can promote aerobic glycolysis and decrease proliferation (*27*). Moreover, NQO1-knockdown cells showed morphological alterations, similar to epithelial cells or undifferentiated forms. NQO1 knockdown induced decreased proliferation rate compared with others, and ATP production was decreased as if dormant. These results are consistent with a previous study.

Meanwhile, NQO1 knockdown made cells more sensitive to complex I inhibition because of declined NAD^+ supply, but ROS levels were not significantly changed compared with control and NQO1^{Y128F} cells. NOQ1 knockdown boosted the GSH/GSSG system to compensate for NQO1 deficiency. Intriguingly, NQO1-knockdown cells showed lower MDA production compared with others, meaning that NQO1 knockdown reduced lipid peroxidation. Because cellular ROS can increase lipid peroxidation and MDA is a final product of lipid peroxidation (*28*), this result suggests that NQO1 knockdown in neuronal cells might be beneficial in response to ferroptosis. Thus, resistance to ferroptosis was compared among control, NQO1 overexpression, NQO1^{Y128F}, and NQO1-knockdown cells. The result showed that NQO1 downregulation attenuated ferroptosis compared with other cells. Interestingly, NQO1-knockdown cells contained lower levels of iron and lipid droplets than other cells. Levels of FTH1 and FPN were decreased, but those of Tfr and NCOA4 increased by NQO1 downregulation. Decreased FTH1 and FPN and increased Tfr indicate that cells were exposed to iron deficiency (*29*). Increased NCOA4 showed that cells tried to store iron because decreased NCOA4 activated ferritinophagy to increase cellular iron levels (*30*). Immunoblotting results indicate that NQO1-knockdown cells were undergoing iron starvation responses. Although the exact reason was not assessed, decreased iron content is likely linked to reduced proliferation because proliferation requires more iron to make iron-sulfur clusters for producing new enzymes (*31,32*). Increased proliferation of cells overexpressing NQO1 is because of c-fos stabilization by NQO1 (*33*). Thus, decreased proliferation of NQO1-knockdown cells might result from the degradation of c-fos (*33*). Also, increased GPX4 and xCT and decreased ACSL4 in NQO1-knockdown cells would be the key factor in reducing ferroptosis when treated with RSL3 and erastin (*34*). Especially, decreased ACSL4 would explain why NQO1-knockdown cells preferred settlement to moving

because PUFAs are associated with increased membrane fluidity (*35*), and necessary for cellular migration because of their low rigidity (*14,36*). Moreover, morphological changes and expression levels of EMT-related molecules support that their different responses to ferroptosis are resulted from changes in cell characteristics because decreased e-cadherin can increase ferroptosis sensitivity (Figure S2A-D, *https://www.biosciencetrends.com/supplementaldata/196*) (*15*). In NQO1-knockdown cells, increased e-cadherin induced a partial EMT-like state, endowing cells with more resistance to ferroptosis than cells with low e-cadherin. Maintenance of the antioxidant system is especially important in neurons because of their low capacity of antioxidants (*18*). In this regard, high expression levels of xCT and GPX4 might help to boost the GSH/GSSG system in NQO1-knockdown cells to protect cells from ROS. Considering that many neurodegenerative diseases are related to oxidative stress generated by iron-dependent metabolic dysfunction (*37*), changes in the antioxidant system might be an evolutionary legacy to avoid ferroptosis. In contrast, NQO1 overexpression made cells susceptible to ferroptosis. Increased NQO1 decreased xCT levels because NQO1 can inhibit xCT *via* interacting with p53 (*38*). Increased sensitivity to ferroptosis in NQO1-overexpressing cells is resulted from increased content of iron and lipid droplets. However, iron levels in NQO1-overexpressing cells showed no significant difference compared to those of control cells, meaning that increased sensitivity to ferroptosis is caused by high PUFA contents, consistent with elevated ACSL4 (*34*). Increased PUFAs can promote lipid peroxidation, especially when ferroptosis inducers are existed. Although GPX4 levels were increased in NQO1-overexpressing cells compared with those of control cells, elevated lipid droplets and iron content might promote ferroptosis, causing lipid peroxidation to exceed the cellular capacity of dealing with ROS regardless of NQO1 and GPX4. Even decreased xCT levels would lower GPX4 synthesis (*39*).

Initially, it can be assumed that when NQO1 is overexpressed, mitochondrial biogenesis would be the main factor in cell survival under conditions of mitochondrial complex I inhibition because NAD^+ stimulates the SIRT1-PGC-1α axis (a critical factor for mitochondrial biogenesis) (*40*). However, evidence for mitochondrial biogenesis despite overexpressing NQO1 could not be found. Given that mitochondrial complex I inhibition can induce reductive stress (*41*), cellular protective effects would be because increased NQO1 supplies more NAD^+ and blocks reductive stress induced by mitochondrial complex I inhibition, but not induced by mitochondrial biogenesis. Meanwhile, NAD^+ was mostly consumed by PARP because the affinity of PARP to NAD^+ is higher than that of NQO1 (*42*), meaning that PARP suppression is necessary to increase mitochondrial biogenesis. This phenomenon would be an action to

reduce energetic stress responses because increased NAD^+ can cause energy deficiency (*43*). Although the exact reason why cells evolutionarily allow PARP to exhaust more NAD^+ than SIRT1 is not known, it can be guessed that mostly exhausting NAD^+ by PARP might help them to be ready to repair DNA damage and to inhibit excessive biogenesis due to a limited cellular capacity. Surprisingly, NOQ1 knockdown also increased SIRT1 and PARP expression. Considering that levels of lactate and LDHA were increased (Figure 2D and Figure S3D, *https://www.biosciencetrends.com/supplementaldata/196*) in NOQ1-knockdown cells, this might be due to the enhanced feedback for ATP demand and cellular stress from increasing lactate. Deficient ATP activates the AMPK-SIRT1 axis (*44*), and high lactate levels increase PARP expression (*45*). In addition, unexpectedly, levels of ETC proteins were increased in cells with downregulated NQO1 compared with NQO1-overexpressing cells. Since PGC-1α was not changed but SIRT3 increased, this response might occur due to shortage of NAD^+ supply. Because neurons lack metabolic plasticity (*46*) and increased glycolytic rate or glycogen synthesis can cause apoptosis (*47*), increased ETC proteins in NQO1-knockdown cells may be rebound responses to offset effects of decreased NAD^+ supply and replenished ATP. Moreover, increased *LDHA* mRNA and GSH might help cells recycle NAD^+ for respiration. Mitochondrial superoxide levels were lower under conditions of complex I inhibition, which supports that reductive stress was not increased in NQO1-overexpressing cells compared with others.

Taken together, cellular NQO1 levels have pros and cons. Many studies mainly focused on beneficial effects of increased NQO1 because of lower NQO1 expression in neurons. In addition, increased NQO1 protects cells from mitochondrial dysfunction. However, our results show that both NQO1 overexpression and NQO1 knockdown have advantages and disadvantages. NQO1 overexpression is advantageous to maintaining mitochondria-related functions when complex I is inhibited, but disadvantageous when exposed to ferroptosis inducers. NQO1 knockdown showed the opposite results against NQO1 overexpression. NQO1 knockdown has merits of inhibiting ferroptosis, although it has demerits of mitochondrial dysfunction. This means that different approaches should be used to treat neurodegenerative diseases in an NQO1 level-dependent manner.

There are several limitations to this study. Firstly, why increasing NQO1 led to accumulating lipid droplets could not be elucidated. Secondly, further experiments for lipid metabolites and lipid metabolism should be performed. Thirdly, whether changing different NAD^+-generating proteins produces same results needs to be assessed. Nonetheless, our study is worthwhile in noting that NQO1 can be a potentially useful target in an environment-dependent manner.

In conclusion, this study suggests that NQO1 levels can lead to different responses to complex I inhibition or ferroptosis inducers in neural cells. These might be a potential biomarker to choose an appropriate therapy. Increasing NQO1 may help alleviate Alzheimer's disease (AD) by reducing mitochondrial stress by amyloid β. In contrast, decreasing NQO1 may reduce a risk of α-synuclein aggregation in Parkinson's disease (PD) by reducing hydroxy-2,3-trans-nonenal (4-HNE), potential to α-synuclein aggregation. If combination therapy with NQO1 induction is considered, using ferroptosis inducers should be reconsidered. However, increasing NQO1 would be an effective approach to treat mitochondrial-related diseases induced by complex I dysfunction without ferroptosis induction. Since therapeutic studies using ferroptosis for cancer therapy and neurodegenerative diseases therapy have recently increased, regulating NQO1 would suggest a promising strategy for choosing an effective therapy.

Conflict of Interest: The authors have no conflicts of interest to disclose.

References

1. Spinelli JB, Haigis MC. The multifaceted contributions of mitochondria to cellular metabolism. Nat Cell Biol. 2018; 20:745-754.
2. Covarrubias AJ, Perrone R, Grozio A, Verdin E. NAD$^+$ metabolism and its roles in cellular processes during ageing. Nat Rev Mol Cell Biol. 2021; 22:119-141.
3. Monks TJ, Hanzlik RP, Cohen GM, Ross D, Graham DG. Quinone chemistry and toxicity. Toxicol Appl Pharmacol. 1992; 112:2-16.
4. Hyun DH, Emerson SS, Jo DG, Mattson MP, de Cabo R. Calorie restriction up-regulates the plasma membrane redox system in brain cells and suppresses oxidative stress during aging. Proc Natl Acad Sci U S A. 2006; 103:19908-19912.
5. Kim J, Kim SK, Kim HK, Mattson MP, Hyun DH. Mitochondrial function in human neuroblastoma cells is up-regulated and protected by NQO1, a plasma membrane redox enzyme. PLoS One. 2013; 8:e69030.
6. Bey EA, Reinicke KE, Srougi MC, *et al*. Catalase abrogates beta-lapachone-induced PARP1 hyperactivation-directed programmed necrosis in NQO1-positive breast cancers. Mol Cancer Ther. 2013; 12:2110-2120.
7. Eisenbeis VB, Qiu D, Gorka O, Strotmann L, Liu G, Prucker I, Su XB, Wilson MSC, Ritter K, Loenarz C, Gross O, Saiardi A, Jessen HJ. beta-lapachone regulates mammalian inositol pyrophosphate levels in an NQO1- and oxygen-dependent manner. Proc Natl Acad Sci U S A. 2023; 120:e2306868120.
8. Stockwell BR, Friedmann Angeli JP, Bayir H, *et al*. Ferroptosis: A regulated cell death nexus linking metabolism. Redox Biology and Disease. Cell. 2017; 171:273-285.
9. Angeli JPF, Shah R, Pratt DA, Conrad M. Ferroptosis inhibition: mechanisms and opportunities. Trends Pharmacol Sci. 2017; 38:489-498.
10. Hangauer MJ, Viswanathan VS, Ryan MJ, Bole D, Eaton JK, Matov A, Galeas J, Dhruv HD, Berens ME, Schreiber SL, McCormick F, McManus MT. Drug-tolerant persister cancer cells are vulnerable to GPX4 inhibition. Nature. 2017; 551:247-250.
11. Liu L, Liu R, Liu Y, Li G, Chen Q, Liu X, Ma S. Cystine-glutamate antiporter xCT as a therapeutic target for cancer. Cell Biochem Funct. 2021; 39:174-179.
12. Shin CS, Mishra P, Watrous JD, Carelli V, D'Aurelio M, Jain M, Chan DC. The glutamate/cystine xCT antiporter antagonizes glutamine metabolism and reduces nutrient flexibility. Nat Commun. 2017; 8:15074.
13. Jia B, Li J, Song Y, Luo C. ACSL4-mediated ferroptosis and its potential role in central nervous system diseases and injuries. Int J Mol Sci. 2023; 24:10021.511.
14. You JH, Lee J, Roh JL. PGRMC1-dependent lipophagy promotes ferroptosis in paclitaxel-tolerant persister cancer cells. J Exp Clin Cancer Res. 2021; 40:350.
15. Lee J, You JH, Kim MS, Roh JL. Epigenetic reprogramming of epithelial-mesenchymal transition promotes ferroptosis of head and neck cancer. Redox Biol. 2020; 37:101697.
16. Kovalevich J, Langford D. Considerations for the use of SH-SY5Y neuroblastoma cells in neurobiology. Methods Mol Biol. 2013; 1078:9-21.
17. Ma Q, Cui K, Xiao F, Lu AY, Yang CS. Identification of a glycine-rich sequence as an NAD(P)H-binding site and tyrosine 128 as a dicumarol-binding site in rat liver NAD(P)H:quinone oxidoreductase by site-directed mutagenesis. J Biol Chem. 1992; 267:22298-22304.
18. Ahlgren-Beckendorf JA, Reising AM, Schander MA, Herdler JW, Johnson JA. Coordinate regulation of NAD(P)H:quinone oxidoreductase and glutathione-S-transferases in primary cultures of rat neurons and glia: role of the antioxidant/electrophile responsive element. Glia. 1999; 25:131-142.
19. Li N, Ragheb K, Lawler G, Sturgis J, Rajwa B, Melendez JA, Robinson JP. Mitochondrial complex I inhibitor rotenone induces apoptosis through enhancing mitochondrial reactive oxygen species production. J Biol Chem. 2003; 278:8516-8525.
20. Park S, Kim, Y., Lee, J, Seo., H., Nam, S. J., Jo, D. G., Hyun, D. H. 4-Hydroxycinnamic acid attenuates neuronal cell death by inducing expression of plasma membrane redox enzymes and improving mitochondrial functions. Food Science and Human Wellness. 2023; 12:1287-1299.
21. Koh JH, Kim JY. Role of PGC-1alpha in the mitochondrial NAD(+) pool in metabolic diseases. Int J Mol Sci. 2021; 22:4558.
22. Hyun DH, Kim J, Moon C, Lim CJ, de Cabo R, Mattson MP. The plasma membrane redox enzyme NQO1 sustains cellular energetics and protects human neuroblastoma cells against metabolic and proteotoxic stress. Age (Dordr). 2012; 34:359-370.

23. Xiao W, Wang RS, Handy DE, Loscalzo J. NAD(H) and NADP(H) redox couples and cellular energy metabolism. Antioxid Redox Signal. 2018; 28:251-272.
24. Lapenna D. Glutathione and Glutathione-dependent Enzymes: From biochemistry to gerontology and successful aging. Ageing Res Rev. 2023; 92:102066.
25. Zhong O, Wang J, Tan Y, Lei X, Tang Z. Effects of NAD+ precursor supplementation on glucose and lipid metabolism in humans: a meta-analysis. Nutr Metab (Lond). 2022; 19:20.
26. Zamaraeva MV, Sabirov RZ, Maeno E, Ando-Akatsuka Y, Bessonova SV, Okada Y. Cells die with increased cytosolic ATP during apoptosis: a bioluminescence study with intracellular luciferase. Cell Death Differ. 2005; 12:1390-1397.
27. Luengo A, Li Z, Gui DY, Sullivan LB, Zagorulya M, Do BT, Ferreira R, Naamati A, Ali A, Lewis CA, Thomas CJ, Spranger S, Matheson NJ, Vander Heiden MG. Increased demand for NAD(+) relative to ATP drives aerobic glycolysis. Mol Cell. 2021; 81:691-707.
28. Su LJ, Zhang JH, Gomez H, Murugan R, Hong X, Xu D, Jiang F, Peng ZY. Reactive oxygen species-induced lipid peroxidation in apoptosis, autophagy, and ferroptosis. Oxid Med Cell Longev. 2019; 2019:5080843.
29. Lee J, You JH, Shin D, Roh JL. Inhibition of glutaredoxin 5 predisposes cisplatin-resistant head and neck cancer cells to ferroptosis. Theranostics. 2020; 10:7775-7786.
30. Lee J, You JH, Roh JL. Poly(rC)-binding protein 1 represses ferritinophagy-mediated ferroptosis in head and neck cancer. Redox Biol. 2022; 51:102276.
31. Ivan M, Kondo K, Yang H, Kim W, Valiando J, Ohh M, Salic A, Asara JM, Lane WS, Kaelin WG, Jr. HIFalpha targeted for VHL-mediated destruction by proline hydroxylation: implications for O2 sensing. Science. 2001; 292:464-468.
32. Lee J, Roh JL. Targeting iron-sulfur clusters in cancer: opportunities and challenges for ferroptosis-based therapy. Cancers (Basel). 2023; 15:2694.
33. Oh ET, Kim HG, Kim CH, Lee J, Kim C, Lee JS, Cho Y, Park HJ. NQO1 regulates cell cycle progression at the G2/M phase. Theranostics. 2023; 13:873-895.
34. Doll S, Proneth B, Tyurina YY, *et al*. ACSL4 dictates ferroptosis sensitivity by shaping cellular lipid composition. Nat Chem Biol. 2017; 13:91-98.
35. Antonny B, Vanni S, Shindou H, Ferreira T. From zero to six double bonds: phospholipid 20unsaturation and organelle function. Trends Cell Biol. 2015; 25:427-436.
36. Brown MD, Hart C, Gazi E, Gardner P, Lockyer N, Clarke N. Influence of omega-6 PUFA arachidonic acid and bone marrow adipocytes on metastatic spread from prostate cancer. Br J Cancer. 2010; 102:403-413.
37. Rouault TA. Iron metabolism in the CNS: implications for neurodegenerative diseases. Nat Rev Neurosci. 2013; 14:551-564.
38. Zhan S, Lu L, Pan SS, Wei XQ, Miao RR, Liu XH, Xue M, Lin XK, Xu HL. Targeting NQO1/GPX4-mediated ferroptosis by plumbagin suppresses *in vitro* and *in vivo* glioma growth. Br J Cancer. 2022; 127:364-376.
39. Fournier M, Monin A, Ferrari C, Baumann PS, Conus P, Do K. Implication of the glutamate-cystine antiporter xCT in schizophrenia cases linked to impaired GSH synthesis. NPJ Schizophr. 2017; 3:31.
40. Cerutti R, Pirinen E, Lamperti C, Marchet S, Sauve AA, Li W, Leoni V, Schon EA, Dantzer F, Auwerx J, Viscomi C, Zeviani M. NAD(+)-dependent activation of Sirt1 corrects the phenotype in a mouse model of mitochondrial disease. Cell Metab. 2014; 19:1042-1049.
41. Kussmaul L, Hirst J. The mechanism of superoxide production by NADH:ubiquinone oxidoreductase (complex I) from bovine heart mitochondria. Proc Natl Acad Sci U S A. 2006; 103:7607-7612.
42. Bai P, Canto C. The role of PARP-1 and PARP-2 enzymes in metabolic regulation and disease. Cell Metab. 2012; 16:290-295.
43. Higgins CB, Mayer AL, Zhang Y, Franczyk M, Ballentine S, Yoshino J, DeBosch BJ. SIRT1 selectively exerts the metabolic protective effects of hepatocyte nicotinamide phosphoribosyltransferase. Nat Commun. 2022; 13:1074.
44. Price NL, Gomes AP, Ling AJ, *et al*. SIRT1 is required for AMPK activation and the beneficial effects of resveratrol on mitochondrial function. Cell Metab. 2012; 15:675-690.
45. Zhu Y, Zhang JL, Yan XJ, Ji Y, Wang FF. Exploring a new mechanism between lactate and VSMC calcification: PARP1/POLG/UCP2 signaling pathway and imbalance of mitochondrial homeostasis. Cell Death Dis. 2023; 14:598.
46. Almeida A, Almeida J, Bolanos JP, Moncada S. Different responses of astrocytes and neurons to nitric oxide: the role of glycolytically generated ATP in astrocyte protection. Proc Natl Acad Sci U S A. 2001; 98:15294-15299.
47. Herrero-Mendez A, Almeida A, Fernandez E, Maestre C, Moncada S, Bolanos JP. The bioenergetic and antioxidant status of neurons is controlled by continuous degradation of a key glycolytic enzyme by APC/C-Cdh1. Nat Cell Biol. 2009; 11:747-752.

#Present address: Logsynk, Seoul, Korea.
Address correspondence to:
Dong-Hoon Hyun, Department of Life Science, Ewha Womans University, Seoul 03760, South Korea.
E-mail: hyundh@ewha.ac.kr

High-frequency hearing vulnerability associated with the different supporting potential of Hensen's cells: SMART-Seq2 RNA sequencing

Yiding Yu[1,2,3], Yue Li[1,2,3], Cheng Wen[1,2,3], Fengbo Yang[4], Xuemin Chen[5,6], Wenqi Yi[5,6], Lin Deng[1,2,3], Xiaohua Cheng[1,2,3], Ning Yu[5,6,*], Lihui Huang[1,2,3,*]

[1] Otolaryngology Head and Neck Surgery, Beijing Tongren Hospital, Capital Medical University, Beijing, China;
[2] Beijing Institute of Otolaryngology, Beijing, China;
[3] Key Laboratory of Otolaryngology Head and Neck Surgery, Ministry of Education, Beijing, China;
[4] Otolaryngology Head and Neck Surgery, Affiliated Hospital of North Sichuan Medical College, Nanchong, China
[5] College of Otolaryngology Head and Neck Surgery, Chinese PLA General Hospital, Beijing, China;
[6] National Clinical Research Center for Otolaryngologic Diseases, Beijing, China.

SUMMARY   Hearing loss is the third most prevalent physical condition affecting communication, well-being, and healthcare costs. Sensorineural hearing loss often occurs first in the high-frequency region (basal turn), then towards the low-frequency region (apical turn). However, the mechanism is still unclear. Supporting cells play a critical role in the maintenance of normal cochlear function. The function and supporting capacity of these cells may be different from different frequency regions. Hensen's cells are one of the unique supporting cell types characterized by lipid droplets (LDs) in the cytoplasm. Here, we investigated the morphological and gene expression differences of Hensen's cells along the cochlear axis. We observed a gradient change in the morphological characteristics of Hensen's cells along the cochlear tonotopic axis, with larger and more abundant LDs observed in apical Hensen's cells. Smart-seq2 RNA-seq revealed differentially expressed genes (DEGs) between apical and basal Hensen's cells that clustered in several pathways, including unsaturated fatty acid biosynthesis, cholesterol metabolism, and fatty acid catabolism, which are associated with different energy storage capacities and metabolic potential. These findings suggest potential differences in lipid metabolism and oxidative energy supply between apical and basal Hensen's cells, which is consistent with the morphological differences of Hensen's cells. We also found differential expression patterns of candidate genes associated with hereditary hearing loss (HHL), noise-induced hearing loss (NIHL), and age-related hearing loss (ARHL). These findings indicate functional heterogeneity of SCs along the cochlear axis, contribute to our understanding of cochlear physiology and provide molecular basis evidence for future studies of hearing loss.

Keywords   cochlea, Hensen's cells, lipid droplets, RNA sequencing

1. Introduction

The cochlea is a very sophisticated 3D structure. The Organ Corti is a highly specialized hearing organ located within the cochlea that is comprised of hair cells (HCs) and their adjacent supporting cells (SCs). Both HCs and SCs are essential for normal hearing, acting as primary structures for sound perception (*1-3*). Within the cochlea, HCs and SCs form an ordered asymmetrical pattern, extending from the basal to the apical axis. SCs provide the necessary metabolic and electrolyte environment for HCs to maintain their normal physiological functions and form the supporting Corti apparatus structure (*4,5*). The

SCs can be identified as several types: Hensen, Deiter, internal and external Pillar, Boettcher, and Claudius cell. Hensen's cells, a type of SC found on the basement membrane's outer side, are notable for their lipid droplets (LDs) enrichment. Hensen's cells can be individually identified in the cochlea of guinea pigs due to the LDs in the cytoplasm (*1,6*). More studies have shown that Hensen's cells may have some other important functions such as the regulation of sensory cell differentiation and development, maintenance of a stable ionic state, modulation of sensorimotor function, and development of synaptogenesis (*7-12*).

     Smart-seq2 is a single-cell RNA sequencing

technology that enables the extraction and sequencing of RNA from individual cells or cell masses, and we took this approach specifically to examine only pure Hensen's cells to avoid the influence of other parts of the cochlea on the result. We observed a gradient enrichment of LDs in Hensen's cells along the tonotopic axis. Analysis of differentially expressed genes (DEGs) suggests that these disparities might be linked to variations in energy storage and metabolic capacities. Following sonic induction, the low-frequency region (apical turn) recovers faster from the noise stimuli than the high-frequency region (basal turn). The increased vulnerability of high-frequency hearing may be related to the lower "supporting ability and potential" of the Hensen's cells from the basal turn.

2. Materials and Methods

2.1. Animals

Five-week-old healthy adult male albino guinea pigs weighing 230 g were used for this study. The animals were purchased from Vital River Laboratory Animal Technology Co., Ltd. (Beijing, China). The study's animal care and use protocols received approval from the Chinese Capital Medical University's Institutional Animal Care and Use Committee.

2.2. Immunofluorescence

The cochleae were transferred into an Eppendorf tube containing paraformaldehyde and kept overnight at 4 °C. A 10% EDTA solution (Solarbio, China) was used for decalcification at room temperature for 7 days. The sensory epithelium of every turn was dissected out and stained with BODIPY 493/503 (Invitrogen, Cat# D3922, 1:200) for 2 h without light to display the LDs. Then, the sections were rinsed with 0.1 M PBS three times for 5 min each time and drawn onto a glass slide by using a pipette. The slides were carefully covered with Antifade Mounting Medium (Beyotime, Cat# P0131, China). A confocal microscope (Zeiss, Germany) was used to observe the experimental results.

2.3. Frozen sections and oil red O staining

After decalcification with disodium EDTA for 7 days, the cochleae were dehydrated with 15% and 30% sucrose for 1.5 h each and embedded in optimal cutting temperature compound (Sakura, Cat#4583, Japan) overnight at 4°C. Modiolar sections with a thickness of 10 μm were cut, air dried, fixed in formalin, briefly washed with running tap water for 5 min, and then rinsed with 60% isopropanol. The slides were stained with freshly prepared Oil Red O working solution for 15 min and rinsed with 60% isopropanol. The nuclei were lightly stained with 5 dips in alum hematoxylin and rinsed with distilled water. The slides were mounted in glycerine jelly. A microscope

(Zeiss, Germany) was used to observe the samples.

2.4. Dissection and isolation of Hensen's cells

Following anesthesia with pentobarbital sodium (50 mg/kg intraperitoneal injection), guinea pigs were killed by cervical dislocation. The bulla was removed, and the cochlea was exposed. Then, the volute was removed from the basal to the apical turn. Micro tweezers were used to mechanically detach the Hensen's cells from the cochlear basement membrane. A microsyringe was used to transfer the Hensen's cell mass to a 1 ml Eppendorf (EP) tube with 500 μL of extracellular fluid (pH 7.35 and 300 mOsm) and 500 μg of trypsin (Gibco, United States) for digestion. After 10 min of incubation at room temperature, 200 μl of extracellular fluid was added to the EP tube to terminate digestion and gently blown with a pipette gun to digest the tissue into single cells and cell masses. The cell masses were transferred to a new plastic chamber containing an enzyme-free culture medium. Hensen's cells were separated after gentle trituration of the tissue with a small pipette and observed under an inverted microscope (Leica, Germany). One guinea pig was used to collect 2 cell masses from apical and basal turns separately, and three guinea pigs were used for three biological repeats.

2.5. Collection of isolated Hensen's cells

Two glass pipettes pulled by an electrode puller (Narishige, Japan), 70-100 μm in diameter, were used to collect solitary Hensen's cells separately to prevent contamination. These pipettes were mounted in two separate electrode holders on two micromanipulators (Narishige, Japan). A 1 mL syringe was connected to the suction port of the pipette to aspirate or expel the cells. The Hensen's cells were identified based on their specific morphological features. Cells from the apical and basal turns were collected separately in different EP tubes, and stored on ice. Each sample contained 10-15 identified Hensen's cells. All samples were from three animals. Only the identified HCs were aspirated into the first glass micropipette and expelled into the Bovine Serum Albumin (BSA) on the adjacent coverslip for washing. Washed cells were transferred using another clean glass micropipette and expelled into a 0.2 mL thin-walled PCR tube containing 2 μl of a mild hypotonic lysis buffer composed of 0.2% Triton X-100 (Sigma, United States) and 2 U/μL RNase inhibitor (Clontech, Canada).

2.6. Library preparation and RNA sequencing

We followed the Smart-Seq2 protocol for reverse transcription with a few modifications (*13,14*). The library was prepared by using the Smart-Seq v4 Ultra Low Input RNA Kit (Clontech Laboratories, Canada) and Nextera Library Preparation Kit (Illumina, Canada).

The concentration of total extracted RNA from cells ranged from 5 to 10 ng/μL. Subsequently, amplified samples were purified and selected with AMpure XP beads (Beckman, United States). The DNA quality was examined using an Agilent 2100 BioAnalyzer system (Agilent Technologies, CA, United States). The libraries were multiplexed and sequenced on an Illumina X-Ten platform to generate 100-bp paired-end reads. The files from the multiplexed RNA-seq samples were demultiplexed, and fastq files representing each library were generated.

2.7. Data analysis

The low-quality reads were filtered, and the linker sequence was trimmed to obtain clean reads by Trimmomatic (v0.39). Then, STAR (2.7.5c) was utilized to align the reads to the guinea pig reference genome (Cavpor3.0). The reads aligned to genes were counted by cufflinks (v2.2.1). The fragments per kilobase of transcript per million mapped reads (FPKM) values were normalized by cuffnorm, and the gene expression levels were calculated by cuffdiff. The resulting P values were adjusted using Benjamini and Hochberg's approach for controlling the false discovery rate. Significant DEGs were identified with threshold P values < 0.05 and fold-change > 1.2. The DESeq R package was used to conduct differential expression analysis of the two groups, with three biological replicates per condition. Gene Ontology (GO) enrichment analysis was performed using TopGO (v2.24.0), Kyoto Encyclopedia of Genes and Genomes (KEGG) enrichment analysis was performed using DAVID (v6.8), and the results were visualized using ClusterProfiler and ggplot2 package in R (v4.3.1).

3. Results

3.1. Morphological differences between apical and basal turn Hensen's cells.

The presence of LDs is one of the main features of Hensen cells and can be easily identified from the cochlea epithelium. The Hensen's cells were distributed in the outer part of the Corti organ, and those from different turns had different morphologies, especially regarding the volume of LDs. We observed a larger cell body and a greater volume of LDs in the apical turn compared to that in the basal turn (Figure 1A-E). Oil Red O staining's longitudinal observations corroborated the LD distribution patterns across various turns: the LDs were dyed red, and the apical LDs were larger (Figure 2A-F). At the same time, the cochlea basilar membrane from different turns showed that the size and number of LDs decreased along the longitudinal cochlea toward the basal turn, and became unobservable (especially the basal turn) (Figure 1E).

3.2. Analysis of gene expression profiles.

The reads containing adapters or multiple unidentifiable nucleotides and low-quality reads were deleted from the raw reads to obtain clean data (FPKM ≥ 0.5). 1389 DEGs between apical and basal Hensen's cells were identified, 567/1389 (40.8%) DEGs were upregulated in apical cells, while 822/1389 (59.2%) DEGs were upregulated in basal cells (Figure 3A). The heatmap and PCA plot compared the gene expression of six samples from different turns and showed that the six samples from the apical turn and the basal turn could be clustered
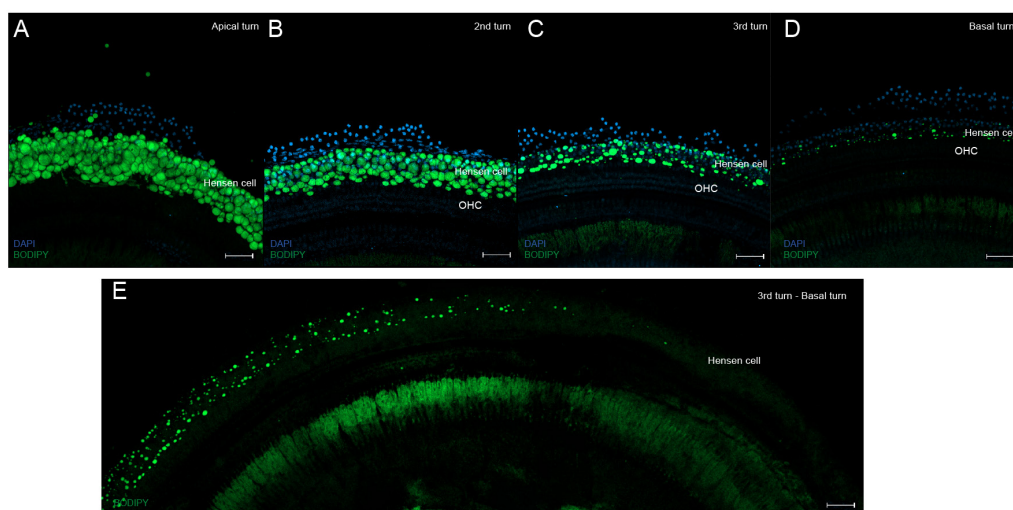
Figure 1. Morphological characteristics of Hensen's cells and the LDs in different turns. A-D: Confocal images scanned on the surface of each turn; green represents the LDs stained by BODIPY, and blue represents cell nuclei stained by DAPI. **E**: LDs gradually become smaller until they disappear. Green represents the LDs stained by BODIPY. The size of the LDs decreases along the longitudinal cochlea apical toward the basal turn, becoming progressively unobservable. Scale bars = 50 μm (apply to A-E). HC: Hair Cell.
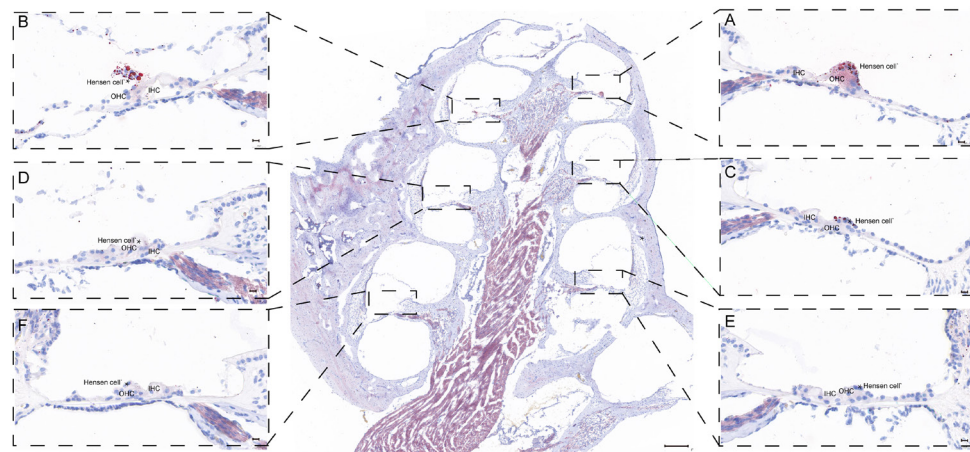
Figure 2. Longitudinal observation of the distribution of LDs in different turns. Oil Red O staining of whole frozen cochlear sections. **A-F**: Oil Red O staining of each turn; red represents the LDs. Longitudinal observation of the distribution of different turns of LDs confirmed the distribution characteristics of LDs, the apical turn enrichs more LDs.**.** Scale bars = 200 μm in the whole cochlea; scale bars = 20 μm in **A-F**. HC: Hair Cell.
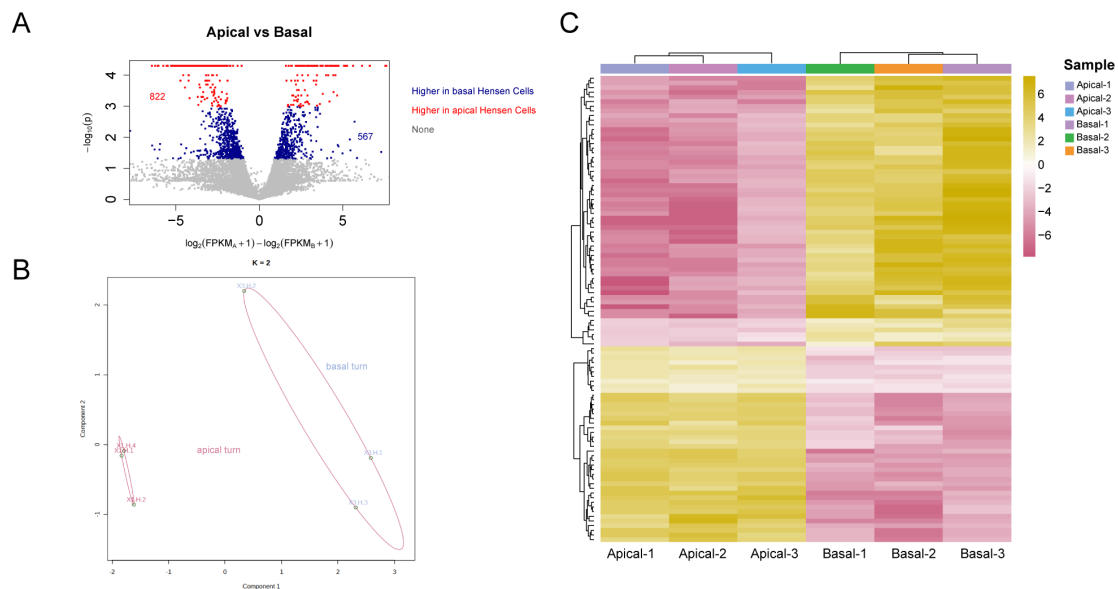
Figure 3. Analysis of DEGs between apical and basal Hensen's cells. A: Volcano plot with the red and blue dots representing the up- and downregulation of differentially expressed genes, respectively. **B**: K-means clustering shows that the samples from the apical and basal turns can be clustered together. **C**: Heatmap generated by the clustering analysis of DEGs and samples. The samples from the apical turn and basal turn could be clustered into two groups, and Hensen's cells from the same site had similar expression patterns.

into two groups, indicating different transcriptional profiles between apical and basal Hensen's cells (Figure 3B, C).

3.3. GO enrichment analysis

The ontology covers three domains: molecular function (MF), cellular component (CC), and biological process (BP). We summarized some of the most significantly enriched GO terms from our analysis, revealing that the DEGs were predominantly associated with the CC, such as extracellular exosome, peroxisomes, and lipid biosynthesis proteins. In terms of MF, the DEGs

were significantly involved in processes and functions critical for cellular energy management and metabolic regulation, including activities related to ion transport *via* ATPase activity, redox reactions *via* oxidoreductases, and lipid metabolism *via* fatty acid-CoA ligase activity and lipid transporter activity. In addition, these DEGs played critical roles in metabolic pathways, particularly in lipid oxidation, fatty acid metabolism, and response to decreased oxygen levels. These findings highlight the essential functions of the genes in lipid metabolism and their impact on the cellular antioxidant system, which may affect the cell's ability to maintain redox homeostasis (Figure 4A).
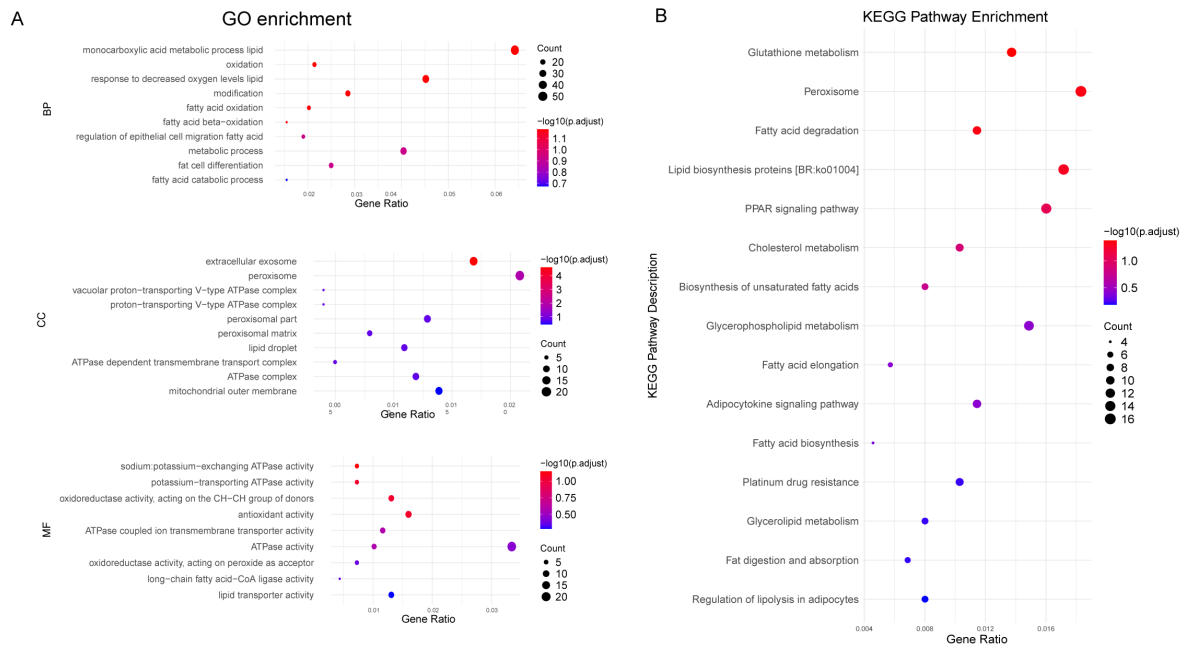
Figure 4. GO bar chart showing significant accumulation and significant KEGG enrichment scatter. A: GO bar chart showing significant accumulation: significantly enriched GO terms based on $p \leq 0.05$; the horizontal axis shows the logarithm of the p value, the vertical axis shows the GO terms, BP terms are shown in green, CC terms are shown in orange, MF terms are shown in blue. **B**: Each dot represents a KEGG pathway; the names of the pathways are shown on the vertical axis, and enrichment factors are shown on the horizontal axis. The larger the enrichment factor is, the more reliable the significant enrichment of the DEGs in the pathway. Both the GO and KEGG enrichment analyses showed that the different pathways between the two groups may be associated with lipid metabolism and oxidative energy supply.

3.4. KEGG enrichment analysis

KEGG pathway analysis revealed a cluster of key pathways that are central to lipid homeostasis and energy balance within Hensen's cell. These pathways range from fatty acid degradation and biosynthesis, including the critical involvement of peroxisomes, to the regulation of these processes by the PPAR signaling pathway. In addition, cholesterol metabolism and unsaturated fatty acid biosynthesis indicate a complex interplay in lipid management. Glycerophospholipid metabolism and the adipocytokine signaling pathway suggest a link between lipid storage and signaling mechanisms. These pathways also emphasize the cellular focus on the regulation of energy storage and utilization, as demonstrated in the pathways for fat digestion and absorption, and regulation of lipolysis in adipocytes. In addition, glutathione metabolism indicates a link to the antioxidant defense system, highlighting the multiple roles of these genes in cellular metabolism (Figure 4B).

3.5. Expression of HHL, NIHL, and ARHL candidate genes

3.5.1. HHL Genes

Mutations in deafness-related genes have been linked to inherited syndromic or non-syndromic hearing loss,

and the mutations affect different hearing phenotypes. Therefore, we analyzed the expression of deafness-related genes. Many of these deafness-related genes can be expressed in SCs, and some exclusively in SCs. We compared 36 deafness-related genes (3 of these genes were not found in our samples) that may be expressed in Hensen's cells (*15*). At least 16 of these genes differed in expression by 2-fold or more ($|\log2FC|>1$); among them, *GJB2 and P2RX2* were significantly more highly expressed in the apical turn, and only *COL11A1* was more highly expressed in the basal turn (FDR *q*-value < 0.05) (Table 1).

3.5.2. Candidate NIHL susceptibility genes

There is increasing evidence that genetic factors may increase susceptibility to noise-induced hearing loss (NIHL), and by conducting a review of previous studies, we compiled a list of some of the genes that may contribute to increased noise sensitivity and compared the expression of these genes in Hensen's cells at different locations. A total of 47 possible NIHL susceptibility genes (*16*) were compared; 7 of these genes were not detected in our samples, and the expression of 25 genes differed 2-fold or more ($|\log2FC|>1$), including 11 genes with higher expression in the apical turn, 1 with a significant difference, and 14 genes with higher expression in the basal turn, 2 with significant differences (FDR *q*-value < 0.05) (Table 2).

Table 1. Summary of deafness genes that differ between apical and basal Hensen's cells

NO.	Gene Symbol	Apical (FPKM)	Basal (FPKM)	log2 FC	*FDR q*-value	
1	*GJB2*	875.50	43.73	-4.41	0.003*	
2	*P2RX2*	353.00	19.64	-4.25	0.003*	
3	*COL11A1*	2.66	41.62	3.88	0.021*	
4	*GJB6*	99.85	16.33	-2.69	0.150	
5	*WFS1*	50.93	18.04	-1.58	0.170	
6	*SMPX*	604.61	6.60	-6.60	0.474	
7	*EYA4*	4.37	11.99	1.37	0.491	
8	*CIB2*	46.08	23.02	-1.08	0.508	
9	*ILDR1*	15.27	5.76	-1.49	0.513	
10	*TMPRSS3*	28.43	1.81	-4.05	0.527	
11	*ELMOD3*	1.44	10.22	2.75	0.569	
12	*SYNE4*	17.93	4.84	-1.97	0.572	
13	*SOX10*	46.41	22.05	-1.15	0.614	
14	*TPRN*	7.11	2.11	-1.82	0.655	
15	*KARS*	61.08	98.88	0.61	0.694	
16	*MYH9*	18.27	13.37	-0.53	0.716	
17	*CLPP*	17.09	27.47	0.60	0.727	
18	*CLDN14*	8.07	3.38	-1.33	0.733	
19	*EDN3*	0.01	13.99	10.30	0.750	
20	*MSRB3*	7.72	1.57	-2.38	0.759	
21	*TRIOBP*	17.52	11.97	-0.63	0.824	
22	*PNPT1*	18.98	17.51	-0.20	0.889	
23	*GPSM2*	8.38	6.99	-0.35	0.940	
24	*TJP2*	16.68	18.89	0.10	0.941	
25	*CCDC50*	13.14	16.26	0.22	0.958	
26	*COL11A2*	2.04	2.15	0.00	0.997	
27	*EYA1*	45.72	48.71	0.01	0.997	
28	*ESRRB*	0.00	0.00	0.00	1.000	Not detected
29	*ADCY1*	0.00	0.00	0.00	1.000	Not detected
30	*CEACAM16*	0.00	0.00	0.00	1.000	Not detected
31	*GRXCR1*	0.29	0.07	-2.09	1.000	
32	*LHFPL5*	0.10	0.46	2.06	1.000	
33	*MYH14*	0.74	0.00	-7.31	1.000	
34	*OTOGL*	0.90	0.24	-1.95	1.000	
35	*TMC1*	0.05	0.25	2.29	1.000	
36	*TMIE*	0.12	0.17	0.36	1.000	

FPKM: Fragments per kilobase of transcript per million mapped reads. *q-value < 0.05

3.5.3. Candidate ARHL-associated genes

Similarly, we conducted a literature survey and summary of the studies related to pathogenic genes associated with ARHL, focusing on genes that may be mainly expressed in SCs, including *CDH23, CEP104, DCLK, ERBB3, EYA4, GJB2, GRHL2, GRM7, ILDR1, ISG20, KCNQ4, KCNQ5, P2RX2, PCDH20, SLC28A3,* and *TRIOBP* (*17-22*). Some of these candidate genes were not detected in our samples, such as *SLC28A3, KCNQ4, KCNQ5,* and *PCDH20* (FPKM ≤ 0.5). The expression of 7 genes differed 2-fold or more (|log2FC|>1) in different groups, among which 3 were highly expressed in the apical turn, 2 with significant differences (FDR *q*-value < 0.05), and 4 had higher expression in the basal turn, none with a significant difference (Table 3).

4. Discussion

SCs are involved in ionic circulation, structural support, and repair in the inner ear, similar to glial cells for neuronal cells, including the provision of mechanical and nutritional support for HCs (*4,5*). The inherent challenges posed by the deep location and limited quantity of cochlear cells limit research investigating gene expression in cochlear SCs. Most previous studies on cochlear cells have inevitably mixed a variety of different cell types, and potentially important information may be lost in the context of data on complex SC populations (*23-25*). One of the biggest difficulties is obtaining enough cells of one single cochlear type for sequencing. Smart-seq2 RNA sequencing technology has provided new ideas and methods to construct libraries from very small amounts of cells and obtain full-length RNA sequencing (*1,13,14,26-28*). As far as we know, there have been no RNA studies have been conducted using pure Hensen's Cells, this is the first data to investigate the difference between apical and basal Hensen's cells using SMART-seq2 RNA sequencing.

4.1. The morphological differences implied that Hensen's cells have different energy storage capacities and metabolic potential

Table 2. Summary of candidate NIHL-related genes that differ between apical and basal Hensen's cells

NO.	Gene Symbol	Apical (FPKM)	Basal (FPKM)	log2 FC	*FDR q*-value	
1	*GJB2*	814.75	44.35	-4.41	0.003*	
2	*ITGA8*	9.52	103.38	3.84	0.003*	
3	*SLC12A4*	1.63	22.42	3.36	0.020*	
4	*GJB6*	112.94	21.58	-2.69	0.150	
5	*ATP2B2*	18.68	4.57	-2.42	0.204	
6	*GAPDH*	2406.65	1182.68	-1.37	0.336	
7	*CAT*	34.48	80.23	1.11	0.348	
8	*SOD2*	123.31	350.11	1.19	0.403	
9	*PER1*	4.19	14.82	1.92	0.409	
10	*KCNQ1*	35.90	8.48	-1.97	0.434	
11	*SIK3*	11.25	26.95	1.20	0.470	
12	*EYA4*	4.01	15.98	1.37	0.491	
13	*SOD1*	3433.96	2187.52	-0.84	0.525	
14	*HDAC2*	28.34	45.42	0.85	0.565	
15	*NRN1*	0.13	97.16	10.45	0.588	
16	*KCNE1*	9.47	132.04	4.43	0.603	
17	*GRM7*	0.01	6.26	9.81	0.635	
18	*NOTCH1*	7.66	0.97	-3.15	0.645	
19	*DNMT1*	0.61	2.22	2.66	0.656	
20	*CDH23*	0.02	1.60	6.02	0.705	
21	*OGG1*	1.06	5.08	1.66	0.705	
22	*KCNJ10*	1.14	0.40	-2.13	0.743	
23	*PON2*	46.28	62.41	0.31	0.793	
24	*WHRN*	2.13	0.55	-2.02	0.798	
25	*CASP3*	1.78	5.68	1.81	0.814	
26	*FOXO3*	13.63	11.57	0.30	0.819	
27	*NCL*	83.30	91.37	0.25	0.843	
28	*MAPK8*	2.81	2.67	-0.73	0.848	
29	*XRCC1*	9.31	14.21	0.46	0.853	
30	*NFE2L2*	55.98	83.58	0.15	0.897	
31	*UBAC2*	13.45	14.60	-0.20	0.903	
32	*GRHL2*	1.48	1.71	-0.50	0.914	
33	*DNMT3A*	21.61	12.26	-0.17	0.920	
34	*AUTS2*	18.13	14.54	-0.12	0.933	
35	*APEX1*	9.01	10.75	0.18	0.942	
36	*MAPK1*	38.32	42.46	-0.06	0.955	
37	*DFNA5*	0.16	0.05	-3.69	1.000	
38	*FAS*	0.00	0.00	0.00	1.000	Not detected
39	*GJB3*	0.00	0.00	0.00	1.000	Not detected
40	*GJB4*	0.00	0.00	0.00	1.000	Not detected
41	*HSPA1L*	1.03	0.24	-2.22	1.000	
42	*KCNMA1*	0.00	0.00	0.00	1.000	Not detected
43	*KCNQ4*	0.00	0.00	0.00	1.000	Not detected
44	*MYH14*	0.71	0.01	-7.31	1.000	
45	*NOX3*	0.00	0.00	0.00	1.000	Not detected
46	*PCDH15*	0.00	0.00	0.00	1.000	Not detected
47	*POU4F3*	0.39	0.13	-0.21	1.000	

FPKM: Fragments per kilobase of transcript per million mapped reads. *q-value < 0.05

Our morphological analysis showed that cell size and LD size were consistent with a gradual decrease from the apical to the basal turn, especially the gradual disappearance near the basal turn (Figure 1E), which was also confirmed by oil red O staining of frozen sections (Figure 2 A-E). In previous studies, LDs have been considered dynamic lipid storage organelles that respond to external stimuli, participate in a variety of metabolic processes, and are involved in maintaining a relatively stable morphological equilibrium They may not only be composed of lipids, but also contain steroids and various proteins that are thought to play important roles in energy metabolism, protein synthesis, and other biological processes, and may regulate relevant cellular signaling pathways (*29,30*). As seen in the structure of the enriched LDs of Hensen's cells, the cells may have a high energy supply capacity and play an important role in the nutritional support of sensory cells. (*31,32*). In the 1980s, Merchan and his team suggested a possible role for Hensen's cell in hearing. Using a scanning electron microscope, they observed that Hensen's cells showed a partial loss of the plasma membrane to form vacuoles. They hypothesized that cytoplasmic material might be extruded through the vacuoles into the endolymph (*33*). Further studies have described that high-intensity noise exposure resulted in the secretion of LDs from Hensen's

Table 3. Summary of candidate ARHL-related genes that differ between apical and basal Hensen's cells

NO.	Gene Symbol	Apical (FPKM)	Basal (FPKM)	log2 FC	*FDR q*-value	
1	*GJB2*	875.50	44.35	-4.41	0.003*	
2	*P2RX2*	353.00	43.73	-4.25	0.003*	
3	*EYA4*	4.37	19.64	1.37	0.491	
4	*ILDR1*	15.27	11.99	-1.49	0.513	
5	*GRM7*	0.01	5.76	9.81	0.635	
6	*DCLK1*	0.00	9.29	11.16	0.645	
7	*CDH23*	0.02	10.53	6.02	0.705	
8	*CEP104*	2.87	1.20	0.66	0.790	
9	*TRIOBP*	17.52	4.80	-0.63	0.824	
10	*ISG20*	5.36	11.97	0.80	0.863	
11	*GRHL2*	1.72	9.80	-0.50	0.914	
12	*ERBB3*	19.01	1.28	0.13	0.924	
13	*SLC28A3*	0.00	21.94	0.51	1.000	Not detected
14	*KCNQ5*	0.00	0.00	0.00	1.000	Not detected
15	*KCNQ4*	0.00	0.00	0.00	1.000	Not detected
16	*PCDH20*	0.00	0.00	0.00	1.000	Not detected

FPKM: Fragments per kilobase of transcript per million mapped reads. *q-value < 0.05

cells into the endolymphatic space in the guinea pig cochlea. (*34,35*). From the different volumes of the LDs, we can see that the large volume LDs of the apical Hensen's cells have more energy storage potential than those in the basal turn.

Our analysis delved into the gene expression of Hensen's cells from different turns and revealed that DEGs were predominantly enriched in biological processes such as lipid and fatty acid oxidation, along with monocarboxylic acid cycle metabolism. At the same time, pathways involved regulation of lipolysis in adipocytes, fat digestion and absorption, and PPAR signaling were also highlighted (Figure 4B). These patterns suggest that Hensen's cells not only exhibit marked differences in the distribution and volume of LDs but also in the expression of genes involved in lipid synthesis and metabolism. This observation implied that LDs function beyond mere energy reserves; they may also be underpinned by a sophisticated gene regulatory framework poised for rapid adaptive responses to stimuli such as noise and pharmacological agents.

The specific causes of the differences in the distribution of LDs in cells at different turns and whether they exhibit differential gene expression are still not well known. We found a variety of lipid metabolism-related genes were differentially expressed, such as *DGAT2, HACD3,* and *ACOT7*. Among them, the diacylglycerol acyltransferase (*DGAT2*) apical–basal expressed significantly differed, and the gene expression level was 477-fold higher (|log2FC|=8.90) in the apical turn than in the basal turn. *DGAT* is a glycerol-restricted transferase with two isoforms, *DGAT1* and *DGAT2*. *DGAT1* is mainly responsible for the synthesis of triacylglycerol during fat absorption and storage, while DGAT2 is responsible for the balance of basic fat in various tissues (*36-38*). The high expression of *DGAT2* in the apical turn may be responsible for the abundance of LDs from the apical turn and needs to be further confirmed.

4.2. Apical Hensen's cells may have a better response to the stimulation

Individuals with sensorineural hearing loss, including HHL, NIHL, and ARHL, usually experience a decrease in high-frequency hearing at first (*39-43*). Hearing loss usually begins as high-frequency hearing loss (*39-44*). For example, in conditions such as NIHL, high-frequency hearing is the first to decline after stimulus onset; high-frequency hearing thresholds also recover more slowly after stimulus disappearance (*41,44*). This suggests that cells in different parts of the cochlea usually have different survival abilities and differ in their recoverability from stimulation.

The reasons for high-frequency vulnerability remain unclear, potentially relating to diverse factors. This vulnerability may be attributed to various cells, such as HCs, SCs, spiral ganglion cells, and other cochlear cells. For the hair cells, such as IHCs, their ability to recover in response to stimuli may differ. For instance, the protective genes *PRKD1* and *SNCG*, associated with IHC survival, exhibited upregulation at the apical turn. Conversely, the negative regulatory genes *NME2* and *FBXO32* manifested upregulation at the basal turns (*26*). Basal HCs demonstrate reduced tolerance to oxygen free radicals, increasing their susceptibility to apoptosis (*44*). Sensory neuron cells exhibit molecular variations across the subtypes of spiral ganglion neurons on the tonotopic axis. Genes such as *LRRC52*, *KCNIP4*, *ANXA5*, and *RYR3*, relevant to functionality, displayed regional differences (*27*). Considering the crucial role of Hensen's cells in maintaining the auditory epithelium's integrity, it is important to also examine their function in high-frequency vulnerability (basal turn).

There was not just a morphological difference between the Hensen's cells from apical and basal turns. These cells exhibit significant differences in genetic expression, particularly within pathways related to

energy and lipid metabolism, which correlate with their morphological characteristics. Hensen's cells are dynamic entities actively involved in lipid and energy homeostasis. We proposed that apical Hensen's cells may have enhanced capacities for energy storage and metabolic processing, involving intricate processes such as oxidation and peroxide transport. Such features could potentially contribute to the recovery and maintenance of the organ of Corti function following environmental stimulation. Notably, the GO term "response to decreased oxygen levels" was enriched. This kind of response is critical for cochlear cell survival under oxygen-deprived environments, which could be indicative of the difference in resilience and adaptability between cells in the apical and basal turn. Simultaneously, the KEGG pathway enrichment for "Platinum drug resistance" suggested that these cells may possess enhanced mechanisms for dealing with the cytotoxic effects of platinum-based chemotherapeutic agents. This could reflect a sophisticated network of genes involved in DNA repair, and apoptosis regulation, endowing the Hensen's cells with the capacity to survive and maintain function during drug exposure.

4.3. Many SNHL-associated gene mutations are expressed at low levels in Hensen's cells at the basal turn, leading to clinical hearing loss in high-frequency

Cochlear function is influenced by both genetic and environmental factors. A significant number of deafness-causing genes are mainly expressed in SCs (*45*), and deafness genes are the most important factors causing HHL (*46,47*), especially *GJB2, GJB3,* and *SLC26A4*, which have a high carriage rate (*1,48-50*). Under specific circumstances, the gene expression patterns observed in the basal turn of the cochlea may contribute to greater challenges in maintaining normal cochlear function. This can cause a more rapid decline below a critical threshold when the gene loses its function compared to that in the apical turn. This disparity arises due to a gene expression gradient that is more pronounced in the basal turn, leading to early progressive loss of high-frequency hearing (*51*). Investigating the SCs across various turns can enhance our understanding of the pathology associated with specific-frequency hearing loss.

In Hensen's cells, we analyzed the susceptibility genes for HHL, NIHL, and ARHL at different turns. Notably, certain genes demonstrated significant differences in their expression levels, as indicated in Tables 1, 2, and 3. *GJB2, GJB6,* and *P2RX2* are all associated with HHL, NIHL, and ARHL. Mutations in *GJB2* significantly contribute to non-syndromic deafness, representing nearly half of all moderate-to-profound congenital cases. *GJB2* can either form a homomeric gap junction on its own or a heteromeric gap junction in conjunction with *GJB6*. Our research indicates a higher expression of *GJB2* and *GJB6* at the apical turn (high-frequency region), aligning with findings from previous studies (*52*).

P2RX2, also known as Purinergic Receptor *P2X2*, plays a pivotal role in several auditory processes. This includes regulating sound transduction, auditory neurotransmission, outer hair cell electromotility, and inner ear gap junctions. Additionally, it mediates K+ recycling and facilitates synaptic transmission between neurons and smooth muscles (*53*). Patients harboring mutations in *P2RX2* can experience progressive hearing loss accompanied by heightened noise sensitivity. Notably, *P2RX2* expression has been observed to decline with age (*21*). Studies conducted with animal models have found that noise can reduce sound transduction and synaptic transmission between HCs by increasing ATP levels and thus activating *P2X2* receptors and reducing *P2RX2* receptor-mediated regulation of endocochlear potential in the aging mouse cochlea resulting in hearing sensitivity impairment (*54,55*).

Our comprehensive analysis has shown that Hensen's cells display significant morphological variations that reflect their different energy storage and metabolic capabilities. The data demonstrated that Hensen's cells from different cochlear turns exhibit pronounced disparities in lipid metabolism, oxidative capacity, and gene expression that are consistent with their morphological characteristics. It appears that Hensen's cells from the basal turn (high-frequency region) may have reduced resilience to environmental challenges such as acoustic trauma and ototoxic agents. This compromised metabolic functionality could lead to an inadequate energy supply to sensory cells, culminating in damage or death of hair cells near the basal turn. Genes such as *GJB2, GJB6*, and *P2RX2* show variable expression along the cochlear axis, which may be clinically critical in initiating cochlear dysfunction and subsequent high-frequency hearing loss. This study emphasized the significance of conducting a thorough investigation of supporting cells to gain a better understanding of the complex physiology of the cochlea and to identify effective measures for preserving high-frequency hearing.

References

1. Cederholm JME, Ryan AF, Housley GD. Onset kinetics of noise-induced purinergic adaptation of the 'cochlear amplifier.' Purinergic Signal. 2019; 15:343-355.
2. Waldhaus J, Durruthy-Durruthy R, Heller S. Quantitative High-Resolution Cellular Map of the Organ of Corti. Cell Rep. 2015; 11:1385-1399.
3. Scheffer DI, Shen J, Corey DP, Chen ZY. Gene Expression by Mouse Inner Ear Hair Cells during Development. J Neurosci. 2015; 35:6366-6380.
4. Monzack EL, Cunningham LL. Lead roles for supporting actors: critical functions of inner ear supporting cells. Hear Res. 2013; 303:20-29.
5. Wan G, Corfas G, Stone JS. Inner ear supporting cells: Rethinking the silent majority. Semin Cell Dev Biol. 2013; 24:448-459.
6. Raica M. A short story of Victor Hensen and a cell of the internal ear. Published online. 2012:3.
7. Spicer SS, Schulte BA. Differences along the place-frequency map in the structure of supporting cells in the gerbil cochlea. Hear Res. 1994; 79:161-177.
8. Spicer SS, Schulte BA. The fine structure of spiral ligament cells relates to ion return to the stria and varies with place frequency. Hear Res. 1996; 100:80-100.
9. Sugasawa M, Erostegui C, Blanchet C, Dulon D. ATP activates a cation conductance and Ca^{2+}-dependent Cl^{-} conductance in Hensen cells of guinea pig cochlea. Am J Physiol. 1996; 271:C1817-1827.
10. Fechner FP, Nadol JB JR, Burgess BJ, Brown MC. Innervation of supporting cells in the apical turns of the guinea pig cochlea is from type II afferent fibers. J Comp Neurol. 2001; 429:289-298.
11. Urrutia RA, Kalinec F. Biology and Pathobiology of Lipid Droplets and their Potential Role in the Protection of the Organ of Corti. Hear Res. 2015; 330(Pt A):26-38.
12. Zhao HB, Liu LM, Yu N, Zhu Y, Mei L, Chen J, Liang C. Efferent neurons control hearing sensitivity and protect hearing from noise through the regulation of gap junctions between cochlear supporting cells. J Neurophysiol. 2022; 127:313-327.
13. Picelli S, Faridani OR, Björklund AK, Winberg G, Sagasser S, Sandberg R. Full-length RNA-seq from single cells using Smart-seq2. Nat Protoc. 2014; 9:171-181.
14. Picelli S, Björklund ÅK, Faridani OR, Sagasser S, Winberg G, Sandberg R. Smart-seq2 for sensitive full-length transcriptome profiling in single cells. Nat Methods. 2013; 10:1096-1098.
15. Nishio SY, Hattori M, Moteki H, Tsukada K, Miyagawa M, Naito T, Yoshimura H, Iwasa Y, Mori K, Shima Y, Sakuma N, Usami S. Gene expression profiles of the cochlea and vestibular endorgans: localization and function of genes causing deafness. Ann Otol Rhinol Laryngol. 2015; 124 Suppl 1:6S-48S.
16. Chen XM, Xue XM, Yu N, Guo WW, Yuan SL, Jiang QQ, Yang SM. The Role of Genetic Variants in the Susceptibility of Noise-Induced Hearing Loss. Front Cell Neurosci. 2022; 16:946206.
17. Xu K, Chen S, Xie L, Qiu Y, Bai X, Liu XZ, Zhang HM, Wang XH, Jin Y, Sun Y, Kong WJ. Local Macrophage-Related Immune Response Is Involved in Cochlear Epithelial Damage in Distinct Gjb2-Related Hereditary Deafness Models. Front Cell Dev Biol. 2021; 8:597769.
18. Trebusak Podkrajsek K, Tesovnik T, Bozanic Urbancic N, Battelino S.. Novel *GRHL2* Gene Variant Associated with Hearing Loss: A Case Report and Review of the Literature. Genes. 2021; 12:484.
19. Wells HRR, Newman TA, Williams FMK. Genetics of age-related hearing loss. J Neurosci Res. 2020; 98:1698-1704.
20. Di Stazio M, Morgan A, Brumat M, Bassani S, Dell'Orco D, Marino V, Garagnani P, Giuliani C, Gasparini P, Girotto G. New age-related hearing loss candidate genes in humans: an ongoing challenge. Gene. 2020; 742:144561.
21. Bouzid A, Smeti I, Dhouib L, Roche M, Achour I, Khalfallah A, Gibriel AA, Charfeddine I, Ayadi H, Lachuer J, Ghorbel A, Petit C, Masmoudi S. Down-expression of *P2RX2*, *KCNQ5*, *ERBB3* and *SOCS3* through DNA hypermethylation in elderly women with presbycusis. Biomarkers. 2018; 23:347-356.
22. Haider HF, Flook M, Aparicio M, Ribeiro D, Antunes M, Szczepek AJ, Hoare DJ, Fialho G, Paço JC, Caria H. Biomarkers of Presbycusis and Tinnitus in a Portuguese Older Population. Front Aging Neurosci. 2017; 9:346.
23. Xu Z, Tu S, Pass C, Zhang Y, Liu H, Diers J, Fu Y, He DZZ, Zuo J. Profiling mouse cochlear cell maturation using 10× Genomics single-cell transcriptomics. Front Cell Neurosci. 2022; 16:962106.
24. Langlie J, Finberg A, Bencie NB, Mittal J, Omidian H, Omidi Y, Mittal R, Eshraghi AA. Recent advancements in cell-based models for auditory disorders. BioImpacts BI. 2022; 12:155-169.
25. Hoa M, Olszewski R, Li X, Taukulis I, Gu S, DeTorres A, Lopez IA, Linthicum FH Jr, Ishiyama A, Martin D, Morell RJ, Kelley MW. Characterizing Adult Cochlear Supporting Cell Transcriptional Diversity Using Single-Cell RNA-Seq: Validation in the Adult Mouse and Translational Implications for the Adult Human Cochlea. Front Mol Neurosci. 2020; 13:13.
26. Tang F, Chen X, Jia L, Li H, Li J, Yuan W. Differential Gene Expression Patterns Between Apical and Basal Inner Hair Cells Revealed by RNA-Seq. Front Mol Neurosci. 2020; 12:332.
27. Shrestha BR, Chia C, Wu L, Kujawa SG, Liberman MC, Goodrich LV. Sensory neuron diversity in the inner ear is shaped by activity. Cell. 2018; 174:1229-1246.e17.
28. Liu H, Pecka JL, Zhang Q, Soukup GA, Beisel KW, He DZ.. Characterization of Transcriptomes of Cochlear Inner and Outer Hair Cells. J Neurosci. 2014; 34:11085-11095.
29. Olzmann JA, Carvalho P. Dynamics and functions of lipid droplets. Nat Rev Mol Cell Biol. 2019; 20:137-155.
30. Walther TC, Chung J, Farese RV. Lipid Droplet Biogenesis. Annu Rev Cell Dev Biol. 2017; 33:491-510.
31. Engstrom H, Wersall J. Is there a special nutritive cellular system around the hair cells in the organ of Corti. Ann Otol Rhinol Laryngol. 1953; 62:507-512.
32. Zhao LD, Liu J, Hu YY, Sun JH, Yang SM. Supporting Cells–a New Area in Cochlear Physiology Study. J Otol. 2008; 3:9-17.
33. Merchan MA, Merchan JA, Ludeña MD. Morphology of Hensen's cells. J Anat. 1980; 131(Pt 3):519-523.
34. del Cañizo Alvarez A, Merchán Cifuentes MA. A possible function of Hensen cells of the internal ear in the guinea pig. An Otorrinolaringol Ibero-Am. 1986; 13:627-638.
35. del Cañizo-Alvarez A, Merchan-Cifuentes MA, Arevalo M. Changes induced by sonic stimulation in the cells of Hensen of the inner ear. Rev Laryngol - Otol - Rhinol. 1987; 108:327-329.
36. Chen G, Harwood JL, Lemieux MJ, Stone SJ, Weselake RJ. Acyl-CoA:diacylglycerol acyltransferase: Properties,

physiological roles, metabolic engineering and intentional control. Prog Lipid Res. 2022; 88:101181.

37. Bhatt-Wessel B, Jordan TW, Miller JH, Peng L. Role of *DGAT* enzymes in triacylglycerol metabolism. Arch Biochem Biophys. 2018; 655:1-11.

38. Liu Q, Siloto RM, Lehner R, Stone SJ, Weselake RJ. Acyl-CoA:diacylglycerol acyltransferase: molecular biology, biochemistry and biotechnology. Prog Lipid Res. 2012; 51:350-377.

39. Fetoni AR, Pisani A, Rolesi R, Paciello F, Viziano A, Moleti A, Sisto R, Troiani D, Paludetti G, Grassi C. Early Noise-Induced Hearing Loss Accelerates Presbycusis Altering Aging Processes in the Cochlea. Front Aging Neurosci. 2022; 14:803973.

40. Cunningham LL, Tucci DL. Hearing Loss in Adults. N Engl J Med. 2017; 377:2465-2473.

41. Kurabi A, Keithley EM, Housley GD, Ryan AF, Wong AC. Cellular mechanisms of noise-induced hearing loss. Hear Res. 2017; 349:129-137.

42. Ding D, Jiang H, Salvi RJ. Mechanisms of Rapid Sensory Hair-Cell Death Following Co-administration of Gentamicin and Ethacrynic Acid. Hear Res. 2010; 259:16.

43. Ou HC, Bohne BA, Harding GW. Noise damage in the C57BL/CBA mouse cochlea. Hear Res. 2000; 145:111-122.

44. Sha SH, Taylor R, Forge A, Schacht J. Differential vulnerability of basal and apical hair cells is based on intrinsic susceptibility to free radicals. Hear Res. 2001; 155:1-8.

45. Usami SI, Nishio SY, Moteki H, Miyagawa M, Yoshimura H. Cochlear Implantation from the Perspective of Genetic Background. Anat Rec Hoboken. 2020; 303:563-593.

46. Lieu JEC, Kenna M, Anne S, Davidson L. Hearing Loss in Children: A Review. JAMA. 2020; 324:2195.

47. Richardson GP, de Monvel JB, Petit C. How the Genetics of Deafness Illuminates Auditory Physiology. Annu Rev Physiol. 2011; 73:311-334.

48. Dai P, Huang LH, Wang GJ, *et al*. Concurrent Hearing and Genetic Screening of 180,469 Neonates with Follow-up in Beijing, China. Am J Hum Genet. 2019; 105:803-812.

49. Wang QJ, Zhao YL, Rao SQ, Guo YF, Yuan H, Zong L, Guan J, Xu BC, Wang DY, Han MK, Lan L, Zhai SQ, Shen Y. A distinct spectrum of SLC26A4 mutations in patients with enlarged vestibular aqueduct in China. Clin Genet. 2007; 72:245-254.

50. Xia J, Liu C, Tang B, *et al*. Mutations in the gene encoding gap junction protein β-3 associated with autosomal dominant hearing impairment. Nat Genet. 1998; 20:370-373.

51. Yoshimura H, Takumi Y, Nishio S ya, Suzuki N, Iwasa Y ichiro, Usami S ichi. Deafness Gene Expression Patterns in the Mouse Cochlea Found by Microarray Analysis. PLoS ONE. 2014; 9:e92547.

52. Zhao HB, Yu N. Distinct and gradient distributions of connexin26 and connexin30 in the cochlear sensory epithelium of guinea pigs. J Comp Neurol. 2006; 499:506-518.

53. Morton-Jones RT, Vlajkovic SM, Thorne PR, Cockayne DA, Ryan AF, Housley GD. Properties of ATP-gated ion channels assembled from *P2X2* subunits in mouse cochlear Reissner's membrane epithelial cells. Purinergic Signal. 2015; 11:551-560.

54. Yan D, Zhu Y, Walsh T, *et al*. Mutation of the ATP-gated *P2X2* receptor leads to progressive hearing loss and increased susceptibility to noise. Proc Natl Acad Sci U S A. 2013; 110:2228-2233.

55. Telang RS, Paramananthasivam V, Vlajkovic SM, Munoz DJ, Housley GD, Thorne PR.. Reduced *P2x₂* receptor-mediated regulation of endocochlear potential in the ageing mouse cochlea. Purinergic Signal. 2010; 6:263-272.

*Address correspondence to:
Lihui Huang, Otolaryngology Head and Neck Surgery, Beijing Tongren Hospital, Capital Medical University, Beijing 100730, China; Beijing Institute of Otolaryngology, Beijing 100005, China; Key Laboratory of Otolaryngology Head and Neck Surgery, Ministry of Education, Beijing 100005, China.
E-mail: huanglihui@ccmu.edu.cn

Ning Yu, College of Otolaryngology Head and Neck Surgery, Chinese PLA General Hospital, Beijing 100853, China; National Clinical Research Center for Otolaryngologic Diseases, Beijing 100853, China.
E-mail: yuning@301hospital.org

Original Article

Efficacy and effect on lipid profiles of Ainuovirine-based regimen versus Efavirenz-based regimen in treatment-naïve people with HIV-1 at week 24: A real-world, retrospective, multi-center cohort study

Hai Long[1,§], Quanying He[2,§], Yanmei Bi[3], Yingchun Ke[4], Xiaoxin Xie[1], Xiuhong Zhao[3], Si Tan[5], Yanhe Luo[6], Zhong Chen[5], Xiaoli Yu[6], Linghua Li[4,*]

[1] Department of Infectious Disease, GuiYang Public Health Clinical Center, Guiyang, Guizhou, China;
[2] Department of Outpatient, Yunnan Provincial Infectious Disease Hospital, Kunming, Yunnan, China;
[3] Department of Dermatology, Shandong Public Health Clinical Center, Shandong University, Jinan, Shandong, China;
[4] Infectious Disease Center, Guangzhou Eighth People's Hospital, Guangzhou Medical University, Guangzhou, Guangdong, China;
[5] Department of Infection and Immunology, The First Hospital of Changsha City, Xiangya School of Medicine of Central South University, Changsha, Hunan, China;
[6] Department of Infection and Immunology with Chinese Integrative Medicine, Wuhan Jinyintan Hospital, Tongji Medical College of Huazhong University of Science and Technology, Hubei Clinical Research Center for Infectious Diseases, Wuhan Research Center for Communicable Disease Diagnosis and Treatment, Chinese Academy of Medical Sciences, Joint Laboratory of Infectious Diseases and Health, Wuhan Institute of Virology and Wuhan Jinyintan Hospital, Chinese Academy of Sciences, Wuhan, China.

SUMMARY   This study aimed to compare the efficacy and effect on lipid profiles of Ainuovirine (ANV)- and efavirenz (EFV) -based regimens in treatment-naïve people living with HIV-1 (PLWH) at week 24. The proportion of PLWH achieving HIV-1 RNA < the limit of quantification in the ANV group was significantly higher than that in the EFV group (89.18% *vs.* 76.04%, $P = 0.002$). The mean change of $\log_{10}$ HIV-1 RNA from baseline was greater (-4.34 *vs.* -4.18, $P < 0.001$), the median change from baseline in CD4+ T cell count increased more (106.00 cells/μL *vs.* 92.00 cells/μL, $P = 0.007$) in the ANV group, while the CD4+/CD8+ ratio was similar (0.15 *vs.* 0.20, $P = 0.167$) between the two groups. The mean changes from baseline in total cholesterol (-0.02 for ANV *vs.* 0.25 mmol/L for EFV, $P < 0.001$), triglyceride (-0.14 for ANV *vs.* 0.11 mmol/L for EFV, $P = 0.024$), and low-density lipoprotein cholesterol (-0.07 for ANV *vs.* 0.15 mmol/L for EFV, $P < 0.001$) was significantly different between the two groups. The percentage of patients with improved lipid profiles was significantly higher in the ANV group (37.44 %) than in the EFV group (29.55%, $P = 0.0495$). The incidence of any adverse events in the ANV group was significantly lower than that in the EFV group at week 12 (6.2% *vs.* 30.7%, $P < 0.001$) and was comparable at week 24 (3.6% *vs.* 5.5%, $P = 0.28$). The ANV-based regimen was well tolerated and lipid-friendly in treatment-naïve PLWH.

Keywords   Ainuovirine, efavirenz, HIV infection, lipid profile, safety, treatment-naïve

1. Introduction

Antiretroviral therapy (ART) significantly reduces acquired immunodeficiency syndrome-related mortality and extends life expectancy in people living with HIV-1 (PLWH) (*1-3*). However, we are still far away from achieving the fourth 90, which is 90% of HIV-1 virologically suppressed PLWH achieving good health-related quality of life (*4*).

Ainuovirine (ANV, also known as ACC007) is a novel non-nucleoside reverse transcriptase inhibitor developed in China (*5,6*). The 96-week data from Phase III study demonstrated that the efficacy of ANV was non-inferior to efavirenz (EFV) and the treatment-related adverse effects (AEs), such as liver toxicity, dyslipidemia, neuropsychiatric symptoms, were less frequent (*7*). In a previous real-world study, we have verified good efficacy and favorable lipid changes of ANV in treatment-experienced PLWH versus EFV (*8*). In this paper, we want to verify these results further in treatment-naïve PLWH from real-life clinical practice. Compared with virologically suppressed PLWH, high HIV duplicate in treatment-naïve PLWH is the predominant reason that cause several metabolic disorders such as blood lipid

abnormalities, weight gain and adipocyte metastasis due to chronic inflammation and chronic immune activation (*9-11*). Reportedly, dyslipidemia occurred in up to 51.7% ART-naïve PLWH (*12*), which was significantly higher than that in general population in China (40.4%) (*13*). Therefore, "metabolically friendly" antiviral drugs are preferred to avoid further exacerbation of metabolic abnormalities. (*14*). In addition to metabolic safety, other drug safety profile also raises concerns in ART-naïve patients, whom are usually prone to adverse events, such as central nervous system (CNS) toxicities and rash due to tolerance has not yet been established. It is reported that AEs in CNS increased from 74.5% to 95.6% after 3 months of treatment in PLWH newly received ART in the first year, which had a great impact on their health-related quality of life (*14*). These AEs usually reduced with the extension of drug treatment time (*15*). Drug toxicity and intolerance are important reasons for at least one drug discontinuance (*16*). Thus, initial ART regimen can be a powerful predictor of long-term compliance and effectiveness.

This study is a multicenter, real-world, retrospective cohort study, aiming to compare the efficacy and safety of ANV- and EFV-based regimens in treatment-naïve PLWH after 24 weeks of treatment, and to further verify the advantage of ANV in altering lipid profiles.

2. Materials and Methods

2.1. Study design and participants

The data of participants receiving ANV-based or EFV-based treatment regimens were collected through the HIV real-world research platform (i-Study) from six clinical centers in China (Table S1, *http://www.biosciencetrends. com/action/getSupplementalData.php?ID=199*). Written informed consent form were signed by all participants. Participants in the ANV group received once-daily oral therapy comprising either ANV (75 mg/tablet × 2 tablets) + 3TC (lamivudine, 300 mg/tablet × 1 tablet) + TDF (tenofovir, 300 mg/tablet ×1 tablet) (ANV group) or an ANV/3TC/TDF fixed-dose compound tablet. The regimens for the EFV group were EFV (600 mg/tablet ×1 tablet) + 3TC (300 mg/tablet × 1 tablet) + TDF (300 mg/tablet ×1 tablet) (EFV 600 mg group) or EFV (200 mg/tablet × 2 tablets) + 3TC (300 mg/tablet × 1 tablet) + TDF (300 mg/tablet ×1 tablet) (EFV 400 mg group).

2.2. Inclusion and exclusion criteria

The inclusion criteria were (1) age ≥ 18 years; (2) diagnosis of HIV-1-positive, never received ART, and judged suitable for ART by a physician; and (3) complete data on four items of lipid profile, including total cholesterol (TC), total triglyceride (TG), high-density lipoprotein cholesterol (HDL-C), and low-density lipoprotein cholesterol (LDL-C).

The exclusion criteria were as follows: (1) currently suffering from serious chronic, metabolic, cardiovascular, and neurological and psychiatric diseases; (2) pregnant or lactating females or females of childbearing age who were unable to use effective contraception or whose partners were unable to use effective contraception; (3) those who had participated in other clinical trials within 8 weeks prior to enrollment in this study; and (4) those who were judged by the investigator to be unsuitable for participation in the trial based on the results of laboratory tests or for other reasons.

2.3. Procedures/Measurements

Data from visit 0 at baseline, visit 1 at 12 ± 2 weeks, and visit 2 at 24 ± 2 weeks were collected from participants, including demographic data (age, sex, height, weight, body mass index (BMI), and blood pressure), HIV infection information (plasma HIV-1 RNA level, CD4+ T cell count and CD4+/CD8+ ratio), biochemical indexes (hematology, liver enzyme levels, total bilirubin, direct bilirubin, blood glucose, uric acid, serum creatinine, and serum urea nitrogen as well as lipid profiles, including TC, TG, HDL-C, and LDL-C) and disease information (World Health Organization (WHO) staging and complications). HIV-1 RNA level was quantified in the clinical laboratory at each center using a real-time polymerase chain reaction-based assay. Safety was assessed during the study through self-reports by the participants or evaluations conducted by the investigators. AEs recorded at weeks 12 and 24 were collected.

2.4. Study endpoints

The maximum duration of observation was 24 weeks. The primary endpoints included the efficacy of the HIV-1 RNA suppression rate calculated by the HIV-1 RNA below the LOQ (the definition or standard of LOQ in each center is shown in Table S2, *http://www. biosciencetrends.com/action/getSupplementalData. php?ID=199*) at week 24 and the lipid profile changes, including TC, TG, HDL-C, and LDL-C from the baseline at week 24.The secondary endpoints included changes in immune function (CD4+ T-cell count and CD4+/CD8+ ratio) at weeks 12 and 24 from baseline, TC/HDL-C and TG/HDL-C changes at weeks 12 and 24 from the baseline, and lipid profile changes, including TC, TG, HDL-C, and LDL-C at week 12 from the baseline. The safety endpoint was the incidence of AEs over 24 weeks.

2.5. Statistical analysis

All statistical analyses were performed using R 4.2.2 (Lucent Technologies, Mount Murray, NJ, USA) and SAS 9.4 (SAS Institute Inc., Cary, NC, USA). Baseline

information, including age, sex, weight, WHO stage, comorbidities, baseline HIV-1 RNA level, and CD4+ T cell count, was weighted according to the overlap weights calculated by the propensity score. Continuous variables were displayed as mean (standard deviation). Independent-samples *t*-test or paired *t*-test were used for intergroup and intragroup comparisons, respectively. Categorical variables were displayed as number of cases (percentage), and comparisons between the two groups were performed using χ^2 test. The lipid profile changes at week 12/24 from baseline were described as the mean (95% CI). Covariate adjustment was performed for balancing baseline covariates. According to the lipid profile changes at week 12/24 from baseline, the patients were further divided into unchanged, improved, and worsened groups, and the data were weighted for description. Improved of four items of lipid profile defined as improved in any of the four items and without any item become worsen. Comparisons between groups were performed using χ^2 test. Results were visualized using GraphPad Prism 9.5.1 (Boston, MA, USA).

3. Results

3.1. Baseline demographics of participants

We retrospectively identified 274 eligible patients treated with ANV+3TC+TDF or ANV/3TC/TDF and 541 patients treated with EFV+3TC+TDF. After propensity score weighting using overlapping weights, the baseline information of the participants was generally balanced between the two groups (Table 1). Majority of the patients in both groups (ANV group: 78.8%, EFV group: 82.8%) were male (*P* = 1.000), and the mean ages of the ANV and EFV groups were 41.66 ± 14.28 and 40.15 ± 14.54 years, respectively (*P* = 1.000). No significant difference was observed in the proportion of comorbidities between the two groups at baseline (*P* = 1.000). Moreover, there were no significant differences in baseline plasma HIV-1 RNA levels, mean CD4+ T cell counts, or the CD4+/CD8+ ratios between the two groups (*P* > 0.05).

The mean concentrations of TC, TG, HDL-C, and LDL-C at baseline were 4.06 ± 0.95, 1.80 ± 1.42, 0.98 ± 0.33, and 2.39 ± 0.78 mmol/L for the ANV group and 4.13 ± 1.08 (*P* = 0.138 *vs.* ANV), 1.79 ± 1.24 (*P* = 0.727), 1.08 ± 0.39 (*P* < 0.001), and 2.49 ± 0.93 mmol/L (*P* = 0.014) for the EFV group, respectively. The percentage of patients with normal HDL-C in the ANV group was significantly lower than that in the EFV group (41.2% *vs.* 53.4%, *P* = 0.001); however, the percentage of patients with normal LDL-C in the ANV group was markedly higher than that in the EFV group (90.2% *vs.* 83.6%, *P* = 0.013).

3.2. Efficacy
The percentage of PLWH achieving HIV-1 RNA level

below the LOQ in the ANV group was obviously higher than that in the EFV group (89.18% for ANV *vs.* 76.04% for EFV, *P* = 0.002, Table 2) and the $\log_{10}$ (HIV-1 RNA) at week 24 from baseline had a more pronounced decrease in the ANV group than in the EFV group [−4.34(−4.46 to −4.21) for ANV *vs.* −4.18(−4.27 to −4.10) for EFV, *P* < 0.001] despite different EFV doses (EFV 400 mg: −4.19(−4.31~−4.07) and EFV 600mg: −4.20(−4.33~−4.08); *P* < 0.05) (Table 2).

As shown in Table 3, both ANV and EFV treatments significantly improved the CD4+ T cell count at weeks 12 and 24 from baseline (*P* < 0.001). The median increase of CD4+ T cell count at week 24 from baseline in the ANV group was 106.00 cells/μL (interquartile range [IQR], 30.00 to 208.00), which was greater than that in the EFV group (92.00 cells/μL, IQR, 19.00 to 173.00) (*P* = 0.007). The median increase in CD4+ T cell count at week 12 from baseline in the ANV group was 122.00 cells/μL (IQR, 67.00–189.00), which was also greater than that in the EFV group [87.00 cells/μL (IQR, 25.00 to 163.00)] (*P* = 0.038). Both ANV and EFV treatments could improve CD4+/CD8+ ratio at week 24 from baseline [0.15 (IQR, 0.06 to 0.28) in the ANV group; 0.20 (IQR, 0.08 to 0.37) in the EFV group] and week 12 from baseline [0.12 (IQR, 0.05 to 0.22) in ANV group; 0.13 (IQR, 0.04 to 0.25) in EFV group] (all *P* < 0.01). There were no statistical differences between the two groups (*P* = 0.167 at week 24, *P* = 0.546 at week 12).

3.3. Changes in lipid profiles

There were significant differences in the mean changes of TC, TG, and LDL-C levels at week 24 from baseline between patients treated with ANV and EFV (*P* < 0.05; Table 4 and Figure 1A). The mean (95% confidence interval [CI]) changes in TC were −0.02 mmol/L (−0.13 to 0.09) for ANV and 0.25 mmol/L (0.16 to 0.34) for EFV (*P* < 0.001). TG levels were decreased with ANV (−0.14 mmol/L; 95% CI, −0.37 to 0.09) and increased with EFV (0.11 mmol/L; 95% CI, −0.01 to 0.23; *P* < 0.001). The increases in HDL-C were 0.14 mmol/L (0.10 to 0.19) and 0.11 mmol/L (0.07 to 0.16) for ANV and EFV, respectively (*P* = 0.088). The LDL-C was decreased to −0.07 mmol/L (−0.15 to 0.02) with ANV and increased to 0.15 mmol/L (0.08 to 0.22) with EFV (*P* < 0.001). The ANV group revealed a more pronounced reduction in TC/HDL-C, TG/HDL-C, and log (TG/HDL-C), although the difference between the groups was not significant (*P* = 0.055, *P* = 0.141, and *P* = 0.069, respectively).

Patients were further stratified into baseline dyslipidemia, never taken lipid-lowing drugs, and baseline dyslipidemia & never taken lipid-lowering drugs subgroups for further analysis in order to exclude the confounding factor of lipid-lowering drugs (Table 4). In the baseline dyslipidemia subgroup, the mean

Table 1. The baseline demographics and clinical characteristics

Items	Unweighted				Propensity score overlap weighting			
	ANV group (n = 274)	EFV group (n = 541)	P	SMD	ANV group	EFV group	P	SMD
Age (mean (SD)), years	41.66 (14.28)	40.15 (14.54)	0.159	0.105	40.96 (14.01)	40.96 (14.86)	1.000	<0.001
Sex, n (%)								
Male	216 (78.8)	448 (82.8)	0.199	0.101	140.7 (80.3)	140.7 (80.3)	1.000	<0.001
Female	58 (21.2)	93 (17.2)			34.5 (19.7)	34.5 (19.7)		
CD4+ count (mean (SD)), cells/μL	313.12 (216.50)	285.70 (200.10)	0.073	0.132	304.88 (215.12)	304.88 (223.06)	1.000	<0.001
CD4+/CD8+ (mean (SD))	0.34 (0.25)	0.32 (0.27)	0.521	0.051	0.33 (0.24)	0.35 (0.32)	0.336	0.082
HIV RNA (%), copies/mL								
<100,000	206 (75.2)	364 (67.3)	0.016	0.220	127.6 (72.8)	127.6 (72.8)	1.000	<0.001
100,000-500,000	45 (16.4)	137 (25.3)			33.6 (19.2)	33.6 (19.2)		
>500,000	23 (8.4)	40 (7.4)			14.0 (8.0)	14.0 (8.0)		
WHO stage (%)								
I stage	148 (54.0)	246 (45.5)	0.056	0.208	90.0 (51.4)	90.0 (51.4)	1.000	<0.001
II stage	44 (16.1)	89 (16.5)			28.7 (16.4)	28.7 (16.4)		
III stage	21 (7.7)	68 (12.6)			15.6 (8.9)	15.6 (8.9)		
IV stage	61 (22.3)	138 (25.5)			40.8 (23.3)	40.8 (23.3)		
Complications (hypertension, diabetes), n (%)								
Yes	38 (13.9)	46 (8.5)	0.024	0.171	19.9 (11.4)	19.9 (11.4)	1.000	<0.001
No	236 (86.1)	495 (91.5)			155.3 (88.6)	155.3 (88.6)		
Weight (mean (SD)), kg	61.84 (11.91)	63.65 (11.00)	0.031	0.158	62.52 (12.09)	62.52 (10.65)	1.000	<0.001
Height (mean (SD)), cm	166.97 (9.21)	168.57 (8.17)	0.012	0.184	167.43 (9.13)	167.93 (8.40)	0.455	0.057
BMI (mean (SD)), kg/m^2	22.10 (3.28)	22.34 (3.16)	0.316	0.074	22.23 (3.33)	22.11 (3.03)	0.632	0.037
<18.5	33 (12.1)	55 (10.2)	0.621	0.100	19.8 (11.4)	19.7 (11.3)	0.711	0.088
18.5-24	162 (59.6)	334 (61.7)			102.1 (58.7)	109.7 (62.6)		
24-28	69 (25.4)	129 (23.8)			46.5 (26.7)	40.7 (23.2)		
≥28	8 (2.9)	23 (4.3)			5.4 (3.1)	5.1 (2.9)		
Systolic pressure (mean (SD)), mmHg	117.51 (12.82)	123.80 (11.19)	<0.001	0.523	117.45 (12.61)	124.39 (11.85)	<0.001	0.567
Diastolic pressure (mean (SD)), mmHg	77.59 (9.12)	74.53 (9.41)	0.001	0.330	77.52 (9.13)	74.81 (9.60)	0.005	0.290
Red blood cell count (mean (SD))	4.63 (0.75)	4.67 (0.67)	0.488	0.052	4.64 (0.75)	4.67 (0.66)	0.597	0.042
Hemoglobin (mean (SD)), g/L	139.58 (23.43)	141.57 (23.52)	0.255	0.085	139.78 (23.47)	141.37 (23.69)	0.375	0.067
Blood platelet count (mean (SD))	209.26 (72.20)	212.39 (70.70)	0.556	0.044	209.30 (71.74)	211.85 (69.13)	0.633	0.036
White blood cell count (mean (SD))	5.45 (1.92)	5.48 (2.07)	0.852	0.014	5.47 (1.95)	5.46 (2.04)	0.977	0.002
Alanine transaminase (mean (SD)), U/L	33.39 (38.23)	28.71 (24.99)	0.037	0.145	33.63 (38.92)	28.21 (23.90)	0.039	0.168
Aspertate aminotransferase (mean (SD)), U/L	32.67 (25.21)	29.59 (19.48)	0.056	0.137	32.68 (25.26)	29.56 (19.75)	0.080	0.138
Total bilirubin (mean (SD)), mmol/L	13.37 (9.38)	12.36 (7.46)	0.095	0.120	13.31 (9.40)	12.57 (7.38)	0.263	0.087
Direct bilirubin (mean (SD)), mmol/L	4.61 (5.71)	3.82 (2.71)	0.011	0.178	4.62 (5.78)	3.84 (2.81)	0.045	0.171
Blood glucose (mean (SD)), μmol/L	5.85 (1.87)	5.52 (1.83)	0.020	0.177	5.82 (1.81)	5.54 (1.90)	0.051	0.150
Uric acid (mean (SD)), μmol/L	365.13 (105.74)	364.06 (121.38)	0.903	0.009	367.05 (106.35)	358.08 (117.70)	0.282	0.080
Serum creatinine (mean (SD)), μmol/L	69.50 (14.60)	67.07 (13.94)	0.022	0.170	69.58 (14.66)	66.51 (14.22)	0.006	0.212
Serum urea nitrogen (mean (SD)), mmol/L	4.68 (1.51)	4.60 (3.41)	0.700	0.032	4.65 (1.51)	4.61 (3.28)	0.827	0.015

Table 1. The baseline demographics and clinical characteristics (continued)

Items	Unweighted				Propensity score overlap weighting			
	ANV group (n = 274)	EFV group (n = 541)	P	SMD	ANV group	EFV group	P	SMD
TC (mean (SD)), mmol/L	4.06 (0.95)	4.13 (1.08)	0.394	0.065	4.03 (0.95)	4.14 (1.05)	0.138	0.109
Normal	238 (86.9)	482 (89.1)	0.411	0.069	153.0 (87.3)	155.4 (88.7)	0.567	0.043
Abnormal	36 (13.1)	59 (10.9)			22.2 (12.7)	19.8 (11.3)		
TG (mean (SD)), mmol/L	1.80 (1.42)	1.79 (1.24)	0.912	0.008	1.82 (1.45)	1.78 (1.24)	0.727	0.027
Normal	181 (66.1)	334 (61.7)	0.258	0.090	114.9 (65.6)	109.2 (62.3)	0.372	0.068
Abnormal	93 (33.9)	207 (38.3)			60.3 (34.4)	66.0 (37.7)		
HDL-C (mean (SD)), mmol/L	0.98 (0.33)	1.08 (0.39)	< 0.001	0.274	0.97 (0.33)	1.08 (0.38)	< 0.001	0.321
Normal	117 (42.7)	284 (52.5)	0.010	0.197	72.2 (41.2)	93.5 (53.4)	0.001	0.246
Abnormal	157 (57.3)	257 (47.5)			103.0 (58.8)	81.7 (46.6)		
LDL-C (mean (SD)), mmol/L	2.39 (0.78)	2.49 (0.93)	0.105	0.124	2.38 (0.79)	2.54 (0.96)	0.014	0.184
Normal	247 (90.1)	460 (85.0)	0.054	0.156	158.0 (90.2)	146.5 (83.6)	0.013	0.197
Abnormal	27 (9.9)	81 (15.0)			17.1 (9.8)	28.7 (16.4)		
TC/HDL-C (mean (SD))	4.51 (1.51)	4.24 (1.80)	0.040	0.157	4.53 (1.52)	4.24 (1.78)	0.015	0.178
$\log_{10}$(TC/HDL-C) (mean (SD))	0.63 (0.14)	0.60 (0.16)	0.002	0.232	0.63 (0.14)	0.60 (0.16)	0.001	0.251
TG/HDL-C (mean (SD))	2.26 (2.64)	2.07 (2.36)	0.284	0.078	2.32 (2.74)	2.05 (2.36)	0.181	0.106
$\log_{10}$(TG/HDL-C) (mean (SD))	0.21 (0.32)	0.17 (0.34)	0.076	0.132	0.22 (0.32)	0.17 (0.33)	0.022	0.172

EFV 400 mg group and EFV 600 mg group were combined into EFV group for data analysis. Propensity scoring factors: age, sex, WHO stage, complications (hypertension, diabetes), CD4+ cell count, baseline HIV RNA level and weight. All results were weighted according to the overlap weighting calculated by propensity score. ANV, ainuovirine; BMI, body mass index; EFV, efavirenz; HDL-C, high-density lipoprotein; HIV, human immunodeficiency virus; LDL-C, low-density lipoprotein; SD, standard deviation; SMD, standardized mean difference; TC, total cholesterol; TG, triglyceride; WHO, world health organization. Comparisons between groups were performed by independent-samples t-test for continuous data or χ^2 test for categorical data. $P < 0.05$ regarded as statistical significance level.

Table 2. The outcome of $\log_{10}$ (HIV-1 RNA) at week 24

Comparisons	ANV group ($n = 274$)	EFV group ($n = 541$)	P
Below the LOQ, %	89.18	76.04	0.002
Above the LOQ, %	10.82	23.96	
[20, 200)	7.19	17.12	
[200, 400)	1.50	2.13	
≥ 400	2.13	4.71	
$\log_{10}$ (HIV-1 RNA) at week 24 from baseline, mean (95% CI)	−4.34 (−4.46~−4.21)	−4.18 (−4.27~−4.10)	< 0.001
EFV 400 mg group		−4.19 (−4.31~−4.07)	< 0.001
EFV 600 mg group		−4.20 (−4.33~−4.08)	0.003

The sample size was unweighted, and the remaining results were obtained through weighted analysis on propensity score. Comparisons between groups were performed by covariance analysis. ANV, ainuovirine; CI, confidence interval; EFV, efavirenz; HIV, human immunodeficiency virus; LOQ, limit of quantification (definition or standard of LOQ in each center is shown in Table S2, *http://www.biosciencetrends.com/action/getSupplementalData.php?ID=199*).

Table 3. The median changes from baseline of immune functions at week 12 and week 24

Variations	ANV group ($n = 274$)	EFV group ($n = 541$)	t	P
The CD4+ cell count change at week 24 from baseline, cells/μL			2.71	0.007
Median (IQR), cells/μL	106.00 (30.00~208.00)***	92.00 (19.00~173.00)***		
The CD4+/CD8+ change at week 24 from baseline			−1.38	0.167
Median (IQR)	0.15 (0.06~0.28)***	0.20 (0.08~0.37)**		
The CD4+ cell count change at week 12 from baseline, cells/μL			2.08	0.038
Median (IQR), cells/μL	122.00 (67.00~189.00)***	87.00 (25.00~163.00)***		
The CD4+/CD8+ change at week 12 from baseline			−0.60	0.546
Median (IQR)	0.12 (0.05~0.22)***	0.13 (0.04~0.25)***		

The number of samples was unweighted, and the remaining results were obtained through weighted analysis on propensity score. Covariance analysis was used for inter-group comparisons, and paired *t*-test was used for intra-group comparisons (follow-up vs baseline). The χ2 test was used to compare the categorical variables between groups. **, ***indicated $P < 0.01$, $P < 0.001$ for intra-group comparisons. ANV, ainuovirine; CI, confidence interval; EFV, efavirenz; IQR, interquartile ranges.

changes of TC, TG, LDL-C, TC/HDL-C, TG/HDL-C, and $\log_{10}$ (TG/HDL-C) were more favorable with ANV than with EFV ($P < 0.05$). HDL-C at week 24 from baseline increased in the ANV (0.21 mmol/L; 95% CI, 0.16 to 0.26) and EFV groups (0.17 mmol/L; 95% CI, 0.10 to 0.23; $P = 0.335$). For participants who had never taken lipid-lowering drugs, the mean changes of TC and LDL-C from baseline were −0.01 (−0.14 to 0.13) and −0.12 (−0.22 to −0.02) in ANV group whereas TC and LDL-C were increased by 0.23 (0.15 to 0.31) and 0.18 (0.10 to 0.26), respectively, in the EFV group (all $P < 0.001$). No statistical differences were observed in the other variables, including TG, HDL-C, TC/HDL-C, TG/HDL-C, and $\log_{10}$ (TG/HDL-C) between the ANV and EFV groups ($P > 0.05$). However, the data showed a decreasing trend in the ANV group. For participants in baseline dyslipidemia & never taken lipid-lowering drugs subgroup, the mean changes in TC, TG, LDL-C, TC/HDL-C, TG/HDL-C, and $\log_{10}$ (TG/HDL-C) from baseline were more favorable with ANV than with EFV at week 24. HDL-C was increased in both ANV (0.24 mmol/L; 95% CI, 0.17 to 0.30) and EFV groups (0.14 mmol/L; 95% CI, 0.05 to 0.22; $P = 0.713$).

For sub-group analysis between ANV and EFV 400 mg groups, the mean changes of TC (−0.03 *vs.* 0.30 mmol/L, $P < 0.001$) and LDL-C (−0.04 *vs.* 0.09 mmol/L,

$P = 0.018$) from baseline was significantly different. The mean changes of all variables from baseline, except TC/HDL-C, were significantly different between the ANV and EFV 600 mg groups ($P < 0.05$) (Table 4).

For the secondary endpoints of mean changes of lipid profiles between the groups at week 12 from baseline, TC, TG, and LDL-C were significantly lower in the ANV group than in the EFV group ($P < 0.05$), whereas no significant difference was observed in the mean change in HDL-C ($P > 0.05$, Figure 1B).

According to the lipid profile change at week 12/24 from baseline, the patients were further divided into unchanged, improved, and worsened subgroups. As shown in Figure 2, at week 24, the percentage of patients with improved TC was about two-fold higher in the ANV group (10.33%) than in the EFV group (5.75%), whereas the percentage of patients with worsened LDL-C levels in the ANV group (2.42 %) was only approximately a quarter of that in the EFV group (9.21%). Overall, the percentage of patients with improved 4 items of lipid profiles was significantly higher in the ANV group (37.44 %) than in the EFV group (29.55%), whereas the percentage of patients with worsened lipid profiles was significantly lower in the ANV group (23.53 %) than in the EFV group (35.18%) ($P = 0.0495$). No significant difference was observed between the two groups at week

Table 4. The mean changes from baseline of lipid profiles at week 24

Variables	ANV group (n =274), mean (95% CI)	EFV group (n =541), mean (95% CI)	Inter-group difference (95% CI)	P
ANV group *vs.* EFV group (EFV 400 mg + EFV 600 mg)				
TC, mmol/L	−0.02 (−0.13~0.09)	0.25 (0.16~0.34)	−0.33 (−0.44~−0.22)	< 0.001
TG, mmol/L	−0.14 (−0.37~0.09)	0.11 (−0.01~0.23)	−0.23 (−0.42~−0.03)	0.024
HDL-C, mmol/L	0.14 (0.10~0.19)	0.11 (0.07~0.16)	−0.05 (−0.10~0.01)	0.088
LDL-C, mmol/L	−0.07 (−0.15~0.02)	0.15 (0.08~0.22)	−0.29 (−0.38~−0.19)	< 0.001
TC/HDL-C	−0.67 (−0.86~−0.47)	−0.27 (−0.44~−0.11)	−0.18 (−0.36~0.00)	0.055
TG/HDL-C	−0.58 (−0.94~−0.21)	−0.15 (−0.38~0.07)	−0.21 (−0.48~0.07)	0.141
Log$_{10}$(TG/HDL-C)	−0.10 (−0.15~−0.06)	−0.03 (−0.06~−0.01)	−0.04 (−0.08~0.00)	0.069
Baseline dyslipidemia subgroup				
TC, mmol/L	−0.01 (−0.15~0.13)	0.25 (0.12~0.37)	−0.39 (−0.53~−0.25)	< 0.001
TG, mmol/L	−0.37 (−0.62~−0.12)	0.04 (−0.13~0.21)	−0.45 (−0.67~−0.22)	< 0.001
HDL-C, mmol/L	0.21 (0.16~0.26)	0.17 (0.10~0.23)	−0.04 (−0.11~0.04)	0.335
LDL-C, mmol/L	−0.07 (−0.17~0.03)	0.09 (0.01~0.18)	−0.28 (−0.39~−0.17)	< 0.001
TC/HDL-C	−0.99 (−1.22~−0.77)	−0.48 (−0.71~−0.25)	−0.35 (−0.58~−0.12)	0.003
TG/HDL-C	−0.98 (−1.44~−0.52)	−0.33 (−0.65~−0.00)	−0.48 (−0.84~−0.12)	0.010
Log$_{10}$(TG/HDL-C)	−0.18 (−0.23~−0.14)	−0.08 (−0.12~−0.04)	−0.08 (−0.13~−0.03)	0.001
Never taken lipid-lowering drugs subgroup				
TC, mmol/L	−0.01 (−0.14~0.13)	0.23 (0.15~0.31)	−0.28 (−0.40~−0.16)	< 0.001
TG, mmol/L	−0.12 (−0.44~0.19)	0.10 (−0.03~0.23)	−0.17 (−0.41~0.08)	0.184
HDL-C, mmol/L	0.16 (0.10~0.22)	0.08 (0.03~0.13)	−0.04 (−0.11~0.03)	0.246
LDL-C, mmol/L	−0.12 (−0.22~−0.02)	0.18 (0.10~0.26)	−0.31 (−0.42~−0.20)	< 0.001
TC/HDL-C	−0.72 (−0.96~−0.48)	−0.17 (−0.35~0.02)	−0.19 (−0.41~0.03)	0.086
TG/HDL-C	−0.53 (−0.96~−0.10)	−0.10 (−0.35~0.15)	−0.16 (−0.49~0.17)	0.344
Log$_{10}$(TG/HDL-C)	−0.12 (−0.17~−0.06)	−0.02 (−0.05~0.01)	−0.04 (−0.09~0.01)	0.084
Baseline dyslipidemia & never taken lipid-lowering drugs subgroup				
TC, mmol/L	−0.00 (−0.17~0.16)	0.22 (0.12~0.32)	−0.33 (−0.48~−0.18)	< 0.001
TG, mmol/L	−0.41 (−0.71~−0.11)	0.01 (−0.17~0.20)	−0.46 (−0.72~−0.20)	< 0.001
HDL-C, mmol/L	0.24 (0.17~0.30)	0.14 (0.05~0.22)	−0.02 (−0.12~0.08)	0.713
LDL-C, mmol/L	−0.13 (−0.25~0.00)	0.11 (0.02~0.21)	−0.30 (−0.43~−0.17)	< 0.001
TC/HDL-C	−1.09 (−1.35~−0.82)	−0.35 (−0.62~−0.08)	−0.43 (−0.72~−0.15)	0.003
TG/HDL-C	−0.96 (−1.45~−0.48)	−0.27 (−0.66~0.11)	−0.55 (−0.99~−0.10)	0.015
Log$_{10}$(TG/HDL-C)	−0.20 (−0.26~−0.15)	−0.07 (−0.12~−0.03)	−0.10 (−0.16~−0.04)	< 0.001
ANV group *vs.* EFV 400 mg group				
TC, mmol/L	0.03 (−0.08~0.14)	0.22 (0.10~0.34)	−0.25 (−0.38~−0.12)	< 0.001
TG, mmol/L	−0.10 (−0.34~0.14)	0.08 (−0.07~0.23)	−0.09 (−0.33~0.15)	0.464
HDL-C, mmol/L	0.16 (0.11~0.20)	0.15 (0.10~0.19)	−0.01 (−0.06~0.04)	0.672
LDL-C, mmol/L	−0.04 (−0.12~0.04)	0.09 (0.02~0.16)	−0.11 (−0.20~−0.02)	0.018
TC/HDL-C	−0.69 (−0.89~−0.50)	−0.45 (−0.65~−0.25)	−0.19 (−0.39~0.02)	0.074
TG/HDL-C	−0.57 (−0.95~−0.19)	−0.20 (−0.53~0.13)	−0.14 (−0.49~0.22)	0.448
Log$_{10}$(TG/HDL-C)	−0.11 (−0.15~−0.06)	−0.06 (−0.10~−0.02)	−0.03 (−0.08~0.02)	0.219
ANV group *vs.* EFV 600 mg group				
TC, mmol/L	−0.03 (−0.14~0.08)	0.30 (0.17~0.42)	−0.39 (−0.53~−0.25)	< 0.001
TG, mmol/L	−0.21 (−0.43~0.02)	0.16 (−0.01~0.34)	−0.39 (−0.62~−0.15)	0.001
HDL-C, mmol/L	0.14 (0.09~0.19)	0.08 (−0.00~0.17)	−0.09 (−0.18~−0.01)	0.037
LDL-C, mmol/L	−0.08 (−0.17~0.01)	0.21 (0.08~0.34)	−0.45 (−0.59~−0.31)	< 0.001
TC/HDL-C	−0.65 (−0.84~−0.46)	−0.07 (−0.33~0.19)	−0.18 (−0.42~0.07)	0.153
TG/HDL-C	−0.65 (−1.01~−0.28)	−0.08 (−0.38~0.22)	−0.33 (−0.65~−0.02)	0.038
Log$_{10}$(TG/HDL-C)	−0.11 (−0.15~−0.07)	−0.00 (−0.04~0.04)	−0.06 (−0.11~−0.01)	0.015

The sample size was unweighted, and the remaining results were obtained through weighted analysis on propensity score. Baseline dyslipidemia was defined as those with baseline total cholesterol ≥5.2 mmol/L or triglyceride ≥1.7 mmol/L or HDL-C < 1 mmol/L or LDL-C ≥3.4 mmol/L. Never used lipid-lowering drugs were those reported no for whether lipid-lowering drugs were used at baseline, week 12 and week 24. Comparisons between groups were performed by covariance analysis. ANV, ainuovirine; CI, confidence interval; EFV, efavirenz; HDL-C, high-density lipoprotein; HIV, human immunodeficiency virus; LDL-C, low-density lipoprotein; TC, total cholesterol; TG, triglyceride.

12 (P > 0.05, data not shown).

3.4. BMI changes

We compared the BMI changes of participants at week 12/ 24 from baseline in the ANV or EFV group, as well as between the ANV and EFV groups, and no significant difference was found in intra- or inter-group comparisons (P > 0.05, Table S3, *http://www.biosciencetrends.com/action/getSupplementalData.php?ID=199*).
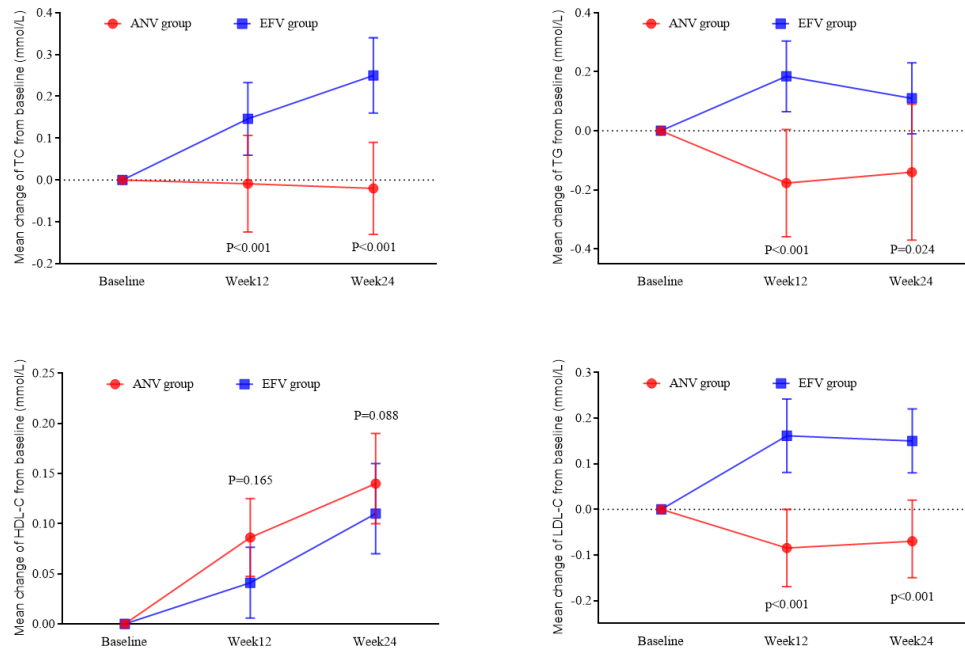
3.5. Safety evaluation

Figure 1. Mean changes in lipid profile at week 24 (A) and week 12 (B) from baseline. The results were obtained through weighted analysis on propensity score. Inter-group comparisons were completed by the analysis of covariance and intra-group comparisons were performed by paired *t* test. ANV, ainuovirine; EFV, efavirenz; HDL-C, high density lipoprotein cholesterol; LDL-C, low density lipoprotein cholesterol; TC, total cholesterol; TG, triglyceride. *indicates *P* < 0.05 for lipid parameters at week 24 from baseline.
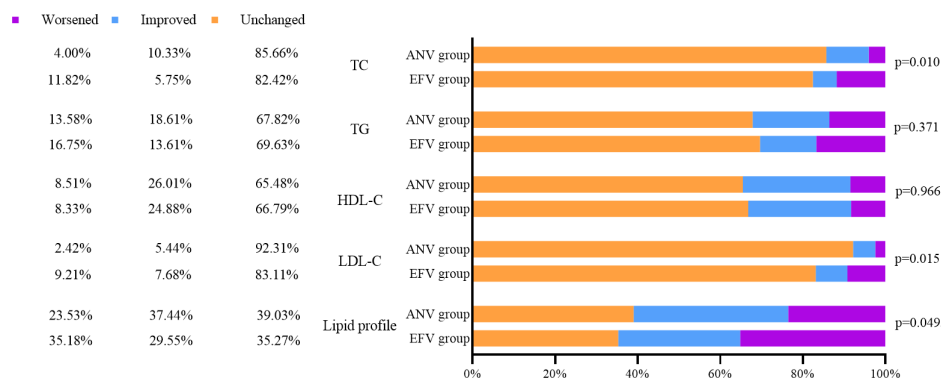

Figure 2. Percentage of patients with worsened, improved, and unchanged lipid profile at week 24. The results were obtained through weighted analysis on propensity score. TC ≥ 5.2 mmol/L, TG ≥ 1.7 mmol/L, HDL-C < 1.0 mmol/L and LDL-C ≥ 3.4 mmol/L were considered abnormal. In the analyses, worsen defined as the lipid level changed from normal at baseline to abnormal; improve defined as the lipid level changed from abnormal at baseline to normal; the lipid level remained normal or abnormal defined as unchanged. Improve of four items of lipid profile defined as improved in any of the four items and without any item become worsen. ANV, ainuovirine; EFV, efavirenz; HDL-C, high density lipoprotein cholesterol; LDL-C, low density lipoprotein cholesterol; TC, total cholesterol; TG, triglyceride.

At week 12, only 17 AEs (6.2%), including 11 mild AEs (4%) and 6 moderate AEs (2.2%), were reported in the ANV group. In contrast, there were 134 AEs (30.7%) in the EFV group, including 109 mild AEs (25%), 21 moderate AEs (4.8 %), and 4 severe AEs (0.9 %). The incidence of any AEs at week 12 in the ANV group was significantly lower than that in the EFV group (*P* < 0.001). The most common AEs in the EFV group were related to the CNS (95, 21.8%), including 76 (17.4%) cases of dizziness, 2 (0.5%) of abnormal dreams, 15 (3.4%) of insomnia, and 2 (0.5%) of anxiety/depression. There were 12 cases of CNS-related AEs (4.4%) in the ANV group, including 7 (2.5%) cases of dizziness, 3 (1%) of abnormal dreams, and 2 (0.8%) of insomnia.

The incidence of rashes was also significantly lower in the ANV group than in the EFV group (1.5% *vs.* 4.6%, *P* = 0.03). There were three (0.2%) cases of severe rashes in the EFV group, two of which remitted after treatment. At week 24, the incidence rate of AEs in the ANV group was reduced to 3.6%, which was lower than that in the EFV group (5.5%), but the difference was not statistically significant (*P* = 0.28) (Table 5).

4. Discussion

In this multicenter, real-world, retrospective cohort study, we found that 89.18% of the treatment-naïve PLWH in the ANV group and 76.04% of those in the EFV group

Table 5. Adverse events in ANV group and EFV group at week 12 and week 24

Adverse events	Week 12							Week 24						
	ANV group (n = 274)			EFV group (n = 541)			P	ANV group (n = 274)			EFV group (n = 541)			P
Severity	mild	moderate	severe	mild	moderate	severe		mild	moderate	severe	mild	moderate	severe	
Any adverse event, n (%)	11 (4)	6 (2.2)	0	109 (25)	21 (4.8)	4 (0.9)	< 0.001	5 (1.8)	2 (0.7)	3 (1)	13 (3)	9 (2.1)	2 (0.5)	0.28
Dizziness	6 (2.2)	1 (0.4)	-	63 (14.4)	12 (2.7)	1 (0.2)	< 0.001	-	-	-	7 (1.6)	2 (0.5)	-	-
Abnormal dreams	3 (1)	-	-	2 (0.5)	-	-	-	2 (0.7)	-	-	-	1 (0.2)	-	0.28
Insomnia	1 (0.4)	1 (0.4)	-	12 (2.7)	3 (0.7)	-	0.06	1 (0.4)	-	1 (0.4)*	3 (0.7)	3 (0.7)	-	-
Anxiety/depression	-	-	-	1 (0.2)	1 (0.2)	-	-	1 (0.4)	-	1 (0.4)	1 (0.2)	-	-	-
Rash	1 (0.4)	3 (1)	-	14 (3.2)	3 (0.7)	3 (0.2)&	0.03	1 (0.4)	1 (0.4)	-	-	2 (0.5)	-	-
Facial numbness	-	-	-	-	1 (0.2)	-	-	-	-	-	-	-	-	-
Palpitation	-	1 (0.4)	-	2 (0.5)	-	-	-	-	-	-	-	-	-	-
Weakness	-	-	-	4 (0.9)	1 (0.2)	-	-	-	-	-	-	-	-	-
Diarrhea	-	-	-	-	-	-	-	1 (0.4)	1 (0.4)	-	-	-	-	-
Nausea/abdominal distension	-	-	-	6 (1.4)	-	-	-	-	-	-	-	1 (0.2)	-	-
Decreased vision	-	-	-	-	-	-	-	-	-	1 (0.4)*	-	-	-	-
Osteopenia/osteoporosis	-	-	-	-	-	-	-	-	-	-	2 (0.5)	-	-	-
Other	-	-	-	5 (1.1)	-	-	-	-	-	-	-	2 (0.5)	-	-

*Remission or improvement after treatment; &2 patients remitted after treatment.

had HIV-1 RNA levels below the LOQ ($P = 0.002$) at week 24. Compared with the EFV group, ANV exhibited superior HIV RNA suppression efficacy and favorable lipid profile changes. In terms of safety, the results of this study showed that the incidence of AEs in the EFV group was higher (30.7% *vs.* 6.2%, $P < 0.001$), especially in the early stage of treatment (week 12). To the best of our knowledge, this is the first multicenter, real-world study in China to evaluate the efficacy, safety and lipid profiles of treatment-naïve PLWH treated with ANV-based regimen in China.

The most prominent AEs caused by EFV were CNS-related AEs, such as dizziness (17.4%), insomnia (3.4%), and cutaneous AEs, such as rash (3.9%). We speculated that these AEs may significantly affect ART adherence in intolerant patients during the early treatment period, thereby resulting in a relatively low EFV efficacy (76.04%). Simultaneously, ANV appears to be "CNS friendly," with much lower incidences of AEs, such as dizziness (2.5%) and insomnia (0.7%) than those with EFV, even though the CNS-related AEs were also the main AEs of ANV. This result is consistent with a previous prospective study that ANV improves the patient's symptom experience, such as dizziness, nervousness and anxiety, compared to the EFV regimen (*17*). After 24 weeks of treatment, the AEs of EFV significantly reduced, indicating improved tolerance. However, it is noteworthy that the early AEs may prompt some patients to switch treatment regimens, thus affecting treatment efficacy. Studies have shown that HIV RNA suppression in the early stages of treatment is associated with a good prognosis and reduces the risk of HIV transmission to the uninfected partners (*18*).

Notably, our results found that HIV RNA inhibition rates were similar regardless of EFV doses of 400 or 600 mg, which was in line with previous non-inferiority studies (*19,20*). In this study, although 400 mg of EFV achieved a non-inferior efficacy to 600 mg, AEs were not reduced, suggesting that for patients with extreme intolerance, it may still be necessary to switch treatment regimens. In addition, we speculate that there may be another reason for the efficacy of EFV drug resistance. The prevalence of drug resistance to EFV has increased from 1.6% in 2004–2007 to 6.3% in 2020–2022 in China (*21-24*). Owing to limited resources, baseline drug resistance is generally not tested in treatment-naïve PLWH in China, which may lead to treatment failure. Preliminary *in vitro* studies have shown that ANV can overcome the HIV-1 resistance mutations K103N and V106M (*6*), which are non-polymorphic resistance mutation sites selected by EFV. Overall, our real-world study showed that ANV significantly improved tolerability while achieving viral suppression.

Regarding lipid changes, patients in the ANV group showed decreases in the mean changes in TC, TG, and LDL-C at weeks 12 and 24, whereas these lipid parameters were all increased in patients treated with

EFV. The advantage of ANV in changing lipid profiles still exists after excluding the confounding factors in subgroup analyses. These results suggest that ANV might be less associated with increase of cardiovascular disease (CVD) risk, which is consistent with the results of phase III with a study period of 96 weeks (*7*). An increase in CVD risk is proportional to dyslipidemia, indicated by increase in LDL-C, TC, and TG levels (*25*). However, these results seem more likely that ANV does not lead to lipid deterioration than EFV. Therefore, we further analyzed the proportion of PLWH with improved lipid profiles and worsened lipid profiles. The percentage of patients with improved lipid profiles was significantly higher in the ANV group (37.44 %) than in the EFV group (29.55%), whereas the percentage of patients with worsened lipid profiles was significantly lower in the ANV group (23.53 %) than in the EFV group (35.18%). For the treatment-naïve PLWH, EFV caused a significant proportion of lipid deterioration even at the early treatment periods of week 12 or week 24, and this metabolic disorder may become more serious with the extension of treatment time (*17*). On the other hand, the favorable lipid changes by ANV may provide a better option for the initial ART of treatment-naïve PLWM.

Weight gain, central obesity, and lipodystrophy in PLWH during ART have attracted increasing attention. PLWH initiating ART gain excess weight, which is associated with a higher risk of metabolic disease (*26*). In our study, ANV had no significant effect on body weight no mater in treatment-naïve or treatment-experienced PLWH. This may also be due to the short follow-up period after ANV treatment, which typically requires extended reobservation.

Our study has some limitations. First, this is a retrospective study and a bias might still exist though we have balanced all the factors that can be collected. Second, the follow-up period was only 24 weeks, and the long-term effects of ANV on lipid profiles may be different. Third, there may have been other unavoidable confounding factors or biases. Therefore, the results should be interpreted with caution and further prospective studies are warranted.

In conclusion, the ANV-based regimen was well tolerated and more lipid-friendly while achieving viral suppression and immune reconstitution in treatment-naïve PLWH. This study, together with the previous study in treatment-experienced PLWH, comprehensively demonstrated the good efficacy and advantages on lipid metabolism of ANV in PLWH. ANV deserves more attention in treatment-naïve PLWH. However, further prospective studies with longer follow-up periods are required to validate our conclusions.

Acknowledgements

References

1. Yoshimura K. Current status of HIV/AIDS in the ART era. J Infect Chemother. 2017; 23:12-16.
2. Wang N, Lan G, Zhu Q, *et al.* HIV Epidemiology, Care, and Treatment Outcomes Among Student and Nonstudent Youths Living With HIV in Southwest China Between 1996 and 2019: Historical Cohort Study. JMIR Public Health Surveill. 2023; 9:e38881.
3. Farahani M, Mulinder H, Farahani A, Marlink R. Prevalence and distribution of non-AIDS causes of death among HIV-infected individuals receiving antiretroviral therapy: a systematic review and meta-analysis. Int J STD AIDS. 2017; 28:636-650.
4. Naghavi M. Global, regional, and national burden of suicide mortality 1990 to 2016: systematic analysis for the Global Burden of Disease Study 2016. Bmj. 2019; 364:l94.
5. Cha YJ, Lim KS, Park MK, Schneider S, Bray B, Kang MC, Chung JY, Yoon SH, Cho JY, Yu KS. Pharmacokinetics and tolerability of the new second-generation nonnucleoside reverse- transcriptase inhibitor KM-023 in healthy subjects. Drug Des Devel Ther. 2014; 8:1613-1619.
6. Huang XS, Luo RH, Hu XL, Chen H, Xiang SY, Tang CR, Zhang CT, Shen XN, Zheng YT. The New NNRTI ACC007 Combined with Lamivudine and Tenofovir Disoproxil Fumarate Show Synergy Anti-HIV Activity *In Vitro*. Curr HIV Res. 2020; 18:332-341.
7. Su B, Gao G, Wang M, *et al.* Efficacy and safety of ainuovirine versus efavirenz combination therapies with lamivudine/tenofovir disoproxil fumarate for medication of treatment-naïve HIV-1-positive adults: week 48 results of a randomized controlled phase 3 clinical trial followed by an open-label setting until week 96. Lancet Reg Health West Pac. 2023; 36:100769.
8. Wang C, Yu X, Ke Y, Fu Y, Luo Y, Li Y, Bi Y, Chen X, Li L, Zhao X, Chen Z. Efficacy and effect on lipid profiles of switching to ainuovirine-based regimen versus continuing efavirenz-based regimen in people with HIV-1: 24-week results from a real-world, retrospective, multi-center cohort study. Antimicrob Agents Chemother. 2024; e0166823.
9. Grunfeld C. Dyslipidemia and its Treatment in HIV Infection. Top HIV Med. 2010; 18:112-118.
10. Willig AL, Overton ET. Metabolic Complications and Glucose Metabolism in HIV Infection: A Review of the Evidence. Curr HIV/AIDS Rep. 2016; 13:289-296.
11. Waters DD, Hsue PY. Lipid Abnormalities in Persons Living With HIV Infection. Can J Cardiol. 2019; 35:249-259.
12. Guo F, Hsieh E, Lv W, Han Y, Xie J, Li Y, Song X, Li T. Cardiovascular disease risk among Chinese antiretroviral-

naïve adults with advanced HIV disease. BMC Infect Dis. 2017; 17:287.

13. Jun-Ren ZHU, Run-Lin GAO, Shui-Ping Z, Guo-Ping LU, Dong Z, Jian-Jun LI. 2016 Chinese guidelines for the management of dyslipidemia in adults. Journal of Geriatric Cardiology. 2018; 15:1-29.

14. Dai L, Su B, Liu A, Zhang H, Wu H, Zhang T, Shao Y, Li J, Ye J, Bai S, Guo X, Sun L. Adverse events in Chinese human immunodeficiency virus (HIV) patients receiving first line antiretroviral therapy. BMC Infect Dis. 2020; 20:158.

15. Hongo H, Nagao T, Nakamura K, Kitaichi T, Maeno Y, Tokunaga T, Fukuda A, Koga I. Safety and Effectiveness Analysis of Dolutegravir in Patients with HIV-1: Interim Report of Post-Marketing Surveillance in Japan. Advances in Therapy. 2021; 38:4480-4504.

16. Gebrezgabher BB, Kebede Y, Kindie M, Tetemke D, Abay M, Gelaw YA. Determinants to antiretroviral treatment non-adherence among adult HIV/AIDS patients in northern Ethiopia. AIDS Res Ther. 2017; 14:16.

17. Ma S, Xie X, Fu Y, Gan L, Yang X, Kong L, Li J, Long H. Clinical benefits of novel non-nucleoside reverse transcriptase inhibitors: A prospective cohort study. Immun Inflamm Dis. 2024; 12:e1217.

18. Robbins RN, Spector AY, Mellins CA, Remien RH. Optimizing ART adherence: update for HIV treatment and prevention. Curr HIV/AIDS Rep. 2014; 11:423-433.

19. Carey D, Puls R, Amin J, *et al.* Efficacy and safety of efavirenz 400 mg daily versus 600 mg daily: 96-week data from the randomised, double-blind, placebo-controlled, non-inferiority ENCORE1 study. Lancet Infect Dis. 2015; 15:793-802.

20. Carey D. Efavirenz 400 mg daily remains non-inferior to 600 mg: 96 week data from the double-blind, placebo-controlled ENCORE1 study. J Int AIDS Soc. 2014; 17:19523.

21. Lin B, Sun X, Su S, Lv C, Zhang X, Lin L, Wang R, Fu J, Kang D. HIV drug resistance in HIV positive individuals under antiretroviral treatment in Shandong Province, China. PLoS One. 2017; 12:e0181997.

22. Chen M, Wu M, Zeng L, Zhang Y, Huobu-Mo M, Li J, Li C, Xiao H. Virologic status and pattern of drug resistance mutation among ART-experienced HIV-infected patients in Butuo County, China. J Glob Antimicrob Resist. 2023; 32:98-103.

23. Dong K, Ye L, Leng Y, Liang S, Feng L, Yang H, Su L, Li Y, Baloch S, He F, Yuan D, Pei X. Prevalence of HIV-1 Drug Resistance among Patients with Antiretroviral Therapy Failure in Sichuan, China, 2010-2016. Tohoku J Exp Med. 2019; 247:1-12.

24. Liu X, Wang D, Hu J, Song C, Liao L, Feng Y, Li D, Xing H, Ruan Y. Changes in HIV-1 Subtypes/Sub-Subtypes, and Transmitted Drug Resistance Among ART-Naïve HIV-Infected Individuals - China, 2004-2022. China CDC Wkly. 2023; 5:664-671.

25. Galindo J, Amariles P, Mueses-Marín HF, Hincapié JA, González-Avendaño S, Galindo-Orrego X. Effectiveness and safety of generic version of abacavir/lamivudine and efavirenz in treatment naïve HIV-infected patients: a nonrandomized, open-label, phase IV study in Cali-Colombia, 2011-2012. BMC Infect Dis. 2016; 16:532.

26. Lam JO, Leyden WA, Alexeeff S, Lea AN, Hechter RC, Hu H, Marcus JL, Pitts L, Yuan Q, Towner WJ, Horberg MA, Silverberg MJ. Changes in Body Mass Index Over Time in People With and Without HIV Infection. Open Forum Infect Dis. 2024; 11:ofad611.

§These authors contributed equally to this work.
Address correspondence to:
Linghua Li, Infectious Disease Center, Guangzhou Eighth People's Hospital, Guangzhou Medical University, No. 8 Huaying Road, Baiyun District, Guangzhou, Guangdong, 510440, China.
E-mail: llheliza@126.com

Brief Report

Vitamin C alleviates rheumatoid arthritis by modulating gut microbiota balance

Yanjie Zhang[1,2,3]**, Sibin Zhen**[1,2,3]**, Hao Xu**[1,2,3]**, Songfang Sun**[1,2,3]**, Ziwei Wang**[1,2,3]**, Mian Li**[1,2,3]**, Liang Zou**[1,4]**, Yangyang Zhang**[1,2,3]**, Yan Zhao**[1,2,3,*]**, Yazhou Cui**[1,2,3,*]**, Jinxiang Han**[1,2,3,*]

[1] Biomedical Sciences College & Shandong Medicinal Biotechnology Centre, Shandong First Medical University & Shandong Academy of Medical Sciences, Ji' nan, Shandong, China;
[2] NHC Key Laboratory of Biotechnology Drugs (Shandong Academy of Medical Sciences), Ji'nan, Shandong, China;
[3] Key Lab for Rare & Uncommon Diseases of Shandong Province, Ji'nan, Shandong, China;
[4] Bone Biomechanics Engineering Laboratory of Shandong Province, Neck-Shoulder and Lumbocrural Pain Hospital of Shandong First Medical University, Shandong First Medical University & Shandong Academy of Medical Sciences, Ji'nan, China.

SUMMARY Rheumatoid arthritis (RA) is a systemic autoimmune disease characterized by chronic and symmetric in-flammation. Our previous research revealed an imbalance in the gut flora of RA patients and showed that certain gut microbiota can accelerate RA progression by enhancing vitamin C degradation. However, it is unclear whether vitamin C supplementation could improve the gut microbiota to prevent the development of arthritis by interfering with the gut-joint axis. In this work, we aimed to evaluate the effects of vitamin C in regulating the gut microbiota and to elucidate its potential role in the onset and progression of RA in a mouse model, thus providing a basis for the development of new intervention strategies and treatments for RA. In this study, collagen-induced arthritis (CIA) mouse models, biochemical, histological and 16S rRNA microbiological methods were used to investigate the role and possible mechanism of vitamin C in rheumatoid arthritis. The results showed that treatment of CIA mice with vitamin C effectively rescued the gut mi-crobiota imbalance and suppressed the inflammatory response associated with RA, and effectively alleviated arthritis symptoms in mice in which levels of the pro-inflammatory cytokines IL-6 and TNF-α were specifi-cally reduced. In conclusion, our results demonstrate the potential of vitamin C as a potential therapeutic choice for RA.

Keywords 　　rheumatoid arthritis, vitamin C, gut microbiota, intestinal dysbiosis

1. Introduction

Rheumatoid arthritis (RA) is a chronic autoimmune disease that affects 0.5% to 1% of the population, mak-ing it the second leading cause of disability in China (*1*). It is characterized by symmetric arthritis and progressive destruction of the synovium and articular cartilage (*2*). While the primary treatments for RA, including glucocorticoids (GCs), disease-modifying antirheumatic drugs (DMARDs) and biologics, can provide some relief of symptoms, they also have several drawbacks, including limited distribution in inflamed joints and potential toxic side effects (*3*).

　　Recent research has shown a link between gut microbiota and several extra-intestinal tissue diseases, including RA (*4*). The gut microbiota plays an important role in maintaining immune homeostasis in the body and has been implicated in the pathogenesis

and progression of RA (*4,5*). Given the critical role of the gut microbiota in the development and progression of RA, there is a need to further investigate innovative treatment strategies that address and promote a healthy gut microbiota balance (*6*). Such approaches may lead to more effective and less toxic treatments for this debilitating disease.

　　In a previous study, we found that the degradation of vitamin C by the gut microbiota in RA patients was positively correlated with the pro-inflammatory cytokines TNF-α and IL-6. This suggests that the gut microbiota may contribute to the progression of RA by promoting vitamin C degradation (*7*). However, there is currently no evidence to support the use of vitamin C supplementation to restore gut microbiota balance and prevent RA exacerbation *via* the gut-joint axis.

　　In this study, we supplemented vitamin C in a CIA (collagen-induced arthritis) mouse model to evaluate its

regulatory effect on gut microbiota and RA development. Our findings suggest that vitamin C supplementation may provide a non-toxic and potentially side-effect-free intervention strategy for RA.

2. Materials and Methods

2.1. Establishment of a collagen-induced arthritis (CIA) mouse model

Seven-week-old male DBA/1 mice, weighing 20 g, were housed in an ultra-clean animal laboratory (SPF grade) with a humidity of 55% and a temperature of 26°C. The animal study protocol was approved by the Institutional Animal Care and Use Committee of the Institutional Review Board of the Shandong Research Center for Medicinal Biotechnology (2020S307). Mice were maintained according to institutional guidelines.

CIA models were established as described previously (*8*). Mice were immunized with collagen II and randomly divided into three groups: (*i*) the CIA-VC group, consisting of mice successfully induced with CIA and treated daily with 100 mg/kg vitamin C for 6 weeks (*n* = 6); (*ii*) the CIA group, consisting of mice induced with CIA (*n* = 6); and (*iii*) the control group (*n* = 6). Both the CIA and control groups received 0.9% normal saline.

2.2. Assessment of arthritis severity in CIA

To continuously monitor the progression of arthritis in the animals, the severity of arthritis was scored after the first immunization using an established grading system as described previously (*9*). The arthritis score for each mouse was determined by summing the scores of all four paws, and the average score for each treatment group was calculated. Scoring of arthritis severity in each category was performed independently by two observers to ensure objectivity.

2.3. Micro-computed tomography (micro-CT)

Micro-computed tomography (Micro-CT) (Quantum GX, Perkin Elmer, USA) was used to scan and reconstruct the three-dimensional structure of the hind paw joint. The settings were 209m, 90kV X-ray tube voltage, 160uA current and 3 minutes scan time. The angle of the X-ray scan was rotated 180 degrees. The resolution is 2μm and the field of view is 12.8 mm × 12.8 mm.

2.4. Hematoxylin and eosin (HE) staining

H&E stained sections were used to evaluate the degree of cartilage degeneration and synovial invasion.Tissue samples were fixed in 4% paraformaldehyde solution for 24 hours. After fixation, the tissues were embedded in paraffin and cut into 5μm slices. The slices were then incubated at 65°C for 4 hours and then dehydrated

through a gradient of ethanol. The sections were then stained with haematoxylin for 5 minutes. After a short differentiation step in 1% hydrochloric acid-alcohol for 2 seconds, the sections were incubated in ammonia water for 2 minutes and stained with eosin for 1 minute. Finally, the sections were dehydrated, cleared and mounted in neutral resin. The sections were examined by light microscopy (Olym-pus Corporation, Tokyo, Japan).

2.5. Enzyme-linked immunosorbent assay (ELISA)

Mouse plasma was collected and centrifuged (3,000 g, 15 min) for serum collection. The levels of in-flammation were determined by ELISA (mlbio, Shanghai, China), total necrosis factor-α (TNF-α) and inter-leukin-6 (IL-6), strictly following the reagent manufacturer's protocols. Absorbance was measured at 450 nm.

2.6. Faecal sample collection and DNA extraction

Faecal samples were collected at the end of the experiment and stored at -80°C for extraction of total faecal DNA (Bacterial DNA Kit, TIANGEN), with the tube containing PBS as an environmental control. Only samples with sufficient bacteria had sufficient bacterial DNA content ($\geq$ 10 ng) for high-throughput sequencing of the bacterial 16S rRNA gene.

2.7. 16S rRNA gene sequencing and analysis

The V1-V2 regions of the 16S rRNA gene were sequenced on the Illumina Hiseq 2500 (Illumina Inc., San Diego, CA, USA). Using split_libraries.py in QIIME (v.1.9.1) to trim raw reads for adapter and primer se-quences, paired-end sequences were then joined using FLASH with default parameters. In addition, chimer-ic sequences were identified and removed using de novo chimera detection in USEARCH (v.6.1). Finally, the resulting sequences were clustered into operational taxonomic units (OTUs) for subsequent analysis. The UCLUST algorithm was used to analyze and determine the community composition of each group at multiple levels of classification, including phylum, family and genus. Rarefaction analysis based on Mothur (v.1.21.1) was used to determine diversity indices, including Chao 1, ACE and Shannon diversity indices. All statistical analyses were performed using the R stats package. Linear discriminant analysis effect size (LEfSe) analysis was performed to identify biomarkers of high-dimensional gut bacteria. Species with significant differences in abundance between different groups were detected using non-parametric Kruskal-Wallis rank sum, consistency of differences was tested using Wilcoxon rank sum, followed by linear discriminant analysis (LDA) was used to estimate the effect size of each distinctly abundant taxa.

2.8. Statistical analysis

GraphPad Prism software version 9.0 and R software version 4.1.3 were used for statistical analysis and presentation. Pearson correlations and Mantel tests were analyzed using the packages 'linkET 0.0.7.4' and 'ggplot2 3.3.3'. A significance level of $p < 0.05$ was considered statistically significant. Data are presented as mean ± standard error of the mean (SEM) or mean ± standard deviation (SD). Statistical significance be-tween groups was assessed using unpaired t-tests and one-way analysis of variance (ANOVA) for the indicators. Corrected p-values were used to adjust for multiple testing.

3. Results and Discussion

3.1. Vitamin C balances the immune response and reduces arthritis progression in CIA mice

Clinical scores were measured every four days during the study. The CIA mice developed severe arthritis with paw thickness increasing continuously until day 12 after booster immunisation, and the clinical scores increased rapidly in the late period (Figure 1A and 1B). The late-stage progression of altered arthritic symp-toms in mice treated with vitamin C was similar to that observed in CIA mice, albeit with significantly less severe arthritis compared to CIA mice (see Figure 1A and 1B). In addition, serum pro-inflammatory cyto-kines were essential indices to assess arthritis activities, and the relative levels of serum pro-inflammatory cytokines were measured by ELISA (Figure 1C). The concentrations of serum TNF-α and IL-6 in the CIA group were significantly higher than those in the control group, while oral administration of vitamin C effec-tively restored the levels of TNF-α and IL-6 in early immunization compared with CIA ($p < 0.01$) (Figure 1C). Overall, oral

administration of vitamin C during early immunization rebalances the immune response and partially rescues the arthritis phenotype.

3.2. Vitamin C attenuated cartilage destruction and inflammation in joint tissue

Imaging studies revealed a higher degree of cartilage damage and bone erosion in the interphalangeal joint of the paws of CIA mice, whereas VC-treated CIA mice showed reduced levels of bone erosion and destruction as shown by micro-CT images (Figure 2A). Therefore, these findings suggest that early administration of vitamin C is effective in delaying disease onset and preventing joint destruction.

In addition, we used histological H&E staining to assess the effect of vitamin C on joint pathology and cartilage destruction. Significant inflammatory cell infiltration and cartilage destruction, granulation tissue prolif-eration, lymphocyte infiltration and chronic inflammation were observed in all CIA mouse groups, whereas the vitamin C group showed few of these symptoms and had significantly lower histological and cartilage destruction than the CIA group (Figure 2B). Taken together, these results suggest that early administration of vitamin C is effective in delaying disease onset and preventing joint destruction. In conclusion, the above re-sults demonstrate that vitamin C supplementation is effective in ameliorating the symptoms and phenotype of RA in CIA mice.

3.3. Vitamin C altered gut microbial diversity and composition in CIA mice

To gain insight into the effect of vitamin C on arthritis-induced dysbiosis, faeces were analysed to compare their microbial composition. Alpha diversity was assessed
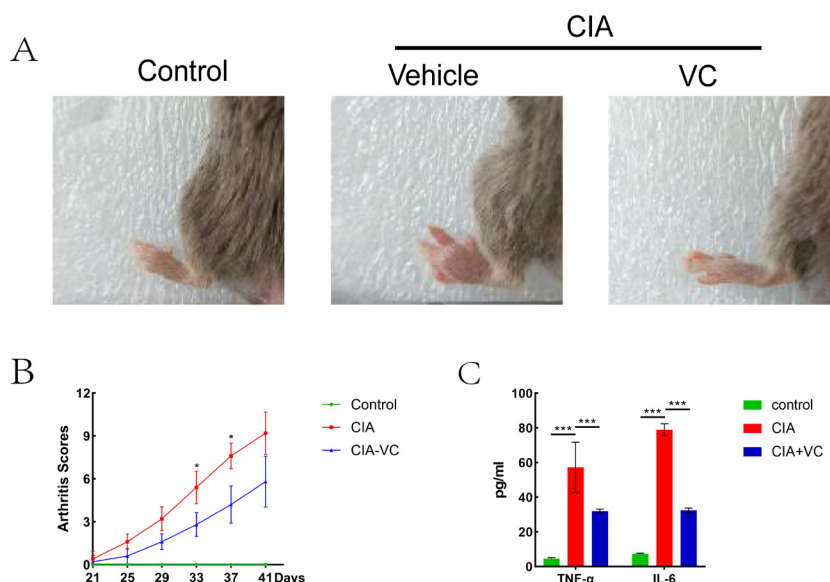

Figure 1. Vitamin C supplementation attenuated the progression of rheumatoid arthritis in CIA. (A) Representative images of paws in each group prior to sacrifice. **(B)** Arthritis scores of CIA were monitored every four days. **(C)** The levels of pro-inflammatory factors, IL-6 and TNF-α, in the serum of mice were de-termined by ELISA. Values are expressed as mean ± SD. One-way ANOVA between groups. (ns: not sig-nificant, *$p < 0.05$, **$p < 0.01$, ***$p < 0.001$).
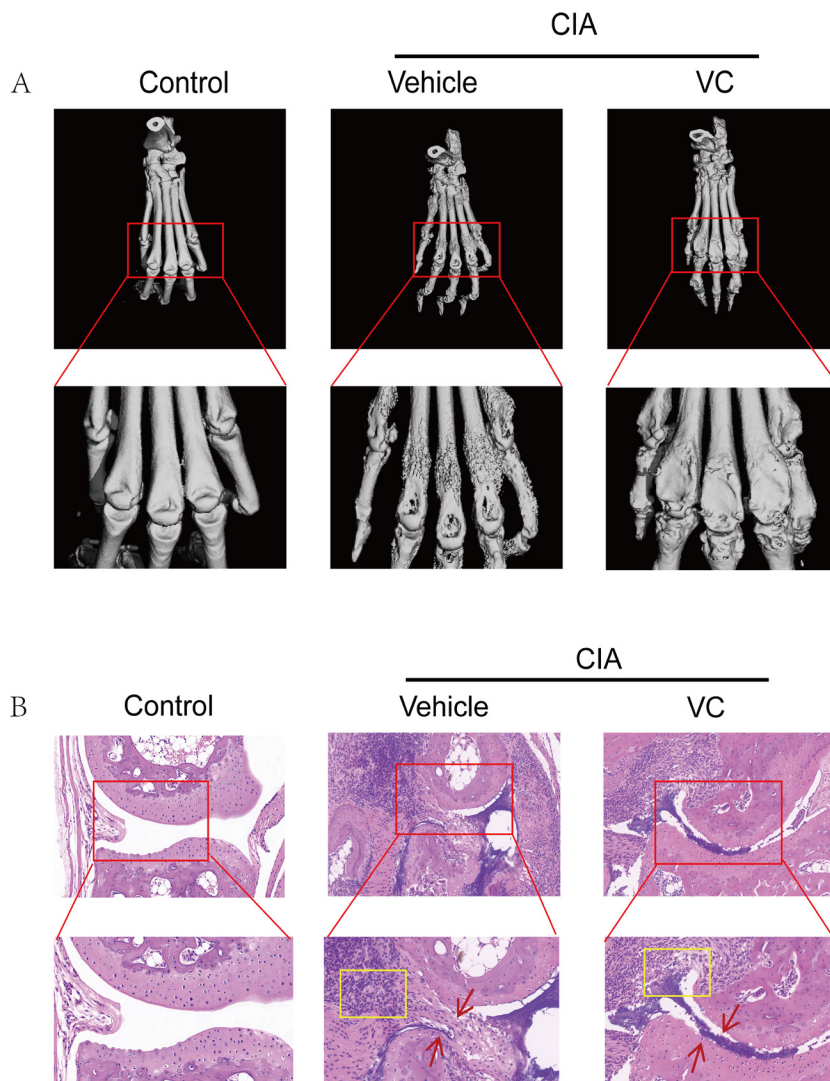
Figure 2. Vitamin C supplementation ameliorates joint pathology and cartilage destruction of rheuma-toid arthritis in CIA. (A) Representative micro-CT images of hind paws and interphalangeal joints. **(B)** Rep-resentative histological images of H&E stained interphalangeal joint showing pathological changes including synovial proliferation and joint destruction.

using Shannon, Richness, ACE and Chao indices. Compared to control mice, the diversity indices of ACE and Chao were significantly decreased in CIA mice, and the other two alpha diversity indices (Richness and Shannon) were also significantly altered. Compared to the model group, Chao1 and ACE indices were significantly higher in the early vitamin C intervention group (CIA-VC group), and Richness and Shannon also increased (Figure 3A). Vitamin C treatment was able to modestly restore gut microbial diversity in CIA mice to near normal levels, thereby reducing gut damage.

Among the dominant phyla, Firmicutes and Proteobacteria were slightly downregulated in the CIA group, while Bacteroidetes were enriched (Figure 3B). Compared to the CIA group, the proportion of Bacteroidetes and Tenericutes was reduced in the vitamin C treatment group, while that of Firmicutes was significantly increased (Figure 3B).

At the family level, Bacteroidaceae, Muribaculaceae and Lachnospiraceae were dominant in both control and CIA model groups, Lachnospiraceae and Bacteroidaceae were decreased, Muribaculaceae and Helicobacter-aceae were increased in CIA mice, and the relative abundance of Bacteroidaceae and Muribaculaceae was decreased in the vitamin C treatment group, whereas Lachnospiraceae and Helicobacteraceae were upregu-lated (Figure 3C). At the genus level, Bacteroides and Odoribacter were significantly more abundant in CIA mice than in control mice. After vitamin C intervention, Bifidobacterium, Kineothrix and Helicobacter in-creased while Odoribacter and Phocaeicola decreased (Figure 3D).

Consistent with the changes in diversity at both phylum and family level, the microbial composition changed after CII or vitamin C intervention. The domain phyla were Bacteroidetes and Firmicutes, followed by Pro-teobacteria and Tenericutes in all groups (Figure 3E). LEfSe was used to identify the major bacterial markers responsible for the observed dissimilarity between groups. The LDA bars of taxa with differential abundance after conventionalisation with the microbiome showed that there were five, five and fourteen dominant bacterial biomarkers in the control, CIA and CIA-VC treatment groups, respectively. Among the identified markers, the relative abundance of a well-known probiotic Lactobacillales was significantly enriched in the control
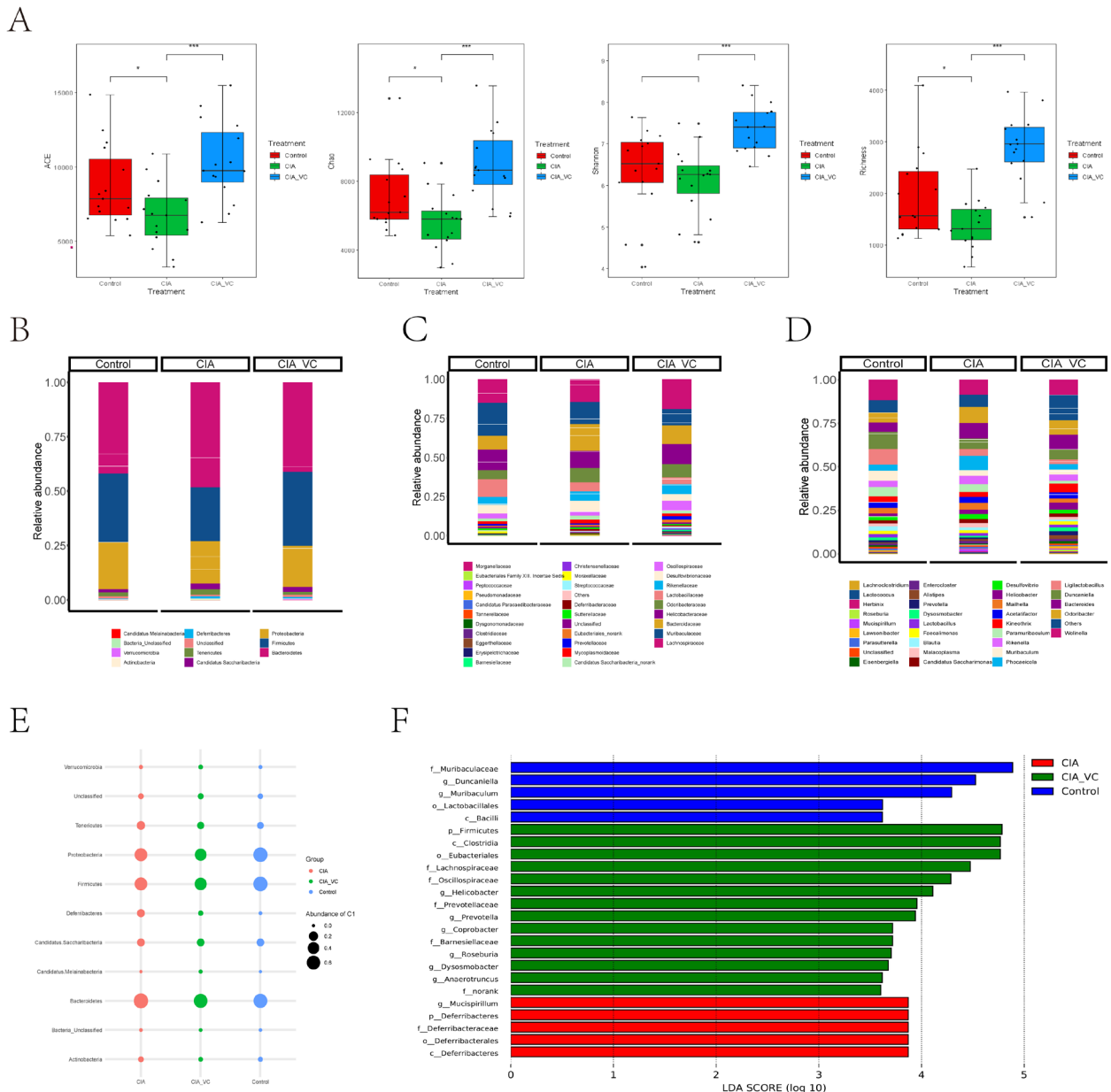
Figure 3. Effects of vitamin C in gut microbiota regulation on diversity and abundance. **(A)** Alpha di-versity analysis of faecal microbiota OTU at different taxonomic ranks including ACE, Chao, Shannon and Richness indices. The gut microbial composition profiles. **(B)** The relative abundance and bacterial taxonomic analysis of major differentiated gut taxa at the phylum level. **(C)** The relative abundance and bacterial taxo-nomic analysis of key differentiated gut taxa at the family level. **(D)** The relative abundance and bacterial taxonomic analysis of key differentiated gut taxa at the family level. **(E)** The bubble plot shows domain phy-la in all groups. **(F)** Histogram of linear discriminant analysis (LDA) showing significant differences in gut microbiota abundance between groups, LDA score > 3.5 and $p < 0.05$.

group (Figure 3F). Meanwhile, among the markers affected by vitamin C intervention, Lachnospiraceae, Barnesiellaceae, Oscillospiraceae and Prevotel-laceae were dominant families considered as candidates for next-generation probiotics (NGPs), whereas Mu-cispirillum and Deferribacteraceae were more abundant in CIA mice. These changes indicated that the gut microbiota in CIA mice tended to restore the normal flora balance after vitamin C administration.

3.4. Correlation between pro-inflammatory cytokines and microbial communities in CIA mice

To verify the correlation between pro-inflammatory cytokines and microbial communities, and to identify potential co-abundance and co-exclusion interactions in microbial communities, we correlated taxonomic community composition with that of inflammatory factors at the family level. Manteltest correlation showed that Muribaculaceae was the strongest correlate of both IL-6 and TNF-α, being positively associated with IL-6 and TNF-α ($p < 0.05$). Lachnospiraceae was also positively associated with IL-6 ($p < 0.05$), while no statistically significant correlation was found for TNF-α. Furthermore, Pearson's r showed that there was
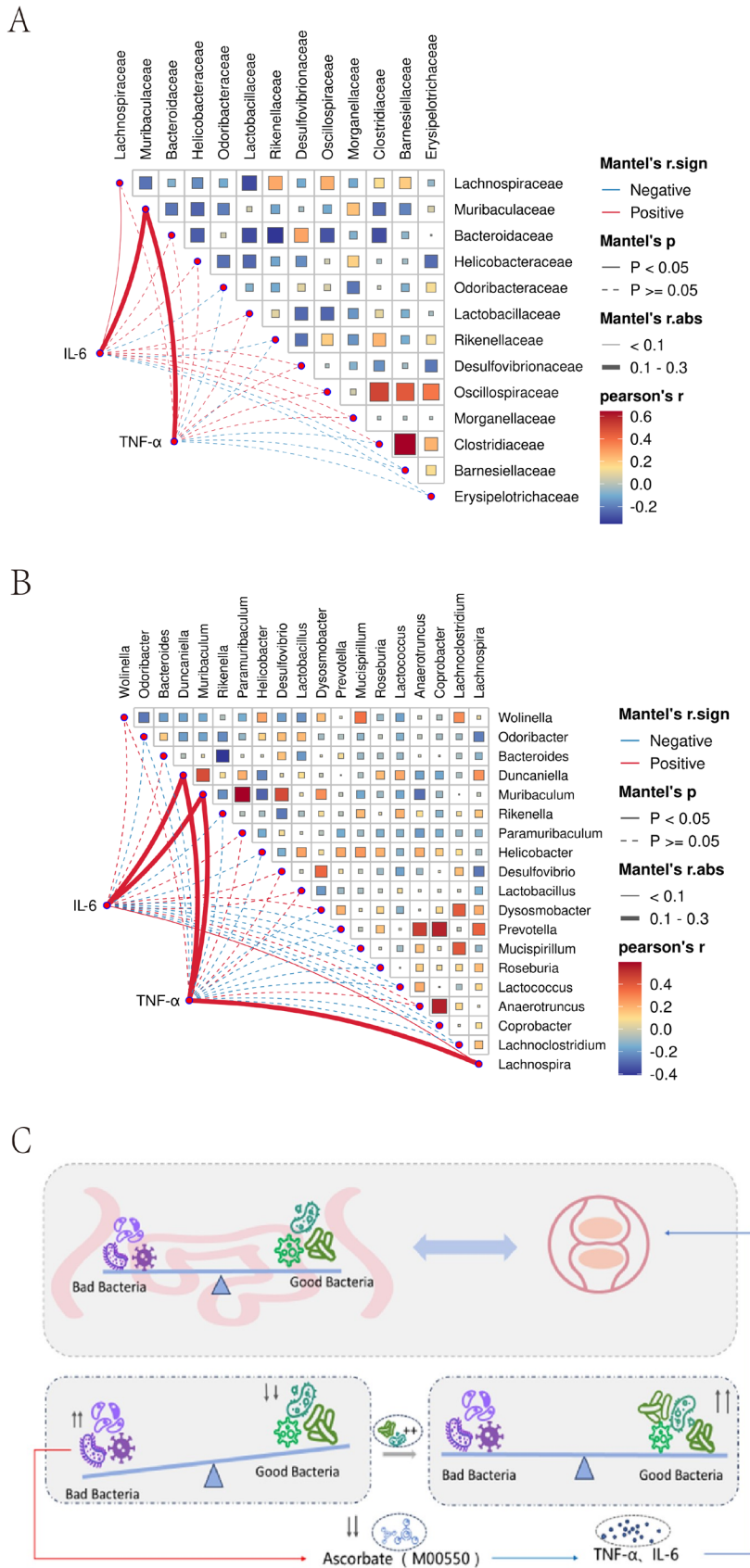
Figure 4. The correlation analysis between gut microbiota composition and pro-inflammatory factors. (A) The correlation analysis between gut microbiota composition at the family level and pro-inflammatory factors, and (B) the correlation analysis between gut microbiota composition at the genus level and pro-inflammatory factors.The community composition was related to each pro-inflammatory factor by partial Mantel tests. Edge width corresponds to Mantel's r statistic for the corresponding distance correlations, red is a positive correlation and blue is a negative correlation. Data are presented as mean ± SEM, *p* < 0.05 was considered significant. Pairwise comparisons of microbial components are shown, with a colour gradient in-dicating Spearman's correlation coefficients. (C) Graphical summary of this study. Based on the gut-joint axis interactions, ascorbic acid alleviated RA symptoms by regulating and balancing the gut microbiota.

a strong positive correlation between Clostridiaceae and the relative content of Barnesiellaceae, Oscillospiraceae was positively associated with the relative abundance of Clostridiaceae, Barnesiellaceae and Erysipelotri-chaceae, while Bacteroidaceae was negatively correlated with Clostridiaceae, Oscillospiraceae, Rikenellaceae and Lactobacillaceae (Figure 4A).

At the genus level, both Muribaculum and

Duncaniella were strongly correlated with IL-6 and TNF-α, there are positive correlations between Muribaculum and Duncaniella with IL-6 and TNF-α ($p < 0.05$), as well as Lachnospira was positively associated with IL-6 and TNF-α, while IL-6 was only weakly correlated, except for Muribaculum, Lachnospira and Duncaniella, the correlations were not statistically significant with other genera. In addition, there was a strong negative correlation between Rikenella and the relative abundance of Bacteroides, Coprobacter was positively correlated with Prevotella and Anaerotruncus, Muribaculum was positively associated with the relative abundance of Paramuribaculum (Figure 4B).

Our previous study showed that the gut microbiota may promote RA progression by increasing the break-down of ascorbate (vitamin C) and may provide a potential approach to prevent the development of arthritis by interfering with the gut-joint axis (7). The aim of this study was to determine whether vitamin C supple-mentation could reverse these pathological processes, which remains to be investigated. In this study, we demonstrated the regulatory effects of oral vitamin C supplementation on the structure of the gut flora in CIA mice. We preliminarily confirmed that vitamin C effectively suppressed various RA phenotypes in the CIA model, as evidenced by the reduction of joint swelling, articular cartilage and bone destruction, and in-flammatory cell infiltration. These data provide further evidence for the therapeutic potential of vitamin C in the treatment of RA.

Vitamin C, also known as ascorbic acid, is one of the most effective antioxidants (10). Previous studies have evaluated the effects of vitamin C as an antioxidant supplement intervention on the levels of plasma inflammatory molecules and disease severity in RA patients (11). This study has shown the noteworthy ef-fect of vitamin C on the gut microbiome, particularly in terms of microbial alpha diversity. Other data also confirmed the effect of high-dose vitamin C to improve both alpha and beta diversity of the bacterial community, including an increase in Collinsella, which is a producer of SCFAs such as butyrate and propionate (12-14). This suggests that vitamin C may be a potential modulator of the gut microbial community (13). The results in the mice model reliably validated the regulatory effect of vitamin C on the balance of gut microbiota. Lachnospiraceae which exhibited high abundance in CIA mice with vitamin C supplementation, was also specifically enriched in the intestinal tract of CIA mice after vitamin C intervention. Lachnospiraceae, Oscil-lospiraceae, Morganellaceae, Barnesiellaceae, and Clostridiaceae were enriched in CIA-VC compared to CIA. Among these families, Muribaculaceae and Lachnospiraceae were revealed to enhance gut microbiota metabolite production, such as SCFAs and polyamines (15). The Lachnospiraceae

family, consisting of Lachnospira, Fusicatenibacter, Roseburia, and Lachnoclostridium, is able to produce SCFAs such as acetic acid, which play important roles in kidney protection, including anti-inflammatory, anti-atherosclerosis, and anti-oxidation effects (16,17). Other studies have also confirmed the anti-inflammatory properties of SCFAs (including valerate, butyrate, propionate, and acetate), produced by the gut microbiota (18,19). Most of these microbes listed above, which are positively associated with vitamin C, are considered as candidate probiotics for producing SCFAs (20). SCFAs are revolved in the body's redox process, regulating intestinal balance and improving intestinal function (20-22). Together, these microbes may serve as a mediator for vit-amin C to exert its anti-inflammatory effects on RA pathology. In this study, vitamin C intervention was found to effectively inhibit various RA phenotypes in the CIA model, as evidenced by reductions in joint swelling, articular cartilage and bone destruction, and infiltration of inflammatory cells. Importantly, vitamin C could effectively ameliorate the inflammatory phenotype in CIA model mice, downregulating IL-6 and TNF-α, suggesting the previous findings that vitamin C regulates immune response and further showing that inflammatory cytokines are decreased in mice gavaged with vitamin C (23,24).

In view of the above results, vitamin C intervention alleviates RA symptoms and also improves the composition of the gut microbiota. It is reasonable to conclude that vitamin C increases the abundance of potential probiotics in the gut associated with RA, such as Muribaculaceae and Lachnospiraceae, regulate the composition of the gut flora in patients, which could achieve the goal of reducing disease-related inflamma-tory factors, alleviating symptoms and slowing disease progression (Figure 4C). These findings support the prevailing idea that vitamin C can be used as an adjuvant therapy for RA.

Notably, these results were obtained in an experimental mouse model of arthritis, therefore, in-depth studies in RA patients are urgently needed to verify our findings and to assess whether this approach would dramatically improve the prognosis of patients. To elucidate their potential role in the onset and progression of RA, the precise molecular mechanisms underlying the preventive and therapeutic effects of vitamin C and the new probiotics, such as the Muribaculaceae identified in the gut, deserve further experimentation. This will facilitate the development of a novel adjunctive treatment option for RA.

Conflict of Interest: The authors have no conflicts of interest to disclose.

References

1. Smolen JS, Aletaha D, Barton A, Burmester GR, Emery P, Firestein GS, Kavanaugh A, McInnes IB, Solomon DH, Strand V, Yamamoto K. Rheumatoid arthritis. Nat Rev Dis Primers. 2018; 4:18001.
2. McInnes IB, Schett G. Pathogenetic insights from the treatment of rheumatoid arthritis. Lancet. 2017; 389:2328-2337.
3. Rai V, Patel N, Mammen SR, Chaudhary SM, Arshad S, Munazzam SW. Futuristic Novel Therapeu-tic Approaches in the Treatment of Rheumatoid Arthritis. Cureus. 2023; 15:e49738.
4. Miyauchi E, Shimokawa C, Steimle A, Desai MS, Ohno H. The impact of the gut microbiome on ex-tra-intestinal autoimmune diseases. Nat Rev Immunol. 2023; 23:9-23.
5. Wang DW, Pang XT, Zhang H, Gao HX, Leng YF, Chen FQ, Zhang R, Feng Y, Sun ZL. Gut mi-crobial dysbiosis in rheumatoid arthritis: a systematic review protocol of case-control studies. BMJ Open. 2022; 12:e052021.
6. Gupta VK, Cunningham KY, Hur B, Bakshi U, Huang H, Warrington KJ, Taneja V, Myasoedova E, Davis JM, 3rd, Sung J. Gut microbial determinants of clinically important improvement in patients with rheumatoid arthritis. Genome Med. 2021; 13:149.
7. Zhao Y, Cheng M, Zou L, Yin L, Zhong C, Zha Y, Zhu X, Zhang L, Ning K, Han J. Hidden link in gut-joint axis: gut microbes promote rheumatoid arthritis at early stage by enhancing ascorbate deg-radation. Gut. 2022; 71:1041-1043.
8. Brand DD, Latham KA, Rosloniec EF. Collagen-induced arthritis. Nature Protoc. 2007; 2:1269-1275.
9. Zhao Y, Liu F, Liu Y, Zhou D, Dai Q, Liu S. Anti-arthritic effect of chebulanin on collagen-induced arthritis in mice. PloS One. 2015; 10:e0139052.
10. Okamoto K, Kitaichi F, Saito Y, Ueda H, Narumi K, Furugen A, Kobayashi M. Antioxidant effect of ascorbic acid against cisplatin-induced nephrotoxicity and P-glycoprotein expression in rats. Eur J Pharmacol. 2021; 909:174395.
11. Bae SC, Jung WJ, Lee EJ, Yu R, Sung MK. Effects of antioxidant supplements intervention on the level of plasma inflammatory molecules and disease severity of rheumatoid arthritis patients. J Am Coll Nutr. 2009; 28:56-62.
12. Pham VT, Dold S, Rehman A, Bird JK, Steinert RE. Vitamins, the gut microbiome and gastrointesti-nal health in humans. Nutr Res. 2021; 95:35-53.
13. Anwar F, Alhayyani S, Al-Abbasi FA, Nadeem MS, Kumar V. Pharmacological role of Vitamin C in stress-induced cardiac dysfunction *via* alteration in Gut microbiota. J Biochem Mol Toxicol. 2022; 36:e22986.
14. Pham VT, Fehlbaum S, Seifert N, Richard N, Bruins MJ, Sybesma W, Rehman A, Steinert RE. Ef-fects of colon-targeted vitamins on the composition and metabolic activity of the human gut microbi-ome- a pilot study. Gut
15. Microbes. 2021; 13:1-20.
16. Zhou X, Pak S, Li D, Dong L, Chen F, Hu X, Ma L. Bamboo Shoots Modulate Gut Microbiota, Eliminate Obesity in High-Fat-Diet-Fed Mice and Improve Lipid Metabolism. Foods. 2023; 12.
17. Nikkhah A, Ejtahed HS, Ettehad Marvasti F, Taghavi M, Pakmehr A, Hajipour F, Larijani B. The critical role of gut microbiota dysbiosis in skeletal muscle wasting: a systematic review. J Appl Mi-crobiol. 2023; 134.
18. Ohira H, Tsutsui W, Fujioka Y. Are Short Chain Fatty Acids in Gut Microbiota Defensive Players for Inflammation and Atherosclerosis? J Atheroscler Thromb. 2017; 24:660-672.
19. Qiu F, Zhang Z, Yang L, Li R, Ma Y. Combined effect of vitamin C and vitamin D$_3$ on intestinal epithelial barrier by regulating Notch signaling pathway. Nutr Metab (Lond). 2021; 18:49.
20. Dürholz K, Hofmann J, Iljazovic A, Häger J, Lucas S, Sarter K, Strowig T, Bang H, Rech J, Schett G, Zaiss MM. Dietary Short-Term Fiber Interventions in Arthritis Patients Increase Systemic SCFA Levels and Regulate Inflammation. Nutrients. 2020; 12.
21. Schönfeld P, Wojtczak L. Short- and medium-chain fatty acids in energy metabolism: the cellular perspective. J Lipid Res. 2016; 57:943-954.
22. Xia W, Khan I, Li XA, Huang G, Yu Z, Leong WK, Han R, Ho LT, Wendy Hsiao WL. Adaptogen-ic flower buds exert cancer preventive effects by enhancing the SCFA-producers, strengthening the epithelial tight junction complex and immune responses. Pharmacol Res. 2020; 159:104809.
23. Parada Venegas D, De la Fuente MK, Landskron G, González MJ, Quera R, Dijkstra G, Harmsen HJM, Faber KN, Hermoso MA. Short Chain Fatty Acids (SCFAs)-Mediated Gut Epithelial and Im-mune Regulation and Its Relevance for Inflammatory Bowel Diseases. Front Immunol. 2019; 10:277.
24. Schmidt T, Kahn R, Kahn F. Ascorbic acid attenuates activation and cytokine production in sepsis-like monocytes. J Leukoc Biol. 2022; 112:491-498.
25. Li L, Krause L, Somerset S. Associations between micronutrient intakes and gut microbiota in a group of adults with cystic fibrosis. Clin Nutr. 2017; 36:1097-1104.

Address correspondence to:
Yan Zhao, Yazhou Cui and Jinxiang Han, Biomedical Sciences College & Shandong Medicinal Biotechnol-ogy Centre, Shandong First Medical University & Shandong Academy of Medical Sciences; NHC Key La-boratory of Biotechnology Drugs (Shandong Academy of Medical Sciences); Key Lab for Rare & Uncom-mon Diseases of Shandong Province, 6699 Qingdao Road, Ji'nan 250117, Shandong, China.
E-mail: zhaoyan@sdfmu.edu.cn (YZ); yzcui@sdfmu.edu.cn (YC); jxhan9888@aliyun.com (JH)

Comment

Association between abnormal lipid metabolism and Alzheimer's disease: New research has revealed significant findings on the APOE4 genotype in microglia

Xiqi Hu[1], Ya-nan Ma[2], Ying Xia[1],*

[1] Department of Neurosurgery, Central South University, Xiangya School of Medicine Affiliated Haikou Hospital, Haikou, China;
[2] Department of Gastroenterology, Hainan General Hospital, Hainan Affiliated Hospital of Hainan Medical University, Haikou, China.

SUMMARY   *APOE4* is widely recognized as a genetic risk factor for Alzheimer's disease (AD), implicated in 60–80% of all AD cases. Recent research suggests that microglia carrying the *APOE4* genotype display abnormal lipid metabolism and accumulate lipid droplets, which may exacerbate the pathology of AD. Microglia play a critical role in immune surveillance within the central nervous system and are responsible for removing harmful particles and preserving neuronal function. The *APOE4* genotype causes abnormal lipid metabolism in microglia, resulting in excessive accumulation of lipid droplets. This accumulation not only impairs the phagocytic and clearance capabilities of microglia but also disrupts their interactions with neurons, resulting in disorganization and neurodegenerative alterations at the neuronal network level. In addition, the presence of *APOE4* modifies the metabolic landscape of microglia, particularly affecting purinergic signaling and lipid metabolism, thereby exacerbating the pathological processes of AD. In conclusion, the accumulation of lipid droplets and abnormal lipid metabolism may be critical mechanisms in the progression of AD in microglia carrying the *APOE4* genotype.

Keywords   Alzheimer's disease, lipid metabolism, apolipoprotein E, microglia, *APOE4*

Alzheimer's disease (AD) is a neurodegenerative disorder that gradually impairs cognitive function and affects tens of millions of people worldwide (*1*). Genetic studies have shown that 60–80% of the risk of developing AD is dependent on genetic factors (*2*). Over 40 genetic risk loci associated with AD have been identified, including the *APOE* gene (*1,3*). *APOE* is a gene responsible for lipid and cholesterol-related metabolism and transport, as well as neuronal maintenance and repair in the central nervous system. It has three major alleles: *APOE2*, *APOE3*, and *APOE4*. Studies have found that *APOE4* is significantly associated with an increased risk of developing AD. This allele promotes amyloid plaque deposition and neuronal damage (*4*), which may be related to abnormal lipid metabolism.

Abnormal lipid metabolism and lipid droplet accumulation have been observed in the microglia of individuals with AD with the *APOE4* genotype. Research has shown that under conditions related to aging and disease, microglia accumulate lipid droplets (*5,6*). This accumulation is more pronounced in *APOE4* human induced pluripotent stem cells (iPSCs)-derived microglia compared to *APOE3* microglia (*7*). Haney *et*

al. (2024) reported that microglia associated with lipid-droplet-accumulating microglia (LDAM) were found in AD patients with the *APOE4/4* genotype, and these cells displayed significantly increased expression in amyloid plaque regions (*7*). In their study, Claes *et al*. transplanted xenograft microglia (xMG) derived from human iPSCs into the brain of an amyloid mouse model. They observed a similar accumulation of large numbers of lipid droplets around amyloid plaques (6). Global transcriptomic analysis revealed that *APOE4*-driven abnormalities in human-specific lipid metabolism caused dysregulation of lipid metabolism in microglia (*8*).

In AD, APOE4 leads to abnormal lipid metabolism and lipid droplet accumulation in microglia. This may be due to alterations in lipid and cholesterol metabolism and transport, inflammation, oxidative stress, and other factors. Global transcriptomic analysis revealed that APOE4 was linked to increased cholesterol synthesis and decreased catabolism/exocytosis (*8*). ApoE4 was found to be less capable of effluxing cholesterol and phosphatidylcholine (PC) compared to ApoE2 and ApoE3 (*9*). A study found that *APOE4* microglia had impaired lipid reuptake, resulting in cholesterol overload

in the culture medium (*10*). ApoE4 caused disruption of intracellular lipid homeostasis in neuroglia, leading to increased unsaturation of fatty acids and accumulation of intracellular lipid droplets (*11,12*).

ApoE4 enhances microglia MHC-II-dependent antigen presentation and T cell activation while also promoting inflammatory responses in microglia (*12*). Moreover, the expression of ApoE4 in microglia leads to downregulation of complement and lysosomal pathways and promotes stress-related responses (*13*). Studies have shown that in a model of frontotemporal lobe dementia with chronic neuroinflammation, microglia containing lipid droplets were found in the hippocampus and thalamus (*5,14*). Neurons produce lipids due to elevated reactive oxygen species (ROS), which are then transferred to glial cells to form lipid droplets (*15*). Lipid droplets were detected in microglia of adult mice in which ROS were induced with rotenone as well (*16*). Inflammation and oxidative stress may be significant factors in the accumulation of lipid droplets in microglia. According to gene pathway analysis, microglia that are rich in lipid droplets exhibit impaired phagocytosis, produce ROS, and release pro-inflammatory cytokines. This could potentially exacerbate the accumulation of lipid droplets in microglia (*5*).

Single-nucleus RNA sequencing (snRNA-seq) of frontal cortex tissues revealed differential expression of genes associated with lipid metabolism, including *ACSL1*, *DPYD*, and *NAMPT*, in microglial cells of AD patients with the *APOE4/4* genotype compared to the control (*7*). Of these genes, *ACSL1* differed the most in microglial cells (*7*).

ACSL1 is an enzyme associated with lipid droplets that promotes their formation (*17,18*). Inhibition of the adipogenic gene *ACSL1* resulted in a reduction of lipid droplets in *APOE4* microglia and restoration of the purinergic signalling pathway. These findings suggest that ACSL1 expression, triglyceride synthesis, and lipid droplet accumulation are induced in an APOE4-dependent manner in AD.

The abnormal lipid metabolism and droplet accumulation observed in microglia of the *APOE4* genotype in AD have significant implications for an organism. Microglia are immune cells in the central nervous system responsible for clearing microbes, dead cells, redundant synapses, protein aggregates, and other potentially harmful particles (*19,20*). Recent research has shown that microglia with lipid droplets, known as LDAM, have a severe phagocytosis defect compared to microglia without lipid droplets in the aging brain. This is closely associated with increased lipid storage (*5*). Microglia carrying the *APOE4* allele exhibit a decreased ability to scavenge, especially for lipid-rich myelin debris, resulting in impaired myelin regeneration (*21*). Moreover, ApoE4 triggers lipid accumulation, leading to reduced surveillance of neuronal activity by microglia, ultimately resulting in disorganization at the neuronal network level (*10*). As immune cells of the brain, microglia participate in surveillance. Microglia prevent the invasion of foreign pathogens and regulate neuronal activities. The presence of *APOE4* alters the metabolic network of microglia, particularly affecting purinergic signaling and lipid metabolism. These alterations can change the surveillance status of microglia, impacting not only brain regions but also directly affecting neuronal activity, ultimately resulting in neurodegenerative changes (*10*) (Figure 1).

The current work has reviewed the effects of abnormal lipid metabolism and lipid droplet accumulation on an organism as observed in AD
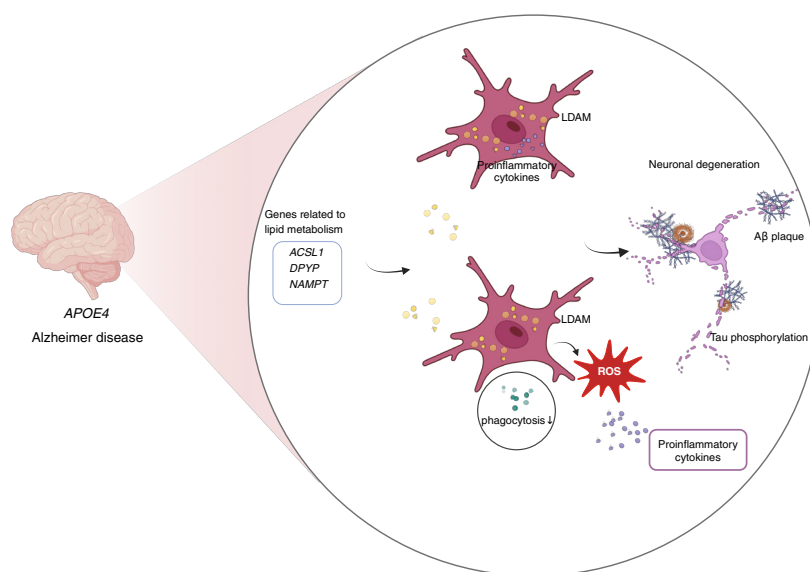

Figure 1. A schematic representation of lipid metabolism in AD microglia with the *APOE4* genotype. *Abbreviations*: ACSL1, acyl-CoA synthetase long-chain family member 1; AD, Alzheimer's disease; APOE4, apolipoprotein E4; DPYP, dihydropyrimidine dehydrogenase; LDAM, lipid-droplet-accumulating microglia; NAMPT, Nicotinamide phosphoribosyltransferase; ROS, reactive oxygen species.

microglia with the *APOE4* genotype. Microglia play a critical role in immune surveillance in the central nervous system and are responsible for eliminating harmful particles and maintaining neuronal function. Abnormal lipid metabolism induced by the *APOE4* genotype in microglia has been found to lead to excessive accumulation of lipid droplets. The presence of lipid droplets affected not only the phagocytosis and clearance ability of microglia but also their interactions with neurons, leading to disorganization at the neuronal network level and neurodegenerative changes. In addition, the presence of *APOE4* altered the metabolic network of microglia, and particularly purinergic signaling and lipid metabolism, further exacerbating pathological changes. In conclusion, abnormal lipid metabolism and lipid droplet accumulation may be important mechanisms in the progression of AD in microglia with the *APOE4* genotype. These findings provide new insights and research directions into the pathogenic mechanism and treatment of AD.

Conflict of Interest: The authors have no conflicts of interest to disclose.

References

1. Scheltens P, De Strooper B, Kivipelto M, Holstege H, Chetelat G, Teunissen CE, Cummings J, van der Flier WM. Alzheimer's disease. Lancet. 2021; 397:1577-1590.

2. Gatz M, Reynolds CA, Fratiglioni L, Johansson B, Mortimer JA, Berg S, Fiske A, Pedersen NL. Role of genes and environments for explaining Alzheimer disease. Arch Gen Psychiatry. 2006; 63:168-174.

3. Jansen IE, Savage JE, Watanabe K, *et al*. Genome-wide meta-analysis identifies new loci and functional pathways influencing Alzheimer's disease risk. Nat Genet. 2019; 51:404-413.

4. Blumenfeld J, Yip O, Kim MJ, Huang Y. Cell type-specific roles of APOE4 in Alzheimer disease. Nat Rev Neurosci. 2024; 25:91-110.

5. Marschallinger J, Iram T, Zardeneta M, *et al*. Lipid-droplet-accumulating microglia represent a dysfunctional and proinflammatory state in the aging brain. Nat Neurosci. 2020; 23:194-208.

6. Claes C, Danhash EP, Hasselmann J, Chadarevian JP, Shabestari SK, England WE, Lim TE, Hidalgo JLS, Spitale RC, Davtyan H, Blurton-Jones M. Plaque-associated human microglia accumulate lipid droplets in a chimeric model of Alzheimer's disease. Mol Neurodegener. 2021; 16:50.

7. Haney MS, Palovics R, Munson CN, *et al*. APOE4/4 is linked to damaging lipid droplets in Alzheimer's disease microglia. Nature. 2024; 628:154-161.

8. Tcw J, Qian L, Pipalia NH, *et al*. Cholesterol and matrisome pathways dysregulated in astrocytes and microglia. Cell. 2022; 185:2213-2233.e25.

9. Michikawa M, Fan QW, Isobe I, Yanagisawa K. Apolipoprotein E exhibits isoform-specific promotion of lipid efflux from astrocytes and neurons in culture. J Neurochem. 2000; 74:1008-1016.

10. Victor MB, Leary N, Luna X, *et al*. Lipid accumulation induced by APOE4 impairs microglial surveillance of neuronal-network activity. Cell Stem Cell. 2022; 29:1197-1212.e8.

11. Sienski G, Narayan P, Bonner JM, *et al*. APOE4 disrupts intracellular lipid homeostasis in human iPSC-derived glia. Sci Transl Med. 2021; 13:eaaz4564.

12. Wang C, Lu J, Sha X, Qiu Y, Chen H, Yu Z. TRPV1 regulates ApoE4-disrupted intracellular lipid homeostasis and decreases synaptic phagocytosis by microglia. Exp Mol Med. 2023; 55:347-363.

13. Liu CC, Wang N, Chen Y, *et al*. Cell-autonomous effects of APOE4 in restricting microglial response in brain homeostasis and Alzheimer's disease. Nat Immunol. 2023; 24:1854-1866.

14. Ghoshal N, Dearborn JT, Wozniak DF, Cairns NJ. Core features of frontotemporal dementia recapitulated in progranulin knockout mice. Neurobiol Dis. 2012; 45:395-408.

15. Liu L, MacKenzie KR, Putluri N, Maletic-Savatic M, Bellen HJ. The glia-neuron lactate shuttle and elevated ROS promote lipid synthesis in neurons and lipid droplet accumulation in glia via APOE/D. Cell Metab. 2017; 26:719-737.e6.

16. Liu L, Zhang K, Sandoval H, Yamamoto S, Jaiswal M, Sanz E, Li Z, Hui J, Graham BH, Quintana A, Bellen HJ. Glial lipid droplets and ROS induced by mitochondrial defects promote neurodegeneration. Cell. 2015; 160:177-190.

17. Li LO, Mashek DG, An J, Doughman SD, Newgard CB, Coleman RA. Overexpression of rat long chain acyl-coa synthetase 1 alters fatty acid metabolism in rat primary hepatocytes. J Biol Chem. 2006; 281:37246-37255.

18. Zhao Z, Abbas Raza SH, Tian H, Shi B, Luo Y, Wang J, Liu X, Li S, Bai Y, Hu J. Effects of overexpression of ACSL1 gene on the synthesis of unsaturated fatty acids in adipocytes of bovine. Arch Biochem Biophys. 2020; 695:108648.

19. Colonna M, Butovsky O. Microglia function in the central nervous system during health and neurodegeneration. Annu Rev Immunol. 2017; 35:441-468.

20. Sarlus H, Heneka MT. Microglia in Alzheimer's disease. J Clin Invest. 2017; 127:3240-3249.

21. Wang N, Wang M, Jeevaratnam S, Rosenberg C, Ikezu TC, Shue F, Doss SV, Alnobani A, Martens YA, Wren M, Asmann YW, Zhang B, Bu G, Liu CC. Opposing effects of apoE2 and apoE4 on microglial activation and lipid metabolism in response to demyelination. Mol Neurodegener. 2022; 17:75.

*Address correspondence to:
Ying Xia, Department of Neurosurgery, Haikou Affiliated Hospital of Central South University Xiangya School of Medicine, Haikou 570208, China.
E-mail: xiaying008@163.com

Letter to the Editor

Elevation of circulating DNAs of disease-associated cytokines in serum cell-free DNA from patients with alopecia areata

Soichiro Sawamura[§], Tselmeg M. Myangat[§], Ikko Kajihara[*], Katsunari Makino, Jun Aoi, Shinichi Masuguchi, Satoshi Fukushima

Department of Dermatology and Plastic Surgery, Faculty of Life Sciences, Kumamoto University, Kumamoto, Japan.

SUMMARY   Alopecia areata (AA) is an autoimmune disease characterized by damage to hair follicles and hair loss. Cell-free DNA (cfDNA) has recently received attention as a biomarker of various disorders including inflammatory skin diseases. In this study, we aimed to investigate the clinical significance of cfDNA and the circulating DNAs of disease-associated cytokines in AA patients. Serum samples were obtained from 63 patients with AA and 32 healthy controls (HC). Using droplet digital polymerase chain reaction, circulating C-X-C motif chemokine ligand (*CXCL*) 9, *CXCL10*, *CXCL11*, C-X-C motif chemokine receptor 3, interferon (*IFN*)-γ, interleukin (*IL*) -7, *IL-15*, and Janus kinase (*JAK*) 2 were detectable in both HC and AA patients. Among the detectable DNAs, copies of circulating *CXCL9*, *CXCL11*, *IL-15*, *IFN-γ*, and *JAK2* were significantly higher in AA patients than in HC. These results suggest that increased circulating DNA levels may reflect damage to hair follicles in AA patients.

Keywords   liquid biopsy, chemokine, Janus kinase, digital PCR

To the Editor,

Alopecia areata (AA) is an autoimmune disease characterized by damage to hair follicles, resulting in the various levels of hair loss (*1*). Some pro-inflammatory cytokines have been shown to play key roles in the pathogenesis of AA (*2*). Circulating cell-free DNA (cfDNA) originates from apoptotic or necrotic cells and reflects the severity of cellular damage (*3*). Although cfDNA has recently received attention as a biomarker for the diagnosis and prognosis of various disorders including inflammatory skin diseases (*4,5*), the clinical significance of cfDNA in patients with AA remains unclear. In this study, we aimed to investigate the clinical significance of cfDNA in patients with AA and assess the circulating DNAs of cytokines associated with AA.

Serum samples were obtained from 63 patients with AA (all of them were diagnosed based on clinical presentation and pathological findings of skin biopsy), including 7 patients with patchy type, 31 with reticular type, 8 with ophiasis type, 11 with alopecia totalis, and 6 with alopecia universalis. Serum samples were collected from 32 healthy controls (HC). The clinical findings of the patients with AA were assessed at the time of serum sampling. cfDNA was isolated from the serum samples using a QIAamp Circulating Nucleic Acid Kit (Qiagen, Hilden, Germany). The cfDNA concentration

was determined using a Qubit 4 fluorometer (Thermo Fisher Scientific, Waltham, MA, USA). The detection of circulating DNAs in cfDNA was performed using droplet digital polymerase chain reaction (ddPCR) according to our previous report (*5*). All probes used in this study were purchased from Bio-Rad (Hercules, CA, USA). All the samples were stored at -80°C before use. Institutional Review Board approval (No. 1452) and written informed consent were obtained in accordance with the principles of the Declaration of Helsinki.

Firstly, no significant difference was observed in the levels of total cfDNA between patients with AA (mean; 882.5 ± 857.7 ng/μL) and HC (mean; 908.5 ± 1260.8 ng/μL) (Table 1). Next, we attempted to detect circulating DNAs of patients with AA using ddPCR (Table 1). Although ddPCR showed that circulating C-X-C motif chemokine ligand (*CXCL*) 9, *CXCL10*, *CXCL11*, C-X-C motif chemokine receptor (*CXCR*) 3, interferon (*IFN*)-γ, interleukin (*IL*) -7, *IL-15*, and Janus kinase (*JAK*) 2 were detectable in both HC and AA patients, circulating *IL-2*, *JAK1*, *JAK3*, tyrosine kinase 2 (*TYK2*) were not detectable. Among the detectable DNAs, copies of circulating *CXCL9*, *CXCL11*, *IL-15*, *IFN-γ*, and *JAK2* were significantly higher in patients with AA than in HC. No significant relationships were observed between their levels and the clinical features such as age, sex, type,

Table 1. Serum cell-free DNA levels and circulating DNAs copies in patients with alopecia areata and healthy controls

Items	Healthy controls ($n = 32$)	Patients with alopecia areata ($n = 63$)	p-value
cell-free DNA levels (ng/mL ± SD)	908.5 ± 1,260.8	882.5 ± 857.7	0.238
circulating DNA levels (copies/mL ± SD)			
CXCL9	6,701.5 ± 11,138.8	7,647.0 ± 7,380.8	*0.015
CXCL10	8,706.6 ± 14,408.8	8,708.2 ± 8,013.0	0.103
CXCL11	5,702.2 ± 9,946.3	6,740.1 ± 7,390.4	*0.030
CXCR3	7,541.8 ± 13,470.7	7,198.7 ± 7,048.7	0.122
IFN-γ	6,634.6 ± 10,282.8	8,123.4 ± 7,847.0	*0.030
IL-7	9,850.4 ± 16,541.4	9,986.3 ± 8,834.0	0.060
IL-15	7,468.2 ± 12,480.2	8,183.2 ± 7,837.6	*0.038
JAK2	6,677.1 ± 10,658.2	7,922.4 ± 7,717.0	*0.041
IL-1	ND	ND	-
JAK1	ND	ND	-
JAK3	ND	ND	-
TYK2	ND	ND	-

The p-value was tested using the Mann–Whitney U test. Statistical significance was set at p-value < 0.05 was considered significant. SD, standard deviation; CXCL, C-X-C motif chemokine ligand; CXCR3; C-X-C motif chemokine receptor 3, IFN-γ, interferon γ; IL, interleukin; JAK, Janus kinase; TYK2, tyrosine kinase 2; ND, not detectable.

disease duration, or disease area (data not shown).

Some pro-inflammatory cytokines involved in the pathogenesis of AA (*2*); in particular, inhibition of JAK signaling has been attracting attention as a new strategy for treating AA, which acts to suppress inflammation (*6*). Serum protein levels of various cytokines such as serum C-C motif chemokine 17 /thymus and activation-regulated chemokine have potential as biomarkers of AA activity (*7*). Recently, elevated cfDNA levels have attracted attention for the potential of biomarkers in various diseases such as skin inflammatory diseases (*4,8*). For example, cfDNA levels in plasma are higher in patients with severe psoriasis vulgaris than those in healthy subjects (*4*). In autoimmune bullous diseases, serum cfDNA levels are increased compared with healthy volunteers. Especially, in patients with bullous pemphigoid (BP), serum cfDNA levels positively correlated with serum anti-BP180 antibody levels (*8*). Elevation of serum α1(I) collagen DNA levels in patients with systemic sclerosis might be useful as the diagnostic marker, reflecting the presence of vasculopathy (*9*). Phospholipase A2 group IV D (*PLA2G4D*) DNA copies in cfDNA in psoriatic patients are significantly higher than that in normal controls, and post-therapeutic circulating *PLA2G4D* DNA copies are significantly decreased after efficient therapy (*10*). We had conducted a comprehensive literature search by PubMed database, there was no literature about the correlation with cfDNA and AA. Thus, to the best of our knowledge, this is the first study to explore the significance of cfDNA levels in patients with AA. Furthermore, the expression of some circulating DNAs (*CXCL9*, *CXCL11*, *IL-15*, *IFN-γ*, and *JAK2*) was higher in patients with AA than in HC. These results suggest that increased circulating DNA levels may reflect damage to hair follicles in patients with AA.

However, these findings were based on a retrospective analysis and did not reveal the significant correlation between cfDNA levels and the clinical features of AA.

Therefore, further extensive investigations are warranted to elucidate the clinical significance of cfDNA in patients with AA.

Conflicts of Interest: The authors have no conflicts of interest to disclose.

References

1. Pratt CH, King LE Jr., Messenger AG, Christiano AM, Sundberg JP. Alopecia areata. Nat Rev Dis Primers. 2017; 3:17011.
2. Rajabi F, Drake LA, Senna MM, Rezaei N. Alopecia areata: A review of disease pathogenesis. Br J Dermatol. 2018; 179:1033-1048.
3. Jahr S, Hentze H, Englisch S, Hardt D, Fackelmayer FO, Hesch RD, Knippers R. DNA fragments in the blood plasma of cancer patients: Quantitations and evidence for their origin from apoptotic and necrotic cells. Cancer Res. 2001; 61:1659-1665.
4. Beranek M, Fiala Z, Kremlacek J, Andrys C, Krejsek J, Hamakova K, Chmelarova M, Palicka V, Borska L. Changes in circulating cell free DNA and nucleosomes in patients with exacerbated psoriasis. Arch Dermatol Res. 2017; 309: 815-821.
5. Sakamoto R, Sawamura S, Kajihara I, Miyauchi H, Urata K, Otsuka-Maeda S, Kanemaru H, Kanazawa-Yamada S, Honda N, Makino K, Miyashita A, Aoi J, Makino T, Fukushima S, Ihn H. Circulating tumor necrosis factor-α DNA are elevated in psoriasis. J Dermatol. 2020; 47:1037-1040.
6. Lensing M, Jabbari A. An overview of JAK/STAT pathways and JAK inhibition in alopecia areata. Front Immunol. 2022; 13:955035.
7. Inui S, Noguchi F, Nakajima T, Itami S. Serum thymus and activation-regulated chemokine as disease activity and response biomarker in alopecia areata. J Dermatol. 2013; 40:881-885.
8. Kakitsuka Y, Sawamura S, Kajihara I, Kanemaru H, Honda N, Makino K, Aoi J, Makino T, Fukushima S, Ihn H.

Elevated circulating cell-free DNA levels in autoimmune bullous diseases. J Dermatol. 2020; 47:e345-e346.

9. Sawamura S, Jinnin M, Shimbara M, Nakamura K, Kudo H, Inoue K, Nakayama W, Kajihara I, Fukushima S, Ihn H. Serum levels of genomic DNA of α1(I) collagen are elevated in scleroderma patients. J Dermatol. 2017; 44:927-931.

10. Yamada-Kanazawa S, Mijiddorj MT, Kajihara I, Kanemaru H, Sawamura S, Makino K, Aoi J, Masuguchi S, Fukushima S. Circulating phospholipase A2 group IV D DNA copies are elevated in psoriasis. J Eur Acad Dermatol Venereol. 2022; 36: e302-e304.

§These authors contributed equally to this work.
Address correspondence to:
Ikko Kajihara, Department of Dermatology and Plastic Surgery, Faculty of Life Sciences, Kumamoto University, 1-1-1 Honjo, Kumamoto 860-8556, Japan.
E-mail: kajiderma@gmail.com

Guide for Authors

1. Scope of Articles

BioScience Trends (Print ISSN 1881-7815, Online ISSN 1881-7823) is an international peer-reviewed journal. *BioScience Trends* devotes to publishing the latest and most exciting advances in scientific research. Articles cover fields of life science such as biochemistry, molecular biology, clinical research, public health, medical care system, and social science in order to encourage cooperation and exchange among scientists and clinical researchers.

2. Submission Types

Original Articles should be well-documented, novel, and significant to the field as a whole. An Original Article should be arranged into the following sections: Title page, Abstract, Introduction, Materials and Methods, Results, Discussion, Acknowledgments, and References. Original articles should not exceed 5,000 words in length (excluding references) and should be limited to a maximum of 50 references. Articles may contain a maximum of 10 figures and/or tables. Supplementary Data are permitted but should be limited to information that is not essential to the general understanding of the research presented in the main text, such as unaltered blots and source data as well as other file types.

Brief Reports definitively documenting either experimental results or informative clinical observations will be considered for publication in this category. Brief Reports are not intended for publication of incomplete or preliminary findings. Brief Reports should not exceed 3,000 words in length (excluding references) and should be limited to a maximum of 4 figures and/or tables and 30 references. A Brief Report contains the same sections as an Original Article, but the Results and Discussion sections should be combined.

Reviews should present a full and up-to-date account of recent developments within an area of research. Normally, reviews should not exceed 8,000 words in length (excluding references) and should be limited to a maximum of 10 figures and/or tables and 100 references. Mini reviews are also accepted, which should not exceed 4,000 words in length (excluding references) and should be limited to a maximum of 5 figures and/or tables and 50 references.

Policy Forum articles discuss research and policy issues in areas related to life science such as public health, the medical care system, and social science and may address governmental issues at district, national, and international levels of discourse. Policy Forum articles should not exceed 3,000 words in length (excluding references) and should be limited to a maximum of 5 figures and/or tables and 30 references.

Communications are short, timely pieces that spotlight new research findings or policy issues of interest to the field of global health and medical practice that are of immediate importance. Depending on their content, Communications will be published as "Comments" or "Correspondence". Communications should not exceed 1,500 words in length (excluding references) and should be limited to a maximum of 2 figures and/or tables and 20 references.

Editorials are short, invited opinion pieces that discuss an issue of immediate importance to the fields of global health, medical practice, and basic science oriented for clinical application. Editorials should not exceed 1,000 words in length (excluding references) and should be limited to a maximum of 10 references. Editorials may contain one figure or table.

News articles should report the latest events in health sciences and medical research from around the world. News should not exceed 500 words in length.

Letters should present considered opinions in response to articles published in *BioScience Trends* in the last 6 months or issues of general interest. Letters should not exceed 800 words in length and may contain a maximum of 10 references. Letters may contain one figure or table.

3. Editorial Policies

For publishing and ethical standards, *BioScience Trends* follows the Recommendations for the Conduct, Reporting, Editing, and Publication of Scholarly Work in Medical Journals issued by the International Committee of Medical Journal Editors (ICMJE, *https://icmje.org/recommendations*), and the Principles of Transparency and Best Practice in Scholarly Publishing jointly issued by the Committee on Publication Ethics (COPE, *https://publicationethics.org/resources/guidelines-new/principles-transparency-and-best-practice-scholarly-publishing*), the Directory of Open Access Journals (DOAJ, *https://doaj.org/apply/transparency*), the Open Access Scholarly Publishers Association (OASPA, *https://oaspa.org/principles-of-transparency-and-best-practice-in-scholarly-publishing-4*), and the World Association of Medical Editors (WAME, *https://wame.org/principles-of-transparency-and-best-practice-in-scholarly-publishing*).

BioScience Trends will perform an especially prompt review to encourage innovative work. All original research will be subjected to a rigorous standard of peer review and will be edited by experienced copy editors to the highest standards.

Ethical Approval of Studies and Informed Consent: For all manuscripts reporting data from studies involving human participants or animals, formal review and approval, or formal review and waiver, by an appropriate institutional review board or ethics committee is required and should be described in the Methods section. When your manuscript contains any case details, personal information and/or images of patients or other individuals, authors must obtain appropriate written consent, permission and release in order to comply with all applicable laws and regulations concerning privacy and/or security of personal information. The consent form needs to comply with the relevant legal requirements of your particular jurisdiction, and please do not send signed consent form to *BioScience Trends* to respect your patient's and any other individual's privacy. Please instead describe the information clearly in the Methods (patient consent) section of your manuscript while retaining copies of the signed forms in the event they should be needed. Authors should also state that the study conformed to the provisions of the Declaration of Helsinki (as revised in 2013, *https://wma.net/what-we-do/medical-ethics/declaration-of-helsinki*). When reporting experiments on animals, authors should indicate whether the institutional and national guide for the care and use of laboratory animals was followed.

Reporting Clinical Trials: The ICMJE (*https://icmje.org/recommendations/browse/publishing-and-editorial-issues/clinical-trial-registration.html*) defines a clinical trial as any research project that prospectively assigns people or a group of people to an intervention, with or without concurrent comparison or control groups, to study the relationship between a health-related intervention and a health outcome. Registration of clinical trials in a public trial registry at or before the time of first patient enrollment is a condition of consideration for publication in *BioScience Trends*, and the trial registration number will be published at the end of the Abstract. The registry must be independent of for-profit interest and publicly accessible. Reports of trials must conform to CONSORT 2010 guidelines (*https://consort-statement.org/consort-2010*). Articles reporting the results of randomized trials must include the CONSORT flow diagram showing the progress of patients throughout the trial.

Conflict of Interest: All authors are required to disclose any actual or potential conflict of interest including financial interests or relationships with other people or organizations that might raise questions of bias

in the work reported. If no conflict of interest exists for each author, please state "There is no conflict of interest to disclose".

Submission Declaration: When a manuscript is considered for submission to *BioScience Trends*, the authors should confirm that 1) no part of this manuscript is currently under consideration for publication elsewhere; 2) this manuscript does not contain the same information in whole or in part as manuscripts that have been published, accepted, or are under review elsewhere, except in the form of an abstract, a letter to the editor, or part of a published lecture or academic thesis; 3) authorization for publication has been obtained from the authors' employer or institution; and 4) all contributing authors have agreed to submit this manuscript.

Initial Editorial Check: Immediately after submission, the journal's managing editor will perform an initial check of the manuscript. A suitable academic editor will be notified of the submission and invited to check the manuscript and recommend reviewers. Academic editors will check for plagiarism and duplicate publication at this stage. The journal has a formal recusal process in place to help manage potential conflicts of interest of editors. In the event that an editor has a conflict of interest with a submitted manuscript or with the authors, the manuscript, review, and editorial decisions are managed by another designated editor without a conflict of interest related to the manuscript.

Peer Review: *BioScience Trends* operates a single-anonymized review process, which means that reviewers know the names of the authors, but the authors do not know who reviewed their manuscript. All articles are evaluated objectively based on academic content. External peer review of research articles is performed by at least two reviewers, and sometimes the opinions of more reviewers are sought. Peer reviewers are selected based on their expertise and ability to provide quality, constructive, and fair reviews. For research manuscripts, the editors may, in addition, seek the opinion of a statistical reviewer. Every reviewer is expected to evaluate the manuscript in a timely, transparent, and ethical manner, following the COPE guidelines (*https://publicationethics. org/files/cope-ethical-guidelines-peer-reviewers-v2_0.pdf*). We ask authors for sufficient revisions (with a second round of peer review, when necessary) before a final decision is made. Consideration for publication is based on the article's originality, novelty, and scientific soundness, and the appropriateness of its analysis.

Suggested Reviewers: A list of up to 3 reviewers who are qualified to assess the scientific merit of the study is welcomed. Reviewer information including names, affiliations, addresses, and e-mail should be provided at the same time the manuscript is submitted online. Please do not suggest reviewers with known conflicts of interest, including participants or anyone with a stake in the proposed research; anyone from the same institution; former students, advisors, or research collaborators (within the last three years); or close personal contacts. Please note that the Editor-in-Chief may accept one or more of the proposed reviewers or may request a review by other qualified persons.

Language Editing: Manuscripts prepared by authors whose native language is not English should have their work proofread by a native English speaker before submission. If not, this might delay the publication of your manuscript in *BioScience Trends*.

The Editing Support Organization can provide English proofreading, Japanese-English translation, and Chinese-English translation services to authors who want to publish in *BioScience Trends* and need assistance before submitting a manuscript. Authors can visit this organization directly at *https://www.iacmhr.com/iac-eso/support.php?lang=en*. IAC-ESO was established to facilitate manuscript preparation by researchers whose native language is not English and to help edit works intended for international academic journals.

Copyright and Reuse: Before a manuscript is accepted for publication in *BioScience Trends*, authors will be asked to sign a transfer of copyright agreement, which recognizes the common interest that both the journal and author(s) have in the protection of copyright. We accept that some authors (*e.g.*, government employees in some countries) are unable to transfer copyright. A JOURNAL PUBLISHING AGREEMENT (JPA) form will be e-mailed to the authors by the Editorial Office and must be returned by the authors by mail, fax, or as a scan. Only forms with a hand-written signature from the corresponding author are accepted. This copyright will ensure the widest possible dissemination of information. Please note that the manuscript will not proceed to the next step in publication until the JPA Form is received. In addition, if excerpts from other copyrighted works are included, the author(s) must obtain written permission from the copyright owners and credit the source(s) in the article.

4. Cover Letter

The manuscript must be accompanied by a cover letter prepared by the corresponding author on behalf of all authors. The letter should indicate the basic findings of the work and their significance. The letter should also include a statement affirming that all authors concur with the submission and that the material submitted for publication has not been published previously or is not under consideration for publication elsewhere. The cover letter should be submitted in PDF format. For an example of Cover Letter, please visit: *https://www.biosciencetrends. com/downcentre* (Download Centre).

5. Submission Checklist

The Submission Checklist should be submitted when submitting a manuscript through the Online Submission System. Please visit Download Centre (*https://www.biosciencetrends.com/downcentre*) and download the Submission Checklist file. We recommend that authors use this checklist when preparing your manuscript to check that all the necessary information is included in your article (if applicable), especially with regard to Ethics Statements.

6. Manuscript Preparation

Manuscripts are suggested to be prepared in accordance with the "Recommendations for the Conduct, Reporting, Editing, and Publication of Scholarly Work in Medical Journals", as presented at *https://www.ICMJE.org*.

Manuscripts should be written in clear, grammatically correct English and submitted as a Microsoft Word file in a single-column format. Manuscripts must be paginated and typed in 12-point Times New Roman font with 24-point line spacing. Please do not embed figures in the text. Abbreviations should be used as little as possible and should be explained at first mention unless the term is a well-known abbreviation (*e.g.* DNA). Single words should not be abbreviated.

Title page: The title page must include 1) the title of the paper (Please note the title should be short, informative, and contain the major key words); 2) full name(s) and affiliation(s) of the author(s), 3) abbreviated names of the author(s), 4) full name, mailing address, telephone/fax numbers, and e-mail address of the corresponding author; 5) author contribution statements to specify the individual contributions of all authors to this manuscript, and 6) conflicts of interest (if you have an actual or potential conflict of interest to disclose, it must be included as a footnote on the title page of the manuscript; if no conflict of interest exists for each author, please state "There is no conflict of interest to disclose").

Abstract: The abstract should briefly state the purpose of the study, methods, main findings, and conclusions. For articles that are Original Articles, Brief Reports, Reviews, or Policy Forum articles, a one-paragraph abstract consisting of no more than 250 words must be included in the manuscript. For Communications, Editorials, News, or Letters, a brief summary of main content in 150 words or fewer should be included in the manuscript. For articles reporting clinical trials, the trial registration number should be stated at the end of the Abstract. Abbreviations must be kept to a minimum and non-standard

abbreviations explained in brackets at first mention. References should be avoided in the abstract. Three to six key words or phrases that do not occur in the title should be included in the Abstract page.

Introduction: The introduction should provide sufficient background information to make the article intelligible to readers in other disciplines and sufficient context clarifying the significance of the experimental findings

Materials/Patients and Methods: The description should be brief but with sufficient detail to enable others to reproduce the experiments. Procedures that have been published previously should not be described in detail but appropriate references should simply be cited. Only new and significant modifications of previously published procedures require complete description. Names of products and manufacturers with their locations (city and state/country) should be given and sources of animals and cell lines should always be indicated. All clinical investigations must have been conducted in accordance Materials/ Patients and Methods.

Results: The description of the experimental results should be succinct but in sufficient detail to allow the experiments to be analyzed and interpreted by an independent reader. If necessary, subheadings may be used for an orderly presentation. All Figures and Tables should be referred to in the text in order, including those in the Supplementary Data.

Discussion: The data should be interpreted concisely without repeating material already presented in the Results section. Speculation is permissible, but it must be well-founded, and discussion of the wider implications of the findings is encouraged. Conclusions derived from the study should be included in this section.

Acknowledgments: All funding sources (including grant identification) should be credited in the Acknowledgments section. Authors should also describe the role of the study sponsor(s), if any, in study design; in the collection, analysis, and interpretation of data; in the writing of the report; and in the decision to submit the paper for publication. If the funding source had no such involvement, the authors should so state.

In addition, people who contributed to the work but who do not meet the criteria for authors should be listed along with their contributions.

References: References should be numbered in the order in which they appear in the text. Citing of unpublished results, personal communications, conference abstracts, and theses in the reference list is not recommended but these sources may be mentioned in the text. In the reference list, cite the names of all authors when there are fifteen or fewer authors; if there are sixteen or more authors, list the first three followed by *et al*. Names of journals should be abbreviated in the style used in PubMed. Authors are responsible for the accuracy of the references. The EndNote Style of *BioScience Trends* could be downloaded at **EndNote** (*https://ircabssagroup.com/examples/ BioScience_Trends.ens*).

Examples are given below:

Example 1 (Sample journal reference):

Inagaki Y, Tang W, Zhang L, Du GH, Xu WF, Kokudo N. Novel aminopeptidase N (APN/CD13) inhibitor 24F can suppress invasion of hepatocellular carcinoma cells as well as angiogenesis. Biosci Trends. 2010; 4:56-60.

Example 2 (Sample journal reference with more than 15 authors):

Darby S, Hill D, Auvinen A, *et al*. Radon in homes and risk of lung cancer: Collaborative analysis of individual data from 13 European case-control studies. BMJ. 2005; 330:223.

Example 3 (Sample book reference):

Shalev AY. Post-traumatic stress disorder: Diagnosis, history and life course. In: Post-traumatic Stress Disorder, Diagnosis, Management and Treatment (Nutt DJ, Davidson JR, Zohar J, eds.). Martin Dunitz, London, UK, 2000; pp. 1-15.

Example 4 (Sample web page reference):

World Health Organization. The World Health Report 2008 – primary health care: Now more than ever. *http://www.who.int/whr/2008/whr08_ en.pdf* (accessed September 23, 2022).

Tables: All tables should be prepared in Microsoft Word or Excel and should be arranged at the end of the manuscript after the References section. Please note that tables should not in image format. All tables should have a concise title and should be numbered consecutively with Arabic numerals. If necessary, additional information should be given below the table.

Figure Legend: The figure legend should be typed on a separate page of the main manuscript and should include a short title and explanation. The legend should be concise but comprehensive and should be understood without referring to the text. Symbols used in figures must be explained. Any individually labeled figure parts or panels (A, B, *etc*.) should be specifically described by part name within the legend.

Figure Preparation: All figures should be clear and cited in numerical order in the text. Figures must fit a one- or two-column format on the journal page: 8.3 cm (3.3 in.) wide for a single column, 17.3 cm (6.8 in.) wide for a double column; maximum height: 24.0 cm (9.5 in.). Please make sure that the symbols and numbers appeared in the figures should be clear. Please make sure that artwork files are in an acceptable format (TIFF or JPEG) at minimum resolution (600 dpi for illustrations, graphs, and annotated artwork, and 300 dpi for micrographs and photographs). Please provide all figures as separate files. Please note that low-resolution images are one of the leading causes of article resubmission and schedule delays.

Units and Symbols: Units and symbols conforming to the International System of Units (SI) should be used for physicochemical quantities. Solidus notation (*e.g.* mg/kg, mg/mL, mol/mm^2/min) should be used. Please refer to the SI Guide *www.bipm.org/en/si/* for standard units.

Supplemental data: Supplemental data might be useful for supporting and enhancing your scientific research and *BioScience Trends* accepts the submission of these materials which will be only published online alongside the electronic version of your article. Supplemental files (figures, tables, and other text materials) should be prepared according to the above guidelines, numbered in Arabic numerals (*e.g.*, Figure S1, Figure S2, and Table S1, Table S2) and referred to in the text. All figures and tables should have titles and legends. All figure legends, tables and supplemental text materials should be placed at the end of the paper. Please note all of these supplemental data should be provided at the time of initial submission and note that the editors reserve the right to limit the size and length of Supplemental Data.

5. Submission Checklist

The Submission Checklist will be useful during the final checking of a manuscript prior to sending it to *BioScience Trends* for review. Please visit Download Centre and download the Submission Checklist file.

6. Online Submission

Manuscripts should be submitted to *BioScience Trends* online at *https://www.biosciencetrends.com/login*. Receipt of your manuscripts submitted online will be acknowledged by an e-mail from Editorial Office containing a reference number, which should be used in all future communications. If for any reason you are unable to submit a file online, please contact the Editorial Office by e-mail at *office@ biosciencetrends.com*

8. Accepted Manuscripts

Page Charge: Page charges will be levied on all manuscripts accepted for publication in *BioScience Trends* (Original Articles / Brief Reports / Reviews / Policy Forum / Communications: $140 per page for black white pages, $340 per page for color pages; News / Letters: a total cost of $600). Under exceptional circumstances, the author(s) may apply to the editorial office for a waiver of the publication charges by stating the reason in the Cover Letter when the manuscript online.

Misconduct: *BioScience Trends* takes seriously all allegations of potential misconduct and adhere to the ICMJE Guideline (*https://icmje. org/recommendations*) and COPE Guideline (*https://publicationethics. org/files/Code_of_conduct_for_journal_editors.pdf*). In cases of suspected research or publication misconduct, it may be necessary for the Editor or Publisher to contact and share submission details with third parties including authors' institutions and ethics committees. The corrections, retractions, or editorial expressions of concern will be performed in line with above guidelines.

(As of December 2022)